(ADP-ribosyl)ation and Ap4A

Thorne, N. M. H.

Award date:
1988

Awarding institution:
University of Bath

(ADP-ribosyl)ation and Ap4A.

Submitted by N.M.H.THORNE

for the degree of Ph.D.

of the University of Bath

1988.

ProQuest LLC
789 East Eisenhower Parkway
P.O. Box 1346
Ann Arbor, MI 48106-1346

Acknowledgements.

I would like to thank my supervisor, Dr. W. J. D. Whish, for his encouragement and consideration. My thanks also go to Ian White, Mrs. Joan Whish and Mrs. Bridget Hunt for their help, and to Rebecca for her patient support.

to Anne and Des.

Abstract.

The (ADP-ribosyl)ation of a low molecular weight molecule was previously observed to be stimulated upon DMS - mediated DNA damage in permeabilised cells. Ap4A (a possible growth regulator) has been found to serve as an acceptor for poly(ADP-ribose) when incubated with NAD^+, histone H1 and highly purified ADPRT.

This project found no evidence to suggest the specific (ADP-ribosyl)ation of a nucleotide - like molecule in response to DNA damage in permeabilised L1210 cells. Although Ap4A caused the inhibition of (ADP-ribosyl)ation of protein in permeabilised cells and salt/PEI-extracted pig thymus nuclei, it was not found to be due to its own preferrential (ADP-ribosyl)ation. TLC analysis of disrupted permeabilised cells incubated with [^{3}H]NAD^+ and Ap4A (although distorted) *did* show the increasing formation with time of a labelled product which had slightly less mobility than Ap4A in this system. The presence of all the other cell components did not allow sufficient resolution of nucleotides due to distortion. The TLC analysis of the complex mixtures of nucleotides harvested from permeabilised cells by extraction with phenol/chloroform/IAA and acidic ethanol also proved to be of limited value, although small amounts of labelled material were also observed to be stimulated by Ap4A. It is unlikely that this material was (ADP-ribosyl)ated Ap4A, however, since it was resistant to base treatment. A more satisfactory technique of chromatography on DEAE cellulose revealed that in nucleotide extracts from dual-labelled permeabilised cells (incubated with [^{3}H]Ap4A and [^{32}P]NAD^+), the [^{3}H]Ap4A was extensively hydrolysed - although this was masked if 200μM unlabelled Ap4A were included in the incubation. Treatment with DMS and/or inhibition of ADPRT with 3AB had no significant effect in terms of the radioactive profiles of the nucleotide extracts on DEAE cellulose.

The possibilty that (ADP-ribosyl)ated Ap4A may have been 'lost' to the extraction procedure was eliminated, since although 200μM Ap4A caused an increase in the amount of [^{3}H]dpm deposited with nucleic acids during ethanol extraction, this was not accompanied by changes in the distribution of [^{32}P]dpm, and when 3AB was present as well, the same effect occurred. It remains possible that (ADP-ribosyl)ated Ap4A *was* produced preferrentially, but that this was followed by its rapid degradation in the cells.

Contents

Introduction.

I: (ADP-ribosyl)ation. Page

Materials and Methods.

III.

Results and Discussion

IV.

Conclusions.

Abbreviations

3AB	3-aminobenzamide
ADO	(in figures only) adenosine
ADP	adenosine diphosphate
ADP-ribose	adenosine diphosphate ribose
ADPRT	poly(ADP-ribose) transferase
AMP	adenosine monophosphate
Ap4A	p^1p^4-diadenosine tetraphosphate
ATP	adenosine tetraphosphate
BHK	baby hamster kidney (cells)
BSA	bovine serum albumin
CHO	chinese hamster ovary (cells)
cpm	(radioactive) counts per minute
Da	daltons (molecular weight unit)
DEAE	diethylaminoethyl
DMS	dimethyl sulphate
DNA	deoxyribonucleic acid
dpm	absolute (radioactive) disintegrations per minute
DTT	dithiothreitol
EDTA	ethylenediamine tetraacetic acid
EGTA	ethylene glycol-bis-(β aminoethyl ether) N,N' tetraacetic acid
[^{3}H]	tritium isotope
HEPES	4-(2-hydroxyethyl)-1-piperazineethanesulphonic acid
HMG	'high mobility' group of nuclear proteins
LiCl	lithium chloride
LMG	'low mobility' group of nuclear proteins

MMS	methyl methanesulphonate
MNNG	N-methyl-N'-nitro-N-nitrosoguanidine
NAD^+	nicotinamide adenine dinucleotide
NaOH	$sodium\ hydroxide_{aq}$
NH_4HCO_3	$ammonium\ bicarbonate_{aq}$
NMN	nicotinamide mononucleotide
NMNU	N-methyl-N-nitrosourea
[^{32}P]	^{32}Phosphorous isotope
PCA	perchloric acid
PEI	polyethyleneimine
PMSF	phenylmethylsulphonyl fluoride
pnp	bis(*p*-nitrophenol) phosphate
PPO	2,5-diphenyloxazole (primary fluor)
POPOP	1,4-di-[2-(5-phenyloxazoyl)]-benzene (secondary fluor)
PRAMP	2'(5''-phosphoribosyl)-5' AMP
Rf	distance sample moved from origin/ distance of solvent front from origin (in TLC).
RNA	ribonucleic acid
SDS	sodium dodecyl sulphate
sf	solvent front (in TLC)
TCA	trichloroacetic acid
TEMED	N,N,N',N'-tetramethylethylenediamine
TLC	thin-layer chromatography
Tpnp	thymidine 5'-monophosph0-*p*-nitrophenyl ester
uv	ultraviolet light

Introduction - (ADP-ribosyl)ation.

(I).

The coenzyme **nicotinamide adenine dinucleotide** (NAD^+) was discovered in the early 1930's and is now known to be the most abundant respiratory coenzyme in nature. Its structure is shown in figure I.1 below.

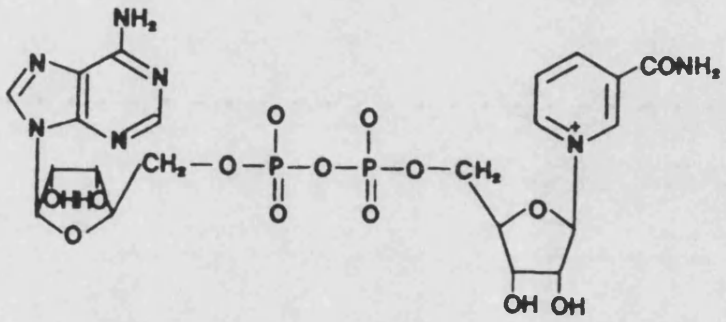

Apart from its major role as an electron carrier associated with oxidation and reduction pathways in aerobic and anaerobic respiration, NAD^+ possesses two "high energy" bonds. Nucleotide pyrophosphatase activity will cleave it into adenosine monophosphate (AMP) and nicotinamide mononucleotide (NMN), and in E.Coli it is the cleavage of this bond by DNA ligase which is coupled to the synthesis of phosphodiester bonds in DNA , rather than the pyrophosphate bond of ATP, which is utilised by eukaryotes (Zimmerman *et.al.*(1967)).

A β-N-glycosidic linkage between the nicotinamide and ADP-ribose moieties constitutes another "high energy" bond ($\simeq$-8.2 kcal.mol^{-1}.

(Zatman *et.al.*(1953))), cleavage of which provides the energy for all so-called **(ADP-ribosyl)ation** reactions.

In 1963 Chambon *et.al.* demonstrated that NMN greatly stimulated the incorporation of ATP (labelled in the adenosine moiety with ^{14}C) into an acid insoluble product from hen liver nuclei. This was later shown to be the homopolymer, **poly(ADP-ribose)** (Nishizuka (1967)). NAD-pyrophosphorylase catalyzed the production of [^{14}C]NAD^+ from the [^{14}C]ATP and NMN, which was then used as a substrate by the chromatin-associated enzyme poly(ADP-ribose) transferase (ADPRT), which covalently attached chains of ADP-ribose molecules to various nuclear proteins (Nishizuka *et.al.*(1968)). At the same time as the discovery of poly(ADP-ribosyl)ation, Honjo *et.al.*(1968) found that diptheria toxin acted as a **mono**(ADP-ribosyl) transferase in rat liver. In the presence of NAD^+, a single ADP-ribose molecule was attached to elongation factor 2 (EF-2). EF-2 is an amino acyl transferase and its mono(ADP-ribosyl)ation subsequently inhibited protein synthesis, causing the cell's death. Thus the study of poly- and mono- (ADP-ribosyl)ation as an important post translational modification of proteins was begun.

What is the biological function of (ADP-ribosyl)ation ? In HeLa cells, the half-life of a molecule of NAD^+ was estimated as one hour, 95 percent of the degradation taking place in the nucleus (Rechsteiner *et.al.*(1976)). The involvement of (ADP-ribosyl)ation in

DNA repair, differentiation, control of proliferation and the transformation of cells has been established. However, after twenty years of research around the world, the exact mechanism by which (ADP-ribosyl)ation acts in these processes has not yet been elucidated. Studies have concentrated on the effective quantitation of ADP-ribose, identification of acceptors for ADP-ribose in the cell, the effects of ADPRT inhibitors upon cellular processes, and the relationship between (ADP-ribosyl)ation and DNA damage. Recently a molecular biological approach to the field has been successful in that the gene for human ADPRT has been isolated (Alkhatib *et.al.*(1987)), which will provide current workers with a powerful tool for determining the function of (ADP-ribosyl)ation *in vivo*.

Mono- and poly((ADP-ribosyl)ation.

(ADP-ribosyl)ation is a group of post-translational modification reactions ubiquitous in all animal tissues investigated so far, as well as in plants and lower organisms. Terminally differentiated skin cells and normal, mature lymphocytes, as well as lacking other chromatin-associated activities, do not exhibit (ADP-ribosyl)ation (Ikai *et.al.*(1980,1981)), but this is unique among mammalian cells - for a list of reviews, see bibliography. Bacteria and archaebacteria also possess (ADP-ribosyl)ating enzymes, however these have extracellular functions. It can be compared to other types of modification such as methylation and phosphorylation in that it affects a variety of different processes and is probably multifunctional, since a bewildering array of acceptors have been identified to date. These are listed in reviews by Gaal & Pearson (1985) and Ueda & Hayaishi (1985). Of the two classes of (ADP-ribosyl)ation reactions, mono(ADP-ribosyl)ation is the simplest and best understood, involving the covalent attachment of a single ADP-ribose moiety (derived from NAD^+) to a specific amino acid residue, generally via an N-glycosidic bond (Ueda & Hayaishi (1985)). Nuclear and cytoplasmic mono(ADP-ribosyl) transferases (monoADPRTs) specific for this function have recently been identified in erythrocytes (Yost *et.al.*(1983), West *et.al.* (1986)), although the nuclear ADPRT

is capable of initiating poly(ADP-ribosyl)ation by attachment of the first ADP-ribose to the acceptor (Kawaichi *et.al.*(1980)).

Much of the early work took place on microbial toxins, with "target" acceptors in eukaryotic cells. These toxins were found to have mono(ADP-ribosyl)ating activity, and their action was lethal to the cell. Examples are Pertussis, Cholera and Diptheria toxins, whose activities and target acceptors have been well understood and characterised (Hayaishi & Ueda (1982), Ueda & Hayaishi (1985)). This aspect of mono(ADP-ribosyl)ation is not discussed further.

It has been established that the predominant class of (ADP-ribosyl)ation in normal mammalian cells is mono(ADP-ribosyl)ation (Bredehorst *et.al.*(1981),Hilz (1981)) residing mainly (but not exclusively - see Wielckens *et.al.*(1982)) in extranuclear compartments (Adamietz *et.al.*(1981)). For example, Adamietz *et.al.*(1981) found that 95 percent of mono(ADP-ribose)-protein conjugates detected in rat liver were located outside the nucleus. In other experiments, it was found that greater than 95 percent of poly(ADP-ribosyl)ating activity resides in the nucleus in a variety of cells (Hayaishi & Ueda (1982), Ikai *et.al.*(1980)). Poly(ADP-ribosyl)ation, involving the further attachment of ADP-ribose molecules (via ribose(1" → 2')ribose linkages) to a mono(ADP-ribose) residue, results in a chain of homopolymer, which may be over 65 residues in length (Tanaka *et.al.*(1978)). Further complication of the

structure has been shown to occur in the form of branching (Miwa *et.al.*(1979)), which involves ribose(1" → 2")ribose - (1" → 2')ribose linkages, probably occuring once every 30-50 ADP-ribose residues (Miwa *et.al.*(1981). Figure I.2. below shows this in diagrammatical form.

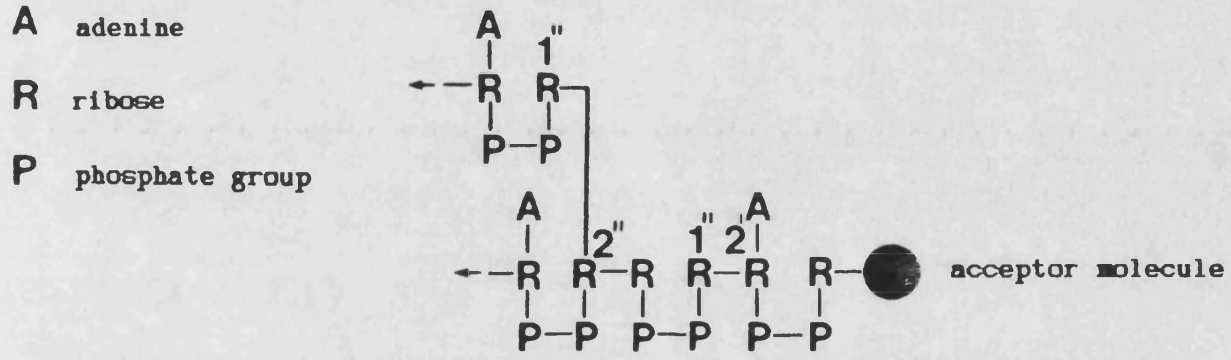

Other workers (Minaga *et.al.*(1983)) have proposed a probable helical structure in long-chain poly(ADP-ribose). As mentioned above, acceptors for poly(ADP-ribose) include histones, other nuclear proteins and the enzyme itself. It has recently been proved that the elongation of poly(ADP-ribose) chains attached to nuclear ADPRT itself proceeds from the ADP-ribose molecule proximal to the enzyme - that is, as each ADP-ribose moiety is added, it 'pushes' the previous one further away from the enzyme (Ikejima *et.al.*(1987)). This is discussed below.

Work by Hilz *et.al.*(1984,1981) supports the consideration of mono- and poly(ADP-ribosyl)ation as independant subclasses of protein modification with different functions. Although modification of an acceptor with a single ADP-ribose is a neccessary event before polymeric ADP-ribose is generated by successive addition of monomers, the discovery that eukaryotic cells possess cytoplasmic and nuclear monoADPRTs (of 32.7, 26 & 25.5 kDa molecular weight) (West *et.al.* (1986)), together with the purported difference in the types of bond between acceptor and mono- or poly(ADP-ribose) (Ueda & Hayaishi (1985)) would seem to suggest that mono(ADP-ribosyl)ation constitutes a type of modification which is separate from that of poly(ADP-ribosyl)ation. Further, Wielckens *et.al.*(1982) found a biphasic degradation of ADP-ribose-protein conjugates when ADPRT activity was stimulated, and then inhibited in Erlich ascites tumour (EAT) cells. Polymeric ADP-ribose degradation proceeded with a half life of < 1 minute, whereas in the degradation of monomeric ADP-ribose, it was ≈ 6 minutes. Bredehorst *et.al.*(1981) found different absolute levels of mono- and poly(ADP-ribose)-protein conjugates in EAT cells. The changes in these levels which were found to accompany differentiation were also different, thus it was proposed that mono(ADP-ribose)-proteins were not derived from degraded poly(ADP-ribosyl)ated proteins, but were autonomous in synthesis and function. It appears that there is some debate about the nature of mono- and poly(ADP-

ribose) - acceptor linkages, sensitivity/resistance to hydroxylamine (NH_2OH) not being the exclusive property of either type. Bredehorst *et.al.*(1979,1981) related the levels of NH_2OH-sensitive mono(ADP-ribosyl)-protein linkages with the rate of proliferation in normal and malignant liver cells, the highest levels being associated with the resting state. Furthermore the degree of terminal differentiation was related to levels of NH_2OH - resistant mono(ADP-ribose)-protein linkages - well differentiated hepatomas possessing elevated levels. To add to the confusion, Hilz *et.al.*(1984) observed *non enzymic* mono(ADP-ribosyl)ation when free monomeric ADP-ribose became attached by a NH_2OH - resistant bond to specific acceptor proteins, and the ribose groups of poly(ADP-ribose) may also take part in a Schiff's base reaction with proteins under certain conditions, forming an irreversible, resistant bond (Kun (1976)). ADP-ribose - protein linkages (often with histones) via glutamic acid and terminal lysine residues are alkali- and NH_2OH- sensitive (Riquelme *et.al.*(1979), Burzio *et.al.*(1979)). Typically, the linkage formed by NAD^+:arginine monoADPRTs are less labile, and differences in NH_2OH-sensitivity between poly(ADP-ribose)-amino acid linkages observed by some (Hilz (1981)) have been attributed to different ADPRTs initiating the chain (West *et.al.*(1986)).

Degradation of poly(ADP-ribose).

Below is a diagram (Fig.I.3) representing poly(ADP-ribose), attached to a protein, and showing the sites of action of phosphodiesterase, poly(ADP-ribose) glycohydrolase and ADP-ribosyl protein lyase.

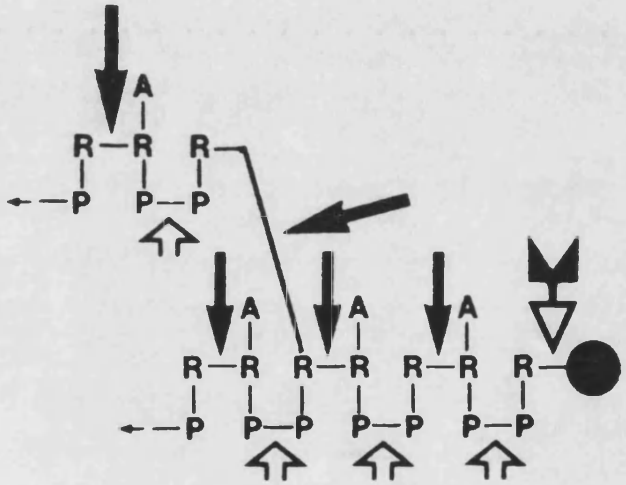


phosphodiesterase


poly(ADP-ribose) glycohydrolase


ADP-ribosyl protein lyase

Phosphodiesterases from rat liver, snake venoms such as Crotalus adamanteus, and tobacco cells are useful analytically, but are probably less important than the glycohydrolase physiologically, since they possess a high pH optimum (10) and a much higher Michaelis constant for poly(ADP-ribose) (Miwa *et.al.*(1982)). Digestion of free poly(ADP-ribose) by phosphodiesterases produces ribose-5'phosphate, 5'-AMP and the unique product 2'-(5-phospho-ß-D-ribosyl)adenosine 5'-phosphate ("PRAMP") which can be quantitatively analysed by thin layer chromatography to give an estimate of the average chain length by the formula: no.of ADP-ribose units = ([AMP] + [PRAMP])/[AMP] . However, "branched" or oligo-ADP-ribose will yield small amounts of "PR-AMP-PR" (using the same abbreviation) plus 5'-AMP, and this often results in miscalculations of chain length !

A recent purification of calf thymus poly(ADP-ribose) glycohydrolase to apparent homogeneity showed that it was monomeric, with a molecular weight of 59 000 (Hatekeyama *et.al.*(1986)). It was demonstrated that its action on poly(ADP-ribose) was exoglycosidic in the direction of the adenosine terminus → ribose terminus and that degradation of large poly(ADP-ribose) chains was biphasic and bimodal. The initial fast production of large polymers (of half the size) was processive, and was followed by a non-processive gradual and even degradation of these polymers at 1/20th the rate. The Michaelis constant for large poly(ADP-ribose) chains was ≈1/100th of

that for the small polymers. This may represent another explanation of the findings of Wielckens *et.al.*(1982) and Bredehorst *et.al.*(1981) who attributed the biphasic degradation of ADP-ribose-protein conjugates to the removal of mono- and poly(ADP-ribose) groups at different rates. Tanuma *et.al.*(1986) also identified two kinds of poly(ADP-ribose) glycohydrolase activities in HeLa s3 cells.

Poly(ADP-ribose) glycohydrolase cannot cleave the ester bond between the proximal ADP-ribose and the acceptor, and the enzyme which specifically does this is ADP-ribosyl protein lyase (Okayama *et.al.*(1978), Oka *et.al.*(1983)). Hardly affecting poly(ADP-ribose)-protein linkages, the enzyme recognises the whole ADP-ribose unit and releases a product similar to ADP-ribose which has been dehydrated, confirming that it works by lyase, rather than hydrolase activity. The molecular weight of this enzyme was estimated to be 83 000 by polyacrylamide gel electrophoresis (Oka *et.al.*(1983)).

Thus degradation of poly(ADP-ribose), attached to protein acceptors appears to be carried out by the combined action of poly(ADP-ribose) glycohydrolase and ADP-ribosyl protein lyase, the ADP-ribose monomer left behind by the former enzyme being liberated from the acceptor protein by the latter enzyme. The existence of this enzyme is further supported by the findings of Wielckens *et.al.*(1982), who showed that the rate limiting step in the turnover of poly(ADP-ribose) groups in EAT cells treated with triazaquonum was

the removal of the initial ADP-ribose monomer from acceptor proteins (Oka *et.al.*(1983).

In addition to the above degrading enzymes, recent work by Moss *et.al.*(1987) suggests that the specific NAD^+:arginine monoADPRT system in avian erythrocytes is reversible. A specific ADP-ribosyl-arginine hydrolase has been isolated and purified, and further work with 2'deoxy-NAD^+ (which acts as a substrate for mono(ADP-ribosyl)ation but prevents elongation) supports the suggestion that the regulation of mono(ADP-ribosyl)ation is independant of the poly(ADP-ribosyl)ating system (Alvarez-Gonzalez *et.al.*(1987)).

ADPRT.

ADPRT (sometimes called poly(ADP-ribose) synthetase or ADPRS) is ubiquitous among animal tissues, plants and lower eukaryotic organisms (Ueda *et.al.*(1982)). It is located in the internucleosomal regions of chromatin (Nishizuka *et.al.*(1967), Kanai *et.al.*(1981), Leduc *et.al.*(1986)) and possibly forms part of a group of cellular ADPRTs, at least in the avian erythrocytes discussed above (West *et.al.*(1986), Yost *et.al.*(1983)). Jongstra-Bilen *et.al.*(1981) found no variations in the molecular mass of the enzyme between various species and tissues, which was found by polyacrylamide gel electrophoresis to be 130 000. As pointed out by Gaal and Pearson (1985), this figure was overestimated, the true molecular weight being 112 000 when corrections were made. This agrees with other laboratories (Jump *et.al.*(1980), Holtlund *et.al.*(1981)) although more recent estimates, based upon the cloning and expression of its cDNA from human hepatoma cells, put the molecular weight of poly(ADP-ribose) transferase at 116 000 (Alkhatib *et.al.*(1987)). The activity of the enzyme is entirely dependent on binding to double stranded DNA and it is stimulated by DNA strand breaks, the most potent stimuli being flush-ended double strand breaks (Benjamin *et.al.*(1980)). The minimum length of DNA necessary for activity is ≈10 base pairs and although there is little specificity for the base sequence (Ueda

et.al.(1982)), DNA which co-purified with the enzyme was found to be many times more stimulatory than "ordinary DNA" by some workers (Yoshihara *et.al.*(1978)). A similar "active DNA" was found more recently in calf thymus by Ittel *et.al.*(1984). There is a plethora of published information about the purified enzyme, its requirements and inhibition which is reviewed in detail by Ueda *et.al.*(1982). Due to the presence of sulphhydryl bridges, a reducing agent such as dithiothreitol or β-mercapto ethanol is required for full enzyme activity (Okayama *et.al.*(1977)), although Zahradka *et.al.*(1984) found that this was not an absolute requirement under certain conditions. Kameshita *et.al.*(1984) have demonstrated that limited proteolysis with α-chymotrypsin, followed by papain, results in the cleavage of ADPRT into three fragments, whose molecular weights were 54 000, 46 000 and 22 000. The large fragment was shown to be solely responsible for binding of the substrate (NAD^+), the others being solely responsible for DNA-binding and ADP-ribose-binding respectively. When antibodies to each of these fragments were prepared, it was shown that HeLa cells synthesize the enzyme directly as a 120 000 Da polypeptide, with a half-life of 18½ hours in the cell (Kameshita *et.al.*(1987).

It is evident that the behaviour of ADPRT and its requirements for activity are extremely variable, particularly when highly

purified enzyme is used (Ueda *et.al.*(1982)). Thus, Tanaka *et.al.*(1981) distinguished two types of activity for the purified enzyme *in vitro* : a "Mg^{++}-dependent" reaction, in which auto-(ADP-ribosyl)ation of the enzyme itself occurs, and a "histone-dependent" reaction, in which histone H1 acts as the major acceptor for poly(ADP-ribose). However, the characteristics of these two reactions vary considerably when the relative proportions of DNA, NAD^+, Mg^{++}, histone and enzyme concentrations are altered (Yoshihara *et.al.*(1981), Shall *et.al.*(1972)). The automodification reaction does occur *in vivo* (Adamietz *et.al.*(1984), Zhang *et.al.*(1987)) as well as in permeabilised cells (Surowy *et.al.*(1983)), and in isolated nuclei (Jump *et.al.*(1980)). This is discussed further in section I.3.

Zahradka *et.al.*(1984) maintain that Zn^{++} is required by the enzyme for interaction or binding with DNA, and found the ion was present at approximately one mole per mole of purified ADPRT. The chelator 1,10 phenanthroline inhibited enzyme activity. They suggest that Zn^{++} may act in a catalytic fashion by interacting with an exposed nucleotide at a nick in the DNA, since DNA strand breaks are required for enzyme activity (Benjamin *et.al.*(1980)). Other workers found that radioactive Zn^{65} was associated only with the 'DNA-binding domain' of the enzyme (see above) which supports this hypothesis (Mazen *et.al.*(1987)), and in this respect, ADPRT may be no

different from many other enzymes, such as nucleotidyl transferases and RNA polymerases (Zahradka *et.al.*(1984), Coleman (1983)).

Inhibitors of the enzyme are mainly competitive analogues of its substrate, NAD^+ (for review, see Ueda *et.al.*(1982)). The benzamide derivatives, substituted at position 3 were found to be potent inhibitors (Purnell & Whish (1980a,b)) and are commonly used in experimental work. Although non-toxic to cultured cells (and even whole animals) at the levels required to inhibit (ADP-ribosyl)ation (Lunec *et.al.*(1984), Purnell & Whish (1980a,b)), 3 amino benzamide (3AB) is not a specific inhibitor of ADPRT. It has been shown to inhibit glucose oxidation (Milam *et.al.*(1984)) and purine synthesis (Borek *et.al.*(1984), Cleaver (1983)) in mammalian cells. Thus, the effects of 3AB, particularly those *in vivo*, must be interpreted according to this. A strange effect of 3 acetamido benzamide has been identified by Skidmore (1987). At μMolar levels, inhibition of (ADP-ribosyl)ation occured in permeabilised L1210 cells. However, at nMolar levels, an *increase* in (ADP-ribosy)lation activity was observed. The mechanism of this stimulation is not yet understood.

Another inhibitor relevant to this thesis is **p^1p^4-diadenosine tetraphosphate** (Ap4A) which was described as a "mixed" inhibitor (exhibiting both competitive and non-competitive kinetics) by Tanaka *et.al.*(1981). This is discussed in section II.

Regulation of (ADP-ribosyl)ation activity in cells could be mediated by stimulation (eg. by DNA strand breakage), or inhibition (eg. by nicotinamide, produced as a result of NAD^+-cleavage), the availability of acceptor molecules, and by two further mechanisms: regulation at the level of *expression* appears to be involved in the granulocytic differentiation of HL 60 cells (Suzuki *et.al.*(1987)) and in the cell cycle of HeLa cells (Alkhatib *et.al.*(1987)), as determined by measurement of the amount of mRNA for the ADPRT gene. This would add another 'tier' to the hierarchy of control, the effects taking place at a slower rate, and presumably having a longer duration compared to, say, the rapid and transient increase in (ADP-ribosyl)ation caused by DNA damaging agents (see I.2).

A further class of regulation appears to be the specific proteolysis ("processing") of the enzyme, investigated in permeabilised L1210 cells (Berger *et.al.*(1985), Surowy *et.al.*(1983a)). Ap4A, and various other phosphodiester-containing nucleotides caused processing of the auto(ADP-ribosyl)ated enzyme into smaller derivatives of molecular weight 96 000, 79 000 and 62 000 Da. (ADP-ribosyl)ated histone H1 was also processed. Interestingly, in human lymphocytes the mitogen phytohaemagglutinin causes the appearance of the 96 000 Da fragment, and DNA strand breakage by MNNG causes the appearance of the 62 000 Da fragment

(Surowy *et.al.*(1983b). The specific proteolysis of other DNA-associated enzymes is known to occur (Chang *et.al.*(1982)), and this probably represents a significant kind of post translational regulation of ADPRT activity.

As mentioned earlier, the process of (ADP-ribosyl)ation appears to account for the turnover of a major proportion of the NAD^+ in the nucleus of eukaryotic cells, and even for this reason alone it is therefore important to discover its function. The following sections do not attempt to comprehensively describe all of the published research to date; rather, they were intended to bring together some of the findings in particular areas of interest, focusing on DNA damage and its repair, DNA replication, and the differentiation and transformation of eukaryotic cells.

DNA damage and excision repair.

Study of the interactions between chemicals and DNA first began with the object of discovering harmful agents which would be incorporated into the DNA of organisms for use in warfare, and later, as a possible treatment for cancer. The hope was that interference with the normal synthesis of DNA in rapidly proliferating tumour cells would retard the cell population's onslaught preferrentially over the slower-replicating normal tissue cells (Friedberg (1985)). Alkylating agents are one such group of compounds which interact with DNA, being electrophilic with an affinity for the nucleophilic centres of macromolecules. Some are bifunctional, such as mitomycin C; others such as dimethyl sulphate (DMS) and streptozotocin (a glucose analogue of methylnitrosourea) attack only one base in the DNA molecule. The effect of the attack is to alter the structure of the base, by the attachment of a methyl- (or ethyl-) group in various places to produce a derivative which then interferes with replication, transcription and other DNA-mediated events in the cell (Friedberg (1985)). Normal cells respond to this damage, and that caused by ionizing radiation by the process of **excision repair**, utilizing various enzymes unique to eukaryotes. This involves incision and removal of a small area containing the defective base (producing a break in the DNA if one has not already occurred due to

the effects upon its configuration), followed by resynthesis of the removed section and its religation into the DNA chain. Major structural changes in chromatin would presumably occur, with at least some dissociation of the DNA strands from nucleosomal proteins and relaxation of superhelical conformation, allowing access by the enzymes concerned. These DNA repair enzymes unique to eukaryotes include DNA polymerase β and DNA ligase II which are not induced on cell proliferation (Kornberg (1980)), unlike DNA polymerase α and ligase I. They are not involved in normal, so-called **scheduled** DNA synthesis and replication, and are presumed to take part in the **unscheduled** synthesis of replacement fragments of DNA and their ligation back into the chain (Lindahl (1982)). Some of the (relatively rare) human diseases associated with the defective repair of damaged DNA are discussed in section I.2.5.

In 1956 the previously observed inhibition of glycolysis which acompanied treatment with alkylating agents was attributed by Roitt to be due to a decrease in cellular levels of NAD^+ , presumably affecting electron transport. Later, this reduction in NAD^+ was shown independently by Smulson *et.al.*(1975) and Whish *et.al.*(1975) to be due itself to the concommitant increase in synthesis of poly(ADPR). Whish *et.al.* showed that this action of streptozotocin was not due to interference with NAD^+ biosynthesis or NAD^+ degradation by NAD^+-glycohydrolase, and therefore that the synthesis of poly(ADP-ribose)

represented a unique and unusual response to DNA damage. The observation by others that the excretion of 1-methyl-nicotinamide also increases upon DNA damage with alkylating agents (Shaikh *et.al.*(1980)) supports this, since the free nicotinamide produced from NAD^+ by release of ADP-ribose would become methylated and excreted by the cell (Shall (1982)). Since then it has been demonstrated that the inhibition of (ADP-ribosyl)ation with nicotinamide analogues prevented the decrease in NAD^+ (Durkacz *et.al.*(1980), Jacobson *et.al.*(1980) and others), and that excision repair was also inhibited, measured as an accumulation of DNA strand breaks after DNA damage (Durkacz *et.al.*(1980), Farzaneh *et.al.*(1985),Greer *et.al.*(1984,1985)). Lunec *et.al.*(1984) found that although the inhibitor 3-acetamido-benzamide did not prevent the ultimate repair of strand breaks in murine lymphoma cells, as measured by the alkaline unwinding method developed by these workers, it did retard the rate of repair, implying that the rate limiting step is mediated by (ADP-ribosyl)ation. Thus it was proposed that (ADP-ribosyl)ation was <u>required</u> for excision repair of DNA in DMS - treated mouse L1210 cells (Creissen *et.al.*(1982),Shall (1982), Durkacz *et.al.*(1980)). Creissen *et.al.*(1982) demonstrated that the incision event and accompanying repair synthesis proceeded without the requirement for poly (ADP-ribose), and proposed that the ligation step was responsible for regulation of excision repair by poly (ADP-

ribosyl)ation. An increase in DNA ligase II activity was reported upon DNA damage in these cells which could be prevented by ADPRT inhibitors; further, they observed a comigration of [^{3}H]NAD$^+$-derived radioactivity with the partially purified enzyme on hydroxylapatite chromatography. This radioactivity increased similarly with enzyme activity upon DNA damage, suggesting its regulation by poly(ADP-ribosyl)ation. Farzaneh *et.al.*(1987) have recently demonstrated the requirement of (ADP-ribosyl)ation for the stable integration of transfected DNA into the genome in a variety of mammalian cells. In the presence of 3AB, ligation of the transfected genes did not occur, in spite of the fact that neither their uptake or expression was affected. This was contrasted by another group's findings (Yoshihara *et.al.*(1984)), who found that DNA ligase II activity was *inhibited* by (ADP-ribosyl)ation *in vitro*. Although little further evidence of regulation of DNA ligase II by <u>direct</u> (ADP-ribosyl)ation has emerged, the findings have been validated by others (eg.Ohashi *et.al.*(1983)) and another explanation has been suggested, in that poly(ADP-ribose) may activate the enzyme by loosening or relaxing the chromatin structure (perhaps by histone modification - discussed in I.3), allowing access to the DNA (Ohashi *et.al*(1983)). It has been suggested (Gaal & Pearson (1985)) that due to DNA ligase II's high affinity for poly(ADP-ribose), the ADPRT molecule which is present at the site of a break in the DNA may "direct" the ligase to the site by

means of (ADP-ribosyl)ation of itself (see earlier). This view of the effects of nuclear (ADP-ribosyl)ation - by means of "opening up" the tightly packed nucleosomal structure in order to gain access to the DNA - is becoming increasingly attractive, and offers at least one explanation for the ubiquitous involvement of ADPRT in nuclear events. As outlined earlier in this introduction, it should be born in mind that the effects of ADPRT inhibitors are not completely specific (Milam *et.al.*(1984)) and interpretation of its action in cells should currently proceed with caution.

Another possible target *in vivo* for poly(ADP-ribose) relating to the repair of DNA strand breaks is a Mg^{++}-sensitive endonuclease (Yoshihara *et.al.*(1974,1975), Tanigawa *et.al.*(1983),Nomura *et.al.*(1984) Tanaka *et.al.*(1984)). The endonuclease is activated and causes random DNA degradation upon exposure to DNA damaging agents (Tanaka *et.al.*(1984)) and appears to be inhibited by (ADP-ribosyl)ation, which suggests that, in order for the DNA repair machinery to operate, the enzyme must be blocked. This suggestion agrees with the findings of Greer *et.al.*(1984,1985,1986) who demonstrated that terminally differentiated T- and B- lymphocytes possessed both a high accumulation of DNA strand breaks and a very low ADPRT activity - high (or un-inhibited) endonuclease activity presumably being the result. Upon stimulation with a mitogen, an early event is the increase in NAD^+ levels, facilitating the (ADP-

ribosyl)ation and inhibition of the endonuclease. This would allow repair of the strand breaks and thus DNA replication and cell proliferation to occur. Greer *et.al.*(1986) suggested that the accumulation of strand breaks in these cells acted as a kind of "safety catch", preventing replication until (ADP-ribosyl)ation caused a temporary halt in DNA enzyme activities, allowing the breaks to be repaired. Presumably, the repair of the breaks would then de-activate the ADPRT (which is known to be dependant on breaks for activity (Benjamin *et.al.*(1980), Jacobson *et.al.*(1983)), allowing normal chromatin functions to proceed. As discussed in the next section, another hypothesis has been put forward proposing that an *active* endonuclease is required for DNA replication, initiating nicks in the DNA strand and so producing a DNA primer for replication (Koide (1982)). The possibility that the separate processes of scheduled and unscheduled DNA synthesis require different endonuclease activities (as well as ligase and polymerase activities) is apparent; mitogen stimulation can be compared to the effects of DNA damage in the sense that the cell's response to both involves the halt of chromatin functions whilst "operations" (such as repair of breaks, whether exogenously or endogenously induced) are carried out by the relevant enzymes. An ADPRT-mediated "emergency halt" was also suggested by Yoshihara *et.al.*(1984).

In opposition to the widely held assumption that regulation of DNA repair by (ADP-ribosyl)ation is mediated at the rate-limiting step of ligation or rejoining of newly synthesized repair patches into the "main strand" of DNA, Cleaver *et.al.*(1985) have proposed that observations made upon cells exposed to both ADPRT inhibitors and alkylating agents may have been misinterpreted. They have suggested that the rapid increase in frequency of single strand breaks occurring when cells which have been damaged by alkylation are exposed to 3AB (and the corresponding decrease upon removal of 3AB) is only measured as a *net* frequency. No distinction is made between an extended lifetime of the breaks caused by alkylation (due to slower repair) and the introduction of *new* breaks, caused by inhibition of the (ADP-ribosyl)ation of an endonuclease (thus activating it). They exposed human lymphoblast cells to MMS in the presence of [^{3}H]thymidine and aphidicolin - a reversible DNA polymerase α inhibitor. This resulted in an increase in the number of incomplete repair patches labelled with [^{3}H], which were found to be sensitive to digestion with exonuclease III (Cleaver *et.al.*(1985)). Upon removal of the aphidicolin, rapid religation of the repair patches was observed, but only the breaks labelled with [^{3}H]thymidine were detectable. Any new breaks would be 'invisible'. This religation occurred both in the presence and absence of 1mm 3AB (higher doses have been found to inhibit *de novo* purine synthesis in

HeLa cells (Cleaver *et.al.*(1983))). Moreover, an observed increase in repair replication caused by inhibition of ADPRT was not accompanied by an increase in patch repair size (as measured by isopicnic centrifugation of the DNA, repaired in the presence of bromo-deoxyuridine). It should be remembered, however, that repair of the MMS-induced strand breaks could be performed by *another* DNA polymerase (eg.β) which is not inhibited by aphidicolin, although the authors above claim that approximately 50 percent of alkylation-induced damage repair is mediated by DNA polymerase α . The two possible mechanisms explaining the (synergistic) potentiation of alkylation damage by ADPRT inhibitors - causing either inhibition of ligation or stimulation of endonuclease activity - result in increased cell killing, and both mechanisms remain viable until accurate experiments can be conducted *in vivo* in which the enzymes' activities can be observed simultaneously with (ADP-ribosyl)ation. Walker *et.al.*(1984), found that the repair synthesis of DNA following exposure of Human T98G cells to DMS was increased by the presence of 5mM 3AB, but that neither the repair patch size, nor the rate of removal of methylated products was affected. Repair synthesis was also increased by 3AB in the presence of hydroxyurea, an inhibitor of semiconservative DNA synthesis. They propose that the stimulatory effect of 3AB upon repair synthesis is due to its influence upon nucleotide pools, in agreement with Cleaver *et.al.*(1983).

DNA replication, Cell cycle & Proliferation

Among the first indications that NAD^+ might be involved in the regulation of the cell cycle was the finding that pre-incubation of isolated rat liver nuclei with 4mM NAD^+ prevented the incorporation of [^{3}H]TTP (thymidine tri-phosphate) into DNA (Burzio *et.al.*(1970)), thus implying that DNA synthesis was inhibited. A quiescent (or 'resting') cell in interphase is described as being in G_0 when no DNA replication and very little, if any RNA synthesis is occurring. When challenged by growth hormones and other growth factors a cell may be stimulated to emerge into the G_1 phase, in which it commits itself to the initiation of DNA synthesis. G_1 is succeeded by S phase, in which DNA synthesis actually takes place. This is followed by G_2, in which no synthesis occurs, but in which chromatin condensation and dispersal proceeds. After G_2, the cell enters prophase, in which the condensed chromosomes first become visible, followed by mitosis and division. The relative length of G_0, G_1, G_2 and S phases varies widely between different tissues, depending upon proliferative activity. Cell cultures may be 'blocked' at a particular stage in the cycle, either by specific inhibition of a certain enzyme activity (such as actinomycin D, which inhibits RNA polymerase by intercalation with double stranded DNA) or by nutrient deprivation. Cell cultures can be synchronised in the laboratory in this way,

allowing the quantitation of certain metabolites etc. throughout the cell cycle. A cell in G_1 can be induced to commit itself to DNA synthesis after treatment with mitogens, tumour promoting viruses and DNA damaging agents (Koide (1982)).

The involvement of (ADP-ribosyl)ation in the cell cycle was indicated, as stated above, when nuclei which had been pre-incubated with NAD^+ were found to have greatly decreased DNA synthesis (Burzio *et.al.*(1970)). ADPRT activity in the isolated nuclei of cells is found by many workers to be high in the G_1 and G_2 phases, and low in S phase (Porteous *et.al.*(1982), Pearson (1982), Farzaneh et.al. (1978), Kidwell (1975), Smulson et.al.(1971) and others).
This suggests that (ADP-ribosyl)ation is involved in the initiation and/or termination of DNA synthesis. Similar findings in synchronous permeabilised L1210 mouse lymphoma cells (Berger et.al.(1978)), concanavalin A (a mitogen) - stimulated lymphocytes (Lehmann et.al. (1974)) and hamster fibroblasts (Furneaux et.al. (1980)) all grown in culture support this hypothesis. However, it was found that great care had to be exercised in comparing findings using different tissues and extraction techniques, due to varying results. For example, NAD^+ -depletion due to anoxia (Ghani et.al. (1978)), and the presence of ADPRT-stimulating DNA strand breaks (Benjamin et.al.(1980)) which can arise due to extraction of nuclei, for

instance, both contribute significantly to the overall level of (ADP-ribosyl)ation in cells.

Burzio et.al.(1980) showed that the inhibitory effect of (ADP-ribosyl)ation on DNA synthesis was influenced by [Ca^{++}] in the medium, and this was related to the presence of a $Ca^{++}.Mg^{++}$-dependant endonuclease in the nucleus, which caused nicks in the DNA template (Koide *et.al.* (1976)). As discussed in the section on DNA breakage and its repair, this enzyme appears to be inhibited by (ADP-ribosyl)ation (Yoshihara et.al.(1975), Tanigawa *et.al.*(1983) and Nomura et.al.(1984)) although it was also shown to be **activated** by DNA damage (Tanaka et.al.(1984)). There appears to be some confusion over the role of the endonuclease in the cell (and even the effect of its (ADP-ribosyl)ation). The enzyme could be <u>activating</u> double stranded DNA as a template primer for DNA polymerase by introducing single strand nicks, allowing synthesis to commence (Koide (1982)). On the other hand, observations in mitogen stimulated T- and B-lymphocytes (Greer et.al.(1984,1985,1986)) suggest a different role for the endonuclease. The presence of high numbers of single stranded breaks in the DNA of quiescent lymphocytes is thought to be due to its action. In agreement with the hypothesis that (ADP-ribosyl)ation inhibits the endonuclease *in vivo*, ADPRT activity was found to be low in these cells, until stimulation with a mitogen (concanavalin A) caused the repair of these strand breaks, concommitant with a rise in

ADPRT activity. ADPRT inhibitors prevented this repair and also the entry into S phase, blocking early events in proliferation such as blast formation. Aphidicolin, an inhibitor of DNA polymerase α, also prevented the repair of the breaks, but did not prevent blast formation: there was no accumulation of strand breaks, as occurred with the ADPRT inhibitor. It was concluded that there was no continuous cycling of strand breaks (nicking and re-ligating), and that inhibitors of DNA repair caused their accumulation: it seemed that the accumulation of strand breaks caused by the ADPRT inhibitor was due to some indirect effect, possibly the inhibition of ADPRT resulting in a fully active $Ca^{++}.Mg^{++}$-dependant endonuclease, causing a halt in DNA replication and thus proliferation. Greer *et.al.*(1986) showed that repair of the breaks was necessary for DNA replication, but not blast formation. They suggest that mitogen stimulation causes the inhibition of the endonuclease via (ADP-ribosyl)ation, and that in the resting state, the strand breaks caused by the (active) endonuclease act as a "safety catch", preventing proliferation of the cell until the right stimulus is received. These conflicting approaches might be resolved by careful monitoring of the activity of the endonuclease during S phase *in vivo*. It should also be noted that although it is known that DNA polymerases α and β participate in scheduled and unscheduled DNA synthesis (Kornberg (1980)), it has not been demonstrated so far how

each of these synthesis pathways interact with the endonuclease. Indeed, it has been reported that cells possess both ADP-ribose-dependant and independant DNA repair pathways (Bohr et.al.(1981)).

Other suggestions have been made as to the possible effects of (ADP-ribosyl)ation upon DNA synthesis: the interaction of polymer chains directly with DNA polymerase α (Nagao et.al.(1972)), and modification of nuclear proteins affecting the binding of DNA polymerase α to DNA (Yoshihara et.al.(1973) could both affect 'scheduled' replication. Yoshihara *et.al.*(1987) have recently showed that the (ADP-ribosyl)ation of histone H1 with chains of up to ten ADP-ribose units does not affect the ability of histone H1 to stimulate DNA polymerase activity in an *in vitro* system using highly purified ADPRT and DNA polymerase α-primase complex from bovine thymus. Thus it was suggested that DNA polymerase α itself was poly (ADP-ribosyl)ated, which was also indicated in earlier experiments (Yoshihara *et.al.*(1985)).

It has been observed that the concentration of Ap4A increases in cells induced to undergo division and decreases upon quiescence (eg. Grummt (1978)). Ap4A has been shown to bind to a protein (possibly an acyl tRNA transferase) closely associated with DNA polymerase α (eg. Rapaport et.al.(1981)) and may affect DNA synthesis in this way. Yoshihara et.al.(1981) and others have shown that it can be (ADP-ribosyl)ated in the presence of histone H1 *in vitro*, and this leads

to the intriguing possibility that (ADP-ribosyl)ation plays its part in the regulation of DNA synthesis via the intermediary, Ap4A. Recently, it has been observed that when Ap4A was (ADP-ribosyl)ated by calf thymus ADPRT, the product suppressed the replication of SV 40 minichromosomes *in vitro*, whereas free poly(ADP-ribose) and Ap4A had no effect. This is discussed more fully in section II. Finally, the many observations of changes in chromatin structure caused by (ADP-ribosyl)ation (eg. Burzio et.al.(1980)) support the hypothesis that the regulation of DNA polymerase α activity and DNA synthesis (leading to cell division) is at least partly dependant upon access of the relevant enzymes to the DNA, and the general effect of (ADP-ribosyl)ation may be the regulation of chromatin structure, rather than the inhibition of DNA polymerase α directly.

Differentiation.

The involvement of (ADP-ribosyl)ation in cellular differentiation has been investigated and debated extensively since the early 1970s, and it is now generally agreed that levels of ADPRT activity are high during the onset of a cell's commitment to differentiation, and low at the final stages when the cell is said to be fully, or terminally differentiated.

However, the importance of assessing the effects of extraction upon (ADP-ribosyl)ation, and knowledge of exactly what stage a cell population under investigation is at, was found to be vital before any model could be suggested, and conflicting results are abundant, sometimes due to these complications!

Working with nuclei extracted from intestinal epithelial cells, Porteous *et.al.* (1982) found that cells undergoing mitosis and DNA synthesis possessed ADPRT activity which all but disappeared in the differentiated cells of the upper crypt and villus. Lehmann *et.al.*(1974) showed a similar drop in ADPRT activity as differentiation proceeded in mitogen-stimulated lymphocytes, as did Furneaux *et.al.*(1980) in hamster fibroblasts. Antigenic variation of surface glycoproteins in Trypanosoma brucei (determined by the expression of VSG genes) was repressed when the host rats were given ≈ 2mM 3AB (the ADPRT inhibitor) in an intraperitoneal infusion

(Cornelissen *et.al.*(1987)). Differentiation in mouse myelomonocytic leukaemia cells (Wu *et.al.*(1987)) and in the protozoan Leishmania mexicana (Williams *et.al.*(1987) was also found to be blocked by 3AB, but in both cases, proliferation was unaffected. Janßen *et.al.*(1987) however, have found that the inhibition of differentiation caused by 10mM 3AB in adipocytes was probably not due to the involvement of ADPRT, since lower levels of the inhibitor *stimulate* differentiation and benzoic acid, the non-inhibitory analogue, also had the same effects. Grey *et.al.*(1984) found changes in the activity of ADPRT in nuclei from pea seedlings during germination. A peak in activity was reached between 24 and 36 hours of germination, after which it declined to the levels observed in non-germinating seeds.

Cherney *et.al.*(1982) suggests a model for the involvement of ADPRT in differentiation which proposes that structural changes in chromatin observed during the onset of differentiation are responsible for the activation of ADPRT. Whether activation is due to this, or to DNA strand breaks spontaneously formed during chromatin rearrangement as suggested by Farzaneh *et.al.*(1980) and others, localized (ADP-ribosyl)ation of nuclear proteins would serve to alter chromatin structure, facilitating transcription of previously inaccessible genes.

The possible mechanism(s) of the action of (ADP-ribosyl)ation upon chromatin structure are discussed in section I.3 . Work on

bipotential granulo-monocytic precursor cells currently being undertaken will provide useful information as to the effects of (ADP-ribosyl)ation upon differentiation and *vice versa*. Kahn *et.al.*(1987) observed rapid changes in chromatin structure on stimulation of these cells with differentiation inducers. The cells differentiate into monocytes on exposure to phorbol esters (eg. 12-O-tetradecanoyl-phorbol-13-acetate or TPA) and Vitamin D, resulting mainly in DNA supercoiling, as measured by nucleoid sedimentation. G-CSA and retinoic acid, on the other hand, induce differentiation into granulocytes, accompanied by a relaxation in chromatin structure. These processes involve different patterns of DNA strand-breakage and rejoining, in which only the religation of pre-existing breaks was sensitive to 3 methoxy benzamide (another ADPRT inhibitor). Differentiation induced in human promyelocytic (HL 60) cells by TPA was found by others to be repressed by ADPRT inhibitors (Patel *et.al.*(1987)) along with re-ligation of strand breaks (Farzaneh *et.al.* (1987)). A different pattern of (ADP-ribosyl)ation was observed in liver cells, where it was found that levels of mono(ADP-ribose)-protein conjugates *increased* by 30-fold from neonatal to adult liver (Bredehorst *et.al.*(1981)). Changes in poly(ADP-ribose) and mono(ADP-ribose)-conjugates were independent, implying their separate derivation, and thus different functions. The same was true in hepatomas, in which ADP-ribose levels were higher in the

differentiated cells. Further subfractionation of the mono(ADP-ribose)-conjugates revealed that the quantity of NH_2OH - resistant (ADP-ribose)-protein linkages correlated with the degree of differentiation, as measured by certain metabolic parameters, including tyrosine aminotransferase activity and glycogen content. Hydroxylamine-sensitive linkages were tentatively correlated with the degree of proliferation. In fact, because normal liver cells and hepatomas have similar proliferation rates, the ratio of hydroxylamine-sensitive/resistant (ADP-ribose)-protein linkages was proposed as a screen, being much higher in undifferentiated hepatomas than adult liver.

Perhaps an important distinction to be made is whether (ADP-ribosyl)ation during differentiation is regulated by changes in the V_{max} of the enzyme due to inhibition, substrate and acceptor availability etc. or by **expressional** regulation via changes in the activity of the ADPRT gene. There is increasing evidence to suggest that the latter occurs, and that increases in (ADP-ribosyl)ation observed at the onset of differentiation and the decreases upon terminal differentiation are due to changes in the **amounts** of ADPRT present. The change in ADPRT activity observed by Jackowski *et.al.*(1987) in differentiating myocardial cells was not due to an increase in the V_{max} of the enzyme, or to a greater quantity of available acceptor molecules. In fact, they identified the major

acceptor as ADPRT itself, and upon extraction of ADPRT from the nuclei of neonatal and adult myocardial cells they found a nine-fold decrease in enzyme content as differentiation progressed. They proposed that this drop in ADPRT activity was therefore due to a decrease in the activity in the ADPRT gene. Similarly, Ben-Ishai *et.al.* (1987) showed that it was the amount of enzyme which changed during myogenesis in muscle cells, and Scovassi *et.al.*(1987) found that stimulation of human lymphocytes with the mitogen phytohaemagglutin caused an increase in ADPRT activity up to ten days after exposure, concommitant with the onset of DNA synthesis. Western blot analysis of ADPRT extracts showed that the increase in activity was due to the presence of a greater amount of the enzyme, implying that the stimulus for proliferation involved increased expression of the gene(s) for ADPRT. The cloning of the gene for ADPRT by Smulson and co-workers (Alkhatib *et.al.*(1987)) and others will probably emerge as the most powerful tool yet available in the study of (ADP-ribosyl)ation, and the techniques already exist whereby, for instance, an accurate quantitation of the enzyme throughout cellular processes *in vivo* is possible, as is the direct monitoring of gene replication.

Transformation.

The close association of ADP-ribose synthesis with chromatin suggests that it may play a part in the regulation of oncogenesis in neoplastic cells. High proliferation rates due to abnormal gene expression is characteristic in these cells, and elevated levels of ADPRT activity have been observed by many workers (for a review, see Hayaishi *et.al.*(1977)). DNA damage is a common effect of treatment with mutagens, alkylating agents or ionizing radiation, and it is the production of DNA strand breaks which may provide a link between ADPRT activity and oncogenesis, since ADPRT requires strand breaks for activity (Benjamin et.al.(1980)). It is important to note that neoplastic transformation may not occur solely as the result of the defective repair of DNA damage, but rather a defect in excision repair tends to increase the susceptibility of a cell to mutagenesis, following some form of DNA damage. Of course, defective DNA repair in a cell can simply increase the cytotoxic effects of damaging agents to such an extent that the cell dies, or that proliferation of the cell is prevented.

Examples of human genetic disorders which seem to be commonly linked by impaired ability to repair DNA damage are well known. Xeroderma pigmentosum (XP) is characterised by phenotypic abnormalities which include defective A P endonuclease activity (and

thus inability to remove pyrimidine dimers often occurring as a result of *uv* irradiation), increased suceptibility to mutagenesis and neoplastic transformation on treatment with mutagens (Friedberg (1985)). Cleaver et.al.(1978) found ADPRT activity in XP lymphocytes which was stimulated by treatment with the DNA damaging agent, MNNG, as were non-XP lymphocytes. However, *uv* irradiation stimulated ADPRT activity only in the control cells, the XP cells remaining unresponsive in this aspect, even though they showed a similar decrease in DNA synthesis after irradiation to that observed in the control cells. The inability to remove pyrimidine dimers caused by *uv* was shown to be due to a defective endonuclease (Cleaver et.al.(1978)) which normally has pyrimidine dimer DNA glycosylase activity (Friedberg (1985)). This fits in with observations that ADPRT requires strand breakage for activity (Benjamin et.al.(1980)), and that when lymphocytes from a 'classical' XP strain were exogenously supplied with "*uv* endonuclease" from M.luteus, *uv* irradiation was shown to stimulate ADPRT activity (Berger et.al.(1981)). Other disorders which have been related to defective DNA repair are Fanconi's anaemia (FA), Cockayne's syndrome (CS), Ataxia telangectasia (AT) and Bloom's syndrome (BS). Carried as autosomal recessive characters (Friedberg (1985)), all show increased susceptibility to neoplastic transformation, often with an increased risk of developing cancer in heterozygotic individuals (*ibid*). In

the case of AT, γ irradiation of lymphocytes not only failed to stimulate ADPRT activity, it also failed to induce the reduction in DNA synthesis observed in normal, irradiated cells (Edwards et.al.(1980)). It was suggested that this 'radiation-resistant' DNA synthesis was due to the absence of stimulated ADPRT activity upon DNA damage in AT cells , since it has been proposed that DNA synthesis is inhibited by (ADP-ribosyl)ation (Burzio et.al.(1970)). Berger et.al.(1982) suggest, however, that qualitative or quantitative differences in the chromosomal proteins of AT cells could affect the ability of DNA lesions to stimulate ADPRT activity, as well as affecting their ability to inhibit DNA synthesis. In FA cells, both MNNG and *uv* treatment was found to stimulate ADPRT levels (Berger et.al.(1982)), but the response was less marked than with normal cells. FA cells were found to have low levels of intracellular NAD^+, and their restricted response to DNA damage was attributed to this. The independant finding by Willis et.al.(1987) and Chan et.al.(1987) that Bloom's syndrome was associated with a deficiency in DNA ligase I conflicts with the idea that the activity of DNA ligase II, thought to be instrumental in DNA repair in eukaryotes (Kornberg (1980)), and sensitive to (ADP-ribosyl)ation (Creissen et.al.(1982)) is in some way impaired in this disease.

The effect of ADPRT inhibitors upon transformed cells is of great interest to medicine, particularly when combined with DNA

damaging treatments, because more effective treatments for cancer may result. The general hypothesis is that an inhibited or retarded DNA repair system would increase the harmful effects of mutagenic agents upon cells.

Whish *et.al.*(1975) observed stimulation of ADPRT activity by streptozotocin (see section I.2.2), which causes single strand breaks in DNA (Smulson *et.al.*(1977)). When NAD^+ was coinjected with the toxin, its oncogenic activity upon pancreatic β cells was prevented (Shinohara *et.al.*(1977)). Lunec *et.al.*(1984) found that after irradiation of murine lymphoma cells, exposure to the potent ADPRT inhibitor 3 acetamido-benzamide (3AAB) caused increased transposition and recombination of DNA, and retarded DNA repair rates which resulted in a marked enhancement of cell killing. The level of 3AAB used was non-toxic towards un-irradiated cells which suggests that "post irradiation sensitization" with ADPRT inhibitors may prove effective as an anti-tumour therapy.

It is commonly argued that 3AB reduces the efficiency of the repair of mutagen-induced DNA damage by inhibiting (ADP-ribosyl)ation, however, Ikejima *et.al.*(1984) isolated a mutant cell line (EM9) which displayed a very similar phenotype to wild type CHO (Chinese hamster ovary) cells which had been grown in the presence of 3AB, and which showed normal ADPRT activities. It was isolated on the basis of its sensitivity to EMS and a reduced rate of

DNA strand-rejoining after exposure to X-ray, EMS and MMS-induced damage as well as by its high baseline sister-chromatid-exchange rate. All these effects are induced in normal CHO cells by growth in medium containing 3AB. However, no differences were observed between wild type CHO and EM9 cells in : the initial rate and progress of (ADP-ribosyl)ation upon DNA damage with DNase 1; the distribution of ADP-ribose acceptors; the size of ADPRT or its fragments; the dependance on DNA strand breakage; the response of ADPRT to 3AB, the time course of degradation and their intracellular NAD^+ concentrations. Thus, it is possible to observe the effects of increased sensitivity to mutagens and X-rays in cells which are apparently normal in ADPRT activity. Further, 3AB could be having an effect via a pathway which is not ADPRT-mediated; it is, after all, a nicotinamide analogue and may interfere with some of the many NAD^+ reactions in cells, apart from its known effects upon the *de novo* synthesis and methylation of DNA precursors (Milam *et.al.* (1984)).

EMS and MMS (ethyl/methyl-methanesulphonate) have toxic and transforming effects upon BALB/3T3 cells as well (Lubet *et.al.*(1984)) and 3AB was found to enhance the toxic effects of EMS and MMS on these cells in a dose dependant manner. The toxic effects of 3-methylcholanthrene (3MCA), a polycyclic hydrocarbon, were not affected by 3AB, however. 3MCA is a relatively poor inducer of the strand breaks (Lubet *et.al.*(1984)) which activate the enzyme

(Benjamin *et.al.*(1983)). 3MCA, like MMS and EMS can induce morphological transformation in 3T3 cells, and again, the effect of 3AB was to enhance EMS/MMS - induced transformation with no effect on that induced by 3MCA, supporting the hypothesis that the action of 3AB is mediated by ADPRT.

3AB caused an increase in γ glutamyl transpeptidase-positive foci in rat liver after DNA damage by diethylnitrosamine (Konishi et.al.(1987)). The quantity of these "GGT-positive" foci are thought to correlate well with the potency of an oncogen, since they are capable of developing into hepatocellular carcinomas without further promotion. The workers suggest that 3AB maintains the damage caused by the carcinogen, producing the aberrant gene expression found in these foci. It was also found that 3AB increased the number and area of GGT-positive foci on exposure to dimethylhydrazine, but not NMNU or N-nitrosobis(2-hydroxypropyl)amine (Konishi et.al.(1987)) . There are many other examples which provide support for the hypothesis that ADPRT inhibitors may act as tumour "promoters" in that they synergistically potentiate the effects of mutagenic agents in cells (Bohr *et.al*(1981), Miwa *et.al.*(1981), Durkacz *et.al.*(1980)). As a treatment, the use of ADPRT inhibitors together with DNA damaging agents does not target transformed cells specifically, although their high proliferative activity does perhaps make them

more vulnerable than untransformed cells to retarded DNA repair rates, because of the sheer 'mobility' of their chromatin.

If there is a general relationship between (ADP-ribosyl)ation and transformation, it is that transformed cells generally possess high ADPRT activity (Ueda *et.al.*(1982b), Hayaishi *et.al.*(1977)). Inconsistent with this is the cytotoxic effect observed on neoplastic cells by Ueda *et.al.*(1982b), who found that exogenously added NAD^+ at 250 μM suppressed the growth of neoplastic cells, but rarely in normal cells, its effects being stronger than adenosine or nicotinamide and its analogues. Others found that mMolar NAD^+ inhibited the growth of EAT cells by 25 percent, and inspite of this, an increase in DNA synthesis (as measured by incorporation of labelled thymidine) over non NAD^+-treated controls was observed (Nolde *et.al.*(1972)). Why, as the substrate for ADPRT, NAD^+ should preferentially affect transformed cells in this way is not known. Of possible relevance is the discovery that intact hepatocytes can take up exogenously supplied NAD^+ in what was proposed as an endocytotic mechanism (Lötscher *et.al.*(1985)) although this has not been confirmed by other groups.

An exiting aspect of (ADP-ribosyl)ation and cancer is the possibility of using a "magic bullet" to selectively kill tumour cells, leaving normal tissue cells unharmed. Recently, the cloning of a cDNA for diptheria toxin (a bacterial mono(ADP-ribose) transferase

which kills cells by preventing protein synthesis) has led a laboratory to synthesize a "chimaeric" toxin which possesses the (ADP-ribosyl)ating fragment of diptheria toxin (fragment A) and amino acids 2 to 133 of interleukin 2 (IL2), by expression in E.coli.K12. This fusion protein ("IL2 toxin") was shown to be exclusively toxic to cells bearing high-affinity IL-2 receptors (Williams *et.al.*(1987).

Nucleosome structure.

If it were stretched out and unpacked, the total length of double stranded DNA in Human cells would be 1.74 metres (Rees *et.al.*(1984)); thus, considerable packaging is required to condense this amount of DNA into a nucleus! Metaphase chromatin has a 'beaded' structure, consisting of **nucleosome** particles, repeated along the length of the DNA. In these, the DNA is wrapped tightly around a central core of protein in a remarkably regular way. In about 1.8 superhelical turns, 145 base pairs are wound around a histone octamer with a diameter of only 11 nm (Travers & Krug (1987)). The compression and extension afflicted on the DNA by such curvature must be accommodated by narrowing and widening of both major and minor grooves on the inside and outside of the nucleosome respectively. The trinucleotides AAA and TTT are often found where the minor groove points inwards, as the trinucleotides GGG and CCC are found where it points away from the core. Since the curvature is regular, this means that these trinucleotides are found with a periodicity of 10 base pairs within the nucleosome (Travers & Krug (1987)). Further condensation of the structure is obviously required, since this nucleosome wrapping only reduces the overall length of the DNA by 5-6 times, and the nature of this is not yet fully understood.

(ADP-ribosyl)ation of histones.

The **histones** are a group of basic proteins (often rich in lysine and arginine) with molecular weights in the range of 13 500 to 21 000 (Panyim & Chalkley (1971)). A nucleosome histone octamer consists of 2 each of histone 2A, 2B, 3 and 4, each of these groups being heteromorphous. External positive charges on these proteins interact with the negative charges on DNA to facilitate the close association described above. The largest histone - H1, is thought to be associated not with the core histones, but with the DNA at the points of entry and exit of the nucleosome. There are three subtypes of histone H1 :- H1A, H1B and H1°, each possessing a central hydrophobic domain responsible for binding two turns of DNA (Allan *et.al.*(1980)). According to one model, the globular portion of histone H1 (with two chains of amino acids extending to the N- and C- termini) interacts with the DNA at entry and exit to the unit (Butt & Smulson (1982)). It has been suggested that histone H1 is further involved in the organization of chromatin by locking nucleosomes into a 'solenoid' nucleosomal fibre, possibly through H1-H1 interaction (Butt & Smulson (1982)).

The (ADP-ribosyl)ation of histones *in vivo* and *in vitro* has been observed by many groups, and there is controversey as to which are the important acceptors *in vivo*, since it has been widely observed

that the behaviour of nuclear poly(ADP-ribose) transferase is variable, depending on the nature of its environment with respect to nucleotide concentrations, the integrity of the DNA and of its higher order structure, and the 'availability' of acceptors for (ADP-ribose)$_n$ ($n \geq 1$). The controversey extends to the mechanism of action and even the *effects* of (ADP-ribosyl)ation of histones, and large amounts of data have accumulated supporting conflicting models. An extreme tendency of (ADP-ribosyl)ated proteins to aggregate, and the labile ADP-ribose - protein bond (Butt & Smulson (1982) creates further difficulties in the detailed analysis of acceptors in chromatin.

To date, only histone H1 (Adamietz & Rudolph (1984) and H2B (Kreimeyer *et.al.*(1984)) have been positively identified as major acceptors of ADP-ribose *in vivo*, both accepting ADP-ribose on glutamic acid residues at position 2. Histone H1 is futher (ADP-ribosyl)ated at positions 14, 116 and at the terminal lysine, position 213 (Burzio (1982)). This means that only the highly basic N- and C- terminal sections of histone H1 are modified. Experiments conducted *in vitro* confirmed this (Riquelme *et.al.* (1979)). Studies indicating that histone H2B is only mono-(ADP-ribosyl)ated *in vitro* (Burzio *et.al.* (1979), and that it was therefore perhaps subject to a specific mono-ADP-ribose transferase in the nucleus (as described by West *et.al.*(1986)) were not confirmed by studies *in vivo*

(Kreimeyer *et.al.* (1984)). In these studies, histone H1 was identified as only a minor acceptor in unstimulated hepatoma cells, stimulation by DNA damage causing a large increase in its (ADP-ribosyl)ation. However, still less than 2% of histone H1 molecules were modified under these conditions, the major acceptors being histone H2B/3, accepting both poly- and mono-ADP-ribose (*ibid*). In addition, (ADP-ribosyl)ation of several non-histone proteins with molecular masses in the range 100-116 000 and 170 000, and minor amounts of histone H4 were also observed *in vivo*.

Mild digestion of isolated nuclei with micrococcal nuclease generates **polynucleosomes**, which have been used for much of the current studies in nuclear (ADP-ribosyl)ation. Aubin *et.al.* (1982) found that maximal ADPRT acivity was associated with polynucleosomes of 3 to 4 units length, after which the activity declined and stabilised towards oligomeric periodicities of 11 to 16 nucleosomes. The hyper-(ADP-ribosyl)ation of histone H1 was also observed by this group at high NAD^+ concentrations. Using isolated rat pancreas polynucleosomes incubated with purified calf thymus ADPRT, Poirier *et.al.* (1982) performed a time course study which firmly related the relaxation of nucleosomal structure (as visualized by sedimentation velocity and electron microscopy) with the extent of histone H1 hyper-(ADP-ribosyl)ation at 200 μM NAD^+. In a further experiment, the activity of DNA polymerase α was observed to be highly stimulated on

(ADP-ribosyl)ation of polynucleosomes, suggesting increased accessibility of DNA for the enzyme (Niedergang *et.al.* (1985)). The same group confirmed these findings recently by demonstrating that this process was reversible (deMurcia *et.al.* (1986)). When partially purified bull testis poly(ADP-ribose) glycohydrolase was added to the relaxed, (ADP-ribosyl)ated polynucleosomes above, the hyper-(ADP-ribosyl)ated histone H1 disappeared, and native chromatin structure was restored.

Smulson and co-workers conducted similar studies with polynucleosomes isolated from HeLa cell nuclei (summarised by Butt & Smulson (1982)), with the difference that no exogenous ADPRT was added. Their conclusions were entirely different, however, in that they observed a *condensation* of nucleosomal structure, and proposed a model whereby (ADP-ribosyl)ation of histone H1 causes the formation of "H1-dimer", consisting of two histone H1 molecules linked by ≈ 15 ADP-ribose units. They suggested that the effect of this would be to shift priority from H1-DNA to H1-H1 interactions, and proposed that this might work to maintain the continuity of the DNA structure whilst repair or replication occurred.

This interpretation (that (ADP-ribosyl)ation causes the condensation of chromatin structure), was supported by melting studies, which showed the increased thermal stability of soluble chromatin after poly(ADP-ribosyl)ation (States & Janakidevi (1983)).

The formation of "H1-dimer" is controversial, however, and the group above recently claimed that, in fact, hyper-(ADP-ribosyl)ated H1 was actually being observed (deMurcia *et.al.* (1986)). Since poly(ADP-ribose) glycohydrolase digests the polymer exoglycosidically from the AMP terminus (Stone *et.al.* (1977)), it is unlikely that it would cause the disappearence of H1-dimer. Renz & Day (1976) showed earlier that the affinity of (ADP-ribosyl)ated histone H1 for DNA was less than that of the unmodified protein, and the contention that the hyper-(ADP-ribosyl)ation of histone H1 causes relaxation of chromatin is supported by recent experiments involving retention gels. Mathis *et.al.* (1987) found that the force required to separate the DNA from nucleosomal core-particles was reduced by about a half upon incubation with ADPRT. Sastry *et.al.* (1987) found a similar relaxation in SV40 minichromosomes. Thoma & Koller (1981) estimated that the removal of 10 percent of histone H1 from nucleosomes would relax the chromatin completely, and Niedergang and co-workers suggest that this might be achieved by hyper-(ADP-ribosyl)ation of only a small proportion of histone H1 molecules, ADP-ribose - mediated relaxation of chromatin forming an early step in the excision repair of DNA (deMurcia *et.al.* (1986)). Free poly(ADP-ribose) was shown to effectively compete with histone H4 for DNA binding at physiological salt concentrations, and also displaced pre-formed H4-DNA complexes

(Sauermann *et.al.* (1986)), which suggests that ADP-ribose may repulse basic proteins from DNA.

Poirier *et.al.* (1982) suggested the coexistence of areas of condensed chromatin within an overall relaxed structure, which may explain the discrepancies between these two main bodies of work.

An explanation of the differences observed in the major acceptors for poly(ADP-ribose) *in vivo* may lie in the findings of Huletsky *et.al.* (1985), which were that the concentration of NAD^+ was critical. Rat pancreas polynucleosomes showed poly(ADP-ribosyl)ation of histones H1, $H1^o$ (cf.States & Janekivedi (1983), Dam *et.al.* (1982)), H2A, A24A and H2B at 1μM NAD^+. However, at concentrations of NAD^+ greater than 10 μM, histone H1 was preferrentially hyper-(ADP-ribosyl)ated. They further observed the hyper-(ADP-ribosyl)ated form of histone H2B at these higher concentrations of NAD^+, suggesting that histone H2B may be modified in the same way as histone H1.

Non-histone nuclear proteins, such as scaffold "lamins" as well as non-structural enzymes associated with DNA also serve as acceptors for $(ADP\text{-}ribose)_n$, and models for the action of poly(ADP-ribosyl)ation in the nucleus which involve these are described below.

Nuclear (ADP-ribosyl)ation of non-histone proteins.

Dam *et.al.* (1982) showed (ADP-ribosyl)ation of HMG proteins in pancreas nuclei, heavily on HMG 14 and 17 and in equal proportions on histone H1 and HMG 1. When permeabilsed cells were used, the pattern of (ADP-ribosyl)ation was different, extensive modification of H2A, H2B and HMG proteins resulting. Burzio (1982) observed similar modification in isolated nuclei. Tanuma *et.al.* (1985) showed the *in vivo* (ADP-ribosyl)ation of HMG proteins as well as histone H1 in mouse mammary tumour cells. When these were treated with the DNA damaging agent MNNG a rapid increase in (ADP-ribosyl)ation of HMG 1,2 and histone H1 was observed, with no changes in the modification of HMG 14 & 17. Further, 3AB inhibited this increase in (ADP-ribosyl)ation, without affecting HMG 14 & 17 again. The authors suggested that (ADP-ribosyl)ation of histone H1 and HMG proteins was involved in the recovery from DNA damage caused by MNNG, and that (ADP-ribosyl)ation of HMG 14 & 17 serves a different purpose. In bull testis nuclei, Mennella *et.al.* (1984) demonstrated that LMG proteins were (ADP-ribosyl)ated preferrentially, with lesser modification of HMG proteins. Both LMG and HMG proteins are thought to be involved in the structural organisation of chromatin, their presence being particularly associated with transcriptionally active chromatin (Weisbrod & Weintraub (1979)) and their (ADP-ribosyl)ation *in vivo*

may affect the process of transcription. Although the direct (ADP-ribosyl)ation of RNA polymerase 1 was inhibited by 4mM NAD^+ in permeabilised cells, Walker & Pearson (1981) showed that this was not prevented by 3AB and not due to its (ADP-ribosyl)ation. Jacob *et.al.* (1987), however, found that the presence of ADPRT was necessary for accurate transcription in an unfractionated nuclear extract from rat hepatoma cells, its absence resulting in the production of random transcripts. The role (if any) of (ADP-ribosyl)ation in transcription is therefore uncertain.

The (ADP-ribosyl)ation of non-histone proteins in the HeLa cell cycle has been reported (Song & Adolph (1983), Adolph (1987), Adolph & Song (1985a,b)). When 'nuclear scaffolds' were isolated from mitotic HeLa cells and nuclei incubated with [^{32}P] NAD^+, autoradiographs of two-dimensional polyacrylamide gels revealed that the main acceptor was ADPRT itself and the lamins, structural components of the nuclear envelope lamina (Song & Adolph (1983)). The previously reported general increase in (ADP-ribosyl)ation during mitosis (Tanuma & Kanai (1982)) was attributed entirely to the auto-(ADP-ribosyl)ation of the enzyme. The function of this auto-modification is not understood, although it is possible that it 'releases' the ADPRT from DNA, since its affinity for DNA decreases upon auto-modification (reviewed by Ueda *et.al.* (1982)).

Other acceptors for (ADP-ribose)$_n$ in the nucleus include various enzymes whose activities are associated with DNA. The (ADP-ribosyl)ation of DNA ligase II (Creissen & Shall (1983), Yoshihara *et.al.* (1984)) and of a Ca^{++}/Mg^{++}-dependent endonuclease is discussed in section I.2. The base-labile (ADP-ribosyl)ation of DNA topoisomerase I was demonstrated *in vitro* by Ferro *et.al.*(1983), and in a continuation of this work, Pearson & Gaal (1987) found that the enzyme appeared to be inhibited in undamaged HeLa cells. When HeLa cells were damaged *in vivo* with the alkylating agent DMS (known to stimulate (ADP-ribosyl)ation (Thi Man & Shall (1982))) , the extracted topoisomerase was active, implying that either (ADP-ribosyl)ation *stimulated* the topoisomerase, or that it was less (ADP-ribosyl)ated under conditions of DNA damage. In *in vitro* (ADP-ribosyl)ation systems terminal deoxynucleotidyl transferase (Tanaka *et.al.*(1986)) and DNA polymerases α and β (Yoshihara *et.al.*(1985)) were all shown to be inhibited by modification. However, the finding that an enzyme *can* be (ADP-ribosyl)ated does not provide the information that it *is* modified *in vivo*, although it seems quite possible that (ADP-ribosyl)ation has multiple functions within eukaryotic cells, perhaps in a similar way to phosphorylation. The modification of other enzymes by (ADP-ribosyl)ation is extensively reviewed by Gaal & Pearson (1985) and Ueda & Hayaishi (1985).

Low molecular weight acceptors.

As mentioned earlier, Yoshihara and Tanaka (1981) discovered that the di-nucleotide Ap4A unusually served as an acceptor for poly(ADP-ribose) when incubated with purified ADPRT in the presence of histone H1. That such a small molecule (M_r: 836) served as an acceptor is made even more interesting by the fact that in addition to ADP-ribose it, too, has been implicated as having a role in the regulation of DNA synthesis in eukaryotic cells (Rapaport *et.al.*(1981)). Does this modification play a part in this *in vivo* ? Part II of this introduction deals with the proposed significance of Ap4A in DNA-associated activities and its relationship (if any exists) with (ADP-ribosyl)ation.

Ap4A

The mitogenic stimulation of resting mammalian cells (for instance by extra cellular growth factors) is characterised by progression through the G_1 phase of the cell cycle and the initiation of DNA synthesis at the G_1/S phase boundary. This ultimately leads to chromosome replication and mitosis. Although the complex chain of metabolic events succeeding this primary mitogenic stimulus are unknown, it is generally accepted that they are regulated by cytoplasmic components, acting as 'positive regulatory signals' which induce DNA replication (Grummt *et.al.*(1978) and references therein). An analogy might be the role of cyclic AMP as a "second messenger" in hormonal action upon eukaryotic cells. Grummt *et.al.*(1978) showed that purine nucleotides play an important role in the regulation of metabolic processes, demonstrating that pool sizes of ATP were tightly correlated with the proliferative growth state of various cell lines. However, although a certain level of ATP was required for proliferation, an increase in ATP concentration alone was not sufficient to trigger DNA replication.

A favourite candidate for the role of a 'signal nucleotide' is Ap4A which was discovered in mammalian cells by Rapaport *et.al.*(1976). They suggested that it was a possible 'pleiotypic

activator' on the basis of observations of a correlation in the intracellular concentration of Ap4A and the proliferative state of the cell, rapidly growing cells having much larger pool sizes than resting or slowly growing cells. This unusual molecule (see fig.II.1 below) was discovered by Zamecnik *et.al.*(1966) as the product in a back- reaction of lysyl-tRNA synthetase - one of the enzymes involved in the activation of amino acids prior to protein synthesis (see below for reaction scheme).

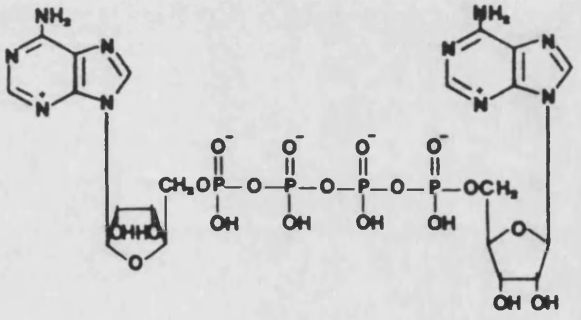

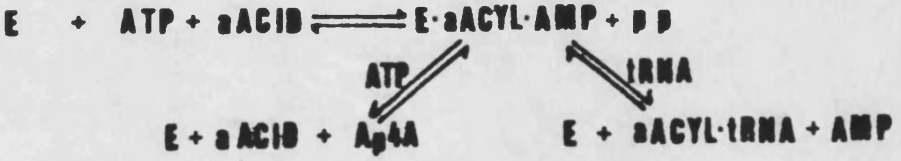

E -aminoacyl tRNA transferase
aACID -amino acid

Figure II.1. The structure of Ap4A (top) and its production by lysyl-tRNA synthetase (after Zamecnik *et.al.*(1966).

A *specific* 'Ap4A synthetase' has not been found in mammalian cells, although Vallejo *et.al.*(1976) demonstrated Ap4A-ase activities in Artemia salina and rat liver. This phosphorylase activity was not specific for diadenosine tetraphosphate, and split all purine and pyrimidine dinucleoside tetraphosphates into NTppp and pN'. In E.Coli., a phenylanalyl tRNA synthetase was found to possess both Ap4A synthesizing and splitting activities, cleavage taking place by hydrolysis of the central phosphodiester bond, giving ADP as the product (Plateau *et.al.*(1981)). As mentioned later, the role of Ap4A in prokaryotes and eukaryotes is probably different, and this Ap4A-ase activity is not observed elsewhere. Recently, the enzyme responsible for cleavage of Ap4A to ATP and AMP in yeast (Guranowski *et.al.*(1985)) was found to be capable of synthesizing Ap4A in a reverse reaction *in vitro* (Brevet *et.al.*(1987)). At pH 7.0, in the presence of a divalent cation such as Ca^{++}, the V_{max} for this was 7.4 s^{-1} (37°C) which makes this enzyme a more likely candidate for Ap4A synthesis *in vivo* than the yeast amino-acyl tRNA synthetases ($V_{max} \simeq$ 3 s^{-1}). Snake venom phosphodiesterase (such as that from C.adamanteus) will also cleave Ap4A into ATP and AMP; however, commercial preparations contain a high proportion of contaminating non-specific phosphatase (exonucleolytic) and 5' nucleosidase (endonucleolytic) activities (Oka *et.al.*(1978)), and any ATP produced will immediately become a substrate for these enzymes unless the

phosphodiesterase is purified. This is relevent because a major procedure used to quantify Ap4A in cells involves the 'removal' of ATP from a nucleotide extract by alkaline phosphatase digestion (to which Ap4A is resistant) followed by digestion with phosphodiesterase, and subsequent quantitation of the ATP produced using the luciferin/luciferase bioluminescence system (eg. Weinmann-Dorsch *et.al.*(1985)).

It is still a matter for speculation whether the regulation of Ap4A pools in cells is controlled at the levels of synthesis, degradation or a combination of the two. Zinc appears to play a major role in this regulation and this is discussed below.

Cell growth

Weinmann-Dorsch *et.al.*(1984b) assayed a large number of widely differing cell types for intracellular Ap4A concentration and found that it varied from 0.01μM to 13μM, depending on the proliferation, transformation, differentiation and cell cycle state of the cells under investigation. When BHK and Swiss 3T3 mouse fibroblasts were released from a block in G_1 (caused by colcemid or serum-deprivation), Ap4A levels increased up to 1000 fold during G_1 to reach 10μM at the beginning of S phase. This increase approaching S phase was less dramatic in cells lacking a defined G_1 phase, such as Physarum polycephalum, although a rapid 8-30 fold increase in Ap4A was found at entry into S phase which is completely prevented by cyclohexamide (a protein synthesis inhibitor) (Weinmann-Dorsch *et.al.*(1984a)). They suggested that inhibition of the synthesis of short-lived proteins required for DNA replication was the reason for the effect of cyclohexamide. Rapaport and Zamecnik (1976) also found a large decrease in Ap4A levels (relative to ATP levels, which were reduced by much less) upon inhibition of protein synthesis. An even larger drop was observed when DNA synthesis was inhibited by hydroxyurea. They too suggested an inverse relationship between the doubling time of cells and Ap4A levels, fast-growing cell lines having up to 200 times the amounts found in slow-growing cells.

The highest levels of Ap4A observed in cells so far were in the sperm of the sea urchin (Psammechinus miliaris) - 28μM compared to 0.2μM in the unfertilized eggs (Weinmann-Dorsch & Grummt (1985)). Upon fertilization of the eggs, Ap4A levels quickly increased, apparently as a result of *de novo* synthesis. Further, microinjection of Ap4A into unfertilized eggs caused an increase in DNA synthesis compared to mock-injected controls. That increases in Ap4A levels can actually *cause* increased DNA synthesis was observed when Ap4A was added to permeabilised, G_1 arrested BHK cells. The incorporation of [^{3}H]dTTP and the number of 'replication eyes' formed in the DNA molecules from these cells increased in a dose dependent manner (Grummt (1978)).

Recently, Plateau *et.al.*(1987) have failed to observe changes in the level of Ap4A in the E.coli cell cycle, which remained constant at 2.42μM in a synchronized culture. The authors doubt whether Ap4A is instrumental in the process of DNA replication in prokaryotes. Lee *et.al.*(1983) found that stresses such as oxidising agents and heat shock resulted in elevated levels of Ap4A in Salmonella typhimurum , and suggested that Ap4A acted as an "alarmone" for the bacterium. It was also suggested by Varshavsky (1983) that Ap4A may act in this way in response to a halt in replication forks occurring sometimes as a result of such stresses.

In opposition to the indications above that Ap4A is associated with the regulation of eukaryotic cell growth, Segal and Le Pecq (1986) could find no variation in the Ap4A pools in NIH 3T3 cells in which growth had been arrested by serum depletion, or when they were subjected to oxidising agents and other stresses. They did, however, observe a 10 fold increase in Ap4A levels when the cells grown in a monolayer reached confluence, and suggest that Ap4A is associated with cell contact inhibition rather than with growth stimulation.

As found when monitoring ADP-ribosylation activity, the exact culture conditions and proliferation states of the cells have a profound effect upon the results observed, and in the case of Ap4A, the establishment of a specific assay (rather than a general one for all dinucleoside tetraphosphates) was also shown to be important when monitoring changes in the intracellular pool size (see Grummt (1983)). The conflicting conclusions based on the observations above have yet to be resolved, but a large amount of evidence has now built up suggesting that Ap4A is associated in some way with the regulation of growth in eukaryotic cells.

Zinc appears to play an important role in the regulation of Ap4A synthesis and degradation. L-phenylalanine tRNA synthetase will produce Ap4A *in vitro* from ATP in a reaction which is entirely dependent upon the addition of Zn^{++} (Plateau *et.al.*(1981)). Grummt (1978) showed that EDTA (which sequesters Zn^{++}) prevents the

stimulation of DNA synthesis caused by Ap4A in permeabilised BHK cells. In later experiments it was demonstrated that Zn^{++} caused a dose dependent increase in Ap4A synthesis, whilst inhibiting Ap4A hydrolysis in the same system (Grummt *et.al.*(1986)). It was also shown that Zn^{++} uptake increased in intact, G_1-arrested BHK cells when they were exposed to mitogenic treatment (*ibid*).

A Possible model for action

The argument that Ap4A is in some way involved with the initiation of DNA synthesis is strongly supported by observations that the dinucleotide interacts with the DNA replication machinery itself. Rapaport *et.al.*(1981b) purified from HeLa cells the enzyme most widely believed to be responsible for DNA synthesis in eukaryotes - DNA polymerase α - as a multi-protein aggregate of high (640 000) molecular weight, or 'holoenzyme'. In this form, it was shown to catalize DNA synthesis with a variety of oligoribo- and oligodeoxyribo adenylates acting as primers with poly(dT) as a template. They found that when Ap4A (at 15μM) was included in the reaction mixture, it too could be utilized as a primer, and observed that it became covalently attached to the 5' end of the poly(A) product. Ap4A was also found to prime DNA synthesis by HeLa DNA polymerase α from a double-stranded synthetic DNA polymer template by Zamecnik *et.al.*(1982). Grummt *et.al.*(1984)) demonstrated similar priming by Ap4A with the purified high-molecular weight form of calf thymus DNA polymerase α, using circular single-stranded M13 phage DNA as a template, as did Zourgi *et.al.*(1986) with the enzyme from Xenopus laevis oocytes using poly(dT) as a template. A recent study has investigated the effect of Ap4A on the effective length and hard core radius of DNA - both indicators of higher order stucture

(Westkaemper & Richard (1987)). At a constant (low) salt concentration, binding of Ap4A caused only a very slight increase in the effective length of DNA, (from 10^{-10} to 10^{-4} M Ap4A) with a similar, very small effect on the core radius. This suggests that Ap4A's stimulating effect upon DNA synthesis is not due to modification of the biological activity of the DNA template itself, but occurs for some other reason(s).

Both HeLa (Rapaport *et.al.*(1981a,b)) and calf thymus (Grummt *et.al.*(1979)) purified DNA polymerase α holoenzymes were found to have highly specific Ap4A-binding activities. Using [^{3}H]Ap4A, it was shown that a protein subunit of molecular weight 57 000 Da was responsible for this binding to the calf thymus enzyme (Grummt *et.al.*(1979)). A similar Ap4A-binding subunit (molecular weight 47 000 Da) was isolated from the HeLa cell enzyme by Baril *et.al.*(1983). The Ap4A-binding protein isolated from calf thymus DNA polymerase α by Rapaport and Feldman (1984) showed great substrate specificity and high affinity for Ap4A (dissociation constant: 13μM). They found most of the protein in a 'free' form, which possessed strong Ap4A-cleaving activity (giving ATP and AMP). Some of the Ap4A-binding protein was found to be non-covalently attached to DNA polymerase α, and in this form it did not possess any Ap4A-cleaving activity. 50-100μM Zn^{++} was found to completely inhibit the cleaving activity, but had no effect on the binding activity of the free protein. Rapaport *et.al.*(1981a)

found that both high (660 000) and low (145 000) molecular weight forms of DNA polymerase α isolated from HeLa cells were associated with several aminoacyl-tRNA synthetase activities. Further purification on hexylagarose and gel filtration media left only the tryptophanyl-tRNA synthetase activity, which also exhibited Ap4A-binding activity, even in the presence of excess ATP or Ap2A, and was enhanced by the presence of L-tryptophan. This suggests a link between DNA replication and the initiation of protein synthesis in mammalian cells. On the basis of these and other experiments it is possible to hypothesize a model for the action of Ap4A in the regulation of DNA synthesis. It has been observed that at the G_1 phase of the cell cycle, the DNA polymerase α complex exists mainly in an un-aggregated form in the cytoplasm (Reddy & Pardoe (1980)) and that during the entry into S phase, the aggregated form predominates (*ibid*). The absence of Ap4A-cleaving activity in the latter form means that it represents a DNA-synthesizing holenzyme which is sensitive to stimulation by Ap4A.

An example of a putative model for the events succeeding mitogenic stimulation was proposed by Grummt *et.al.*(1986)) and this is represented below in Figure II.2 . It proposes that the initial mitogenic stimulus ("extracellular growth factor") is internalized, together with Zn^{++} ions by an endocytotic process. This leads to an increase in the intracellular zinc concentration which stimulates the

synthesis, and inhibits the degradation of Ap4A. The resulting large expansion of the Ap4A pool causes stimulation of DNA polymerase α activity which can lead to replication and cell division. Although tentative, this model is very reminiscent of those for hormone action in vertebrate cells.

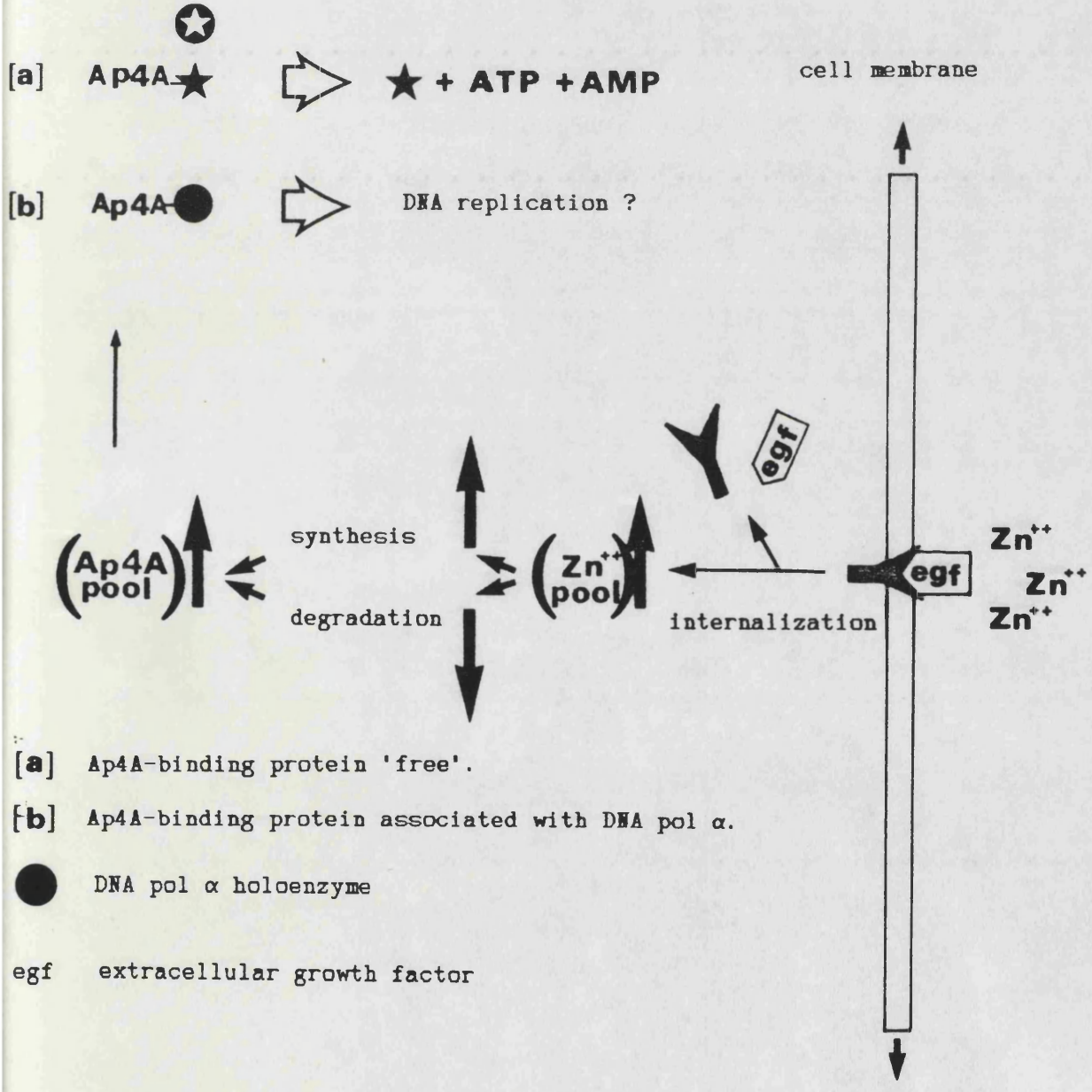

Figure II.2.
Ap4A as a 'third messenger' -a tentative model (after Grummt *et.al.*(1986).

Ap4A : (ADP-ribosyl)ation

Tanaka *et.al.*(1981a) identified two classes of reaction for calf thymus ADPRT *in vitro*: an automodification reaction dependant on the presence of Mg^{++} ions, and the (ADP-ribosyl)ation of histone H1 which is favoured at high histone:DNA ratios. "Active" DNA (which co-purifies with the enzyme at an early stage of extraction (see Hashida *et.al.*(1979)) was used to satisfy ADPRT's requirements for activity and strand breaks in this preparation may have had stimulatory effects. In a search for new inhibitors of the enzyme they discovered that although only weakly effecting the 'Mg^{++}-dependant' reaction, Ap4A was a potent inhibitor of the 'histone-dependant' reaction. A double-reciprocal plot of 1/velocity versus $1/NAD^+$ concentration showed different V_{max} and K_m values at 0, 10 and 30μM Ap4A and it was concluded that Ap4A was an inhibitor of 'mixed type', with a K_i of 5.1μM.

In an investigation of the molecular basis of these findings, it was discovered subsequently that the reason for this apparent inhibition was that Ap4A was serving as a better acceptor for poly(ADP-ribose) than histone H1 under the reaction conditions employed (Yoshihara *et.al.*(1981)). Under conditions of equal proportions of histone H1 and 'active' DNA, and 100μM [^{3}H]NAD^+ the

incorporation of [^{3}H]ADP-ribose into TCA-insoluble products fell from 57 to 7 percent of the added NAD^+ in the presence of 500μM Ap4A. 30 percent of the added NAD^+ was converted into a new product, which was shown by anion-exchange chromatography on DEAE cellulose at pH8.3 to be mono- and oligo-(ADP-ribosyl)ated Ap4A. At 250μM Ap4A and 20μM NAD^+, this figure increased to 90 percent of the NAD^+ added. Using [^{3}H]Ap4A and [^{14}C]NAD^+, digestion of the isolated mono(ADP-ribosyl)ated Ap4A product with snake venom phosphodiesterase yielded phosphoribosyl-[^{3}H]AMP and [^{3}H]AMP, indicating that the linkage between Ap4A and ADP-ribose is via a ribose-ribose (probably a α(1"→2')) bond. This is shown in Fig.II.3 below.

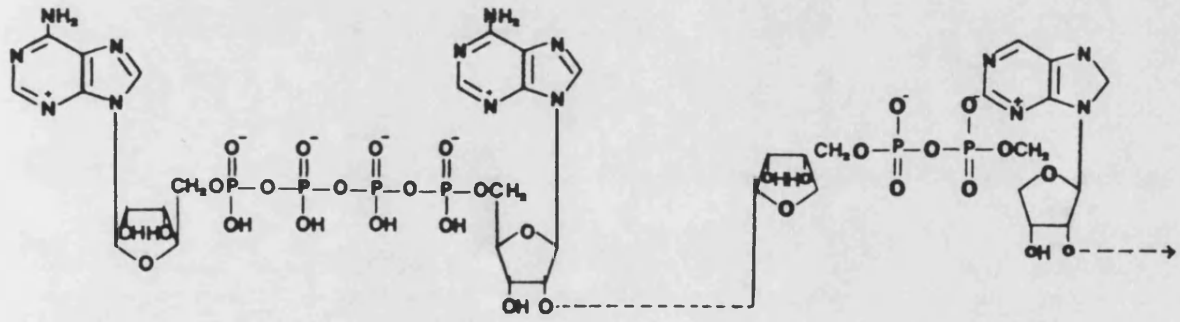

(after Yoshihara and Tanaka (1981)).

Ommission of the histone H1 from the reaction mixture completely inhibited the formation of this product, and it was later shown that all five classes of calf thymus histones could replace histone H1 with similar effects (Tanaka *et.al.*(1981b)). Poly (L-lysine) - a basic polypeptide, allowed the reaction to proceed, but not BSA. Pulse-chase experiments showed that the ADP-ribose in the product was

not derived from histone-bound ADP-ribose, and dialysis experiments indicated that Ap4A was binding non-covalently to histone H1, where it became an acceptor for (ADP-ribose)$_n$. In a recent study, Just and Holler (1987) found that Ap4A binds strongly to two sites on histone H1 and competes with Mg^{++} ions for this binding. They found that Ap4A did not bind to assembled nucleosomes, but that the dissociation constant of the free histone H1:Ap4A complex was roughly equivalent to physiological nuclear Ap4A concentrations sometimes observed (100μM), and concluded that complex formation was likely *in vivo*. Other dinucleoside oligophosphates (eg. Ap5A and Gp4G) also served as acceptors for ADP-ribose, but the combination of Ap4A and histone H1 produced the greatest effect (Tanaka *et.al.*(1981b)). Nucleoside triphosphates, such as 5'ATP and 5'GTP, were moderate inhibitors of the (ADP-ribosyl)ation of histones (50 percent inhibiton at 100μM), but no evidence was found that they acted as acceptors for ADP-ribose, and their effects are probably due, therefore, to some other influence (*ibid*).

The biological significance of dinucleoside oligophosphates is not yet understood, although a possible role for Ap4A is discussed above. However, it seems likely that their modification by poly(ADP-ribosyl)ation would have profound effects upon their biological activities. Recently, Baker *et.al.*(1987) found that poly(ADP-ribosyl)ated Ap4A inhibited the ability of calf thymus DNA polymerase

α to replicate SV40 DNA *in vitro*. This was not observed with activated salmon sperm DNA as a template, which suggests that a specific characteristic of SV40 DNA is required for the effect to occur. 60 percent of the control DNA polymerase α activity could be restored by the addition of 20μM Ap4A - but not Gp4G. This is consistent with the model that following stress such as DNA damage, poly(ADP-ribosyl)ated Ap4A inhibits the initiation of DNA replication by DNA polymerase α, perhaps until damage repair has taken place.

It was reported that the polymerase and primase activities of the high molecular weight form of calf thymus DNA polymerase α were inhibited when the complex was incubated in an (ADP-ribosyl)ating mixture *in vitro* (Yoshihara *et.al.*(1984, 1987)): is this interaction *via* Ap4A, perhaps attached to the 'Ap4A binding-protein' discovered to be associated with DNA polymerase α (Rapaport *et.al*(1981a,b),Grummt *et.al.*(1979)) ?

A previous experiment in this laboratory using permeabilised L1210 cells suggests that DNA damage (caused by DMS) results in a large increase in (ADP-ribosyl)ation of material of low molecular weight (Mullen (1983)). The purpose of this investigation was to look for, identify and ascertain the biological significance of the (ADP-ribosyl)ation of such acceptors, particularly in the case of the cell's response to DNA damage. In the light of the discovery that Ap4A can serve as an acceptor for poly(ADP-ribose) in *in vitro*

experiments, it was pertinent to find out if this unusual modification occurred in a system which was nearer to that *in vivo*, ie: permeabilised cells.

Materials and Methods.

(III).

Cell Culture.

(a) L1210 Mouse Lymphoma cells.

L1210 Mouse Lymphoma cells were obtained from Flow Laboratories Ltd., Irvine, Scotland. They are ideal subjects for biochemical study, being easily cultured repeatedly, with a doubling-time of 12-13 hours. In the medium described below, they exhibit the classical growth kinetics of many bacteria - in that after a variable "lag-phase" caused by subculturing they enter a "logarithmic phase" of exponential growth, after which they enter a "stationary phase" (G_0) at a density of > 1.0×10^6 cells/ml. They can also be stored by slowly freezing in a medium containing dimethylsulfoxide and thawed when required.

(b) Culture Medium.

All ingredients were purchased from Flow Laboratories (see above) and were either guaranteed to be sterile, autoclaved for at least 20 minutes at ≥120°C, or in the case of heat-sensitive solutions, sterilized using a standard filtration procedure through membranes with pores of <0.45μm in size.

A large McCartney bottle (>500ml) was filled with 440ml of double-distilled water and autoclaved as above. In a laminar flow

cabinet, using careful sterile procedure, the following solutions were added:-

50ml 10x RPMI concentrate

50ml donor horse serum (10%v/v final conc.)

20ml penicillin (5000 iu/ml)

& streptomycin (5000 µg/ml)

5ml glutamine (200 mM)

13.5ml sodium hydrogen-carbonate (7.5% v/v)

This medium was stored at 4°C usually one bottle at a time to minimise the possibility of contamination that may develop in a large, frequently used supply.

(c) Subculturing.

Cells were grown in 150ml sterile McCartney glass bottles. Interestingly, they were previously found to be highly sensitive to detergents, and the re-usable bottles and lids had to be washed without detergent in order to sustain healthy L1210 cultures. Cells in the logarithmic phase were put into pre-warmed medium to a level not less than 5×10^4 /ml using a sterile syringe in a laminar flow cabinet. The resulting suspension was gently mixed, loosely capped and the bottle placed in an incubator at 37°C, in which the CO_2 level was monitored and kept at 5% automatically. The function of the CO_2 was to buffer the medium. This occurs due to the dissociation of the

sodium bicarbonate added, producing the (weak) carbonic acid and OH^- ions, which itself dissociates to give CO_2. This equilibrium is held artificially constant by driving it "backwards" with supplied CO_2 gas. The RPMI contained a pH indicator which was red at the optimum pH (7.5). Cells used for experiments were at a density of between 4 and 8 x 10^5 /ml.

(d) Cell counting and viability.

Cells were counted in an improved Neubauer haemocytometer under phase contrast microscopy. Generally, five separate counts were made in different quadrants of the haemocytometer and the average taken. One large square of the haemocytometer, when covered with an optically flat cover slip, was equal to 10^{-4} ml in volume.

Viability was determined by the ability to exclude Trypan blue dye from the cell's cytoplasm. Dead cells take up the dye and are stained an intense blue. Permeable cells (see [2]) are stained a pale blue. A small volume of cells was mixed with an equal volume of trypan blue in a 5%$^{v}/_{v}$ solution in 0.85% ($^{w}/_{v}$) saline. The Trypan blue dye was also purchased from Flow laboratories. *It should be noted that the dye was reported by Flow to be a possible carcinogen and that skin contact should be avoided.* The photographs over show L1210 cells, taken through the microscope at different magnifications in the presence and absence of trypan blue.

L1210 cells photographed

at x 10 magnification .

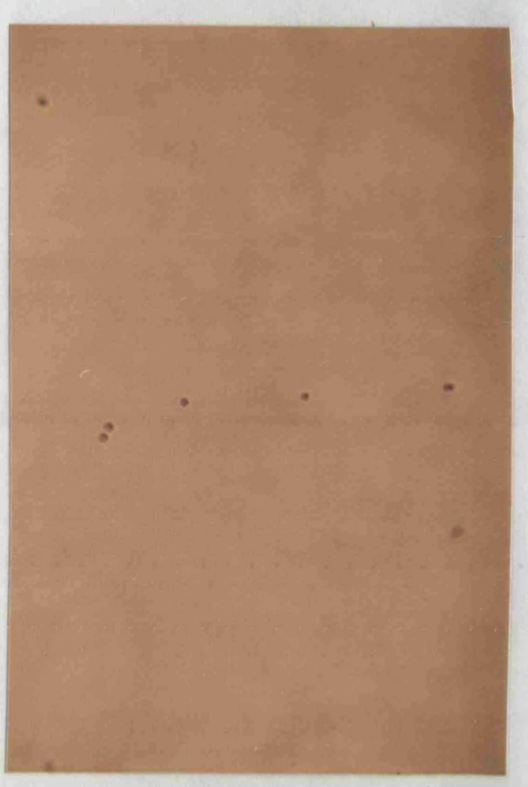

L1210 cells photographed

at x 50 magnification in

Trypan blue (see text) - note

the bright ring around each.

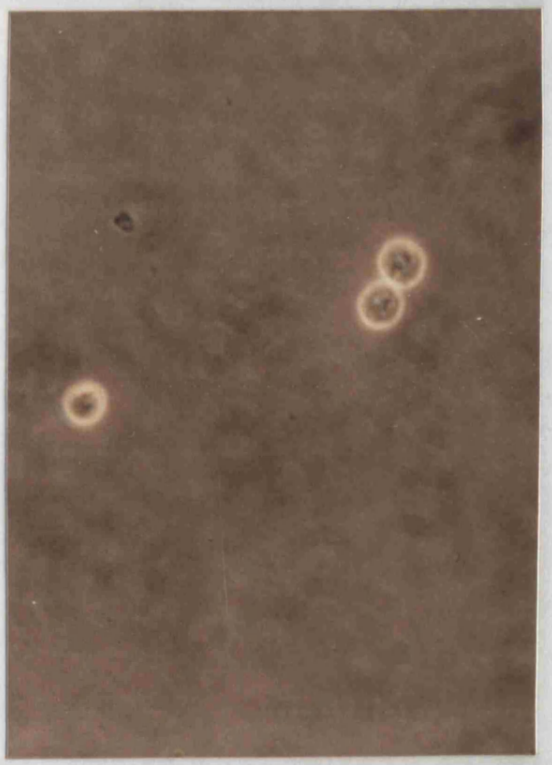

Cell Permeabilisation.

This was performed according to the method of Durkacz *et al.* (1980). Great care had to be taken throughout the procedure to avoid excessive shearing and thus disruption of the cells. The principle behind the method is one of subjecting the cells to cold shock, together with Mg^{++} ions and a lipophilic ionophore (EGTA). This renders the cells permeable to molecules which would otherwise be excluded by the cell membrane (Burr (1980)) - including the substrate for ADPRT - NAD^{+}.

L1210 cells intended for permeabilisation (at a density of between 4 and 8 x 10^{5}/ml) were allowed to settle overnight. If, before permeabilisation, incubation with DMS was performed, the medium over the cells was carefully aspirated using a pasteur pipette until the desired volume was reached (as determined in a warmed measuring cylinder). It was found that the best container for the cells from this point was a round bottomed glass (15ml) tube. This made re-suspension of pellets easier to perform and more gentle on the cells than, say, a conical tube. Plastic tubes did not allow enough visibility when ensuring complete re-suspension of pellets. If the cells were then to be DMS-treated, a culture was split in two, aspirated as above, and placed into two such tubes, pre-warmed in a 37°C water-bath. Into one was added 20µl of the DMS solution

required, the other providing the control cells. *See [15] for important notes concerning DMS.* After incubation for the desired length of time, the tubes were placed in pre-formed wells in ice and allowed to cool for 3 or 4 minutes. When cool, they were placed into pre-cooled centrifuge buckets and centrifuged at no greater than 1000rpm for 2 minutes (MSE bench centrifuge). After replacing the tubes and buckets in ice, the medium above the (visible) cell pellets was aspirated with a pasteur pipette. In the case of the DMS-treated cells, this was done with the utmost caution in a suitable fume hood. The pellets were then re-suspended gently in 10ml of ice-cold Puck's saline (see below) and centrifuged as before. This was repeated once again, but the pellets were this time re-suspended in a small volume of hypotonic buffer (below) such that the cell density was between 3 and 5 x 10^7/ml. At this stage it was imperative that the pellet was fully resuspended. After incubation on ice for 30 minutes the cells were diluted with the isotonic buffer below up to ten-fold and the tubes gently inverted to ensure mixing. The cells were then counted as described in [1](d) in Trypan blue.

It was consistently observed that cells which had been treated with DMS appeared to be larger, with more diffuse edges at this stage. This might possibly be due to a direct effect on the cell membrane by DMS, and is shown in the photographs on the page following. The cells, kept on ice, were then used within the next 20

minutes otherwise re-sealing of the membranes started to occur. The photographs below show how the cells stain a pale blue when permeabilised. Notice the dark-staining non-viable cell (arrow), and the effects of DMS-treatment.

control cells

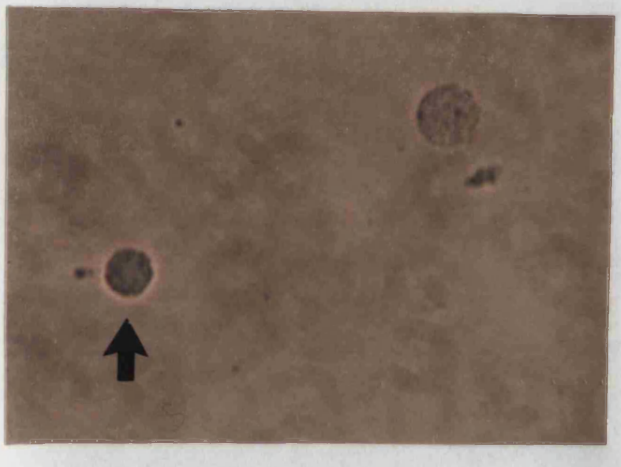

DMS-treated cells

Buffers.

PUCK'S SALINE:	KH_2PO_4	0.400g/litre
(at pH 7.4)	$NaHCO_3$	0.350g/litre
	NaCl	0.008g/litre
	Glucose	1.000g/litre
HYPOTONIC:	HEPES	2.145g/litre
(at pH 7.8)	Dextran	45.000g/litre
	EGTA	0.336g/litre
	$MgCl_2$	0.951g/litre
	DTT	0.771g/litre
ISOTONIC:	HEPES	9.532g/litre
(at pH 7.8)	KCl	9.693g/litre
	Dextran	40.000g/litre
	Sucrose	77.017g/litre
	EGTA	0.672g/litre
	$MgCl_2$	0.468g/litre
	DTT	0.386g/litre

DTT :dithiothreitol

HEPES :N-2-Hydroxyethyl piperazine & N'-2-ethane sulphonic acid.

EGTA :Ethylene glycol-bis-(β-amino ethyl ether)-cv N,N'-tetra acetic acid. All buffers were stored frozen at -20°C in small aliquots.

Extraction and partial purification of nuclei.

Pig thymus nuclei were regularly isolated from fresh thymii in this laboratory, and purified from DNA by mixing with a buffer containing salt and polyethyleneimine (PEI) which is positively charged. Centrifugation of this mixture left a supernatant which was a crudely purified preparation of nuclear proteins, free of DNA, and small aliquots (20µl) of this were used as an *in vitro* (ADP-ribosyl)ating system. The full methodology is described elsewhere (White (1988)). When assaying for ADPRT activity, histone H1 was added to the incubation mixture as an acceptor for $(ADP\text{-}ribose)_n$, as well as DNA, which is required by the enzyme for activity (see section 4).

ADPRT assay.

The activity of ADPRT was measured by the incorporation of radioactivity into material which was insoluble in TCA. Radioactively labelled NAD^+ (either in the adenosine moiety as with [^{3}H], or at the primary (α) phosphate group, as with [^{32}P]) is present as a substrate for the enzyme, which transfers the ADP-ribose moiety to acceptor molecules - usually proteins. The assay used for salt/PEI - extracted pig-thymus nuclei was as follows:-

The reaction took place in an Eppendorf tube in a total volume of 520 µl, in which were 80 µl of a sonicated solution of histone H1 and DNA (salmon sperm) at 1mg per ml each, 10 µl of DTT at 100 mM in water, and 360 µl of triethanolamine buffer (0.1M)/magnesium chloride (50mM) at pH 7.8. 50 µl was then allowed for the labelled NAD and any other additions (eg. inhibitors, [^{3}H]Ap4A etc.), the volume being made up with more of the triethanolamine/magnesium chloride buffer above. The incubation was allowed to procede for 5 minutes in a 26°C water bath with an occasional gentle inversion of the tube, after which aliquots were taken for TCA-precipitation as described in section [5].

Permeabilsed L1210 cells were also assayed for ADPRT activity in a volume of 520 µl. This contained 500 µl cells (between 0.4 and 1.0 x 10^6) in the isotonic buffer described in section [2], with the labelled NAD^+ and any other ingredients contained in 20 µl. When investigating the inhibition caused by Ap4A, the total volume of the reaction was increased to 530 µl, and the extra 10 µl contained Ap4A at different concentrations in 0.25M Tris-HCl buffer (pH 7.8). The incubation was started by the addition of the labelled NAD^+ and was allowed to proceed for 10 minutes in a 26°C water-bath. This has been found in this laboratory to be the optimum time at which to monitor ADP-ribose labelling in cells (Mullen (1983), Durkacz *et.al.*(1980)) after which ADPR-glycohydrolase activity begins to decrease the amount of polymer attached to TCA-insoluble material. However, aliquots were again taken before and after this time for time-course studies.

It should be noted that these assays were conducted purely with the aim of obtaining data concerning the *relative* activity of ADPRT, so that the effects of certain treatments (eg. DMS, 3AB, Ap4A etc.) could be ascertained. Where comparisons of ADPRT activity were made *between* different experiments, it was ensured that the precise reaction conditions (total volume, cell count etc.) were taken into account.

TCA-precipitation.

ADPRT activity was measured by the incorporation of radioctivity (either [^{3}H] or [^{32}P]) into TCA - insoluble proteins. As discussed earlier, this does not provide quantitation of *absolute* amounts of (ADP-ribose)$_n$ present, nor does it distinguish between the distinct processes of mono- and poly-(ADP-ribosyl)ation, but it does provide an indication of the general level of ADPRT activity and allows comparisons to be made (eg.between (ADP-ribosyl)ation in the presence or absence of an inhibitor).

Of course, this method of determinig ADPRT activity would not detect the (ADP-ribosyl)ation of acceptors which are too small to be precipitated by TCA!

After incubating the material to be tested for ADPRT activity under controlled conditions (see [4]), two methods were used and and are described below:

Method 1. Small aliquotes (>5µl<200µl) were pipetted accurately into plastic Lp4 tubes (4ml) containing ice-cold TCA at 20% and were allowed to precipitate for not less than 2hrs on ice. The maximum time allowed for this was overnight; it is later shown that the process produced repeatable results provided that this precaution was observed. Frequently, 100µg of BSA in water (0.1mg/ml) was mixed with the aliquot immmediately beforehand to facilitate precipitation where

the protein concentration was very low. The precipitates were then collected on numbered GFC (Whatman) discs, previously soaked with ice-cold 5% TCA. This was performed using a Millipore filtration apparatus, which draws liquid through the discs in a controlled manner under partial vacuum. The discs were washed three times with ice-cold 5% TCA and then once with 95% ethanol/water. A final wash comprised of Laboratory Reagent ether, which aided drying of the discs (performed in a drying oven at ≈40°C).

The discs were then counted for radioactivity as described in section [6].

Method 2. Aliquots were pipetted accurately onto numbered *paper* discs (Whatman 3mm, 2 cm diameter) which had previously been soaked in a mixture of 20% ˇ/ˇ TCA in ether for 30 minutes and dried. The discs were then washed (together) in 4 successive solutions of 10% TCA for 15 minutes per wash, and then once in 95% ethanol and once in ether. The discs were then dried in the oven and counted for radioactivity as before.

The latter method was useful for handling large numbers of samples, but was found to have two disadvantages: the maximum volume that could be precipitated per disc was 40µl, and with large amounts of TCA *soluble* radioactivity, the blank discs sometimes showed unacceptably high background levels of radioactivity. The first method was reliable in this respect, provided that the glassware of

the Millipore apparatus was kept clean. This was achieved by soaking in concentrated chromic or nitric acid overnight. Blank GFC discs were employed before and after radioactive samples were collected to monitor this. Thus, the first method was usually employed.

Purification of low molecular weight molecules.

This involved separation from the bulk of the cell proteins by phenol/chloroform/iso-amyl-alchohol(IAA) extraction (a). After ether extraction of the phenol (b), nucleic acids were removed by acidic ethanol precipitation followed by centrifugation (c). A final lyophilization ("freeze-drying") step removed the ethanol and most of the acetic acid.

(a). Phenol/chloroform/IAA extraction.

This was adapted from a procedure used routinely to extract DNA and RNA from homogenised tissue (Maniatis,T. (1982)), except that it is the nucleotides and other small molecules which are of interest. The method finally developed (see results section) was used to extract small molecules from permeabilised L1210 cells after they had been incubated under various conditions. In nearly all cases, these incubations took place in a capped Eppendorf tube in a total volume of 500µl to 530µl. A few seconds before the reaction was due to be stopped, 100µl of BSA at 0.1mg/ml in distilled water was quickly added to the cells to facilitate precipitation of proteins. This was shown by experiment to be necessary in order to obtain repeatable results (chapter IV). To stop the incubation, 500µl of an ice-cold mixture of water-saturated phenol (freshly prepared), chloroform and

IAA in the proportions 1:1:1/24 respectively were added to the tube. After tightly sealing, the tube was then vigorously mixed using a bench rotary vortex mixer for 2 x 30 seconds, with 30 seconds resting on ice inbetween. The phenol/chloroform/IAA mixture denatures the proteins which precipitate out of the aqueous solution (this results in an opaque white suspension being formed). The IAA is present as an anti- foaming agent. The tube was then centrifuged for 10 minutes at full speed (approximately 12000 g) using an MSE bench microfuge with a fixed angle rotor at 4°C. This caused the mixture to separate into three layers due to the partition formed between the aqueous phenol and the chloroform. The upper (aqueous) layer contained the small molecules of interest; the central layer (hereafter called the "phenolic interface") contained a layer of precipitated protein forming a disc between the aqueous and chloroform-containing layers. The lower layer of chloroform was shown to contain no material of relevance (by monitoring for radioactivity) and was discarded.

In the next step, 500µl of the upper aqueous layer were carefully and slowly removed by pipette, leaving a film (≈40µl) over the interface. This was placed in a ground glass-stoppered tube on ice in readiness for the next step (b). The remaining phenolic interface was "back-washed" by the further addition of 500µl of 0.1M acetic acid, with mixing and centrifugation as before, which minimised the losses of nucleotides to the interface as shown by

monitoring of radioactivity. This second supernatent was again removed carefully so that the phenolic interface was undisturbed, and it was pooled with the first, ready for ether extaction of the phenol.

(b). Ether extraction.

The pooled supernatants were brought to 2 or 3 mls with 0.1M acetic acid, and an equal volume of dry ether was added in the tube. The ground glass stopper was replaced and the tube was shaken by hand (with careful periodic releasing of pressure) for a few minutes. The aqueous and ether layers were allowed to settle for 10 minutes, and if a clear partition did not occur after this time, the mixture was centrifuged for a few seconds at <1000 rpm in a bench centrifuge. The upper (ether) layer was then aspirated using a pasteur pipette to a few mm above the aqueous layer and discarded (it was again shown to contain no molecules of relevance by monitoring of radioactivity). This procedure was repeated twice more, with the final small amount of ether remaining being evaporated off under a stream of air.
Because the ether absorbs a certain amount of water, the final solution was often less than the original volume.

(c). Acidic ethanol extraction.

This procedure was again adapted from a regularly used method (Maniatis (1982) of precipitating nucleic acids from solution, again with the difference that it was the small molecules that were of interest and not the DNA and RNA ! After ether extraction, the solution above was removed from the glass tube and pipetted into a conical plastic 15 ml centrifuge tube. The glass tube was washed with 2 or 3 x 1 ml of 0.1M acetic acid and these washes were pooled with the solution, which was topped up to either 4 or 5 mls with more 0.1M acetic acid. An equal volume of absolute ethanol was then added, with mixing, and the tube was sealed and left overnight at -20°C to precipitate the nucleic acids.

The tube was then brought to room temperature by hand-warming, placed in a Sorval high-speed centrifuge with a fixed-angle rotor and centrifuged at 10000 rpm for 30 minutes. A visible (but translucent) nucleic acid pellet was formed, and the supernatant was removed to a few mm above it. The pellet was then "back-extracted" with a further 2 ml of 50% ethanol/0.1M acetic acid with mixing and centrifugation as before. This minimised the losses of nucleotides to the pellet, as shown by monitoring of radioactivity. The supernatants were pooled in 25ml round-bottomed glass bulbs, which were then immersed at an angle in liquid nitrogen until the contents had frozen. The bulb was then fixed to a lyophilizing machine and left under vacuum overnight or

at room temperature, until the process had finished. The lyophilizates were then either frozen and stored at -20°C or dissolved in 4 ml of equilibriation buffer, ready for analysis by DEAE cellulose chromatography (section [8]b).

Radioactivity.

(a) Counting tritium.

Liquid samples to be counted were pipetted accurately into scintillation vials and then mixed thoroughly (using a bench top vortex mixer) with scintillation fluid. In order to obtain accurate counts, the general rule was adopted that the scintillation fluid must be present in the ratio of at least nine to one over the (aqueous) sample to be counted.

Samples that had been collected on glass fibre discs and dried were also counted in scintillation vials, but in this case, scintillation fluid was added so that it was sufficient to immerse the disc (2 to 3ml). The discs became transparent almost immediately.

The vials were then placed in either a Packard Tri-Carb or LKB liquid scintillation counter and counted for 2 minutes (or longer, if required). The basic scintillation fluid used was toluene, with PPO (2,5-diphenyloxazole -5%) as the primary fluor and POPOP (1,4-di-[2-(5-phenyloxazoyl)]-benzene) as the secondary fluor. This was supplemented with Triton-X-100 (30% v/v) when counting liquid samples to ensure single phase counting. Later, the commercially prepared scintillation cocktail "Optiphase" (LKB) was used. This was safer to work with (not being toluene based) and is reputedly more

efficient. It also forms a single phase solution when used in conjunction with liquid samples.

Both the LKB and Packard Tri-Carb machines were programmable to give read-outs of chemiluminescence. When this was observed to be >0.5%, the vials were left (overnight, if necessary) until it had subsided and then re-counted.

Unless mentioned otherwise, readings were taken through an "open window" on the spectrometer, and left as cpm (counts per minute). The efficiency of these machines was checked using an authentic standard, and found to be 49-50% efficient for tritium using such an open window.

TLC plates (PEI) were prepared for counting as described in section [8] by the method of Randerath *et al.* (1966).

Gel slices from agarose and polyacrylamide analyses were prepared for counting as described in section [10].

(b) Dual labelling.

Dual labelling experiments were performed using both tritium ([^{3}H]) and the phosphorous isotope [^{32}P]. Since the energy spectra of emission for these are different, it was possible to create two channels (using the LKB counter) which separated readings from the two isotopes. This was done by re-programming the counter's "windows"

to exclude one or the other type of radioactive emission. It was thus possible to count [^{3}H] at 23.8% efficiency and [^{32}P] at 78.9% efficiency. There was a spillover from [^{32}P] to [^{3}H] of ‹0.1%, and no detectable spillover from [^{3}H] to [^{32}P].

The next step was to convert these cpm figures to dpm (absolute disintegrations per minute - as if counted at 100% efficiency) for ease of comparison. A programme was written in basic which performed this task (an example of which can be seen in Appendix 1.). The cpm figures for [^{32}P] and [^{3}H] were entered into a file on the computer and the programme was run. It took each figure from the file, subtracted the appropriate blank from it for background radiation and then converted it to dpm. In the case of [^{3}H], a 0.1% spillover from [^{32}P] was taken into account for each reading.

In the case of [^{32}P], another calculation was performed by the programme: it became necessary to take into account the relatively short half-life of [^{32}P] (14.2 days as opposed to 12.26 *years* for [^{3}H]) in order that results were comparable with each other. This was achieved by including a section of the programme in which a factor could be entered which corresponded to a number on a "decay chart" for [^{32}P] (From 'Radioisotopes':A wall chart by LKB). For instance, if the results of analysis of three different parts of the same experiment were obtained over a period of a week, the results would each be given a factor corresponding to the date of the original

experiment, producing [^{32}P] dpm figures as they would have appeared on that day. This decay chart is also shown in Appendix 1.

(c) Isotopes used.

[^{3}H] NAD^+ was synthesized by Dr.W.J.D.Whish (at Bath University) enzymically from [^{3}H] ATP by a method of Ueda *et al.*(1971). The [^{3}H]ATP (21 Ci/mmol) was from Amersham International plc.

[^{32}P] NAD^+ was synthesized in a similar manner, from adenosine 5'-[α 32P] triphosphate (Amersham International) the specific activity of which was 1.11 TBq/mmol (30Ci/mmol) at 1200 GMT on 13th February, 1987.

Di[2,8 3H]adenosine tetraphosphate ([^{3}H]Ap4A) was at first synthesized from [^{3}H]ATP as described in section [12], but when this became unsatisfactory, it was purchased as the remainder of a custom synthesis, again from Amersham International, at 159 GBq/mmol (4.3Ci/mmol) and it was quoted by them as 95% radiochemically pure. [^{3}H]leucine (130 Ci/mmol), [^{3}H]thymidine (at 40mCi/mmol) and [^{3}Hadenosine (30 Ci/mmol)were all similarly purchased from Amersham International.

Anion Exchange.

(a) TLC.

This was performed on commercially prepared polyethyleneimine (PEI) plates with a plastic backing. PEI is a positively charged anion exchange medium which is ideal for the chromatographic analysis of negatively charged nucleotides and nucleotide derivatives. The plates were washed free of contaminating ions before use by soaking in 2M NaCl for 30 minutes followed by 30 minutes soaking in distilled water. After drying, the plates were stored at -20°C to prevent bacterial infestation.

Samples were applied to the plates in the smallest area possible with the aid of extruded glass tubes, approximately 1.5cm from the bottom of the plate. Repeated application of the sample over the same area was carried out by drying each application under warm air (eg. from a hair-drier) and this was found to be essential in order to obtain adequate separation of nucleotides on the plate. If the application area was too thick, separation was poor, and smudging occurred. The application area could be as *wide* as was desired (which was sometimes necessary when the sample was high in salt concentration) in a direction perpendicular to the solvent flow, but generally an application "spot" of 1-1.5cm was employed.

The plate was placed in a glass tank containing enough of the (aqueous) solvent required to reach 0.5cm up the plate and developed. Unless otherwise stated, two solvent systems were used: a single - step development in 1.6M LiCl (A.R. grade) or a two - step development, first in 1M acetic acid for 2 cm, and then a further 11 cm in 0.9M acetic acid/0.3M LiCl. The solvent front was usually allowed to run 13cm, after which the plate was removed and dried under warm air.

Authentic standards (at 1mg/ml in 50-25% ethanol/water ᵛ/ᵥ) were always run together with the samples, and as was discovered, it was imperative that they be applied first to the area upon which the sample was to be applied. If they were applied separately to a track which was to run parallel to the sample track, discrepancies often occured in the positions the standards migrated to, depending on the ionic strength and nature of the sample. It must be remembered that after several applications with drying, even a fairly weak solution will produce very high concentrations on such a small area on the plate. As the solvent moves through this, there will be a tendency for "leading" and "trailing" ions to form and separate, and the more material applied, the stronger the smudgeing effect. After drying the PEI plate, the positions to which the standards had moved were determined by viewing under a source of "hard" *uv* light (at the small end of the *uv* wavelength range). This was possible because

nucleotides (particularly those containing adenosine) absorb strongly in the *uv* range. Radioactivity was determined by the method of Randerath *et al.*(1966). The plates were marked and cut into 0.5cm strips, each of which was placed in a scintillation vial containing 0.5ml perchloric acid (0.5M). The vials were sealed and heated at 80-90°C for 30 minutes. This procedure was effective in removing the charged adenosine moieties particularly of interest from the PEI. 5ml of suitable scintillant were then added to each vial, and after vigorous mixing in a bench vortex mixer, they were counted for radioactivity as described in section [6].

All standards were of the highest quality obtainable and were purchased either from Sigma(UK) or Boehringer Mannheim. LiCl was also purchased from Sigma. acetic (ethanoic) acid was purchased from BDH.

(b) Column Chromatography.

Anion exchange chromatography was performed with a variety of usually cellulose-based resins, which were prepared according to the manufacturer's (BioRad, BDH) instructions. This involved pre-swelling the material in the equilibriating buffer to be used. De-gassing of buffers before use was not necessary, but careful pouring of columns was important in order to obtain repeatable results. The non-linear disposable plastic columns purchased from BioRad were ideal for analysis of nucleotide extracts with DEAE-cellulose (

Pharmacia) as the ion exchange material. As they tapered slightly toward the font end, a *linear* flow rate (cm/hr/cm^2) was not practically calculable, but as the flow rate (ml/hr) was within the range at which equilibrium could take place over the whole column, this was considered to be of minor importance.

In the case of DEAE cellulose analysis of nucleotide extracts (adapted from a method outlined by Yoshihara *et al.* (1981)) the procedure was as follows : a disposable (BioRad) column with a capped font was fixed by clamping to a stand. 2ml of equilibriation buffer (of either 2 or 5mM ammonium hydrogen carbonate (NH_4HCO_3), pH 8.3) was added and the column was tapped to ensure that no air was trapped. A slurry of DEAE-cellulose, previously left overnight in the same buffer, was carefully poured in to 2/3 of the total volume of the column and allowed to settle and form a 1cm bed for one minute. The cap was then removed from the font and an even bed was allowed to form to a height of approximately 6cm. The column was graduated and this was equivalent to 3ml of the resin when hydrated. More buffer was then supplied to the top of the column by means of fixing a reservoir to it by plastic tubing. The reservoir was clamped at a known head height such that the flow rate was 40ml/hr and connected to the column by an air-tight fixing such that there was sufficient buffer above the resin to avoid disturbance as it entered the column. The whole assembly was made easier to set up by fixing another

plastic tube to the font and adjusting the head hight accordingly as the vertical distance between the exit of this tube and the level of buffer in the reservoir (see Figure 1.).

The column was allowed to equilibriate for at least 30 minutes, and the flow of buffer was halted by means of clamp A on the font - tubing, and after closing clamp B (Figure 1.), the cap was removed from the top of the column and the radioactive sample, previously dissolved in equilibriation buffer, was then applied by gently pipetting it onto the top of the column. With the cap still off, clamp A was opened and the eluate (hereafter called 'the remainder unbound') was collected in a small vial. The column was then washed with a further 4ml of equilibriation buffer and this wash was also collected. By counting the radioactivity in small aliquots of the initial solution applied, the remainder unbound and the wash, it was possible to monitor the initial binding to the column.

After washing, clamp A was closed and 1ml of the same buffer was placed on the top of the column. The air-tight fixing was replaced (open - ended) and this was then connected to the linear gradient maker, ready for elution. Two ml fractions were collected drop-wise in a rotary fraction collector (LKB - bromma 2112 Redirac) at a flow rate of 40ml/hr. After elution, 4ml of 500mM NH_4HCO_3 were then applied to the top of the column, followed by up to 20ml of distilled water. This was in an attempt to remove the NH_4HCO_3 from the resin so

that 0.1M hydrochloric acid could be applied to remove any material still bound. However, even with this extensive water-washing, the application of acid caused effervescence within the column and blockage resulted. It is not clear why this last step was included in the original method (Yoshihara and Tanaka (1981)), as it was impractical to perform and did not yield any useful data. It was thus abandoned.

(c) Setting up linear gradients.

This was performed using a linear gradient maker (2 x 200ml) made by LKB. This is shown diagrammatically in figure III.2, and basically consists of two chambers, interconnected by a closable capillary, with an exit from one of them. The whole apparatus is rigidly clamped and it is obviously important that it remain horizontal. With valves A and B closed, a measured amount (80ml) of low strength buffer (2 or 5mM NH_4HCO_3)is poured into the exit reservoir. Valve A is slowly opened until a drop emerges in the other reservoir, thus excluding air. After re-closing valve A, the same amount of high strength buffer (300 or 400mM NH_4HCO_3) is poured into the other reservoir. Valve A is re-opened and a mixer is placed in the exit reservoir and switched on before valve B is opened. After excluding the air from the exit tubing the gradient is ready for applying to the column and should produce a linear concentration gradient, drop by drop, from the low to the high concentration.

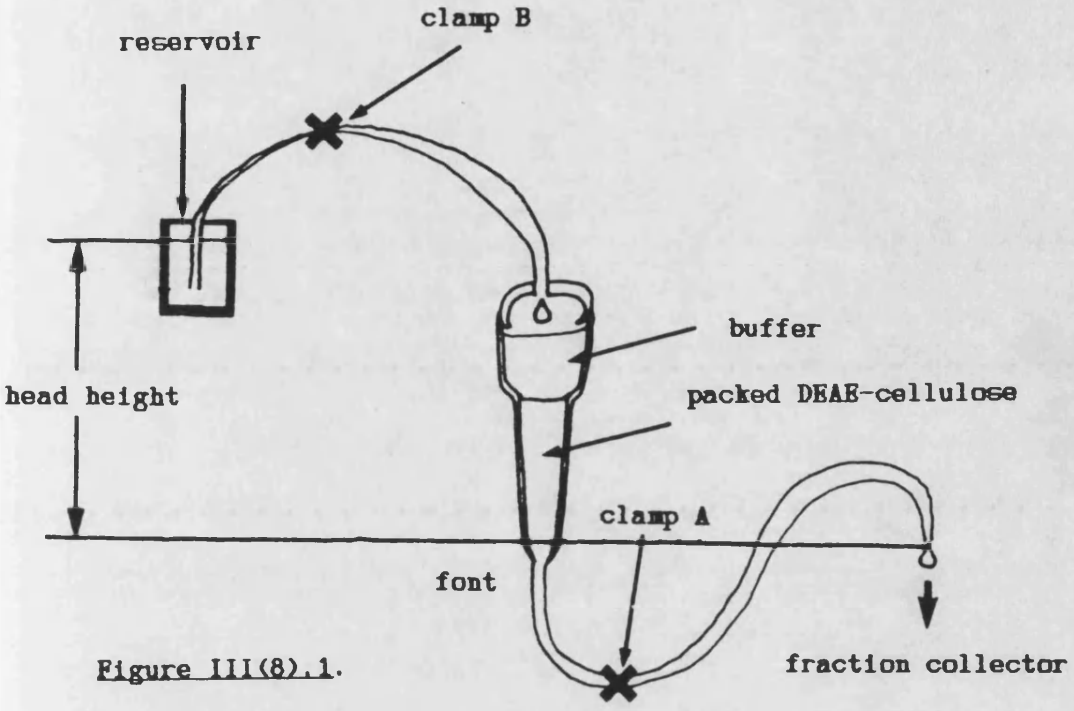

Figure III(8).1.

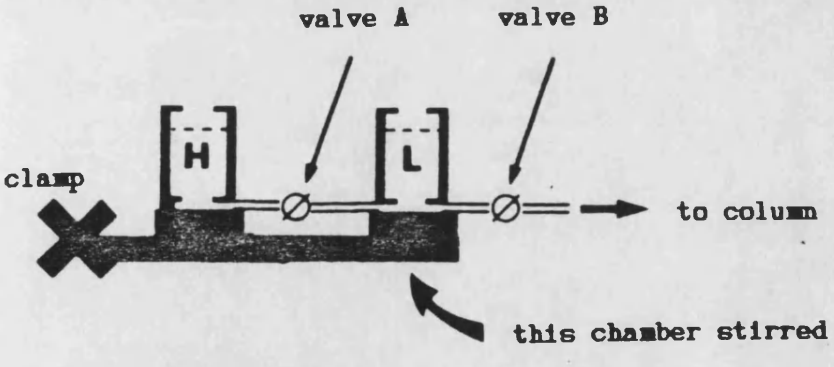

Figure III(8).2

Top - anion exchange column chromatography.

Bottom - linear gradient maker

Gel Filtration.

Gel filtration was conducted using Biogel P2 (BioRad) which has an exclusion limit of 1800 Da (bead diameter 40-80 Microns) and a fractionation range from 100 Da up to 1800 Da, according to the manufacturers. However, Politi *et al.*(1983), after doing extensive work with Biogel P2, concluded that separation of molecules on this medium had less to do with their molecular weight than with hydrophobic interactions with the Biogel, thus analysis of nucleotides by this technique was abandoned after a few attempts. It was still considered a valid tool in one aspect, however, with regards to its exclusion of molecules over ≈2000 Daltons: material appearing in the void volume of the column could be separated from smaller molecules. When [^{3}H]NAD was run on a column of Biogel P2 it was included and a clear radioactive peak was observed, facilitating separation from excluded material.

The gel was prepared according to the manufacturer's instructions by pre-swelling in equilibriation buffer, either overnight at room temperature or at 90°C for one hour. A linear glass column (Pharmacia) of 1.5cm interior diameter was carefully packed with the hydrated resin, also according to BioRad's instructions, and equilibriated for several hours before use. The buffers used consisted of either 0.1M acetic acid or 0.1M sodium acetate (pH 5),

and the gel was stored in the running buffer supplemented with 0.02% (w/v) sodium azide to prevent bacterial infestation. After packing the column at a flow rate of not more than 40ml per hour (using either a peristaltic pump or gravity, as with DEAE cellulose chromatography) the final column volume was 40 mls. Samples were applied in running buffer, to which was added Dextran blue and bromophenol blue dyes (Sigma) and 10% glycerol in a volume not greater than 300µl. Larger volumes were difficult to apply and greatly increase the size of band formed by the dye - an indication that separation was not efficient. Dextran blue was of variable molecular weight, but was excluded from the column and appeared in the void volume (V_o), which appeared after 14 (± 1)mls had eluted. The bromophenol blue band was included and sometimes appeared much later than expected, due to aggregation of the sample on the column (when the dyes were run without the sample, the bromophenol blue appeared after approximately 40ml was eluted). 2ml fractions were collected drop-wise using a rotory fraction collector (LKB - bromma 2112 Redirac).

Electrophoresis

(a). Polyacrylamide gels.

Polyacrylamide gel electrophoresis was performed as described by Mullen (1983) in the analysis of (ADP-ribosyl)ated proteins which had been subjected to the purification and enrichment procedure therein. The protein sample was dialysed and concentrated against 15% poly(ethylene glycol), 0.02M sodium acetate (pH 5.5), 4M urea and 0.1% SDS and then applied to 10cm polyacrylamide rod gels, which consisted of an upper "stack" of 1.5 cm in length, over a lower gel of 8 cm length. The stack consisted of 4M urea and 0.1M sodium acetate in 2% (w/v) glycerol/water at the lower pH of 4.0.

The lower gel consisted of 10% acrylamide in 4M urea, 0.1M sodium acetate and 0.1% (w/v) SDS. The acrylamide was polymerised by mixing this solution together with 20µl each of a solution of TEMED and ammonium persulphate, such that the final concentrations were 0.0015% (v/v) and 0.1 µM respectively. The rods were arranged in a perspex gel apparatus and running buffer (0.1M sodium acetate (pH 5) and 0.1%(w/v) SDS) was poured into the chambers above and below the gels. The samples were brought to 10%(v/v) glycerol and carefully applied to the stacking solution above the gels. "SDS-VI-Dalton Marker" (Sigma) proteins were run simultaneously for molecular weight calibration, and these contained bromophenol blue as a marker. The

gels were run at 8 mAmps per rod until the bromophenol blue reached the end of the gel. The gels were then fixed and either stained or frozen and cut into 1 mm slices for radioactive counting by the method of Aloyo (1979). An apparatus consisting of standard razor blades clamped together with 1mm washers between each was firmly pushed onto the (previously frozen) gel and the slices removed individually using fine tweezers. Each gel slice was incubated for 48 hours at room temperature in 10 mls of a solution containing 0.6%(ʷ/ᵥ) PPO, 1.0%(ʷ/ᵥ) Soluene-350, 1.0% hyamine hydroxide in toluene with occasional mixing.

(b) Agarose gels.

In order to investigate the nature of the radioactivity present in the ethanol precipitates observed during the procedure described in section [6](c), 1% agarose gel electrophesis was performed using the method as described by Maniatis *et al.*(1982). To calibrate the gels, standards of [^{3}H]Ap4A and ECO R1/*Hin*dIII-digested λ phage-DNA were employed; these being visualised by counting for radioactivity and observation under *uv* light respectively.

By using this method it was hoped that if [^{32}P](ADP-ribosyl)ated [^{3}H]Ap4A were present in the samples, it would be visualised by retention on the gel. Similarly, if the radioactivity was associated in some way with the L1210 DNA present, this would be seen as a radioactive peak, co-migrating with a fluorescent band (due to the

intercalation of ethidium bromide with DNA). It was found that the technique was only useful in the latter sense, however, since the majority of the radioactivity (shown to be small molecules by TLC) did not appear to enter the gel, and agarose electrophoresis is only effective in the analysis of DNA larger than approximately 200 base-pairs (Wilson *et al.*(1986). The method employed was as follows:- Agarose (Sigma type II.medium E.E.O.) was poured into a flask containing TBS buffer (consisting of 0.06M Tris-borate, 0.06M boric acid and 0.01M EDTA at pH 8.3) such that the concentration was 1% (ʷ/ᵥ) and held in a boiling water-bath with stirring until completely dissolved (about 15 minutes). After cooling to 50°C, ethidium bromide (Sigma) was added to a final concentration of 1mg per ml, and the solution was poured into the horizontal gel-apparatus being used to a thickness of 3-4 mm and allowed to set. Two types of home-made gel-apparatus were used; a standard "mini-gel" and a longer (15cm) system for which the gel was pre-formed on a glass plate before use. A "comb" was placed at one end of the gel (1cm in) to create sample application wells. After setting, the gels were covered over in TBS buffer and the samples were applied to the wells in 50%ᵛ/ᵥ solution with a buffer containing bromophenol blue marker and glycerol at 2mg per ml and 10%(ʷ/ᵥ) final concentration, respectively. The gel was connected to a D.C. power source and run at 60 mA until the bromophenol blue had migrated to the desired distance from the

positive end of the gel. Visualization of the L1210 and standard DNA was achieved by placing the gel on a transilluminator (GRI, TM 20) and photographing under *uv* light (max.320nm wavelength). After measuring the positions of the standards the gel was cut into either 0.5cm slices in the case of "long" gels or 1mm slices using the apparatus described in (a). Each slice was placed in a scintillation vial containing 2ml distilled water and heated at 95°C for 1 hour before counting for radioactivityy as described in section [7](a,b). Monitoring the radioactivity present in the end buffer was carried out, although the high volume of buffer required for the "long" gel apparatus (2 litres) meant that the dilution factor was so high that the errors in cpm figures obtained were unacceptable. The results are contained in Appendix 3.

Purification of Phosphodiesterase.

Phosphodiesterase from snake venom (SVPDE) is used extensively in the calculation of chain length of (ADP-ribose)$_n$ and for the quantitation of Ap4A - see chapters I and II. Because of the relatively high contamination of commercial preparations with non-specific phosphatase (phosphomonoesterase) and 5'-nucleotidase activities (Oka *et al.*(1978)), which produce erroneous results in both these techniques, it is necessary to purify the enzyme. The method below was finally adopted in this purification, utilizing affinity chromatography on blue Sepharose, which has previously been used in the purification of various enzymes interacting with NAD^+ and other nucleotides (*ibid.*). Affinity for the ligand was attributed to the similarity between the structure of the blue dye Cibacron Blue F-3GA and NAD^+ which can act as a substrate for SVPDE.

Due to the high expense of commercially prepared blue Sepharose (Pharmacia), it was synthesized using a method of Böhme *et al.*(1972), adapted by Heynes *et al.*(1974) for the purification of 3β-hydroxysteroid dehydrogenase. 150 mls of pre-swelled Sepharose 4B (Pharmacia) were carefully mixed with 100 mls of distilled water containing 2.5g disodium carbonate (BDH) and 1.0g of Cibacrom Blue G-3FA (Ciba AG. Basel). After incubation at 45°C for 40hrs with occasional stirring, this was then filtered using 3mm Whatman filter

paper in a Büchner funnel and washed with distilled water until the filtrate ran clear. Coupling was quantified by measuring the absorbance of a 10% (v/v) suspension of the gel in 20% (v/v) glycerol/water at 610nm in a spectrophotometer, and this was estimated as 14.7 +/-0.1 mgs of dye per ml of packed gel. This was comparable to other values reported (Oka *et al.* (1978), Heynes *et al.* (1974)). The prepared gel was stored at 4°C in 0.1% w/v sodium azide to prevent bacterial infestation.

SVPDE from Crotalus adamanteus (Type II, 5.66mgs protein) was dissolved in 1.5 mls of equilibriation buffer, containing 20% (v/v) glycerol, 5mM potassium phosphate, 10mM Tris-HCl and 50 mM sodium chloride at pH 7.5. The enzyme is unstable when purified (Oka *et al.*(1978)) and the presence of glycerol or BSA will remedy this (*ibid.*). After small aliquots were taken for assays, this was applied to a 0.7 x 8cm column of the prepared blue Sepharose, which had been equilibriated in the same buffer. The resulting eluate was then re-applied and the column was washed with 18 mls of the same buffer. The potassium phosphate concentration was brought to 10 mM by the application of 20 mls of a buffer otherwise containing the same ingredients, after which 20mls of the same buffer at 30 mM potassium phosphate were applied. The flow rate throughout was 12 mls per hour and 2 ml fractions were collected (drop-wise) in a rotory fraction collector (LKB bromma 2112 Redirac).

The fractions were then subjected to three assays : a phosphatase assay, a phosphodiesterase assay and a protein assay. The first two (after Oka *et al.*(1978)) utilised the absorbance of *p*-nitrophenol at 400nm when released from bis(*p*-nitrophenol)phosphate (pnp) and thymidine 5'-monophospho-*p*-nitrophenyl ester (Tpnp) respectively. It was found that the absorbance at 280nm used by Oka *et al.*(1978) was not sufficiently sensitive or accurate, and a protein assay using Coomassie blue dye was used instead (section [13]). The assay mixture for phosphodiesterase contained 40 µMoles Tris-acetate (pH8.8), 0.4 µMoles Tpnp, 10µ Moles magnesium chloride in a 1ml plastic cuvette. The addition of either 10 or 20 µl of enzyme sample brought the final volume to 1 ml and started the reaction, which was allowed to proceed at 24°C for 1hr, after which the absorbance at 400nm was taken in a bench spectrophotometer. The phosphatase assay mixture contained 150 µMoles of glycine-NaOH (pH 9.1), 10 µMoles of magnesium chloride, 0.4 µMoles of pnp and the reaction was held in a total volume of 1ml as above, with the addition of enzyme starting the reaction. The reaction was at 37°C and it was determined that 6hrs was the minimum incubation time - although the rate of release of *p*-nitrophenol (again measured by absorbance at 400nm) in this assay was slow and remained linear for some 24hrs.

The relevant fractions (30 mM potassium phosphate) were pooled, concentrated and washed in an Amicon filtration unit with a buffer containing 10 mM magnesium chloride, 30 mM Tris-HCl (pH 8.5) and 2% (v/v) glycerol. A fourth assay was then conducted on this product, which did not utilize α-[^{32}P]AMP as in Oka *et al.*(1978). This was for determination of nucleotide pyrophosphatase activity, which is quoted by Sigma as being present over SVPDE seven times in excess in the original preparation, and involved the digestion of [^{3}H]-ATP and subsequent analysis by TLC (section [8](a)).

The concentrated enzyme was stored at -20°C in 50 µl aliquots, each containing one 'unit' of enzyme activity (one 'unit' is defined as the activity required to release 1 µmole of *p*-nitrophenol (ϵ = 17000 cm^2mol^{-1}) per minute).

The procedure above was attempted several times, purifying SVPDE from other proteins and phosphatase activity, but does not appear to remove nucleotide pyrophosphatase activity from either C.adamanteus or C.atrox venom SVPDE preparations. The results from the above purification procedure are shown in Appendix 2.

Synthesis of [^{3}H]Ap4A.

[^{3}H]Ap4A was prepared chemically according to a modified method of Reiss *et al.*(1965) and Grummt (1978) from [^{3}H]ATP and AMP-morpholidate (adenosine-5'-phosphomorpholidate). Although this method did apparently produce [^{3}H]Ap4A (which was eventually purifiable) it was inefficient and consistantly gave poor yields, possibly due to the problem of ensuring absolute dryness. Khorana (1954) showed that water drastically inhibited the reaction, which is characteristic of these "dismutation" reactions involving morpholidate derivatives. [2,8-^{3}H]Ap4A, in which *both* adenosine molecules are labelled, was obtained eventually from Amersham when it became available as left-over product from a special "custom-synthesis" for another laboratory. This was produced by catalytic exchange using tritium gas - beyond the scope of most laboratory's facilities ! I would suggest that an easier method would be to use the recently published method of Kitebatake *et al.*(1987) which is a much-improved version of a method discovered by Zamecnik *et al.*(1966). Briefly, this involves the enzymic synthesis of Ap4A by leucyl-tRNA synthetase from Bacillus Stearothermophilus. Ap4A is generated in a back reaction of the enzyme from ATP, and when coupled to an ingenious ATP-regenerating system the reaction runs to completion, giving high yields. The

authors did not use radioactive ATP, however, it is difficult to see how the synthesis would be adversely affected by this.

The method used in this work was as follows: AMP-morpholidate (Sigma) was dissolved in dry pyridine (Fisons) and a dilution was made such that 2 mls contained 5 picomoles (the amount of ATP used). The pyridine had been kept as dry as possible over calcium chloride and pipetted into a dry test tube in a polythene bag, filled with nitrogen. In another tube in the bag 100 μCi (5 pmol) of [^{3}H]ATP had been aspirated to dryness, also under nitrogen, and to this was added 2 mls of the AMP-morpholidate in pyridine. A ground glass stopper sealed the tube, which was wrapped in Parafilm before being removed from the bag. The tube was shaken at room temperature for 72 hrs using a shaking machine, after which the pyridine was aspirated in a fume hood. Monitoring of the solution by TLC revealed that no increase in the amount of [^{3}H]Ap4A occurred after this time. The resultant white powder was dissolved in 1 ml of 0.01M sodium acetate pH 7.0 and the tube was shaken for a further 5 minutes, after which the solution was removed and the tube was washed with a further 2 x 1 ml of the same buffer (which were pooled with the first). This was necessary to remove as much material as possible from the long glass tube. TLC analysis showed that [^{3}H]Ap4A was consistently present only as approximately 8% of the total radioactivity, the rest being

[^{3}H]ATP (about 85%) and [^{3}H]adenosine; thus, purification was necessary.

Unsuccessful attempts were made using Dowex-1-acetate and aminoethyl cellulose chromatography and the method finally adopted was that of DEAE-cellulose chromatography using a linear gradient of ammonium bicarbonate, as described in section [8](b). The three resulting peaks (see chapter IV) were confirmed as [^{3}H] adenosine, [^{3}H] ATP and [^{3}H] Ap4A, eluting in order of increasing bicarbonate concentration. The [^{3}H] Ap4A containing fractions (from 180 to 220 mM ammonium bicarbonate) were pooled and lyophilised, and the product was dissolved in distilled water.

Protein assay.

Protein estimation was regularly carried out by the following method (after Bradford (1976)): For one litre of the reagent, 100 mg of Coomassie Brilliant Blue G-250 were dissolved in 50 mls of 95% ethanol/water (v/v)(standard laboratory reagent) to which 100 ml of 85% (w/v) phosphoric acid (BDH) were then added. This was made up to 1 litre with distilled water and filtered regularly before use (Whatman, 3mm). The sample was made up to 100 µl with 0.1M Tris-HCl (pH 7.5) and mixed with 5 mls of the reagent above in a test tube. After standing at room temperature for at least 5 minutes, an aliquot was withdrawn and the absorbance at 595nm was determined in a plastic cuvette using a bench spectrophotometer. The absorbance figure obtained was then related to a protein concentration by means of a standard curve, using BSA (Sigma, type IV) at concentrations ranging from 2 to 150 µg per ml. It was necessary to produce such a curve simultaneously with each batch of samples assayed, due to variations in the absorbance readings; a blank consisted of 5 mls of the reagent mixed with 50 µl of the Tris buffer above and 50 µl of the solution in which the protein sample was dissolved. The lower limit of detection for this assay is 1 µg protein per ml.

Developmental methods.

It should be noted that some of the techniques described in this chapter are the result of a number of developmental steps. For instance, in TLC analysis various problems were encountered, and the adaptations of the basic methods used to try and overcome these are described in the text of chapter IV.

Dangerous chemicals.

Particular care was taken when handling carcinogenic/poisonous and radioactive materials. Users of DMS should be aware that it is volatile, extremely poisonous and carcinogenic. Apart from the usual laboratory precautions, all contaminated solid waste was sealed in plastic bags with a few drops of ammonia (the vapour of which rapidly hydrolyses DMS), and all contaminated liquid waste and glass-ware was immersed in 6M HCl, which again hydrolyses DMS. It is important that the fume cupboard being used is capable of handling such a toxic compound. Standard safety procedures were observed in the use and disposal of [^{3}H]- and [^{32}P]- labelled compounds.

Results and Discussion.

(IV)

Note for figures representing TLCs.

Where more than one TLC is represented in the figure, or where the figure represents [^{3}H] and [^{32}P]dpm in two graphs from the same TLC, the standards have been labelled only once. The length of the area to which the standard has migrated is represented in all cases by a line.

Previous work in this laboratory (Mullen (1983)) has led to the suggestion that L1210 cells may respond to the DNA damage caused by DMS by increased (ADP-ribosyl)ation of low molecular weight material (< 10 000 Da) in addition to an overall increase in the (ADP-ribosyl)ation of proteins. Briefly, the technique developed by Mullen to observe this involved the treatment of these cells with DMS and their permeabilization and incubation with [^{3}H] NAD^+ - the substrate for ADPRT. After precipitation in TCA, the macromolecules were centrifuged into a pellet which was dissolved in a solution of high-strength urea and PMSF - a protease inhibitor. The (ADP-ribosyl)ated proteins were then 'enriched' by passing over a column of DEAE sephadex, which bound tightly to the negatively charged DNA. Proteins which were not closely associated with the DNA were then washed off the column by a buffer containing a low concentration of salt. The DNA-associated proteins (including the majority of (ADP-ribosyl)ated proteins) were then eluted in a solution containing a high concentration of salt, leaving the majority of DNA molecules bound to the DEAE ligands of the column. In a way, this represents a 'DNA-affinity' purification of (ADP-ribosyl)ated proteins. The eluate was dialysed and concentrated before electrophoresis on polyacrylamide rod gels containing urea and SDS, and the radioactive profile of the gels was visualized by the method of Aloyo (1979).

DMS treatment was found to stimulate the overall level of (ADP-ribosyl)ated protein, but particularly high cpm were observed near to the end of the gel, corresponding to material of less than 10 KDa (assuming denaturation and an 'even coating' of SDS on the molecules).

This procedure was repeated as closely as possible in an attempt to verify the result. However, it was not considered worthwhile performing a large number of identical experiments, particularly as the *nature* of the (ADP-ribosyl)ated material is not further described by its position in the radioactive profile of the gel. In a duplicate experiment, 2.95 x 10^6 DMS-treated, permeabilised cells were incubated with 100 µCi [^{3}H]NAD^+ in a final volume of 1ml before the (ADP-ribosyl)ated proteins were enriched and analysed as described above. The incorporation of [^{3}H] into TCA-insoluble material was 605000 cpm (± 11.6%) per x 10^6 cells. At the end of the enrichment, the sample used for electrophoresis contained 876800 cpm, of which only 29.5% was TCA insoluble. However, figure 1.1 shows that over 99.9% remained on the origin when 10 µl were analysed by TLC in a LiCl solvent system . This implies that some of the material is 'too large' (or negatively charged) to move significantly on the TLC plate, and too small to be precipitated out of the solution of 20% TCA.

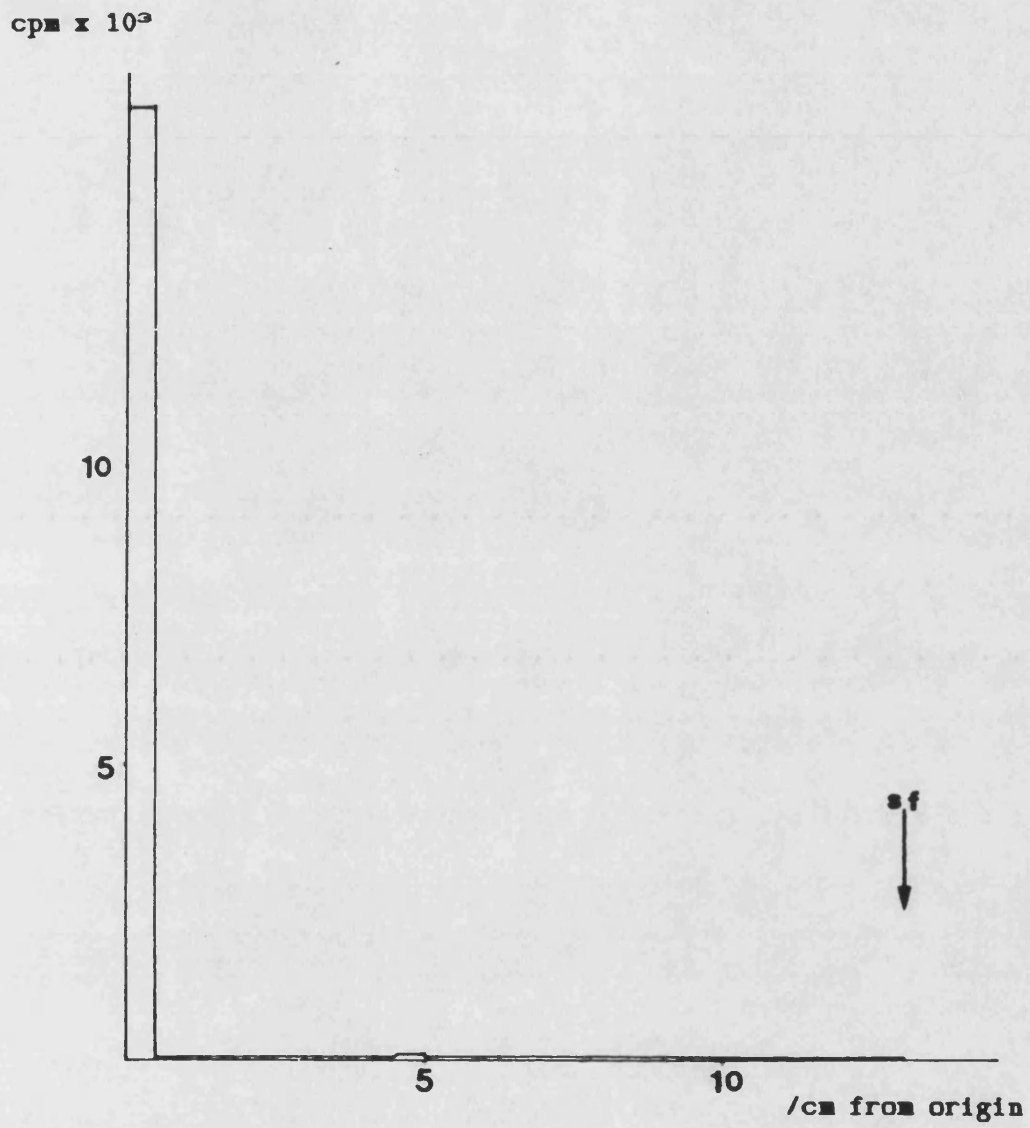

Figure 1.1.

Permeabilised cells were incubated with [³H] NAD^+, and the [³H](ADP-ribosyl)ated proteins were enriched and dialysed after Mullen (1983) - see text for further details. 10µl were applied to a PEI TLC plate which was developed in 0.2M LiCl for 2 min.; 1.0M LiCl for 6 min. and 1.6M LiCl until the solvent front had reached 13cm. The plate was cut into 0.5M strips and each was assayed for radioactivity as described in III.7&8.

(OVER) Figure 1.2.

Polyacrylamide rod gel electrophoresis of enriched (ADP-ribosyl)ated proteins after Mullen (1983). Top: Coomassie Blue-stained "SDS-6 dalton marker proteins" (Sigma). Bottom: radioactive profile after 45µl of the dialysed proteins had been electrophoresed in a parallel gel, fixed, cut into 1mm slices and counted as described in III.10(a).

bpb = bromophenol blue dye.

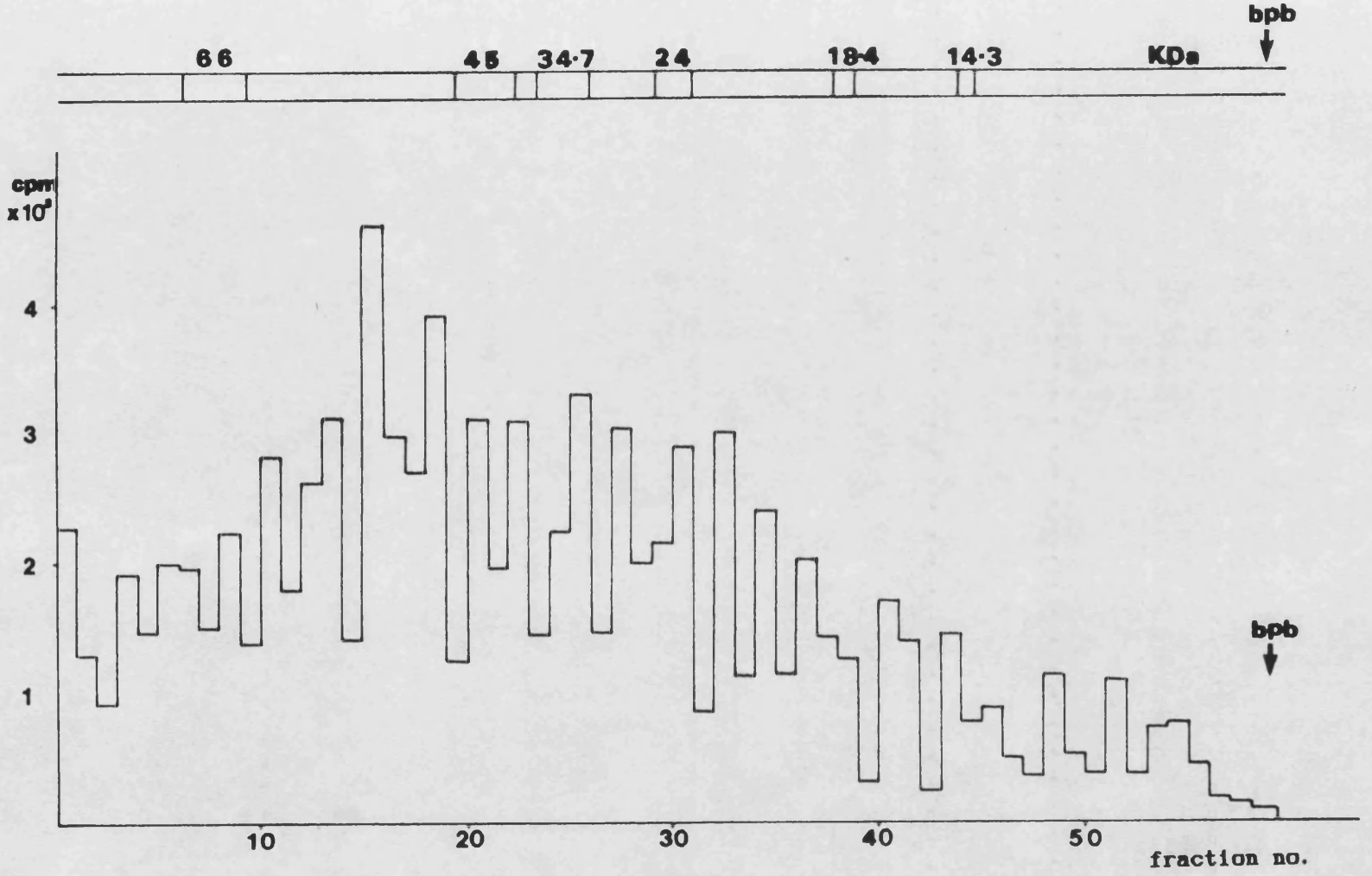
bpb
66
45
34·7
24
18·4
14·3
KDa
cpm
x10³
4
3
2
1
bpb
10
20
30
40
50
fraction no.

45 µl of this solution (approximately 116000 cpm) were used for electrophoresis, and a parallel rod gel was run using a sample of 'SDS-VI' Dalton marker proteins (Sigma) which was stained with Coomassie Blue as described in chapter III.13. Figure 1.2 shows the radioactive profile resulting, and it can be seen that approximately 7.7% of the radioactivity appeared between the bromophenol blue marker (indicating the position of the buffer front) and the position of the 14.3 KDa marker on the stained gel. Although not identical to the findings of Mullen (1983), this does demonstrate that using this technique, [^{3}H] is incorporated (presumably through (ADP-ribosyl)ation) into material of low molecular weight.

Various technical difficulties were encountered with this procedure, particularly in ensuring that the initial pellet resulting from TCA precipitation and centrifugation was fully dissolved (requiring sonication) , and that the majority of (ADP-ribosyl)ated proteins had actually *been* precipitated.

As mentioned in chapter II, it has been reported that under specific conditions highly purified ADPRT, together with 'active' DNA (which co-purified with the enzyme up until a late stage in the procedure) will (ADP-ribosyl)ate the dinucleotide Ap4A in a histone H1-dependant reaction (Yoshihara *et.al.*(1981), Tanaka *et.al.*(1981)).

It was also demonstrated that other nucleotides, such as Gp4G could serve as acceptors for (ADP-ribose)$_n$, always in a histone-dependant reaction (Tanaka *et.al.*(1981)) and it was suggested that binding of the nucleotides to protein is necessary for the reaction to take place. The observation that nucleotides may be (ADP-ribosyl)ated raises the interesting possibility that the effects of these nucleotides upon proteins within the cell may be *regulated* by (ADP-ribosyl)ation. It was also reported by Surowy *et.al.*(1983a) that Ap4A and some other phosphate group-possessing nucleotides caused the apparent proteolytic processing of ADPRT in permeabilised L1210 cells.

The experimental work undertaken in this thesis can be divided into approximately three parts: firstly, an investigation by various means of the results of incubating permeabilised L1210 cells with [^{3}H]NAD$^+$, with emphasis on low molecular weight acceptors for [^{3}H]ADP-ribose, and the effect of DNA damage upon this; secondly, an investigation of the effects of Ap4A upon (ADP-ribosyl)ation in salt/PEI-extracted pig thymus nuclei (a crude extract of nuclear proteins) and in permeabilised cells by again using [^{3}H]NAD$^+$ as a way of labelling the product(s); and thirdly, the use of dual labelling as a means of distinguishing between the adenosine moieties of Ap4A and ADP-ribose. [^{3}H]Ap4A and [^{32}P]NAD$^+$ were incubated with permeabilised L1210 cells in the presence or absence of ADPRT-

inhibiting levels of 3AB and/or Ap4A and the products analysed. The response of the cells to DNA damage under these conditions was also investigated. The latter part of the investigation employed the procedures developed earlier for extracting and isolating the nucleotides from these cells.

To determine whether L1210 cells (ADP-ribosyl)ate small molecules when treated with the DNA-damaging agent DMS, experiments were conducted using [^{3}H]NAD$^+$, the [^{3}H]ADP-ribose moiety of which should become attached to (and therefore label) the acceptors. Initially, it was of interest to see whether such an (ADP-ribosyl)ated molecule was soluble in 20% TCA, and/or whether it was possible to isolate it from the bulk of the larger (ADP-ribosyl)ated molecules of the cell by ultracentrifugation.

A culture of L1210 cells were grown until they reached "log phase", split into two and incubated for one hour with or without DMS (final concentration, 100µM) as described in Chapter III.1 . After permeabilisation (see III.2) 5 x 10^6 cells from each batch were incubated with 20µCi of [^{3}H]NAD$^+$ (at 50µM) for ten minutes at 26°C in a final volume of 1ml (see III.3). Two aliquots of 20µl were removed and assayed for TCA-insoluble radioactivity as described in III.7, and the reaction was stopped by the addition of ice-cold 100% TCA to a final concentration of 20%. The contents of the reaction tube were transferred to a 5ml nitrocellulose ultracentrifugation tube, and the tube was washed with two further 1ml of 20% TCA, which were also added. The final volume was brought to 5ml with more 20% TCA, and the samples were ultracentrifuged for one hour at 45 000 rpm and 4°C, after which the supernatants were carefully removed and shaken with 2

x 2ml of ether (SLR) until the pH was ≥6. The volume of the resulting sample was then determined, and 20µl were applied to a PEI TLC plate, with ADP-ribose and NAD^+ as standards (see III.8.a). The developing system used 0.2M, 1.0M and 1.6M LiCl for 2 minutes, 6 minutes and to 13 cm respectively, and the plate was cut into strips and assayed for radioactivity as described.

Table 1.

	DMS-TREATED	σ_{n-1}	CONTROL	σ_{n-1}
TOTAL TCA-INSOLUBLE RADIOACTIVITY (cpm)	331 000	±1.9%	158 000	±1.4%
TOTAL TCA-INSOLUBLE RADIOACTIVITY ASSAYED FROM ULTRACENTRIFUGE SUPERNATANT (cpm)	118 000	±7.9%	69 000	±15.7%

Table 1 shows that DMS caused a 2.1-fold stimulation of (ADP-ribosyl)ation, as measured by the incorporation of radioactivity into TCA-insoluble material. When some of the ether-extracted supernatant was similarly assayed for TCA-insoluble radioactivity, it was found that a small quantity was retained on the GFC discs which amounted to approximately 20 000 cpm per 10^6 cells. The aliquots taken from the initial incubation mixtures for this assay represented 1/50th of the

total volume and amounted to between 3 and 6000 cpm of TCA-insoluble radioactivity. However, the aliquots taken from the supernatants represented only 1/175th of the total volume, and the amount of TCA-insoluble radioactivity per sample was lower by a factor of 10 (5-700 cpm). Thus, the errors quoted above are higher in the latter case.

Figure 2.1 shows the radioactive profiles of the DMS-treated and control samples on TLC. It is perhaps notable that treatment with DMS appeared to cause elevated levels of free ADP-ribose (from 26.1 to 40.2% of the total radioactivity on the plate), as well as reduced amounts of [^{3}H]NAD$^+$ (from 65.9 to 47.0%). The most relevant observation, however, is that the area on and around the origin of the plate contains only a small amount of radioactivity, and that there is little difference between the DMS-treated and control samples in this aspect. If a figure is extrapolated for the entire supernatant from 5 x 10^6 DMS-treated cells, this would mean approximately 175 000 cpm were "origin material", which is small in comparison to the $\simeq$ 22x10^6 cpm of [^{3}H]NAD$^+$ present! If this material were produced in response to DNA damage, then it should not be present in the TLC profile of the control sample. Non-specific binding of a very small proportion of the total (20 µCi) [^{3}H]NAD$^+$ to the origin of the plate could be the cause of its appearance, although the proportion in relation to the total TCA-insoluble

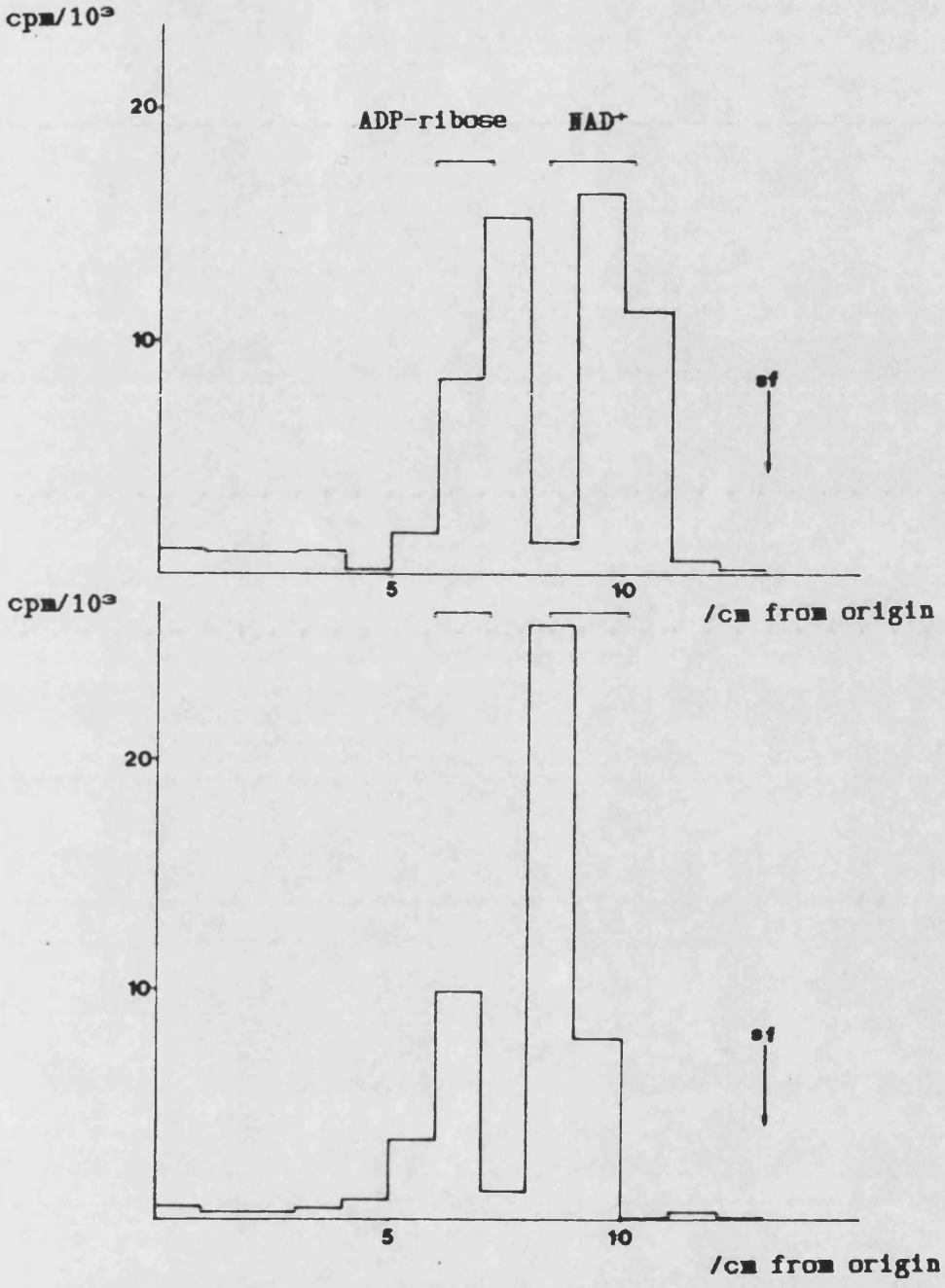

Figure 2.1.

TLC (in 3-step LiCl system - see figure 1.1) of 20µl aliquots of 20% TCA/ultracentrifuged supernatants from (top) 100µM DMS-treated and (bottom) control cells, which had been permeabilised and incubated with [^{3}H]NAD$^+$. See text for further details. ADP-ribose and NAD$^+$ standards (underlaid) migrated as indicated.

radioactivity precipitated initially is *not* small. The amount of radioactivity present on the orgins of these TLC plates is of the same order as the amount retained on a GFC disc when an equal aliquot of the supernatant was passed through it and washed with 5% TCA. This suggests that the material is not (ADP-ribosyl)ated nucleotide, since it is known that such molecules are not TCA-precipitable (Yoshihara *et.al.*(1981)). It is possible that this material is (ADP-ribosyl)ated protein which has been precipitated by the TCA, but remains un-pelleted by the ultracentrifugation procedure, and thus 'contaminates' the supernatant.

In a further experiment, the DNA damage was increased by elevating the DMS concentration to 500μM, and the TLC plate was developed to 15cm in an attempt to exaggerate any unobserved effects, and to increase the separation of [^{3}H]ADP-ribose/NAD$^+$ from the origin. The resulting TLC profile (Figure 2.2) shows a similar (relatively small) amount of radioactivity on the origin.

A cruder separation of 'small' and 'large' (ADP-ribosyl)ated material was also performed by the omission of ultracentrifugation in the above procedure, and its replacement by a step which consisted of filtration of the material (in 20% TCA) through two GFC discs successively laid onto the sintered glass surface of a millipore apparatus. The discs were washed with a further 2 x 1ml of ice-cold 20% TCA and these washes were pooled with the first filtrate. The

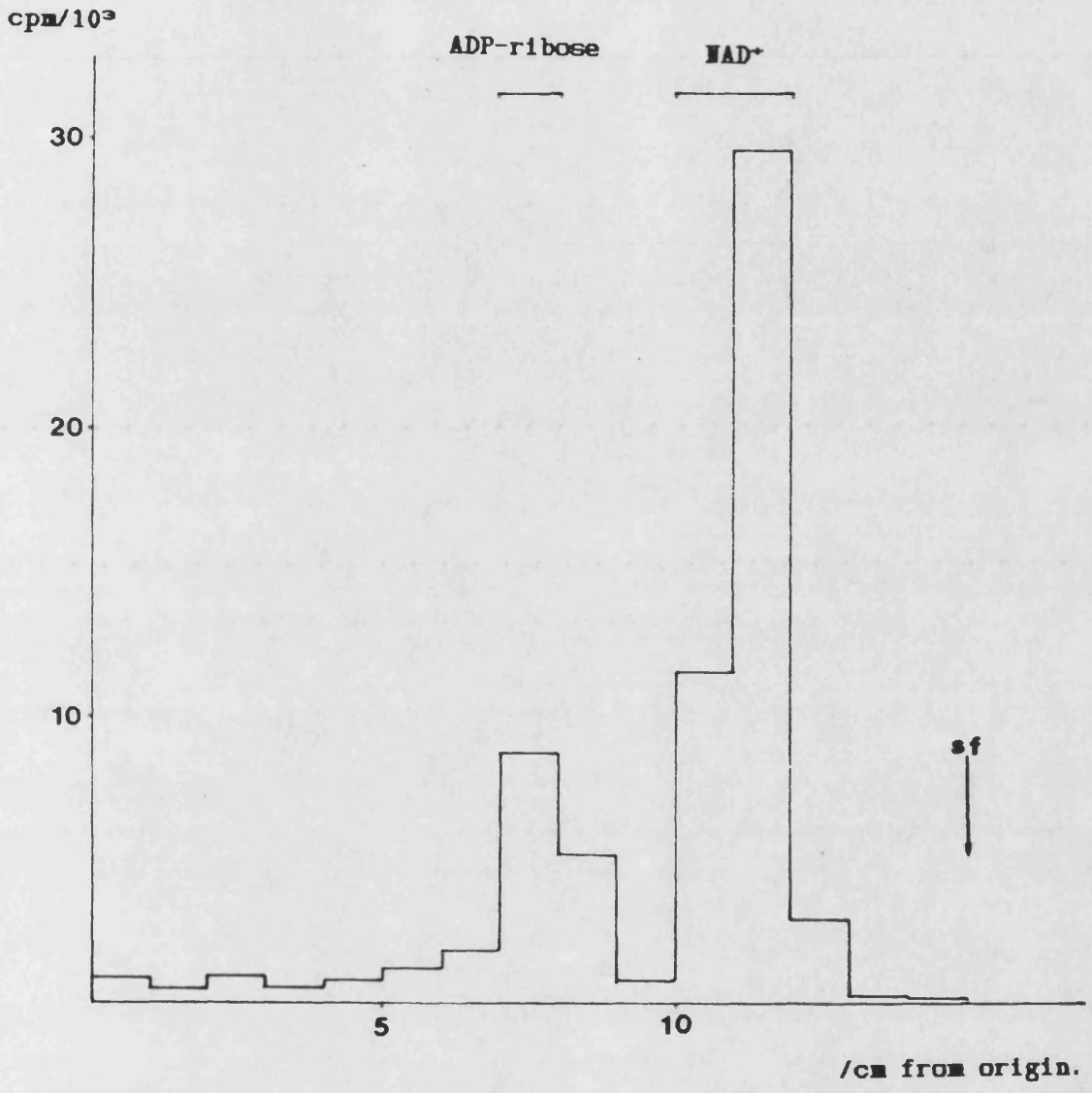

Figure 2.2.

TLC of ultracentrifuged TCA-supernatant as in figure 2.1, except that the cells were treated with 500μM DMS.

discs were then washed with 5ml ethanol 95% (v/v) which was discarded), separated and assayed for radioactivity as described in III.7 .

The filtrate pool was then ether extracted as before until the pH was ≥ 6, and then checked for TCA-insoluble material by re-precipitating 20µl aliquots in 4ml ice-cold 20% TCA and passing through a GFC disc. 20µl aliquots were also subjected to the TLC system described above.

Table 2.

	DMS	σ_{n-1}	CONTROL	σ_{n-1}
INITIAL ASSAY FOR TOTAL TCA-INSOLUBLE RADIOACTIVITY (cpm)	256 200	±8.1%	66 700	±16.8%
TOTAL RADIOACTIVITY COLLECTED ON FILTERS (cpm)	146 111	-	43 380	-
TOP DISC	138 821	-	34 415	-
BOTTOM DISC	7 290	-	8 965	-
TOTAL TCA-INSOLUBLE RADIOACTIVITY IN GFC FILTRATE (cpm)	37 400	±78.0%	19 100	±3.1%

Table 2 shows that 100µM DMS stimulated the incorporation of radioactivity into TCA-insoluble material by 3.8 times - much more than in the previous experiment (2.1 times). This ratio, which was

obtained when aliquots were taken from the incubation just before the end and TCA-precipitated separately, is also approximately the same as that arrived at when the radioactivity on the upper and lower discs from each sample was totalled - although the *amount* of radioactivity is lower than that extrapolated from the first assay.

It was consistantly observed throughout this work that the extent to which DMS stimulated (ADP-ribosyl)ation was variable, and was probably related to the general 'health' of the cell culture, as well as the success of the permeabilisation procedure. Even though great care was taken to standardize this procedure, variations between different batches of cells were always observed - particularly when the cells were DMS-treated. The usual stimulation found was about 1.6 times - a similar figure to that found by others (Kreimeyer *et.al.*(1984)).

The fact that the total radioactivity collected on the discs is less than the total extrapolated from the initial assay may imply that the upper disc was 'saturated' with [^{3}H], or that quenching was occurring. It also appears that TCA-*in*soluble material not only passed through the first disc and onto the second, but that some was present in the filtrate as well (the error here is high because the actual cpm were in the order of 100 above background, and the extrapolation for the 'total' figure involved a multiplication factor of $\simeq$ 150). Thus, the analysis of the TLC profiles of the filtrates

(Figure 2.3.) is made difficult, due to the likelyhood that any (ADP-ribosyl)ated nucleotide(s) appearing at the origin or near-origin would be masked by the presence of contaminating TCA-insoluble material which has 'escaped' the GFC discs.

Radioactivity on the origin *was* observed, (figure 2.3.) however it was present in similar amounts in the filtrate from both DMS-treated and control cells. This further implies that whether the origin material is (ADP-ribosyl)ated nucleotide or 'contaminating' (ADP-ribosyl)ated protein/protein fragments, its presence is not increased by DMS-treatment of the cells. This origin material represents about 300 000 cpm per 5 x 10^6 cells, and in an attempt to characterize it, 30 000 cpm (300µl) were digested with 0.05 units of snake-venom phosphodiesterase (unpurified) as described in III.11 . Figure 2.4 shows the TLC profile of the resulting digest, in which the origin material is seen to have disappeared. This suggests that it was either (ADP-ribose)$_n$ in the form of a dimer, or that it was (ADP-ribosyl)ated nucleotide, however, both of these are soluble in 20% TCA! As mentioned in III.11, commercial preparations of venom phosphodiesterase are contaminated with sometimes high levels of other enzymic activities, among them, 'nucleosidase' activity which acts endonucleolytically to split (eg.) [^{3}H]NAD$^+$ into [^{3}H]AMP and NMN. The single large [^{3}H]AMP peak in Figure 2.4 is the result of this.

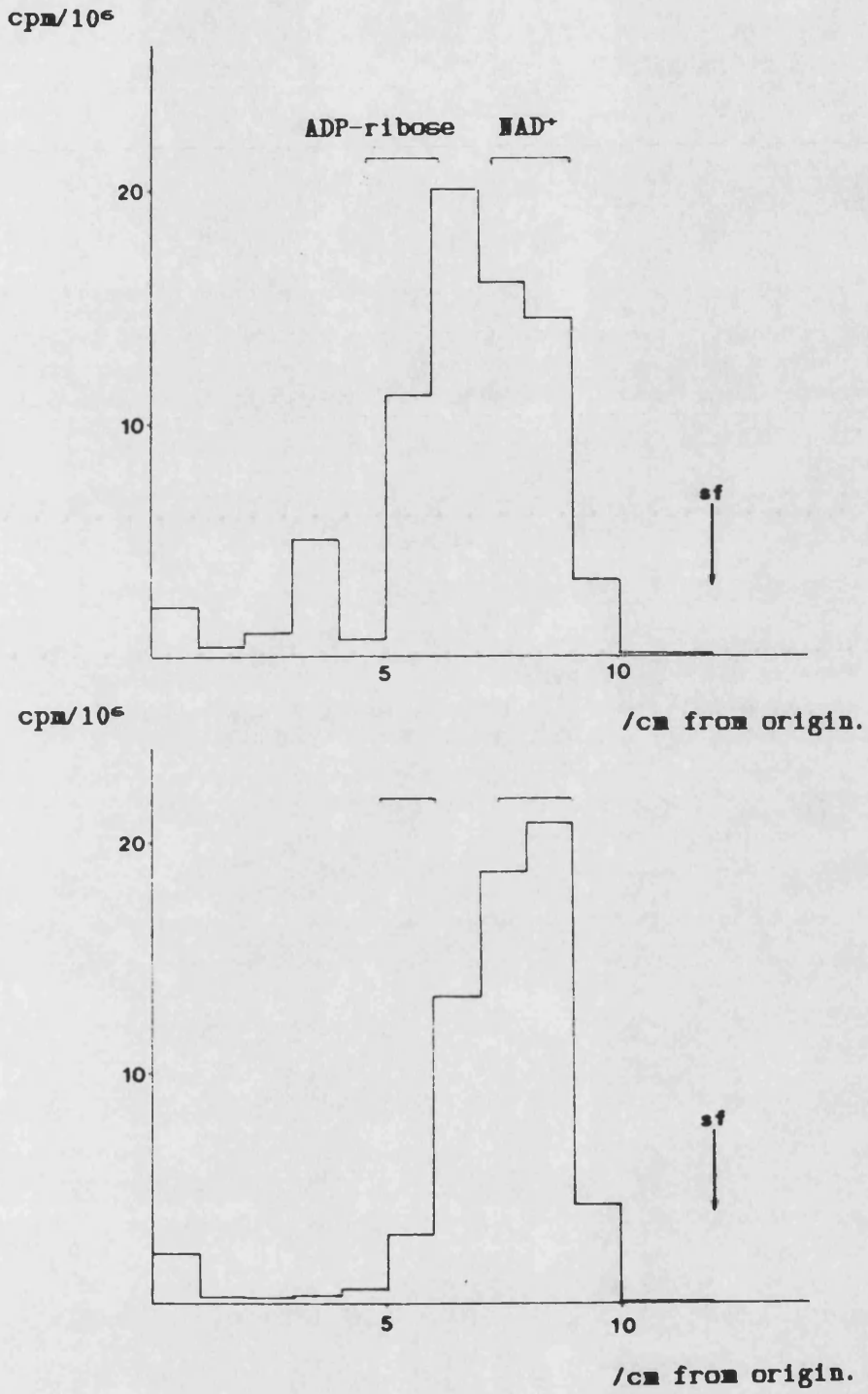

Figure 2.3.

TLC (in 1.6M LiCl system) of small aliquots of the filtrates from 100 μM DMS-treated (top) and control (bottom) cells which had been permeabilised, incubated with [^{3}H]NAD$^+$, TCA-precipitated and then passed through 2 GFC discs. ADP-ribose and NAD$^+$ standards ran as indicated. See text for further details.

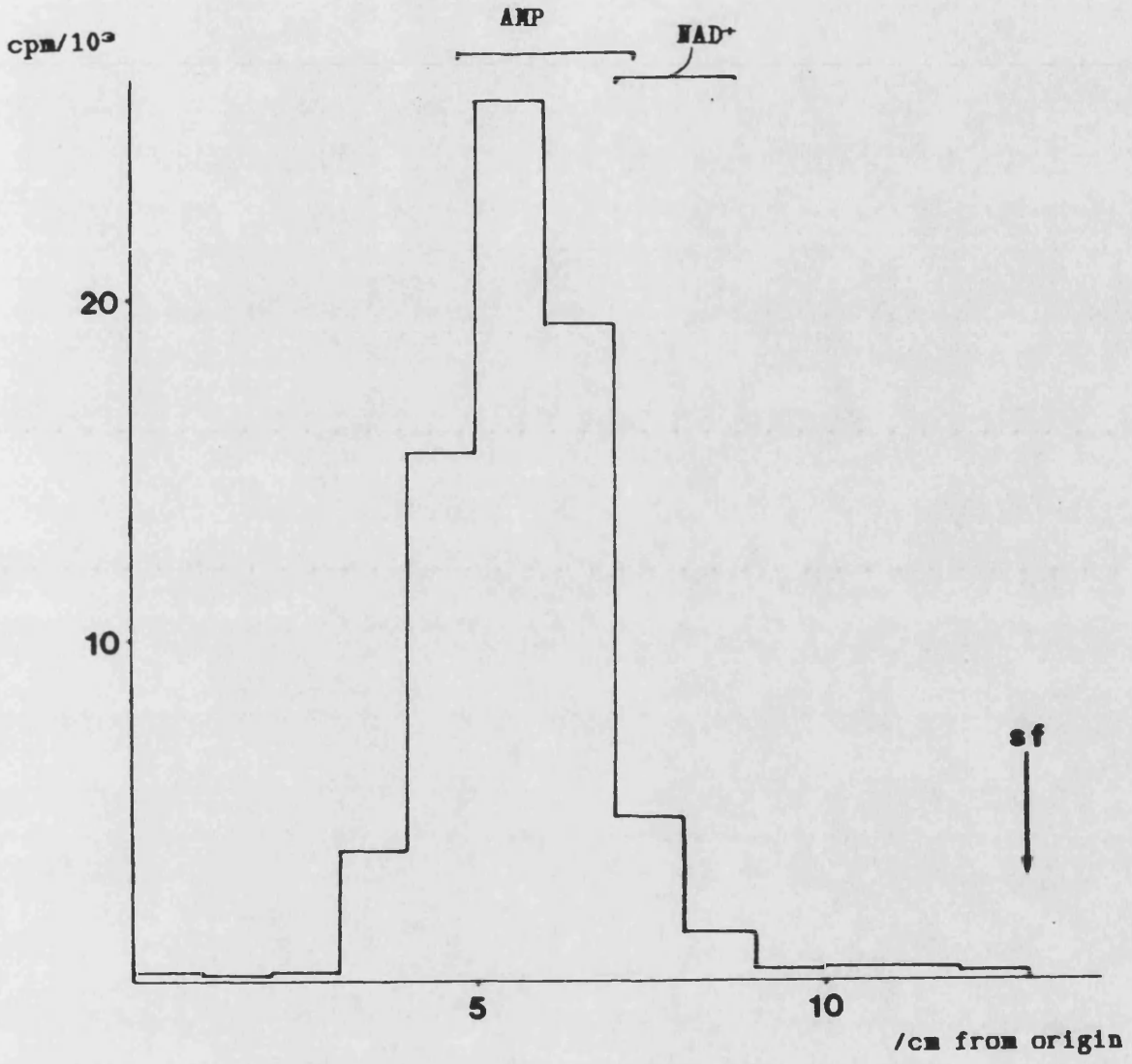

Figure 2.4.

30 000cpm of the filtrate from the DMS-treated cells (figure 2.3) was digested with 0.05 units of snake venom phosphodiesterase, as described in III.11. This is a TLC (1.6M LiCl) of a 20µl aliquot after 1 hour's digestion. Note the disappearence of origin material, and poor separation of NAD^+ and AMP standards.

It was decided that TCA precipitation and ultracentrifugation or GFC-filtration were unsatisfactory methods for the isolation and analysis of 'small material' from the cells.

Attempts to remove the possibility of protein "contamination" in extracts from the cells involved the use of filtration through a semipermeable membrane, similar to that found in dialysis tubing, which allows molecules of less than 10 000 Da to pass through it. This membrane was purchased commercially (from Amicon) and was incorporated into a plastic tube (a "Centricon") which was centrifuged in a fixed-angle rotor at a maximum of 5000g.

As before, L1210 cells were incubated with or without 100μM DMS, permeabilised and then incubated with [^{3}H]NAD^{+}. In order to avoid the problems mentioned above with TCA-precipitation (and because the membrane breaks down in 20% TCA) glacial acetic acid was added to stop the reaction to a final concentration of 0.1M. After vigorously mixing and cooling on ice, the resulting mixture was placed in the upper chamber of a Centricon and centrifuged at 6500 rpm for two hours at 4°C. Because of the angled rotor, the volume of liquid retained in the upper membrane is always ≥30μl, although the time taken for ≈ 970μl to pass through the membrane was found to vary greatly, depending upon the viscosity of the solution to be filtered. This meant that no more than 2 x 10^{6} cells (in a volume of 1ml) could practically be filtered per membrane.

In one such experiment, the filtrates from DMS-treated and control cells (2 x 10^6 each) were assayed for TCA-insoluble radioactivity. It was found that the 'DMS' filtrate contained a total of 3150 cpm against a total of 1080 cpm for the 'control'. 20µl aliquots from these filtrates were then applied to a PEI TLC plate as before and developed in 1.6M LiCl. Figure 2.5 shows the radioactive profiles of the two filtrates and it can be seen that in both cases a small amount of radioactivity remains on the origin. This material represents 2.0% of the total cpm for the control-filtrate and 1.5% for the DMS-filtrate. Comparing the amount of radioactivity (in cpm) remaining on the origin when a 20µl portion of the filtrates is subjected to TLC with the amount which is TCA-insoluble reveals that the filtration was successful in removing (ADP-ribosyl)ated material which is large enough to be precipitated by 20% TCA. Approximately ten times the amount of radioactivity is present in the filtrates as TLC-origin material rather than as TCA-insoluble material. Precipitation of the cells in 20% TCA followed by ultracentrifugation or GFC-filtration still resulted in significant levels of (ADP-ribosyl)ated larger material being present together with the smaller molecules. A simple filtration of the cells after incubation with [^{3}H]NAD^+ has shown that a very small proportion of the filtrate contains radioactive material that stays on the origin of a TLC system in which molecules such as NAD^+ and ADP-ribose will move from

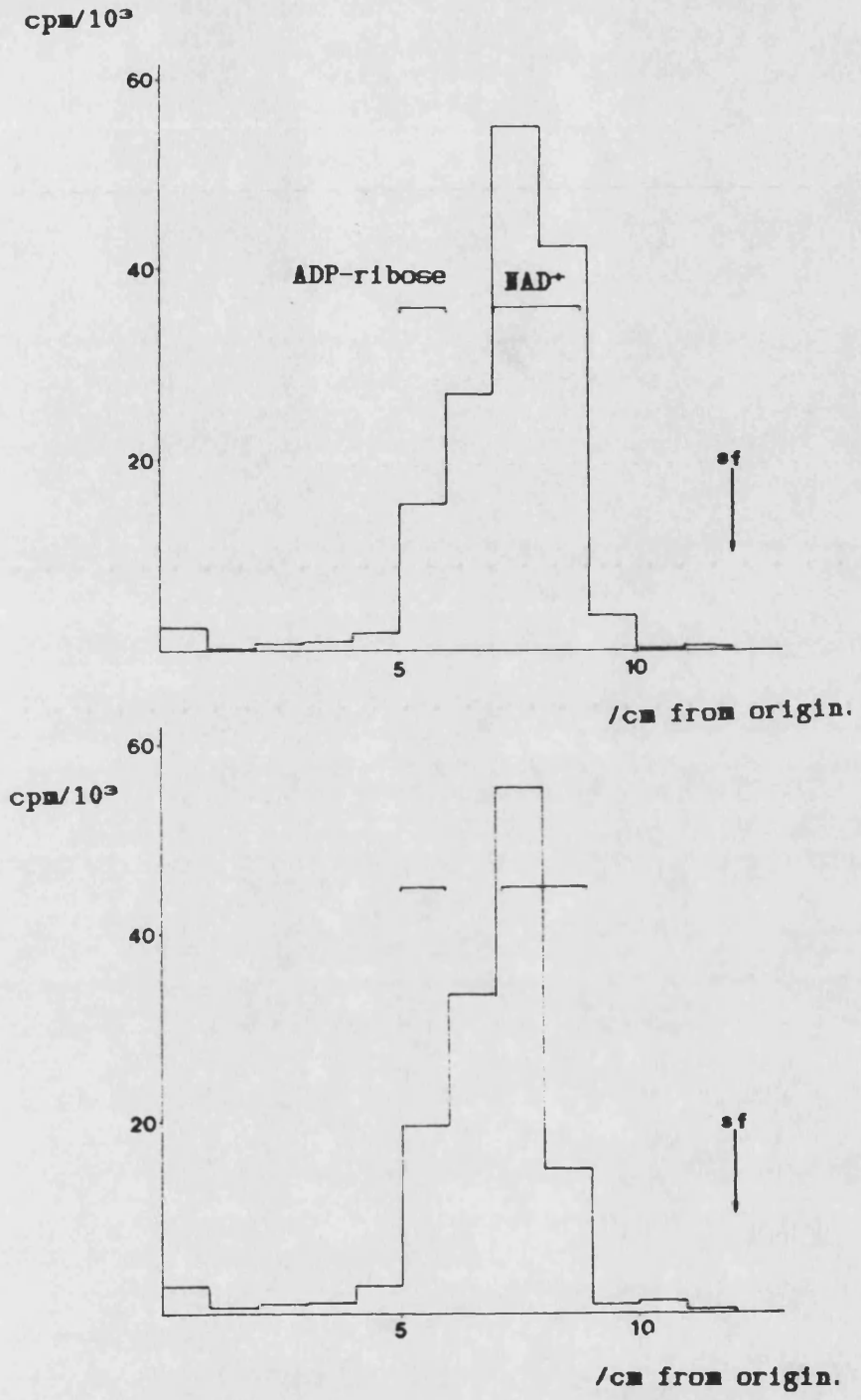

Figure 2.5.

20µl aliquots of the 'Centricon' filtrates from DMS-treated (top) and control (bottom) cells, permeabilised and incubated with [^{3}H]NAD$^+$ were subjected to TLC analysis in the 1.6M LiCl system. ADP-ribose and NAD$^+$ standards ran as indicated. See text for further details.

it. Although small (about 100 000 cpm for 2 x 10^6 of the DMS-treated cells) it was thought that this material warranted further investigation.

The filtrate from the DMS-treated cells was then subjected to digestion with (unpurified) snake venom phosphodiesterase as before. A control incubation was carried out simultaneously, in which the same quantity of filtrate (50µl) was incubated at the same pH (8) with 0.1M Tris-buffer in the same volume (100µl). 20µl aliquots of each were taken after 1 hour's incubation at 37°C for TLC analysis. This time, the developing system used was the three-step 0.2,1.0 & 1.6M LiCl system described above, which provided better separation between NAD^+ and 5'AMP than the one-step 1.6M LiCl system. Figure 2.6 shows the radioactive profiles of the digested and control samples, and it can immediately be seen that the origin material is depleted by the digestion, as found above with the GFC-filtrate. The [^{3}H]NAD^+ has been exhaustively digested by contaminating nucleosidase activity to yield [^{3}H]AMP.

The centrifugal filtration of such a complex mixture as this (basically, disrupted whole cells) is frought with problems, and many experiments were performed in which the macromolecules of the cells aggregated to form a viscous 'gel' which impeded the rate of filtration to almost nil. It was felt that the technique would prove

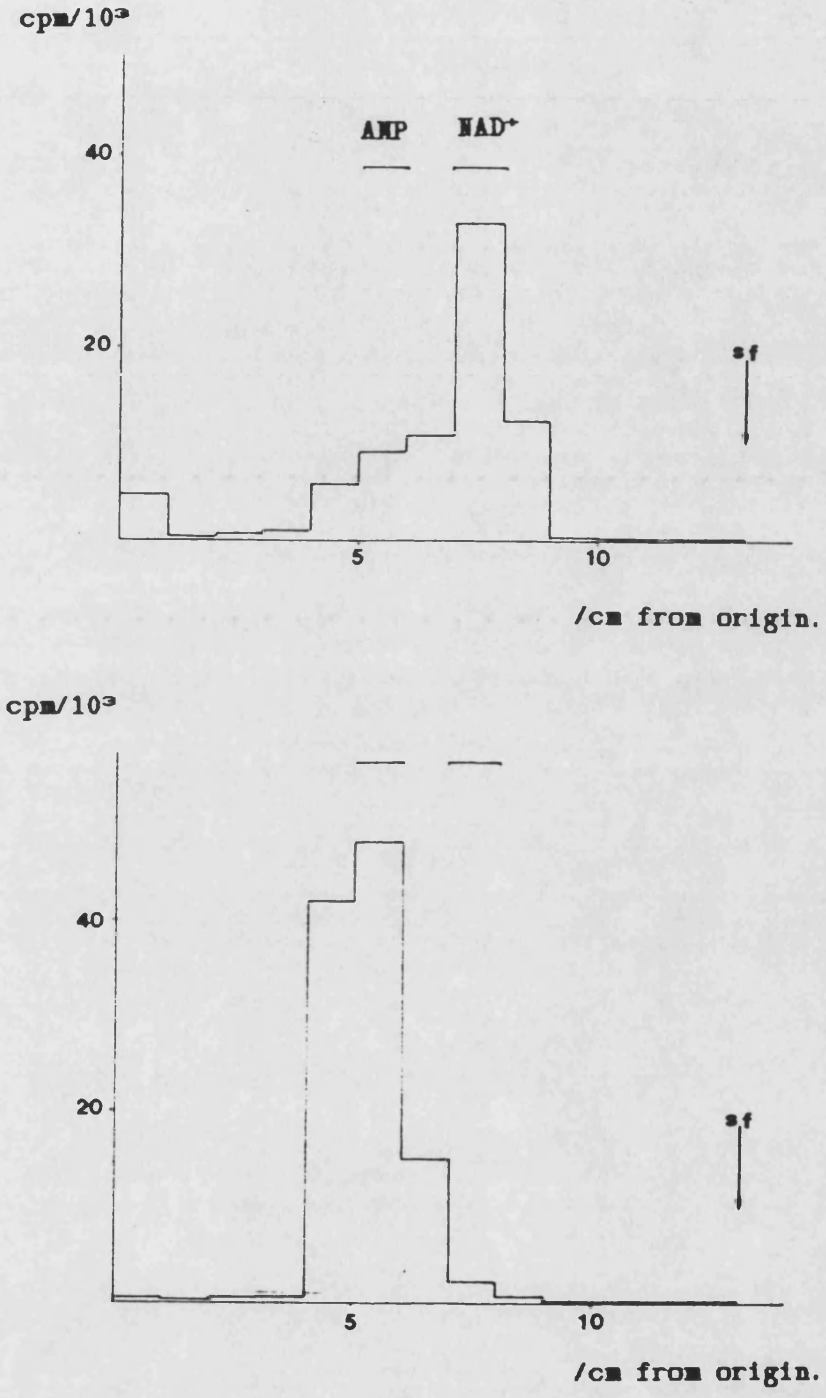

Figure 2.6.

The 'Centricon' filtrate from DMS-treated cells (figure 2.5) was digested with snake venom phosphodiesterase as before and analysed in the three-step LiCl system (as in figure 1.1) to afford better separation of NAD^+ and AMP. Top: control, incubated in Tris. Bottom: digested. See text for further details.

more useful at a later stage in the extraction of small molecules from the cells.

The technique finally adopted for the isolation of small molecules is a modification of a procedure used routinely for the extraction of DNA and RNA. This is described fully in chapter III.6 .

In an early experiment, L1210 cells in log phase were permeabilised and incubated, as before, with [^{3}H]NAD^{+}. After removing aliquots for assaying TCA-insoluble radioactivity, an equal volume (500µl) of a mixture of ice-cold water-saturated phenol, chloroform and IAA in the proportions 1/1/$^{1}/_{24}$ was added, and the tube was sealed and mixed for 2 x 30s, with 30s resting on ice inbetween. The resulting opaque mixture was then centrifuged for 10 minutes at full-speed (12 000 g) in a bench centrifuge (MSE) at 4°C. This caused the mixture to clearly separate into a lower ("chloroformic") layer and an upper ("phenolic"/ aqueous) layer, with a disc of denatured protein sandwiched between them at the interface. The supernatant was carefully extracted, leaving ≈ 40µl above the undisturbed interface, and extracted with ether as described in III.6.

When assayed for TCA-insoluble radioactivity, this supernatant contained 9083 (+/-2243)cpm in total (the small aliquots assayed contained very low levels of TCA-insoluble radioactivity, thus producing a high error figure), which represents the phenol-soluble/TCA-insoluble radioactivity produced by 750 000 cells incubated with 20μCi [^{3}H]NAD$^+$ in a volume of 500μl. This compares with a figure of 131 677 (+/-16.4%) cpm for the total TCA-insoluble radioactivity before phenol extraction, and it means that 7.4+/- 2.9% remains in the supernatant.

A small aliquot of the ether-extracted supernatant was subjected to TLC analysis, using the acetic acid/LiCl developement described in chapter III.8,(a). In addition a third of the supernatant was subjected to gel filtration on Biogel P2, using 0.1M acetic acid as the running buffer and dextran Blue and bromophenol blue as molecular weight markers, as described in III.9 . The object of the former was to determine whether the TCA-insoluble radioactivity found in the supernatant stayed on the origin, and the latter was to determine whether it would be excluded by the Biogel P2 (which excludes material of $\geq$ 10 000 Da).

Figure 2.7 shows the radioactive profile on the TLC plate, and, concentrating on the origin, it can be seen that 2.1% of the total radioactivity remained immobile. This represents approximately 84 000

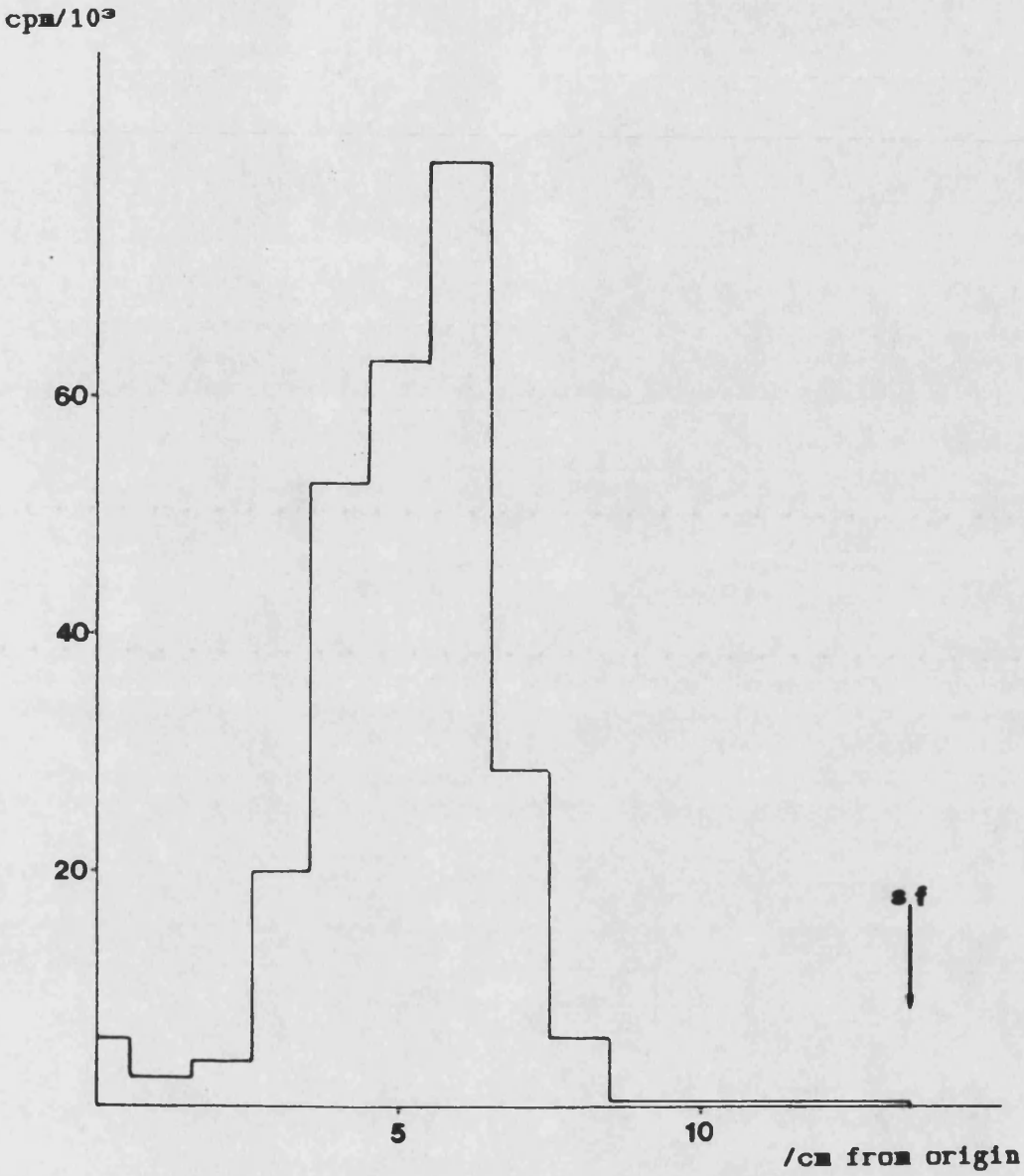

Figure 2.7.

TLC (in the acetic acid/LiCl system see III.8(a)) of 20µl from the ether-extracted phenolic supernatant from permeabilised cells incubated with [³H]NAD⁺. The first cm from the origin was divided into two 0.5cm fractions, since only this area was of interest (see text).

cpm for the whole supernatant, which is clearly greater than the 9000 cpm which were TCA-insoluble! This is probably due to the fact that, in this system, a molecule such as [^{3}H]ATP stays on the origin, thus rendering it impossible to distinguish between it and (ADP-ribosyl)ated protein. Figure 2.8 shows the result when aliquots were taken from the 1ml column fractions (collected at 40ml/hr) and counted for radioactivity. It can be seen that a small quantity (≃ 1000 cpm) is excluded from the gel and appears in the 'void volume'(with the dextran Blue). As explained in chapter III.9, the accurate resolution of nucleotides by gel filtration on Biogel P2 is not reliable, although it is probable that the largest peak consists of [^{3}H]NAD$^+$. The radioactivity in the void volume implies that approximately 3000 cpm in the supernatant would be excluded from Biogel P2, and is thus perhaps TCA-precipitable.

This experiment was repeated with a greater density of permeabilised cells (500µl contained 2 x 10^6), one batch of which had been pre-treated with 100µM DMS as described before. In this case, even more TCA-insoluble radioactivity appeared in the supernatants - 17.1% of the total for the DMS-treated cells and 16.4% for the control cells. Again, filtration on Biogel P2 produced small quantities of radioactivity in the void volume of the column (3 - 4000 cpm for the entire supernatant from 2 x 10^6 cells). This was observed for both the DMS-treated and control cells.

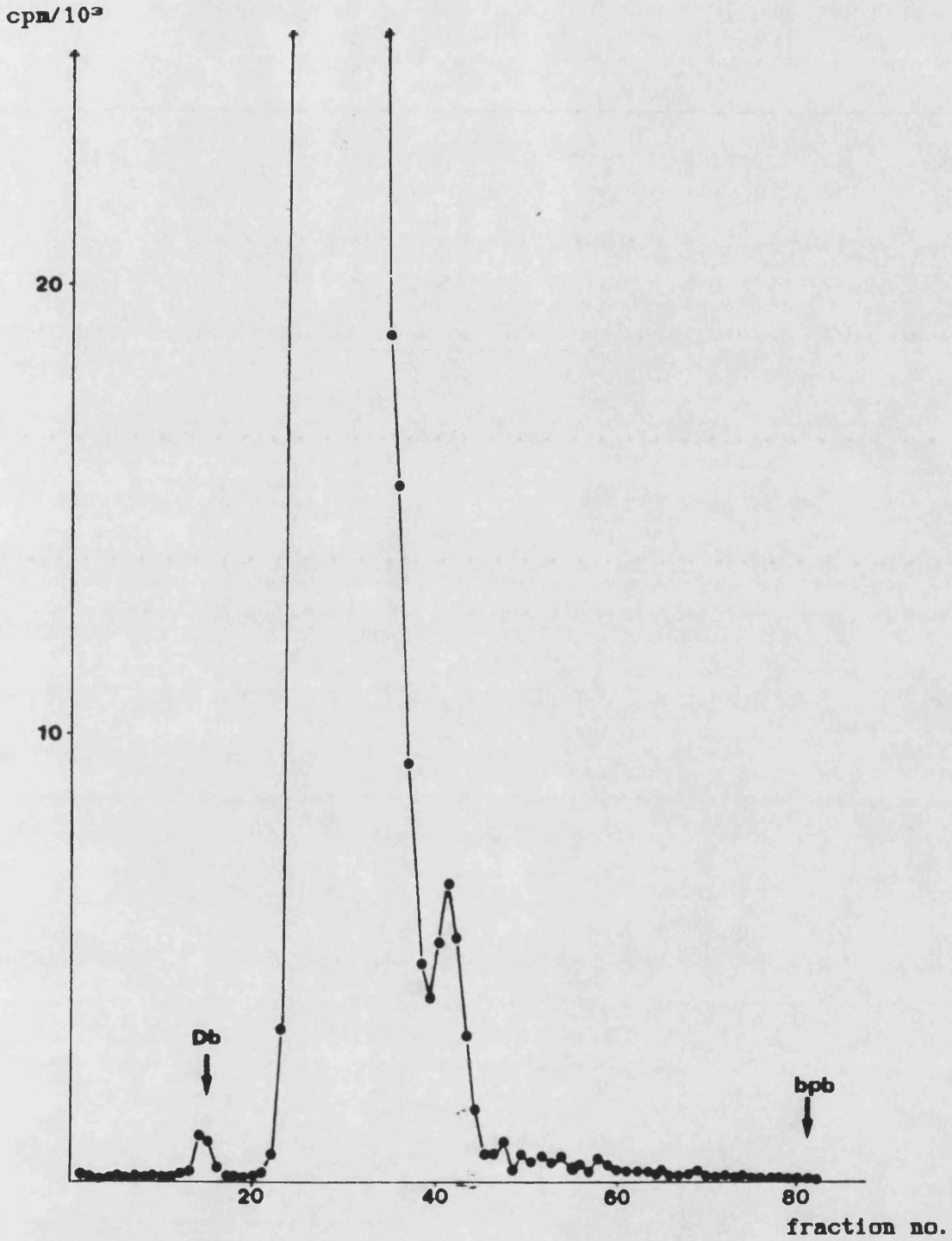

Figure 2.8.

Gel filtration on Biogel P2 of 1/3rd of the ether extracted phenolic supernatant in figure 2.7. 1 ml fractions were collected at 40 ml/hr and assayed for radioactivity as described in the text. Each point represents the entire radioactivity in the fraction. The elution positions of bromophenol blue (bpb) and dextran Blue (Db) are shown (Db is excluded from the column and therefore emerges in the void volume of the column.

An experiment was conducted in order to find out the relationship between the proportion of (ADP-ribosyl)ated protein deposited on the chloroform/phenol interface and that which remains in the supernatant after centrifugation. Five drops of L-(4,5-[^{3}H]) leucine were added to a 50ml cell culture at 4 x 10^5 cells/ml which was allowed to grow for 12 hrs before harvesting and permeabilisation, as before. The [^{3}H]leucine became incorporated into the proteins of the cells, and this typically produced 46 000 cpm of TCA-insoluble radioactivity per 1 x 10^6 permeabilised cells. Batches of these cells were diluted, either with more isotonic buffer (see III.2) or with different amounts of unlabelled, permeabilised cells and then phenol extracted. A further step was added to the phenol extraction procedure which involved 'back-extraction' of the chloroform/phenol interface with 0.5 ml of 0.1M sodium acetate (pH 5.5). This was mixed with the contents of the tube after 450µl of the supernatant had been extracted, and centrifuged as before. Table 3 shows the results of this experiment.

It was found that the amount of TCA-insoluble radioactivity present in this second,'back-extracted' supernatant was indistinguishable from the background cpm; however, back-extraction was adopted on all later occasions in order to extract as many nucleotides as possible from the protein deposited at the chloroform/phenol interface.

Table 3.

[^{3}H]-labelled cells /10^6	unlabelled cells /10^6	TCA-insoluble radioactivity in supernatant (cpm) σ_{n-1}
1.0	-	10773 +/- 18
1.0	0.4	3906 +/- 540
1.0	0.8	1188 +/- 144
1.0	2.0	1129 +/- 90

One million of these cells contained 45 848 +/-(0.3%)cpm of TCA-insoluble radioactivity, and if this is taken as 100%, phenol extraction has resulted in the removal of only 78% from the supernatant when no unlabelled cells are present. When diluted with 2 x 10^6 unlabelled cells, however, it can be seen that 98% (+/- 8.0%) of TCA-insoluble radioactivity is removed from the supernatant. In an attempt to assay the TCA-insoluble radioactivity present in the protein at the chloroform/phenol interface of the latter sample, it was sonicated in a sonicating water bath for 20 minutes in 1ml 8M urea/0.1M sodium acetate, pH 5.5, and portions were TCA-precipitated. Even with sonication, some undissolved protein was still visible, but the soluble portion contained a total of 40 440 (+/- 4300)cpm or 88.2 +/-9.4% of the total TCA-insoluble radioactivity. This compares with 15 +/-0.5 % for the sample to which no unlabelled cells were added. In later experiments, the addition of 100µl of BSA in water (at

0.1mg/ml) was found to be more convenient than permeabilised cells, and had the same effect of acting as a "carrier" in removing proteins from the phenolic supernatant.

In order to see if even more of this remaining TCA-insoluble radioactivity could be removed from the phenolic supernatant, an experiment was performed in which cells were permeabilised, incubated with [^{3}H]NAD$^+$ and phenol extracted exactly as before, exept that one batch was centrifuged at the normal 12 000 g and another was subjected to ultracentrifugation at 45 000 rpm. 100µl of 0.1mg/ml BSA was added to each before mixing with the phenol/chloroform/IAA to facilitate the 'co-precipitation' described above. The supernatants were extracted and assayed for TCA-insoluble radioactivity. Each batch contained 0.98 x 10^6 cells, which were incubated with 5µCi [^{3}H]NAD$^+$. The total TCA-insoluble radioactivity remaining in the bench-centrifuge supernatant was 2040 ± 424 cpm and that left in the ultracentrifuge supernatant was 1764 ± 508 cpm, which means there is no significant difference between the two methods within the margins of the errors (which were relatively large because of the low levels of radioactivity being measured - only 1-200 cpm above background).

Experiments were conducted in an attempt to characterize the TCA-insoluble radioactivity in the phenol supernatant, including

tests for sensitivity to neutral and basic NH_2OH, different pHs and 'digestion' with venom phosphodiesterase, spleen phosphodiesterase, ribonuclease and protease. The results from these, however, were inconclusive due to the very low levels of radioactivity being measured, and so within the margin of the errors, no significant effect was observed with any of these treatments.

In a final attempt to remove the material, the supernatant obtained from 0.5 x 10^6 permeabilised (pre-DMS-treated) cells incubated with 20μCi [^{3}H]NAD^+ was brought to 2ml with 0.1M sodium acetate (pH 5) and filtered through a 'Centricon' membrane, as described previously. When the retentate above the membrane reached the minimum volume of ≃ 40μl, it was diluted with a further 2ml of the same buffer and the mixture was re-centrifuged as before. This was repeated two more times, the retentate being assayed for TCA-insoluble radioactivity each time. Table 4 shows the results from this experiment.

Table 4.

	Total radioactivity (cpm)	σ_{n-1}	TCA-insoluble radioactivity	σ_{n-1}
1st filtration	8 270 200	+/- 31 550	16 100	+/- 800
2nd filtration	3 942 400	+/- 15 040	11 200	+/- 330
3rd filtration	1 584 400	+/- 6 044	6 850	+/- 100
4th filtration	104 851	+/- 400	5 746	+/- 1 794

Even after a total of 6 hours filtration, > 100 000 cpm of radioactivity remained in the retentate, of which only 5% was TCA-insoluble.

A TLC analysis of this retentate (using the three-step LiCl system of development described earlier) shows that only 7% of the radioactivity stays on the origin - the rest having Rf values of between 0.3 and 0.7 (see figure 2.9). The high viscosity of the retentate was expected to affect the mobility of the standards applied to the plate underneath the sample, and this occurred, ADP-ribose, ADP, AMP and NAD^+ all merging into a single smear corresponding with the majority of radioactivity (figure 2.9). However, the fact that the majority leaves the origin of the TLC implies that, even with repeated 'washing', radioactive material *smaller* than 10 000 Da is retained above the membrane, and the technique was not employed further.

In the light of the findings by Tanaka *et.al.* (1981a,b) discussed earlier, it was decided to approach the investigation from another angle: Tanaka *et.al.* (1981a) showed that Ap4A inhibited the (ADP-ribosyl)ation of histone H1 by highly purified ADPRT in a cell-free system. They showed that this was due to the preferential (ADP-ribosyl)ation of Ap4A itself, and further, under certain conditions (ADP-ribosyl)ated Ap4A could account for over 90% of the $[^3H]NAD^+$ initially added. It was of interest to see whether Ap4A had the same

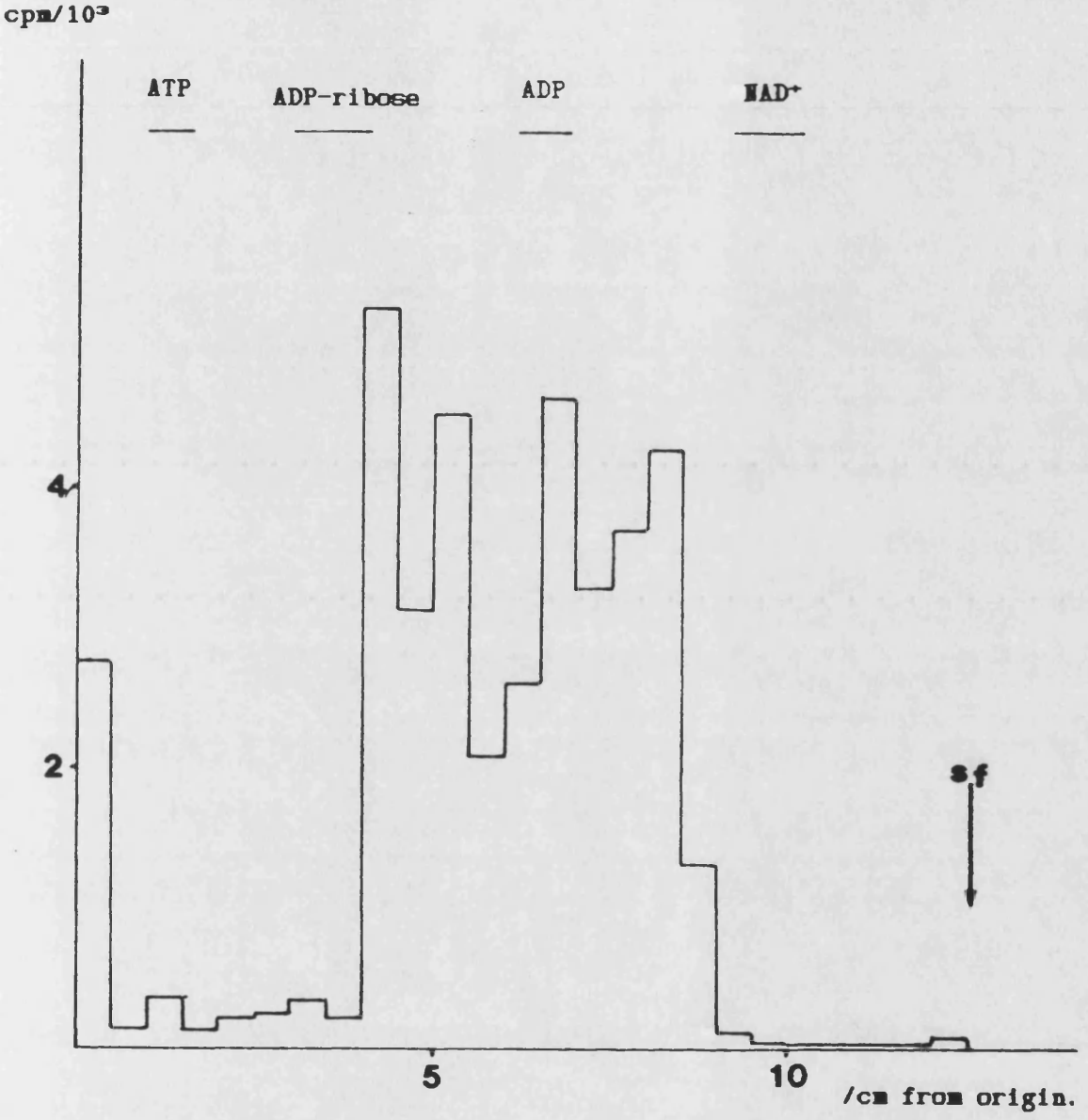

Figure 2.9.

3-step LiCl TLC analysis of 10µl from the 'Centricon' retentate when the phenol supernatant from permeabilised cells, incubated with [^{3}H]NAD$^+$ was subjected to repeated washing with sodium acetate buffer. See text for further details.

effect in a system much closer to that *in vivo* - namely, in permeabilised L1210 cells. Also, it was hoped that the presence of elevated levels of Ap4A might *stimulate* its self-(ADP-ribosyl)ation, so that the product could be observed more easily upon analysis. The next section deals with the results from experiments investigating the effects of Ap4A upon (ADP-ribosyl)ation in salt/PEI-extracted pig thymus nuclei and in permeabilised L1210 cells.

The effect of Ap4A upon (ADP-ribosyl)ation of histone H1 was studied in salt/PEI-extracted pig thymus nuclei. As mentioned before, this is a crude extract of proteins which is essentially free of DNA. Reaction conditions were as described in III.4 and included the addition of DNA and histone H1, together with [^{3}H]NAD$^+$ as a substrate for ADPRT and different concentrations of Ap4A, in a total volume of 500 µl. The (ADP-ribosyl)ation of histone H1 (expressed as TCA-insoluble radioactivity) was measured as described in III.4,5.
Figure 3.1 shows the results from a typical experiment, in which two batches each of the extracted nuclei were incubated for 5 minutes at different levels of Ap4A, three aliquots being assayed for TCA-insoluble radioactivity per batch. After these were extracted, the incubation was stopped by the addition of 125 µl of ice-cold 100% TCA, and kept on ice after mixing.

It is clear from fig.3.1 that Ap4A inhibits the (ADP-ribosyl)ation of histone H1 in a dose-dependant fashion. Table 5 below shows the data from this experiment expressed as 'percentage inhibition', with the control activity (without Ap4A) being taken as 100%. Conversion of the figures to disintegrations per minute (from counts per minute at 50% efficiency) was not considered necessary since this experiment is concerned only with *relative* amounts of (ADP-ribosyl)ated protein.

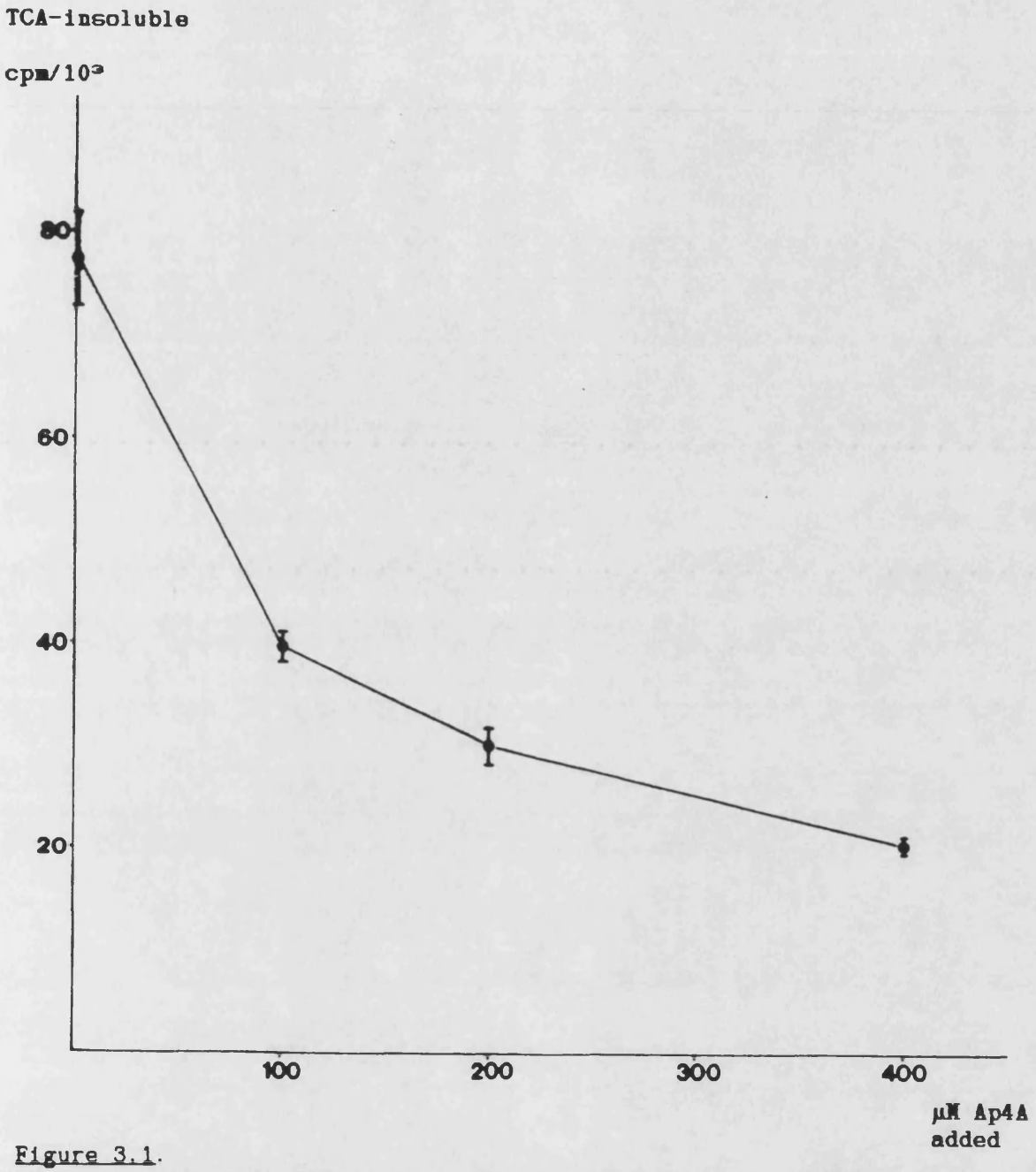

Figure 3.1.

Radioactivity incorporated into TCA-insoluble material (representing (ADP-ribosyl)ation of proteins) in salt/PEI- extracted pig thymus nuclei at different concentrations of Ap4A. The points represent the average total [^{3}H]cpm incorporated by 20µl of the preparation after 5' incubation with 5µCi [^{3}H]NAD$^+$ in two separate experiments at each concentration of Ap4A. The error bars represent the standard deviation from the mean when three assays were made per incubation. See text for further details.

This effect is less dramatic than that found by Tanaka *et.al.*(1981a,b), who showed that 100 μM Ap4A inhibited their highly purified (bovine thymus) ADPRT by greater than 80%. The fact that a crude protein extract (from a different species) was used here may be sufficient to explain this.

Table 5.

Ap4A concentration (μM)	TCA-insoluble radioactivity (cpm)	σ_{n-1}	percentage inhibition %	(σ_{n-1})%
0	77 853	5413	-	6.9
100	39 815	1775	49	4.4
200	30 207	1833	61	6.1
400	20 263	809	74	4.0

In an attempt to investigate the radioactive nucleotide(s) that may have been produced, two of the above incubations (at zero and 400 μM Ap4A) were subjected to analysis on TLC as described in III.8(a). After two hours at 20% TCA on ice, they were centrifuged at 12 000g for ten minutes, and 10μl aliquots from each supernatant were applied to the plate, on top of small quantities of Ap4A, ADP-ribose and NAD^+ as standards. 1.6M LiCl was used as a developing solvent. Figure 3.2 shows the resulting radioactive profiles, and it is immediately evident that radioactive (ADP-ribosyl)ated histone H1 is

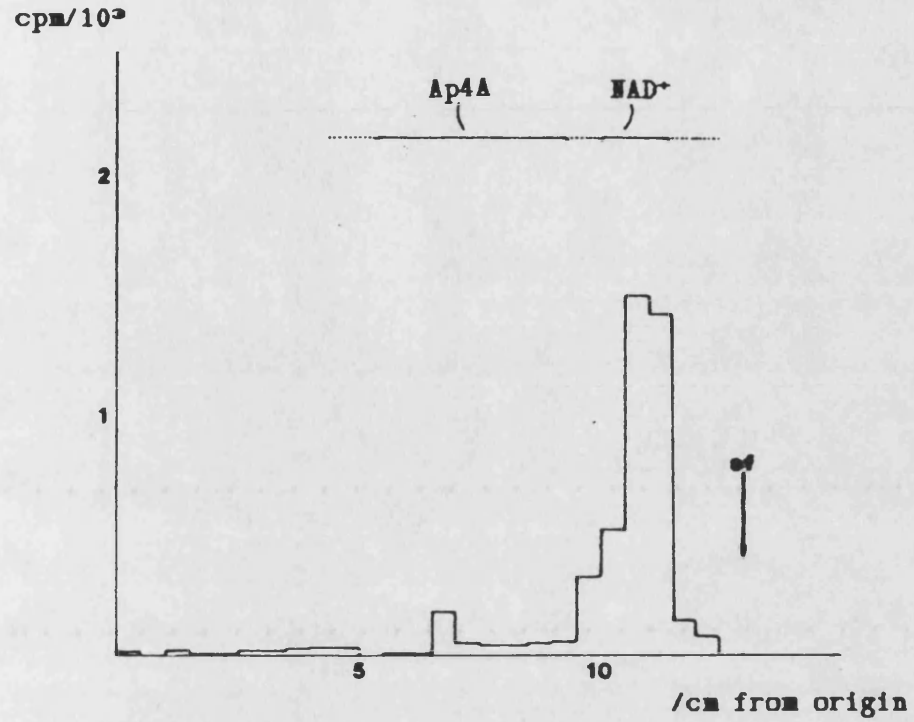

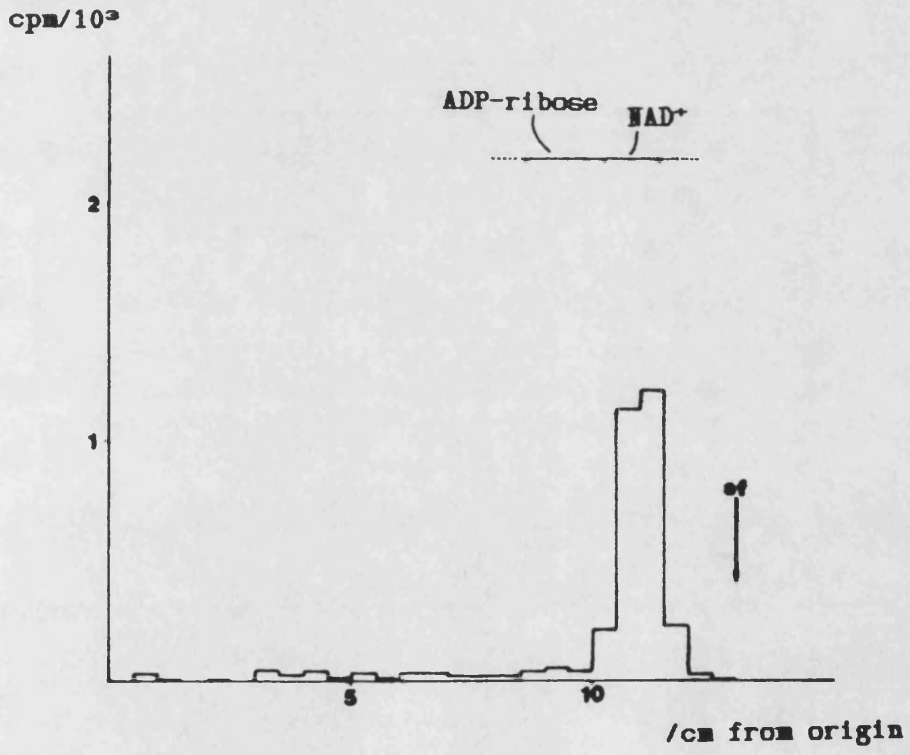

Figure 3.2.

The incubations at 0 (bottom) and 400μM Ap4A (top) from figure 3.1 were TCA precipitated and centrifuged. 10μl aliquots from the supernatants were then analysed by TLC (1.6M LiCl system). Ap4A and NAD^+ standards smeared, as indicated by the dotted line.

not present on the origin, having been removed by precipitation. In the case of the control incubation, this would have amounted to about 1500 cpm. Examination of the plate under *uv*, however, revealed that the nucleotide standards had smeared into a continuous broad band. Even when a broad (2 cm) application spot, and the minimum volume required to obtain measurable radioactivity (10 µl) was employed, this smearing of standards still occurred, which made interpretation difficult.

A possibility was that high concentrations of either TCA or nucleic acids present when the sample was dried onto the plate may have caused this smearing effect. In order to simplify the solution being applied to the plate, another experiment was performed exactly as above, but incubating at only zero and 400 µM Ap4A concentrations. This time the incubation was stopped by the addition of glacial acetic acid and absolute ethanol to final concentrations of 0.1M and 50% v/v, respectively. They were left for two hours at -20°C in an attempt to precipitate some of the nucleic acids out. As well as bringing the enzymic reaction to a halt, the acetic acid can be partially evaporated when dried onto a TLC plate, reducing the final ionic concentration of the sample. Centrifugation as before resulted in the deposition of a visible white pellet, and figure 3.3 shows the resulting radioactive profiles when the supernatants were subjected to TLC analysis as above. The positions to which the standards

(OVER) Figure 3.3.

The incubations at 0 (top) and 400μM Ap4A (bottom) from figure 3.1 were ethanol precipitated and centrifuged. 10μl aliquots from the supernatants were then analysed by TLC (1.6M LiCl system). Ap4A and NAD^+ standards ran as indicated.

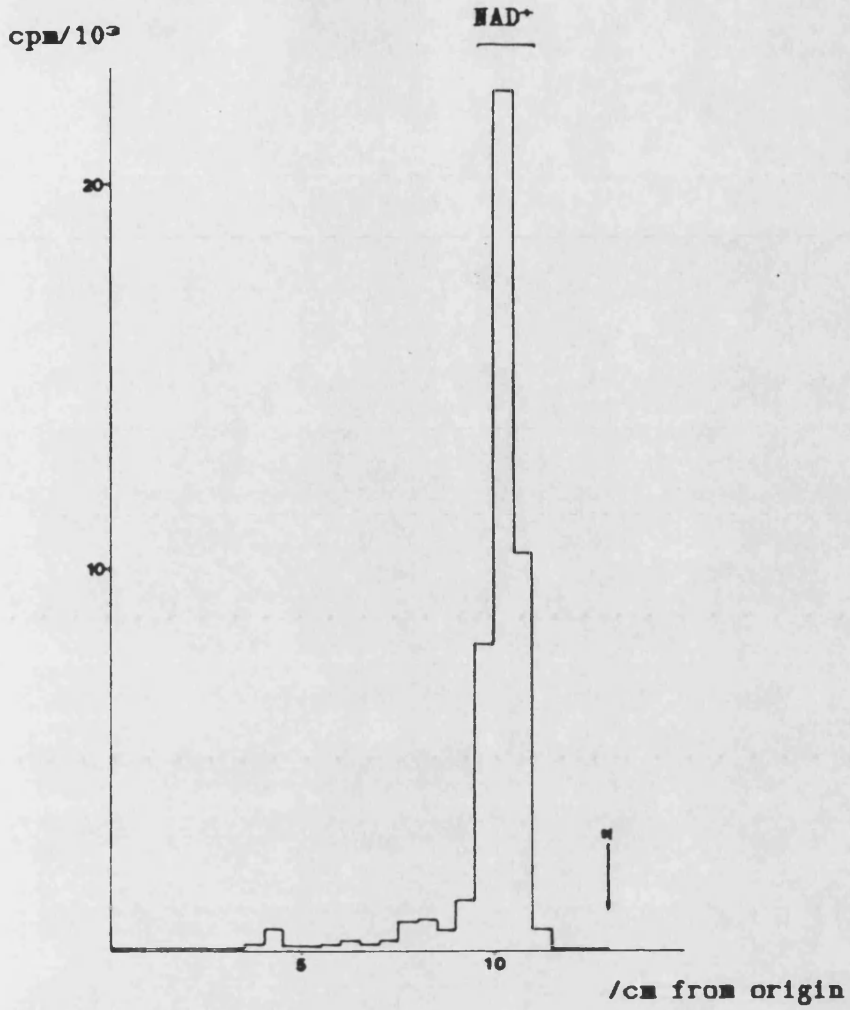
cpm/10³
NAD⁺
20
10
5
10
/cm from origin

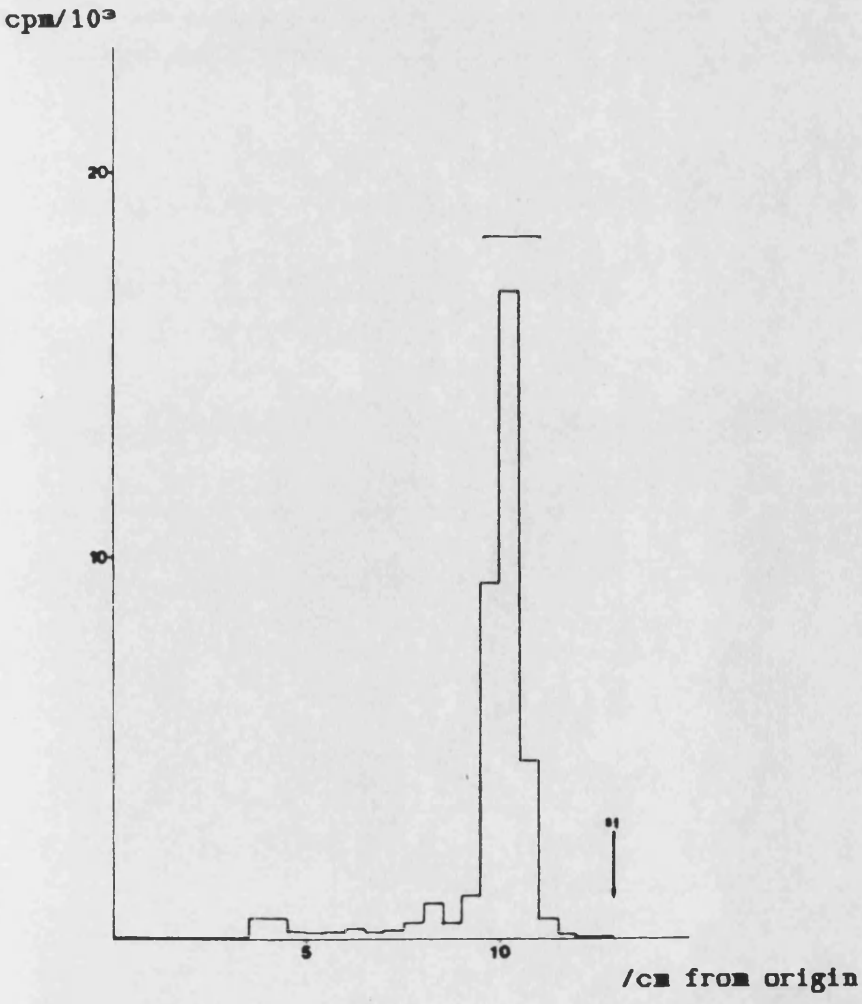
cpm/10³
20
10
5
10
/cm from origin

migrated (without smearing) are shown also in fig.3.3. It is perhaps significant that the supernatant from the incubation at 400 μM Ap4A contains approximately 5-fold less [^{3}H]NAD$^+$ than that from the control. This may imply that the presence of Ap4A has meant that less NAD$^+$ has been used as a substrate for (ADP-ribosyl)ation. However, although this is supported by the fact that less (ADP-ribosyl)ated histone H1 was found, the presence of Ap4A has not produced any detectable (ADP-ribosyl)ated nucleotide(s). It is expected that, by virtue of its negative charge, (ADP-ribosyl)ated Ap4A would remain on, or perhaps move slightly from the origin, and it can be seen from fig.3.3 that there is very little difference in the radioactive TLC profile when Ap4A is present or absent from the incubation.

It was then of interest to see whether Ap4A had the same effect in permeabilised cells. L1210 cells were treated with 200 μM DMS, permeabilised and incubated with [^{3}H]NAD$^+$ (as described in chapter III) at different concentrations of Ap4A. Figure 3.4 shows the results when two aliquots were taken from each incubation and assayed for TCA-insoluble radioactivity, and again, it can be seen that Ap4A caused the inhibition of (ADP-ribosyl)ation of protein in a dose-dependant fashion. This protein is endogenous to the cells, unlike the histone H1 exogenously added to the nuclei extract, and the

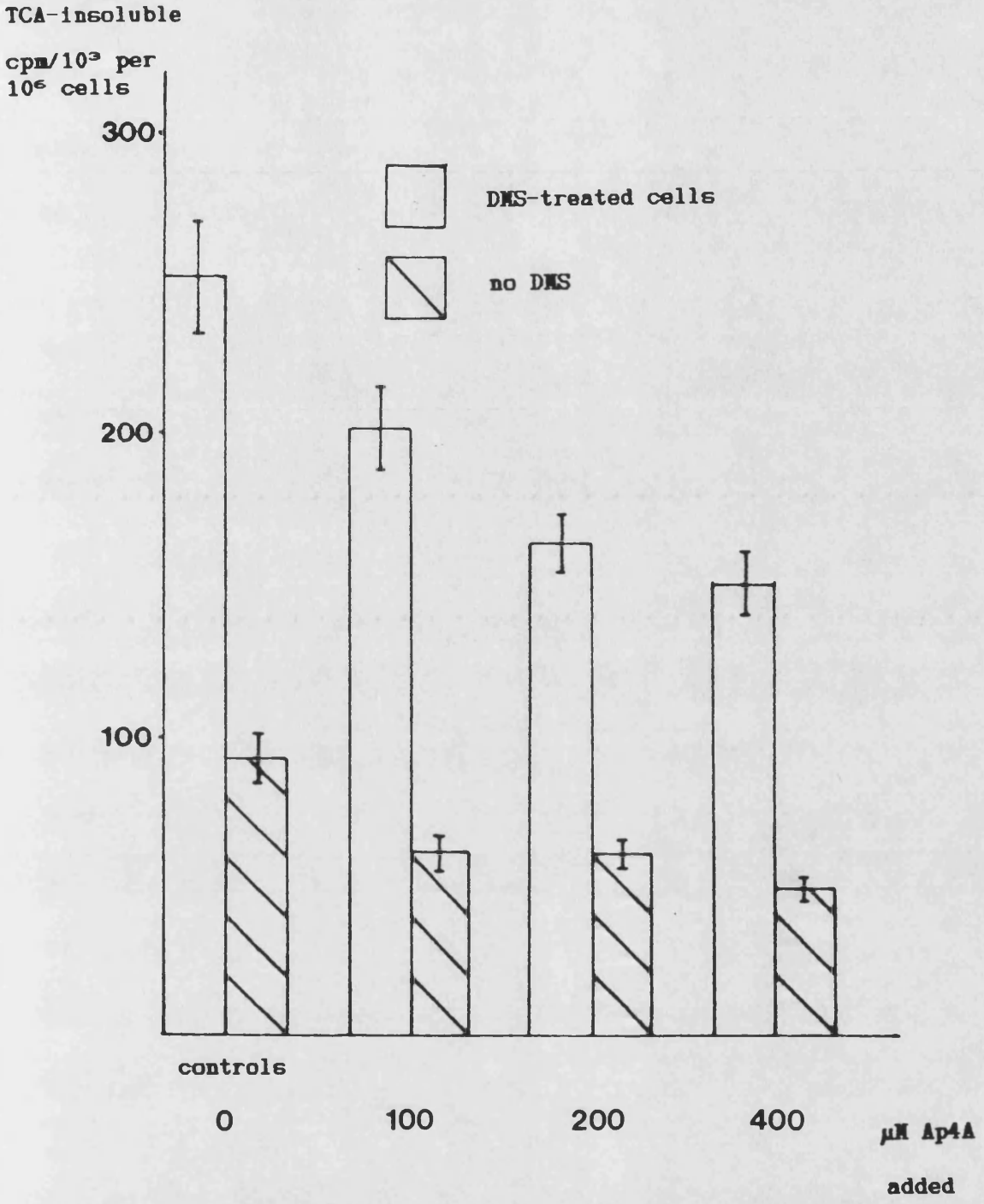

Figure 3.4.

Radioactivity incorporated into TCA-insoluble material (representing (ADP-ribosyl)ation of proteins) in permeabilised L1210 cells at different concentrations of (added) Ap4A. The shaded columns represent cells which had been pre-treated with 200 µM DMS. The errors shown represent the variation (σ_{n-1}) for three assays per batch of cells.

effect was even less than that observed above, with < 50% inhibition at 400 μM Ap4A.

Treatment with DMS appeared to make little difference to the extent of inhibition, and in order to amplify any possible effects, cells were treated with 500 μM DMS (for the same period of one hour). After permeabilisation and incubation as above, TCA-insoluble radioactivity was measured. Figure 3.5 shows that the inhibition of (ADP-ribosyl)ation of protein by Ap4A was more marked in the DMS-treated cells. DMS stimulates ADPRT by inducing DNA-strand breakage, and it can be seen that at 200 μM Ap4A this stimulatory effect is almost completely abrogated. This inhibition/stimulation effect, however, was not always observed and is certainly within the margins of errors in cell-counting and differences in behaviour between batches of cells, and it can be seen that it is not statistically significant. The cells incubated at zero and 100 μM Ap4A (both DMS-treated and not) were brought to 1M acetic acid at the end of the ten minute incubation, and 10μl aliquots were applied in 2cm-wide application spots (on top of nucleotide standards) to a TLC plate and developed in 1.6M LiCl as before. Figure 3.6 shows the radioactive profiles and the single line across the top of each denotes the fact that the nucleotide standards smeared into a single broad band, as before. Although further interpretation is difficult, there does seem to be a shift in the major radioactive peak to a

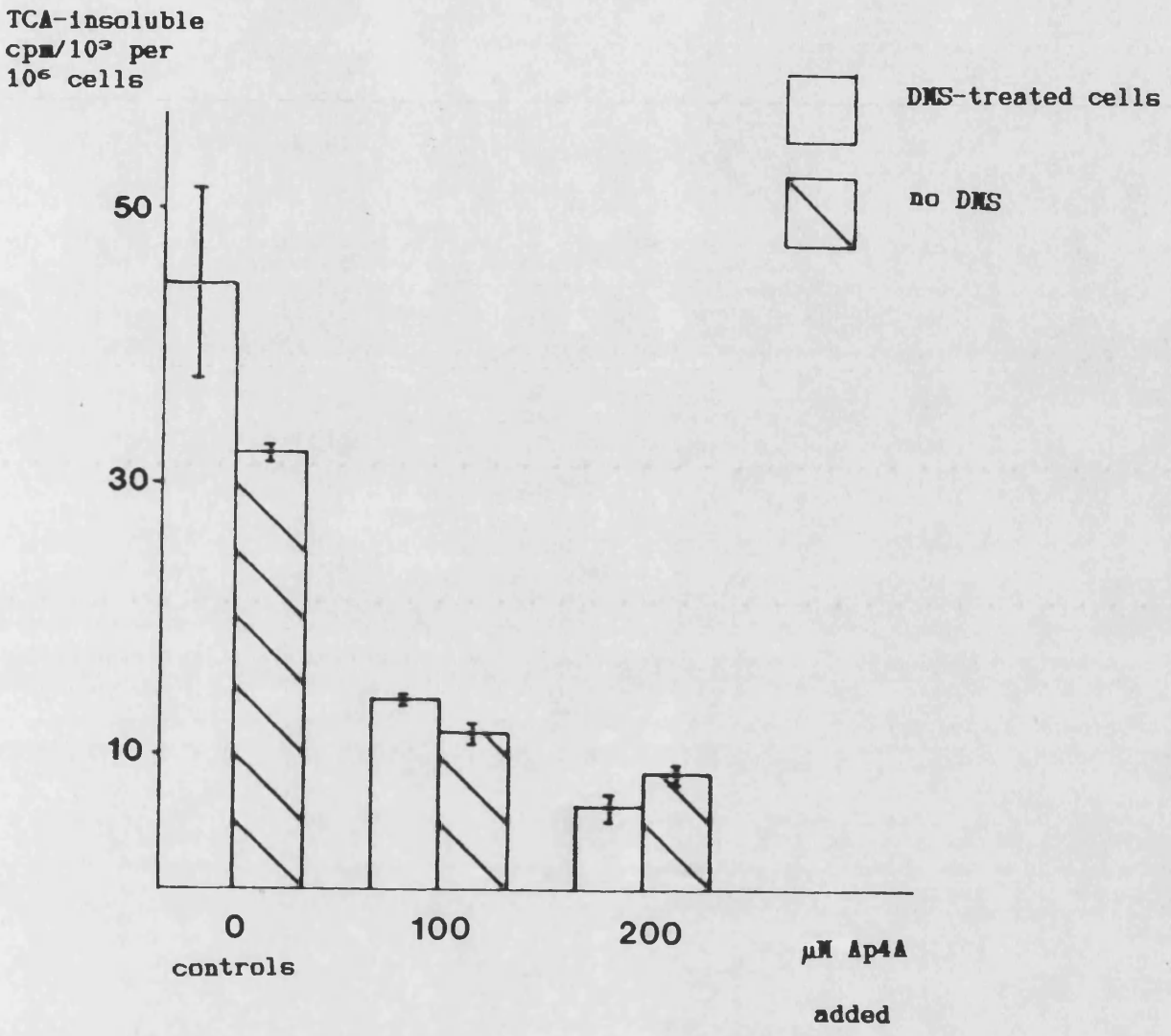

Figure 3.5.

Radioactivity incorporated into TCA-insoluble material (representing (ADP-ribosyl)ation of proteins) in permeabilised L1210 cells at different concentrations of Ap4A. The shaded columns represent cells which had been pre-treated with 500 μM DMS (cf figure 3.4, where it was 200μM). The errors shown represent the variation (σ_{n-1}) for three assays per batch of cells.

(OVER) Figure 3.6.

The incubations from figure 3.5 were brought to 1M acetic acid and a 10µl aliquot from each was analysed by TLC in the 1.6M LiCl system. A - 500µM DMS-treated cells.

B - control cells.

C - 500µM DMS-treated cells, 200µM Ap4A added to incubation.

D - control cells, 200µM Ap4A added to incubation.

All standards smeared badly - see text.

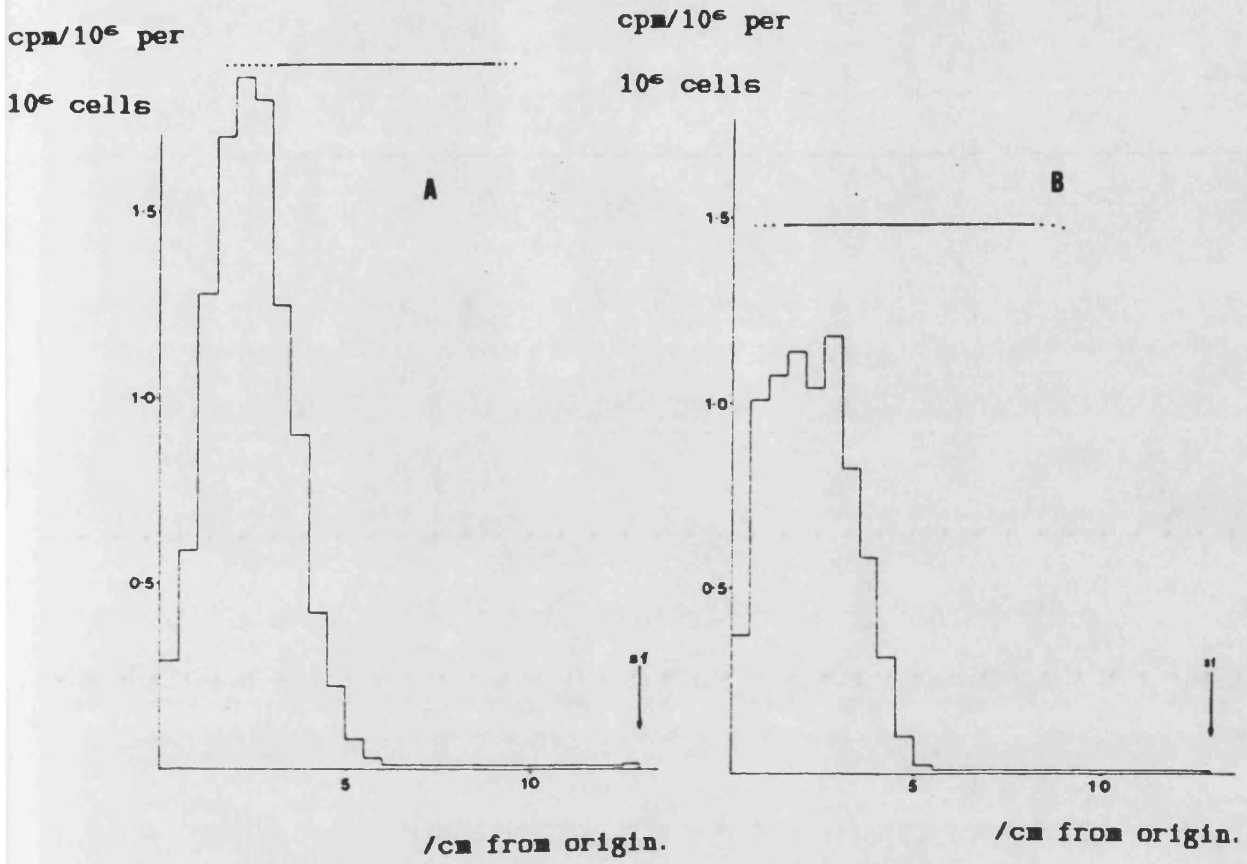
cpm/10⁶ per
10⁶ cells
A
1·5
1·0
0·5
s.f
5
10
/cm from origin.
cpm/10⁶ per
10⁶ cells
B
1·5
1·0
0·5
s.f
5
10
/cm from origin.

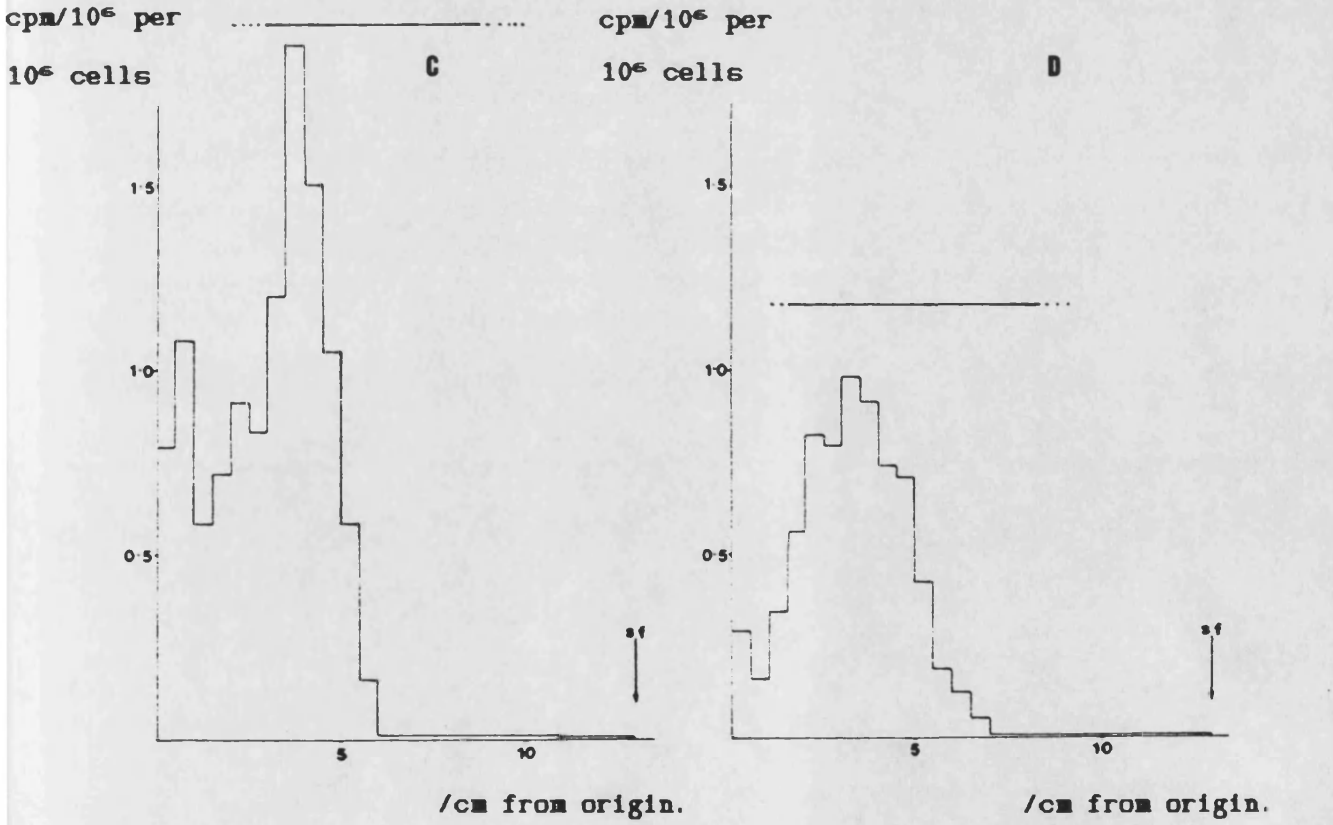
cpm/10⁶ per
10⁶ cells
C
1·5
1·0
0·5
s.f
5
10
/cm from origin.
cpm/10⁶ per
10⁶ cells
D
1·5
1·0
0·5
s.f
5
10
/cm from origin.

position slightly further away from the origin in the profiles of the cells incubated with Ap4A, although equally important may be the increased radioactivity *on* the origin in the case of the cells which had been DMS-treated *and* incubated with 200 μM Ap4A.

The unsuitability of Biogel P2 filtration in the analysis of nucleotides was discussed earlier, and when even small (100μl) portions of the above incubations were applied to a column of this medium (as described in chapter III.9) with 0.1M sodium acetate (pH 5.5) as a running buffer, visible aggregation occured, markedly slowing the flow rate and producing unacceptable resolution, with a staggered entry of material into the matrix of the column.

A distinct improvement in the resolution of The TLC-analysis of this suspension of permeabilised cells was made by the application of only 5μl in a 2cm-wide band to the plate. In order to show that the retardation of [^{3}H]NAD$^+$ apparent in figure 3.6 is real - and not in fact the result of its metabolic conversion by the cells, an experiment was conducted in which 500μl (10^6) permeabilised L1210 cells were mixed with 100μl 6M acetic acid and left on ice for 10 minutes. 5μl of [^{3}H]NAD$^+$ (50μM, 5μCi) were then added, and after mixing a 5μl aliquot was withdrawn and applied to a TLC plate. A small quantity of NAD$^+$ standard had been previously applied to the same area, and the resulting radioactive profile (shown in figure 3.7) demonstrates that the mobility of the [^{3}H]NAD$^+$ is retarded with

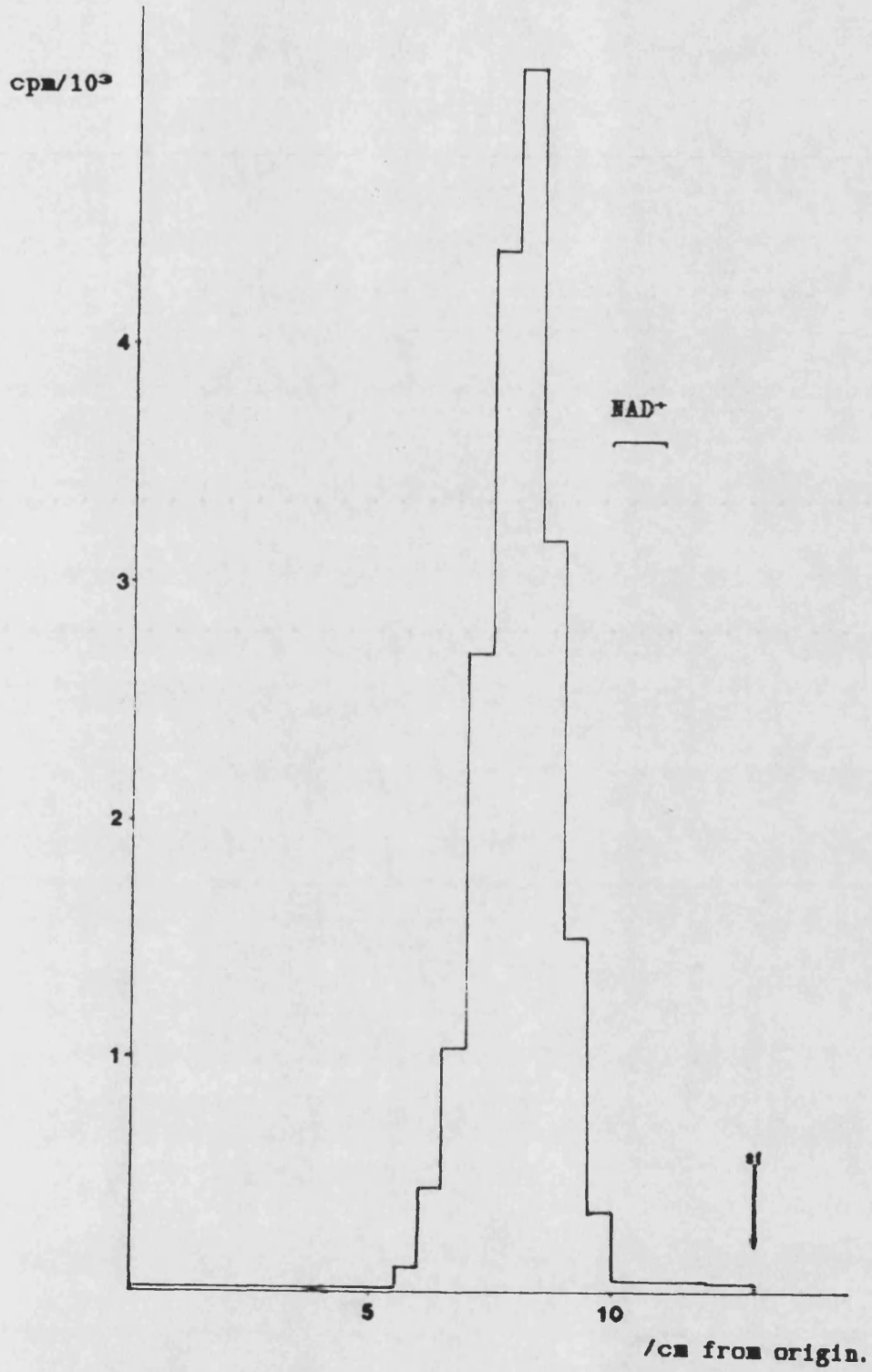

Figure 3.7.

[³H]NAD⁺ was added to permeabilised cells *after* they had been 'killed' by incubation on ice in 1M acetic acid. A 10µl aliquot was then analysed by TLC (1.6M LiCl system) - note retardation of radioactive peak compared to NAD⁺ standard.

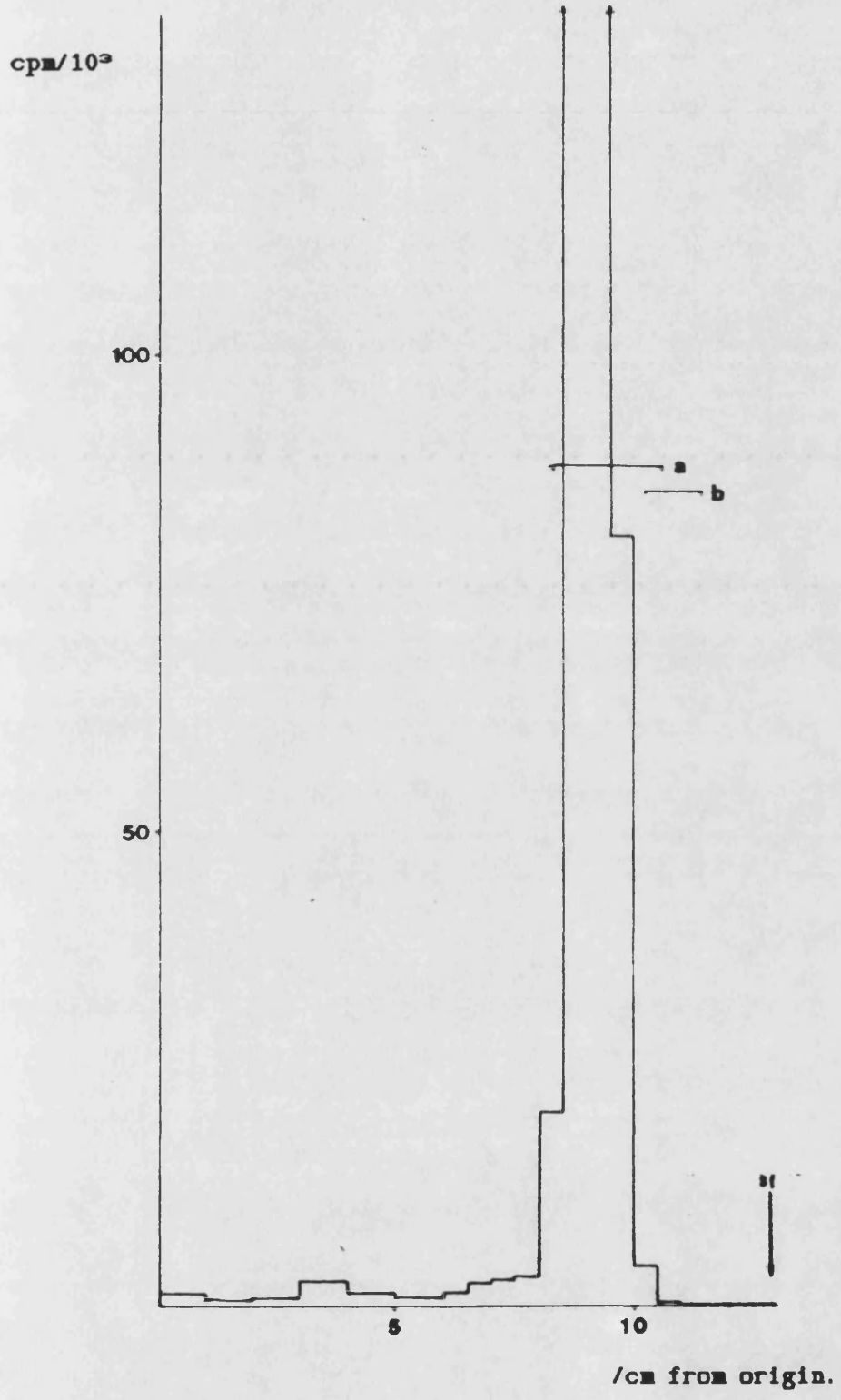

Figure 3.8.

[³H]NAD⁺, in isotonic solution (see text) was subjected to TLC analysis in the 1.6M LiCl system. Note retardation of radioactive peak with respect to the independant NAD⁺ standard (b), but not the underlaid NAD⁺ standard (a).

respect to the *independent* standard (which had been run alongside), but not with respect to the underlaid standard. The fact that the cells were not viable at the time of incubation with [^{3}H]NAD$^+$ makes it very unlikely that the peak observed is metabolically altered NAD$^+$.

It was in fact shown in another experiment that the same effects were obtained when more than 10µl of a solution of [^{3}H]NAD$^+$ in isotonic buffer (see chapter III.2) was applied to the plate. Figure 3.8 shows the radioactive profile when 15µl of a solution of [^{3}H]NAD$^+$(10µM, 0.2µCi) in isotonic buffer was developed as before in 1.6M LiCl.

The resolution of nucleotides with Rf. values >0.5 in a LiCl - based TLC system is improved if the molarity of LiCl is lowered. Further, sharper bands of nucleotide standards were always obtained with the *acidic* LiCl/acetic acid solvent described in chapter III.8(a). However, in the presence of acetic acid, molecules which have a net negative charge of >2 such as ATP and Ap4A tend to remain fixed on the origin and thus will not be resolved. The use of 1.0M LiCl as a solvent causes ATP and Ap4A to overlap during their short migration, and thus was not employed here either. Even so, (see figure 3.7) an Rf. value of 0.62 +/- 0.1 for NAD$^+$ in this situation was considered sufficient to provide the qualitative information required for the next experiment.

The reasoning behind this was that if this dose-dependant inhibition of the (ADP-ribosyl)ation of proteins was, in fact, due to the preferrential formation of (ADP-ribosyl)ated *Ap4A*, this should result in a detectable increase in a new radioactive product of relatively low molecular weight during the time of incubation with [^{3}H]NAD$^+$.

500µl (10^6) permeabilised cells were incubated as before with 10µl [^{3}H]NAD$^+$ (50µM, 10µCi) in the presence or absence of 100µM Ap4A. With gentle inversion of the reaction tube, 20µl aliquots were withdrawn after one, five and ten minutes incubation and mixed with an equal volume of 2M acetic acid (ice cold) and left on ice. At the end of ten minutes, 2 x 20µl aliquots were also withdrawn and assayed for TCA-insoluble radioactivity, as described previously. The latter gave the information that the presence of 100µM Ap4A caused the total TCA-insoluble radioactivity (per 10^6 cells) to drop from 69 870 +/- 4830 to 38 040 +/- 2610 cpm. This inhibition (45.6 +/- 6.9%) is rather more than that obtained in the experiments above, but see the note above on the variability of different batches of cells for a discussion.

After ten minutes on ice, 10µl from each of the time-course aliquots were applied to PEI TLC plates, on top of previously underlaid nucleotide standards, and developed in 1.6M LiCl as before.

(OVER) Figure 3.9.

Permeabilised cells were incubated with [^{3}H] NAD^+ in the presence (A,B,C) or absence (D,E,F) of 100μM Ap4A. 20μl aliquots were withdrawn at 1 minute (A,D), 5 minutes (B,E) and 10 minutes (C,F) and analysed in the 1.6M LiCl TLC system. Note the increasing size of the peak with time, occuring only in the presence of added Ap4A.

All axes have been left unlabelled for clarity. Vertical axes denote cpm/10^6 per 10^6 cells and horizontal axes the distance from the origin of the plate in cm.

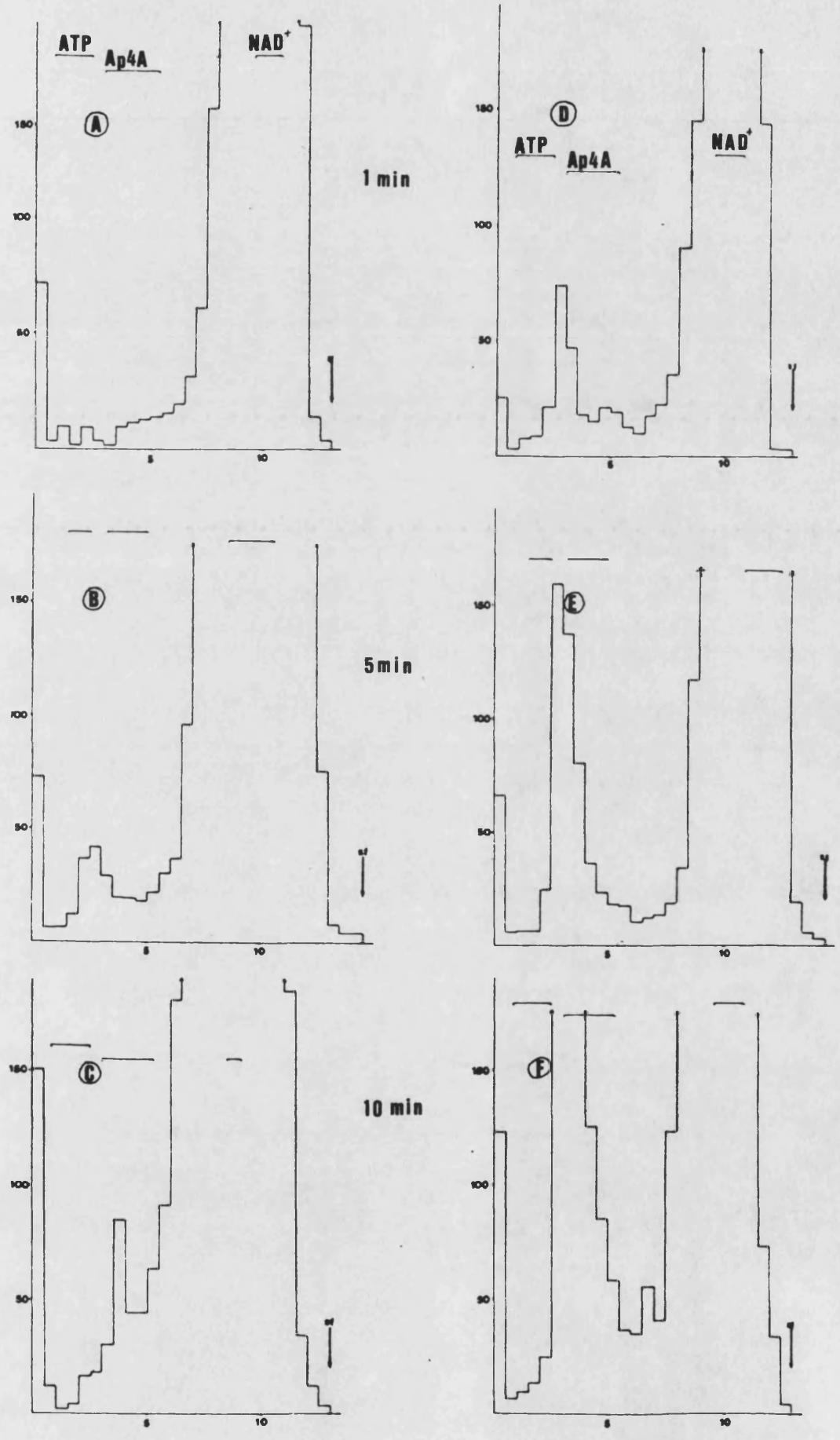
ATP
Ap4A
NAD+
A
1 min
D
ATP
Ap4A
NAD+
B
5 min
E
C
10 min
F

Figure 3.9 shows the changes in radioactive profile throughout the time course for the cells incubated with or without Ap4A.

Immediately apparent is the fact that even though the underlaid standards were reasonably resolved, the expected [^{3}H]NAD$^+$ peak is in fact a broad band, some 6cm in width!

Another clear outcome is that even though the (ADP-ribosyl)ation of proteins (or TCA-insoluble material) was inhibited by 45.6% in the presence of Ap4A, the radioactivity on the origins of both incubations (+ or - Ap4A) steadily increases with time.

The most obvious difference, however, can be seen in the steady increase in formation of a new radioactive peak between 2 and 4cm from the origin, which appears to be absent from the TLC profiles of the control cells (and is therefore presumably Ap4A-dependant).
The last two observations are more clearly summarised in table 6 below, which is concerned only with the one and ten-minute aliquots.

The amount of radioactivity on the origin with respect to the total on the plate increases both in the presence and absence of Ap4A in the initial incubation. Bearing in mind that uncentrifuged, permeabilised cells were applied to the plates, these figures are probably within the margins of error due to the inevitable heterogeneity of the suspension, even though mixing in the acetic acid was thorough.

Table 6.

area of radioactivity on TLC plate	control cells		cells at 100μM Ap4A	
	1 min.	10 min.	1 min.	10 min.
ORIGIN	0.83	1.93	0.32	1.38
2-4cm PEAK	-	2.22	2.07	13.39
8-12cm PEAK	96.71	92.14	95.34	82.36
SUM	97.54	96.29	97.73	97.13

(Figures represent the amount of radioactivity in the area concerned, expressed as a percentage of the total on the plate).

The 2-4cm peak in the profiles from the cells incubated with Ap4A present rises from ≈2 to ≈13 percent of the total radioactivity - which is obviously not matched in the control profiles, even though the peak is apparent, and is increasing with time. It is also apparent that although the [^{3}H]NAD^+ peak (8-12 cm) in the control profiles is reduced from 96.71 % at one minute to 92.14% at ten minutes, the decrease is much larger in the profiles of the cells incubated with Ap4A (95.34 to 82.36%). The fact that there is little difference when the radioactivity in these three areas is added together (see 'sum' in table 6.) implies that the decrease in the 8-12cm peak is due to the increase in the 2-4cm peak. This fits in with

the hypothesis that the [^{3}H]NAD^+ is being used to (ADP-ribosyl)ate Ap4A. However, the data do not suggest that this is *at the expense of (ADP-ribosyl)ated protein.*

Although no further information is provided by this experiment about the *nature* of the material, it has demonstrated that the presence of Ap4A depresses the (ADP-ribosyl)ation of proteins in permeabilised L1210 cells, and causes the time-dependant formation of a substance slightly less mobile than Ap4A on a TLC plate, seemingly at the expense of 'free' NAD^+.

Due to the problems of using a heterogenous suspension of cells, it was thought that the next logical step would be to see if Ap4A has the same effect when the crude phenol extract from cells discussed in section III.2. is analysed. L1210 cells in mid-log phase were permeabilised to 2.9 x 10^6/ml and 500µl aliquots were incubated with 20µl [^{3}H]NAD^+ (50µM, 20µCi) and 20µl of either isotonic solution or Ap4A dissolved in it, such that the final concentration was 100µM. At the end of this ten minute incubation (at 26°C), 100µl of a solution of BSA (0.1mg/ml in dH_2O) were added and the mixture was phenol-extracted as described in section 2. After 'back extraction' the supernatant pools were extracted with dry ether until the pH was >5 as described in III.6(b), and brought to a final volume of 1 ml with 0.1M sodium acetate, pH 5. 5µl aliquots (representing 0.5% of the total volume) of these supernatants were then applied to PEI TLC

plates on top of standards of Ap4A, ADP-ribose and NAD^+ which had been laid previously, and the plates were developed in 1.6M LiCl as before. Figure 3.10 shows the radioactive profiles resulting. It was noticed that, as observed with the unfractionated permeabilised cell suspension above, the standards were smeared and did not form thin discreet bands under *uv* light. Although their mobility was less retarded than in figure.3.9, the ADP-ribose and NAD^+ standards overlapped slightly. From the radioactive profiles in figure 3.10 it is evident that the presence of Ap4A in the incubation mixture causes the appearence of a peak (which is not present for the control) of slightly less mobility than Ap4A. The peak appearing between 7 and 8.5cm from the origin is probably free ADP-ribose monomer, produced by the hydrolysis and/or the action of ADP-ribose glycohydrolase upon poly(ADP-ribosyl)ated acceptors. The [^{3}H]NAD^+ peak is slightly more retarded in the profile containing the Ap4A dependant peak (Fig.3.10(b)). The Ap4A-dependant peak is similar to the one observed in the TLC profiles of unfractionated cells (figure 3.9) in terms of its mobility, and in that it appears to be produced at the expense of [^{3}H]NAD^+. Further TLCs of these supernatants provided no extra information and the standards were consistently found to smear. It was thought that the nucleic acid content of the phenolic supernatant might be contributing to this effect, and an experiment was performed to investigate this. ATP, AMP, Ap4A and NAD^+ standard solutions

(OVER) Figure 3.10.

Permeabilised cells were incubated with [^{3}H]NAD$^+$ in the presence (top) or absence (bottom) of 100 μM Ap4A. Phenol extraction was performed, the supernatants were ether extracted and a small quantity was analysed by TLC (1.6M LiCl system) as before. Note the lack of separation between the NAD$^+$ and ADP-ribose standards.

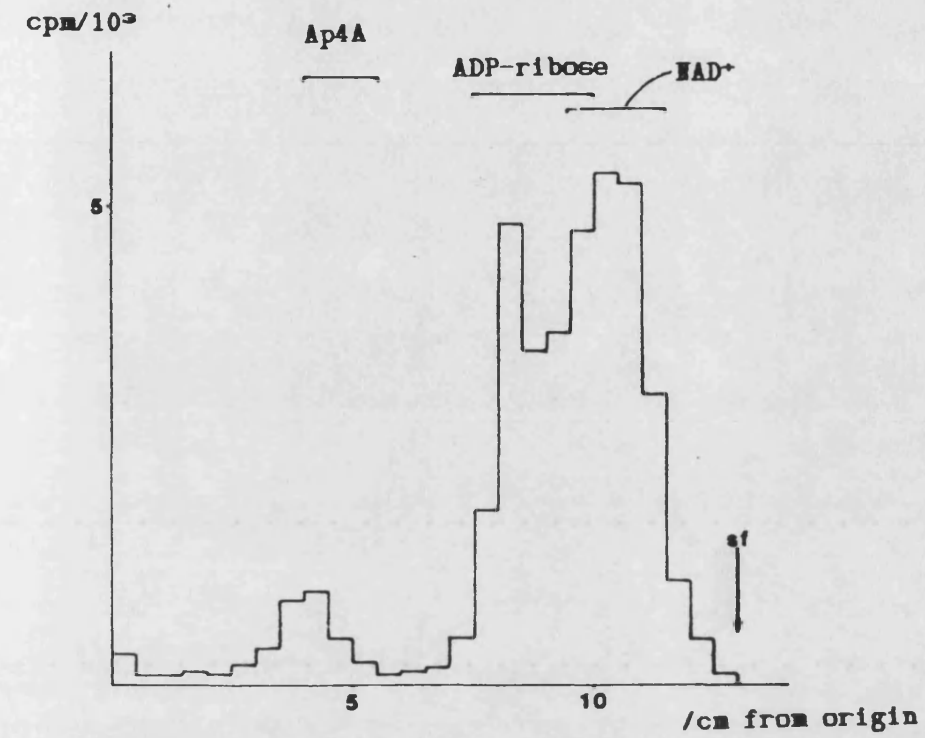
cpm/10³
Ap4A
ADP-ribose
NAD+
5
sf
5
10
/cm from origin

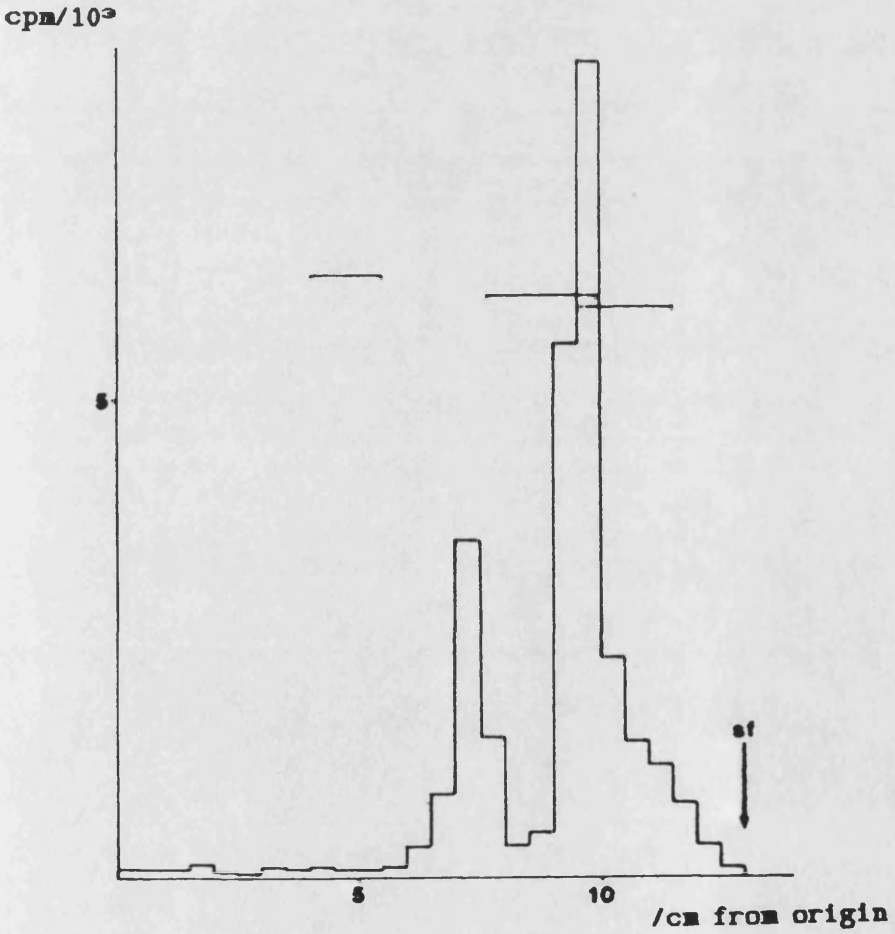
cpm/10³
5
sf
5
10
/cm from origin

(1mg/ml in 50%(v/v) ethanol/water) were dried in 1.5cm-wide application spots onto PEI TLC plates as before, and 5µl solutions of DNA (calf thymus; type I, highly polymerised.SIGMA) and RNA (yeast; highly polymerised. BDH) in distilled water were applied on top. The plates were developed in 1.6 M LiCl, dried and observed under *uv* light. Figure 3.11 shows that solutions of DNA at 2mg/ml and RNA at 1mg/ml cause significant distortion of the standards with respect to a distilled water control. The value of this finding, however, is limited since it is highly likely that the nature of the nucleic acids present in the phenolic supernatants (eg.Fig.3.10) will be different to that of these commercial preparations. In order to minimise any interference by nucleic acids in the resolution of nucleotide extracts by anion exchange chromatography, a procedure was adopted which removed them by precipitation in ethanol. This is described in full in III.6(c). Note the 'back-extraction' of the nucleic acid pellet, which serves to minimise the losses of nucleotides from the supernatant. This is discussed further in section 4. The inclusion of 0.1M acetic acid raised the ionic concentration (facilitating precipitation) and lyophilisation resulted in its disappearence, along with the ethanol.

It was thought that the inclusion of this step in the extraction of nucleotides from cells would improve their resolution upon TLC analysis, and an experiment was performed to test this.

Figure 3.11

Effects of DNA and RNA concentrations on the mobility of ATP, AMP Ap4A and NAD^+ standards when subjected to TLC in the 1.6M LiCl system. See text for further details.

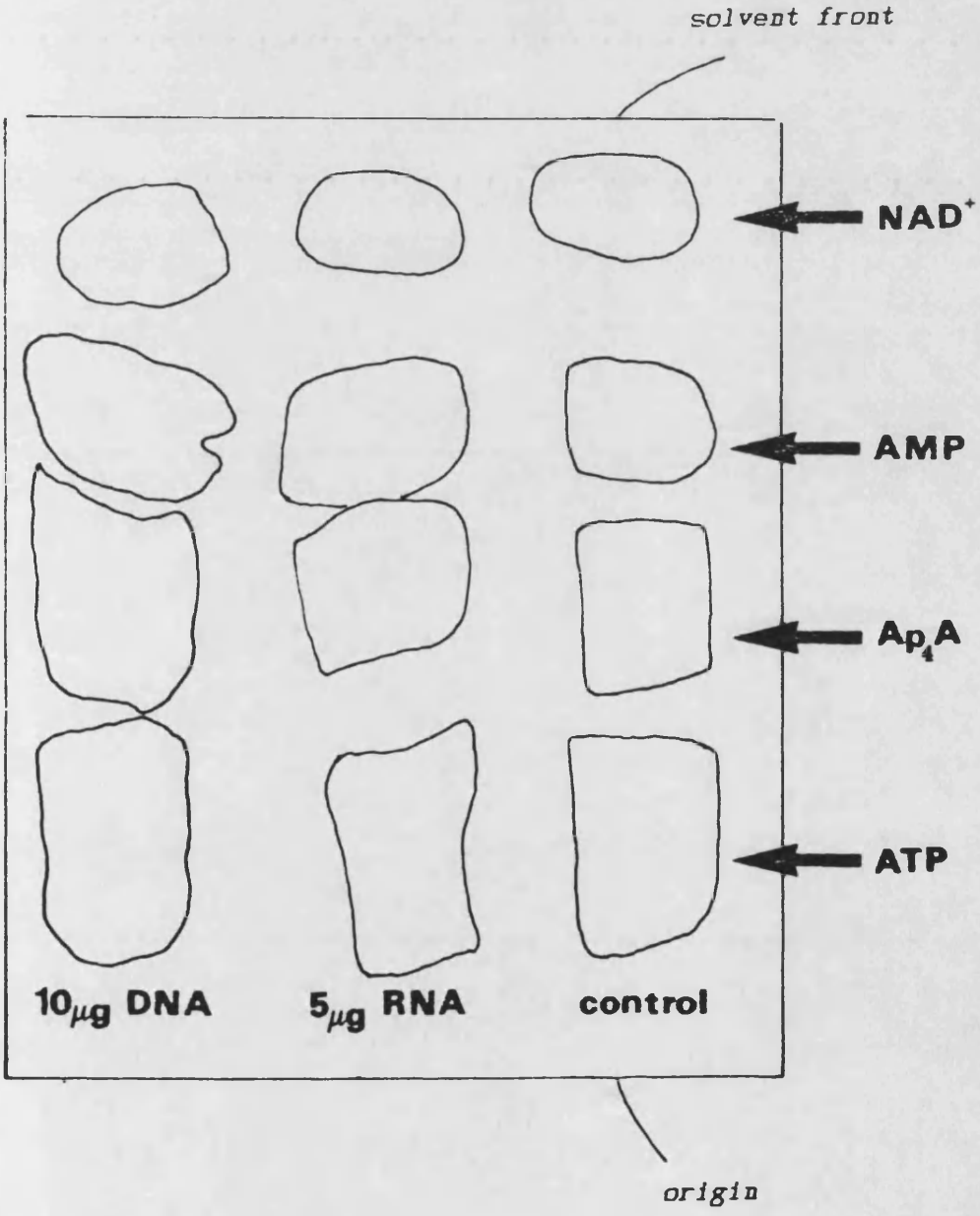

L1210 cells were cultured and permeabilised in mid-log phase to 9 x 10^5 viable cells per ml. 500µl portions of this cell suspension (4.5 x 10^5 cells) were incubated for ten minutes at 26°C with 20µl [^{3}H]NAD$^+$ (20µCi, 50µM) in the presence or absence of 100µM Ap4A, in a final volume of 540µl. After sampling for TCA-insoluble and *total* radioactivity, BSA was added and the mixtures were extracted with phenol/chloroform, ether and acidic ethanol as described. The ethanolic supernatant pools were freeze-dried and the lyophilisates redissolved in 250µl 0.1,M sodium acetate, pH 5.5 .

The control cells (incubated in the absence of Ap4A) incorporated 122 040 +/- 8280 cpm of radioactivity into TCA-insoluble material. This was against a figure of 59 760 +/- 13320 cpm for the cells incubated with Ap4A. This means that Ap4A at 100µM has caused a 2.2 +/- 0.6 - fold reduction in (ADP-ribosyl)ation of TCA-insoluble material. Table 7 shows the recovery of *total* radioactivity, from the amount initially present in the incubation to the amount left in the final nucleotide extract.

When 10µl aliquots of the nucleotide extracts were subjected to analysis in the 1.6M LiCl TLC system, severe distortion of the radioactive profiles and smearing of the standards occured (figure 3.12).

(OVER) Figure 3.12.

Permeabilised cells were incubated with [^{3}H]NAD$^+$ in the presence (top) or absence (bottom) of 100 μM Ap4A. Phenol extraction was performed, the supernatants were ether-extracted and then precipitated in 50% ethanol/0.1M acetic acid as described in chapter III.6(c). After lyophilisation, the ethanolic supernatants were redissolved and 10μl aliquots were analysed by TLC (1.6M LiCl system). Note the smearing of Ap4A, ADP-ribose and NAD$^+$ standards.

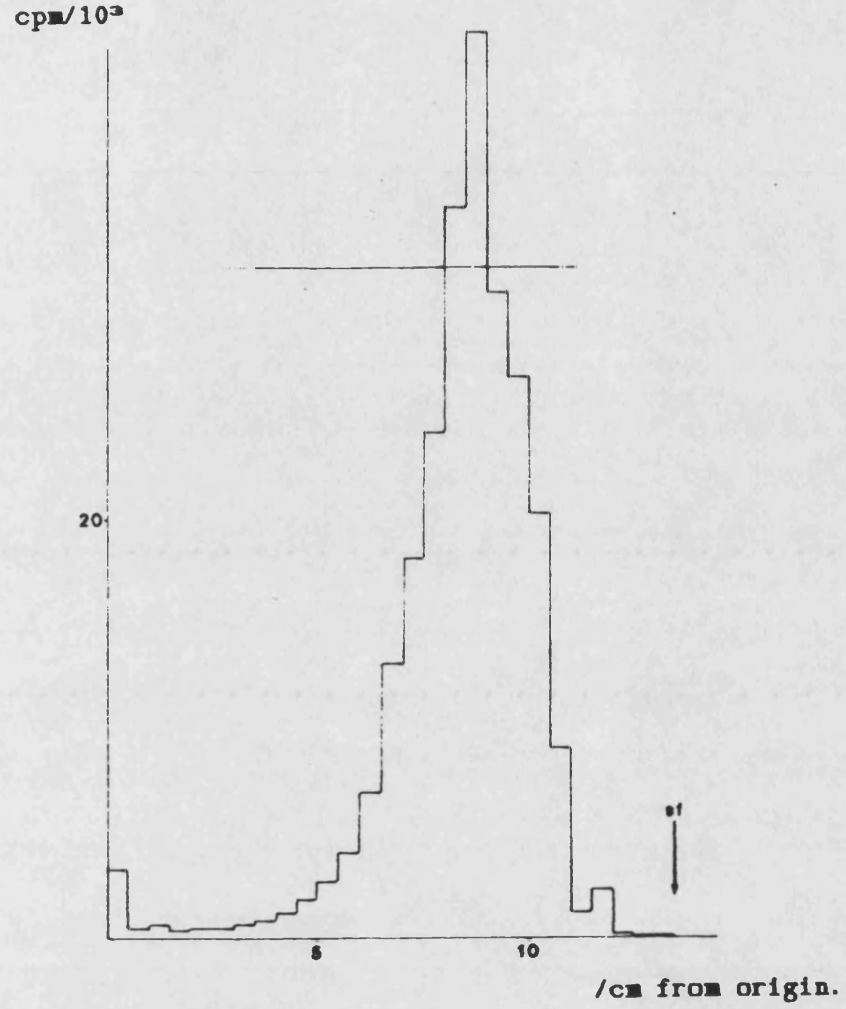
cpm/10³
20
5
10
sf
/cm from origin.

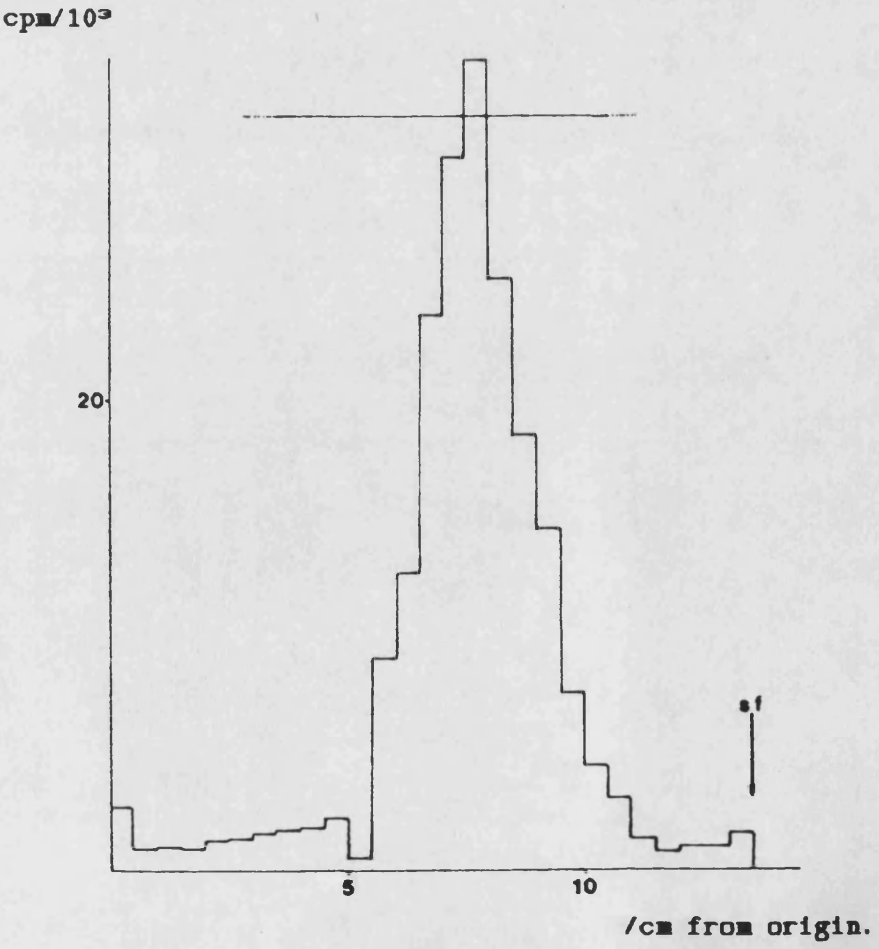
cpm/10³
20
5
10
sf
/cm from origin.

Table 7.

	CONTROL (NO Ap4A)	100μM Ap4A
Initial radioactivity (cpm)	10 685 412 +/- 174 700 σ_{n-1}	9 032 634 +/- 345 762 σ_{n-1}
Radioactivity in nucleotide extract (cpm)	8 629 582 +/- 434 694	8 940 438 +/- 79 742
percentage recovery	80.8 +/- 21.3	99.0 +/- 4.7

In an attempt to resolve the components less negative than ATP, the extracts were analysed in the acetic acid/LiCl TLC system described earlier (and in III.8(a)). This time, the underlaid standards did not smear, and the radioactive profiles are shown in figure 3.13. The profile for the Ap4A-containing extract shows approximately three times more radioactivity on the origin than on the control (and also slightly less comigrating with ADP-ribose). Portions from the nucleotide extracts were incubated overnight at room temperature with an equal volume of 0.4M NaOH and analysed again in the above acidic TLC system. Figure 3.14 shows the resulting radioactive profiles, the figures for which have been doubled to allow comparison, and so that an equal volume (10μl) was applied to

(OVER) Figure 3.13.

TLC analysis of the nucleotide extracts in figure 3.12 in the *acidic* (LiCl/acetic acid) system. Note the better resolution of standards.

Top - 100 μM Ap4A present in incubation.

Bottom - no Ap4A added to incubation.

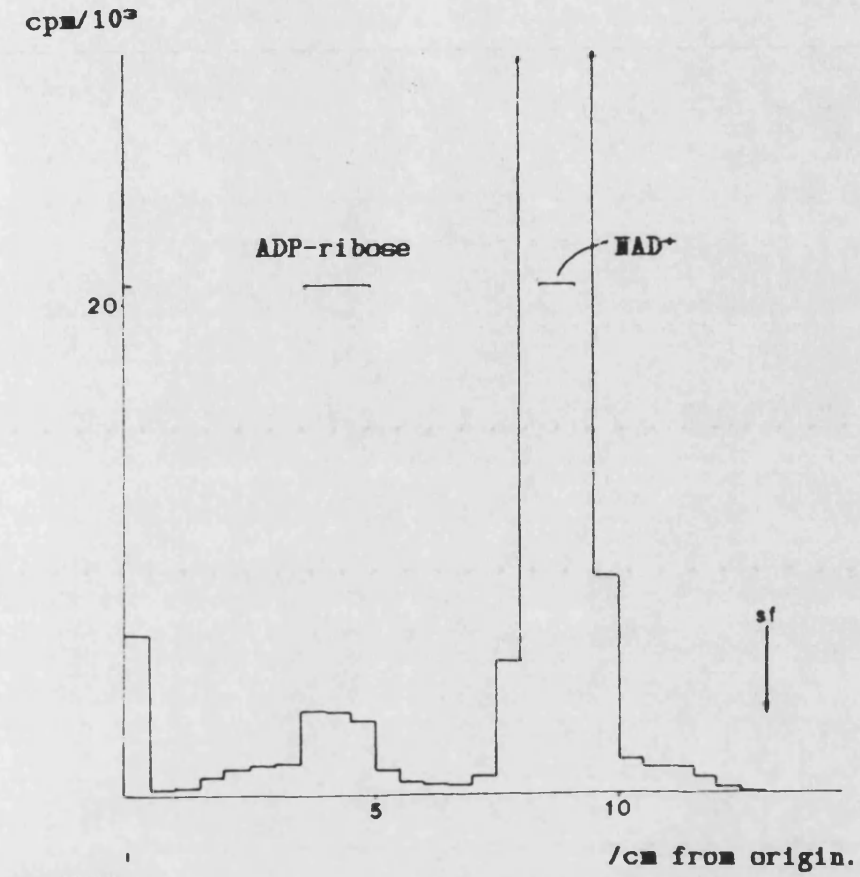
cpm/10³
ADP-ribose
NAD⁺
20
sf
5
10
/cm from origin.

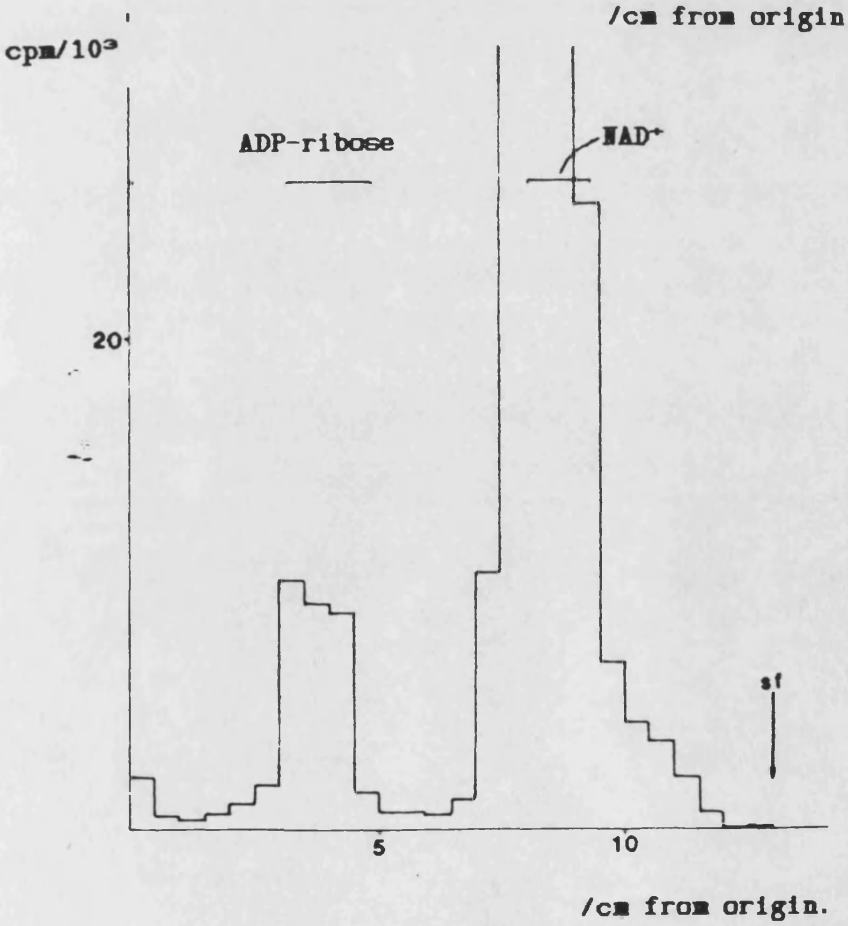
cpm/10³
ADP-ribose
NAD⁺
20
sf
5
10
/cm from origin.

(OVER) Figure 3.14.

The nucleotide extracts in figures 3.12 & 13 were base-treated (see text) and analysed in the LiCl/acetic acid system. Note that the radioactivity on the origin has remained. Top - 100μM Ap4A present in incubation.

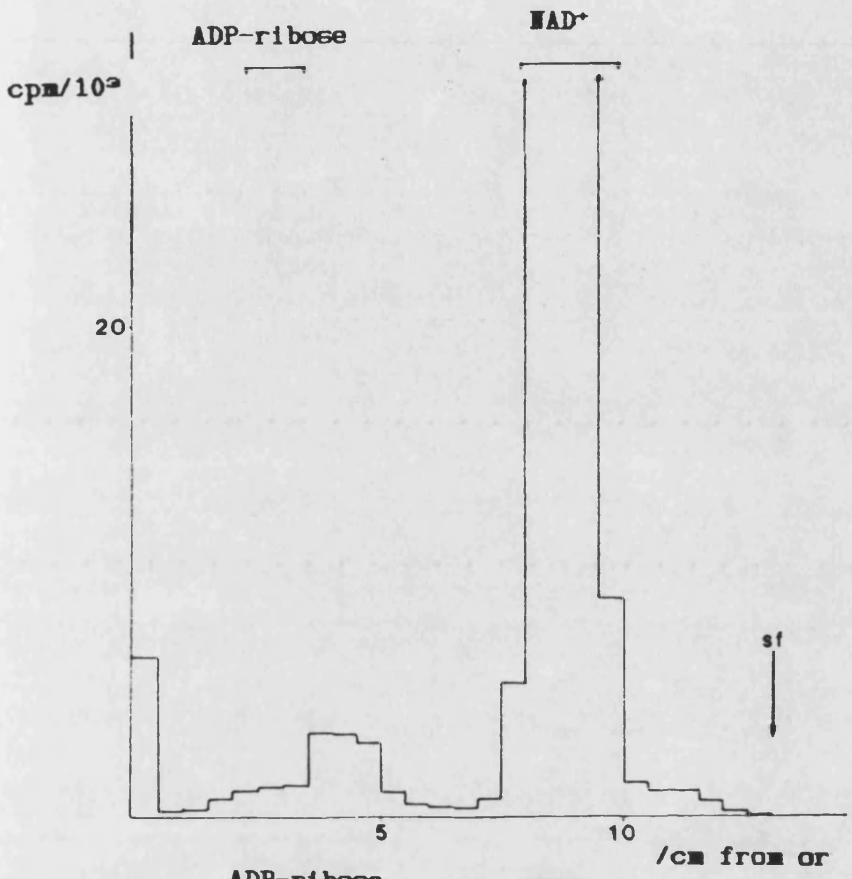
ADP-ribose
NAD+
cpm/10³
20
sf
5
10
/cm from or

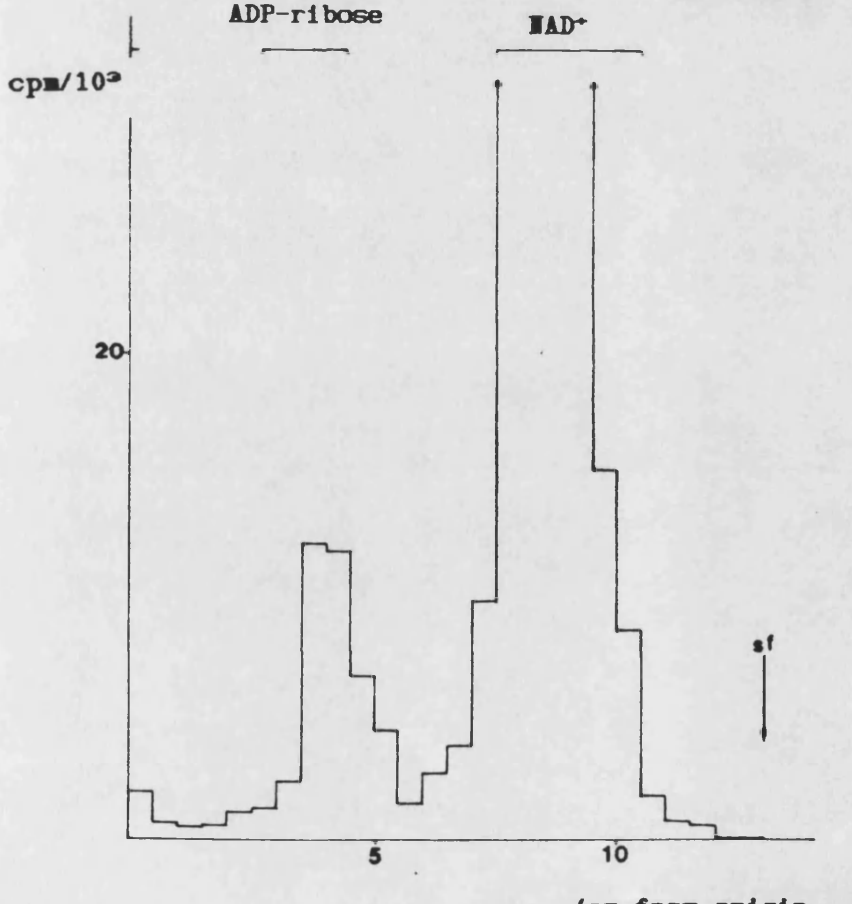
ADP-ribose
NAD+
cpm/10³
20
sf
5
10
/cm from origin.

the plate. It can be seen that the origin material present in the Ap4A-containing extract remains unchanged by treatment with base. If this material were, for instance, Ap4A-([^{3}H]ADP-ribose)n, then it would be expected that base treatment would release [^{3}H]ADP-ribose and it would comigrate with the ADP-ribose standard, resulting in a reduction of radioactivity at the origin. That the linkage between ADP-ribose and Ap4A (an $\alpha(1'' \rightarrow 2')$ inter-ribose bond *in vitro*) is base-labile was established by Yoshihara and Tanaka (1981).

Clearly, since Ap4A remains on the origin in this system, it is only of limited value in the resolution of the radioactive components of these nucleotide extracts. Equally, the 1.6M LiCl TLC system is ineffective due to the distortion and smearing described. Lowering the LiCl concentration to, say, 1.0M does not permit the separation of ADP-ribose, AMP and NAD^+ or Ap4A and ATP, adequately. It was decided that anion exchange chromatography could be better performed in this case using DEAE cellulose as the exchange medium, packed into a column with a linear gradient of NH_4HCO_3 as the mobile eluting phase. Initially, this was employed in the same manner as by Yoshihara and Tanaka (1981) and is described in full detail in chapter III.8(b&c). It was used in the first instance to separate any [^{3}H]Ap4A produced from [^{3}H]ATP in synthesis attempts described in III.12 in which 100μCi of [^{3}H]ATP was reacted with 5 pmol 5'AMP morpholidate under dry pyridine. After the pyridine was blown off,

the nucleotides remaining were dissolved in 5ml column-equilibriation buffer (5mM NH_4HCO_3, pH 8.3). A 10µl aliquot of this was subjected to TLC analysis in the 1.6M LiCl system, with underlaid standards of ATP and Ap4A, and the resulting radioactive profile is shown in figure 3.15. Approximately 6.4% of the total radioactivity is associated with the smaller peak, which comigrated with the Ap4A standard. This relatively low yield was typical. The dissolved nucleotides remaining were applied to a pre-equilibriated 3ml column of DEAE cellulose and after washing with 4ml of equilibriation buffer (5mM NH_4HCO_3), elution was performed with a linear gradient from 5-400 mM NH_4HCO_3 (2 x 80ml). Table 8 shows the amount of radioactivity applied to the column, that emerging unbound and that removed by the 5mM NH_4HCO_3 wash. 95.2% remains bound to the column after the 5mM NH_4HCO_3 wash.

Table 8.

Total radioactivity applied	84 388 500 cpm
Radioactivity left unbound	1 396 200 cpm
Radioactivity removed in wash	2 671 700 cpm

(no error figures were available).

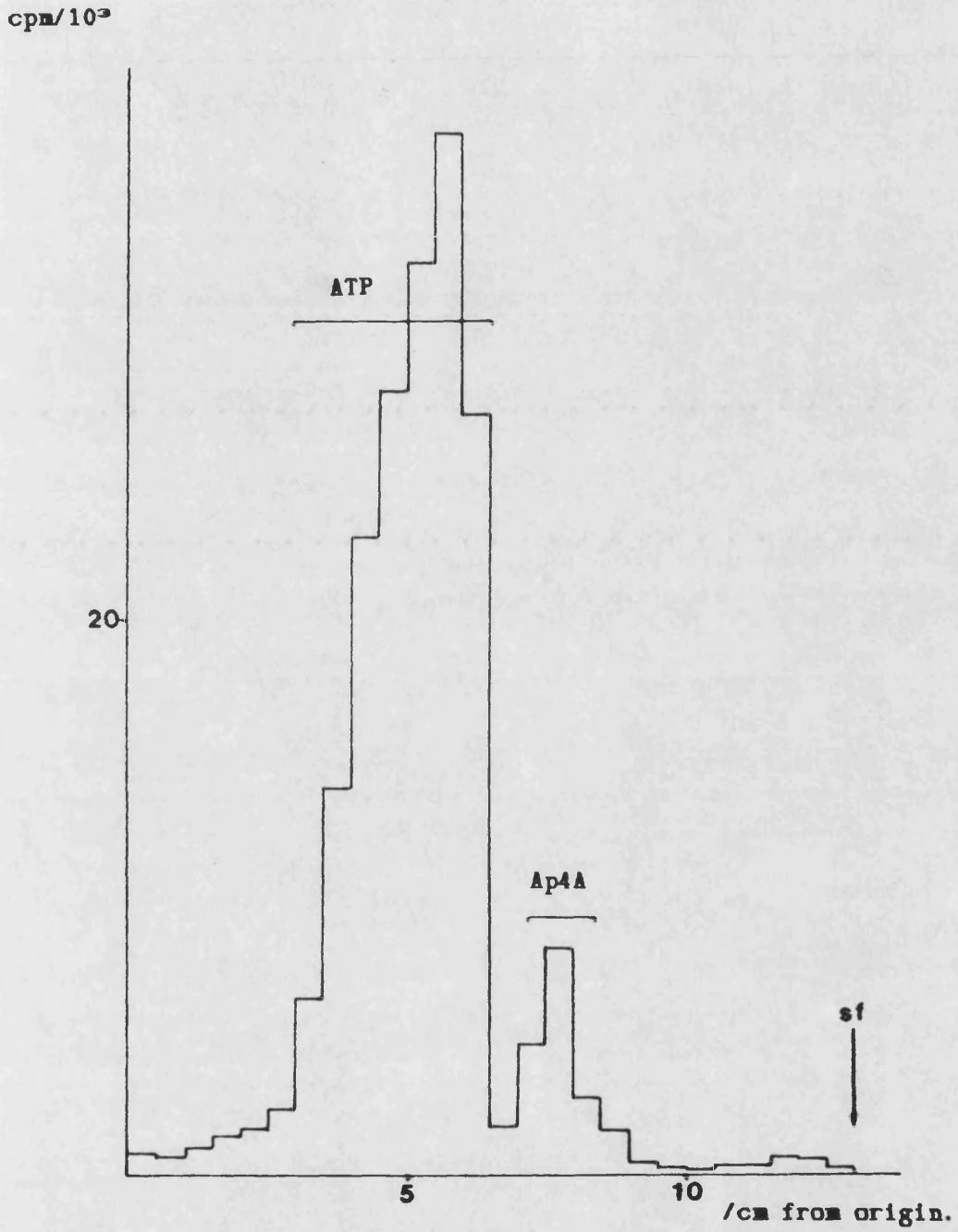

Figure 3.15.

TLC analysis of products when 100μCi [³H]ATP were reacted with 5 pmol 5'AMP-morpholidate under dry pyridine. See text for further details.

After elution with the linear gradient, the column was washed with 10ml of distilled water before attempting to remove any uneluted material with 4ml of 0.1M HCl. As mentioned in III.8(b), this resulted in effervescence and disruption of the medium in the column, and in any case, the level of radioactivity in the two 2ml HCl 'fractions' collected was not significantly above that of the background. When this step was replaced by eluting with 4ml 500 mM NH_4HCO_3, no significant levels of radioactivity were detected either. Figure 3.16 shows the resulting profile when 50µl aliquots were taken from each 2ml fraction and assayed for radioactivity. The smaller peak (fraction 14) amounts to 3.9% of the total radioactivity applied to the column (or 5.6% of the total radioactivity eluted). From figure 3.15, it would be expected that the smaller peak should contain [^{3}H]Ap4A, the larger one consisting of [^{3}H]ATP. Figures 3.17 and 3.18 show the results when 15µl aliquots from fractions 14 and 18 were subjected to TLC analysis (1.6M LiCl, with underlaid standards of Ap4A and ATP). It can be seen that the radioactivity in fractions 14 and 18 comigrates with Ap4A and ATP, respectively, and the fact that Ap4A moves further from the origin in this TLC system (because it is less negatively charged) agrees with the observation that ATP is eluted from the column at a slightly higher concentration of NH_4HCO_3 (100-125 mM) than Ap4A (75 mM).

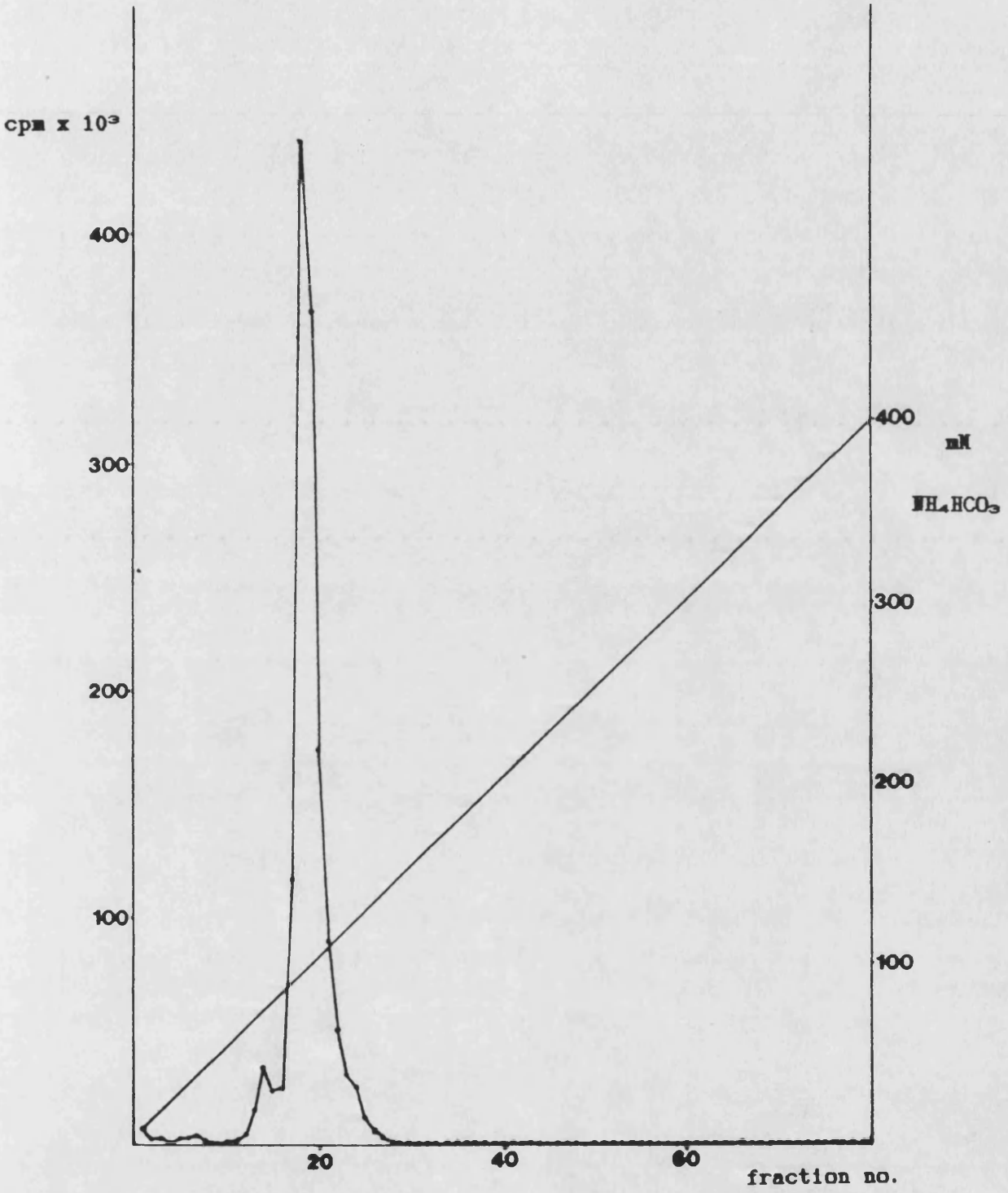

Figure 3.16.

Analysis of the products in figure 3.15 by anion-exchange chromatography on DEAE cellulose, using a linear gradient of NH_4HCO_3 (pH 8.3) from 5 mM to 400 mM. 2ml fractions were collected at 40 ml/hr and a 50µl aliquot from each was counted for radioactivity (cpm).

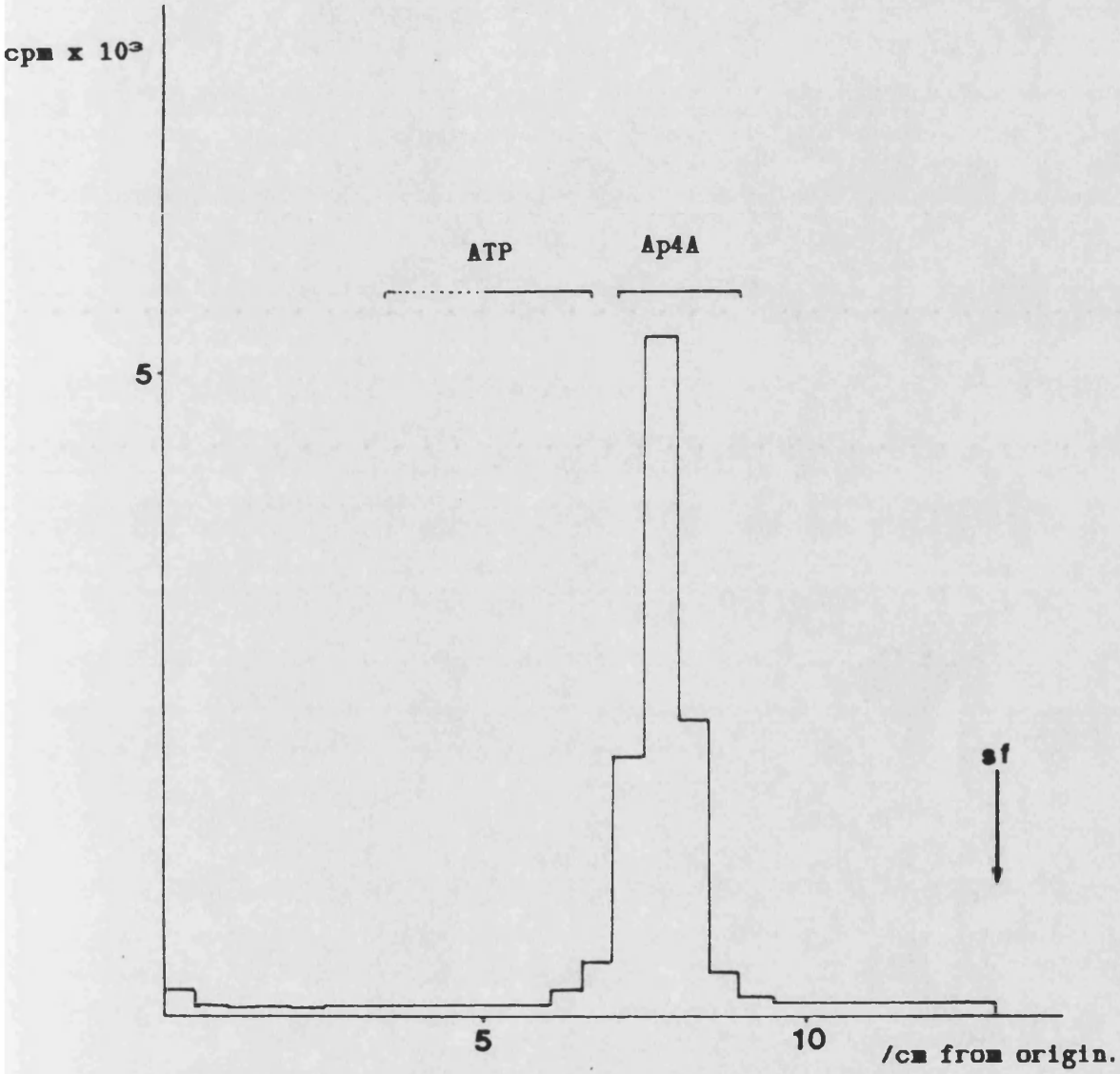

Figure 3.17.

A 15µl aliquot from fraction 14 from the DEAE cellulose column in figure 3.16 was analysed by TLC (1.6M LiCl system). The radioactive material in this fraction co-migrates with the underlaid Ap4A standard.

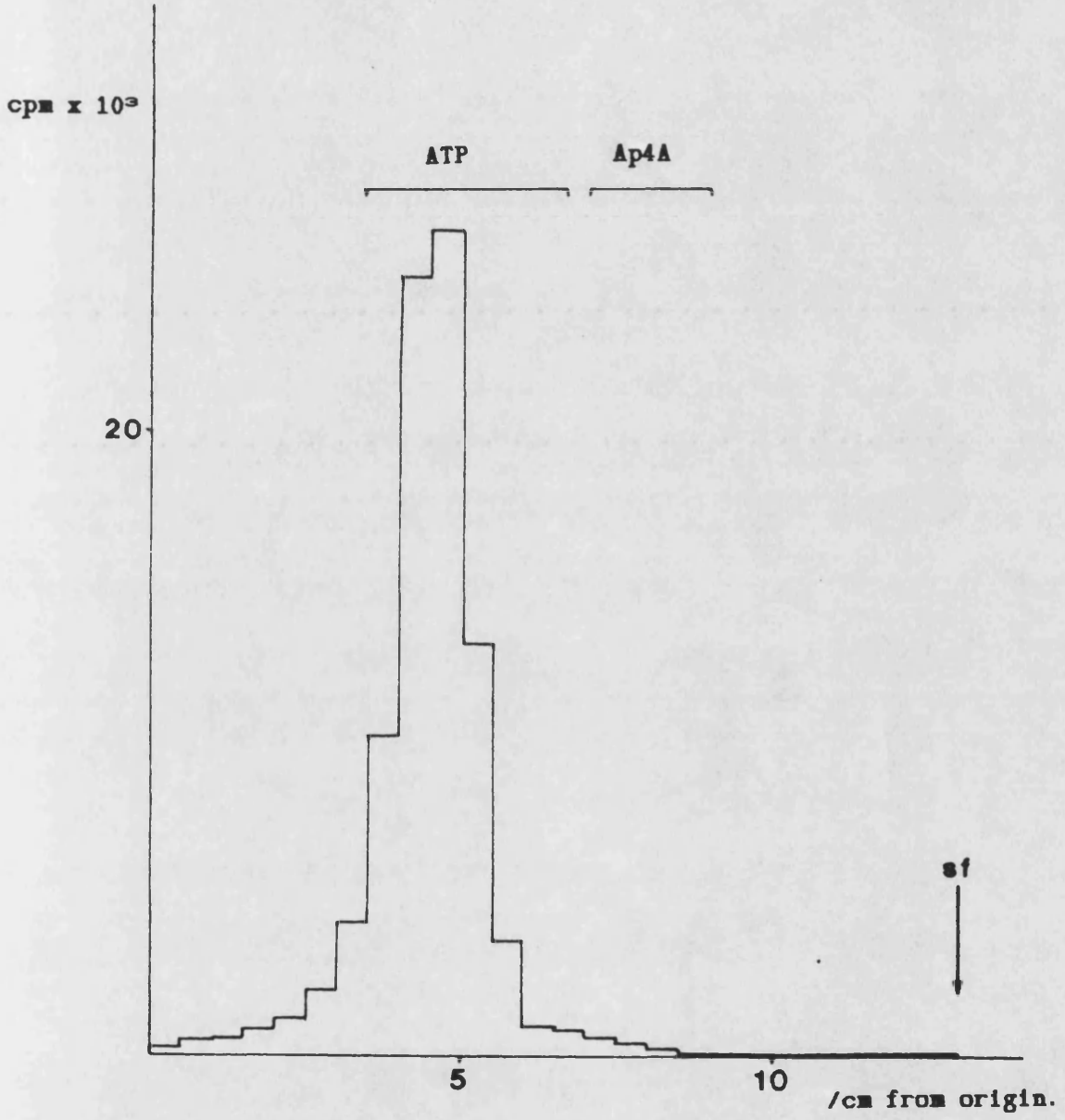

Figure 3.18.

A 15µl aliquot from fraction 18 from the DEAE cellulose column in figure 3.16 was analysed by TLC (1.6M LiCl system). The radioactive material in this fraction co-migrates with the underlaid ATP standard.

Digestion of the two fractions with snake venom phosphodiesterase in order to further characterize them was not feasible, since ATP appeared to serve as a substrate for this enzyme, even when it is purified (see III.11). Thus, the stoichiometric production of ATP and AMP would not be visible, since all the ATP would subsequently be converted to AMP! The exhaustive digestion of ATP by SVPDE is illustrated and discussed in appendix 1.

Thus, it could be said that the material in fraction 14 (figure 3.16) is not in fact Ap4A, since although it comigrates with Ap4A in the TLC system, it is eluted from a DEAE cellulose column at lower concentrations of NH_4HCO_3 (75 mM) than expected from the results of Yoshihara and Tanaka (1981), who found that it eluted at around 175-225 mM. When commercially produced [^{3}H]Ap4A became available for purchase, their results were confirmed in later experiments in that it consistantly appeared to elute at this higher concentration.

It was of interest to see whether anion exchange chromatography on DEAE cellulose could be used to resolve some of the components in the nucleotide extracts from permeabilised cells described earlier. Figure 3.12(b) showed the smeared TLC profile of a nucleotide extract from permeabilised cells, incubated with [^{3}H]NAD^+. 80µl (from a total volume of 250µl) of this extract, amounting to approximately $3.5x10^6$ cpm, was mixed with 5mM NH_4HCO_3 to a final volume of 5ml and applied

to a DEAE cellulose column exactly as before. Table 9 shows the binding figures.

Table 9.

	$\bar{v}_{n-1}$
Total radioactivity applied (cpm).	3 495 600 ± 34 800
Radioactivity left unbound (cpm).	1 775 800 ± 8 900
Radioactivity in NH_4HCO_3 wash (cpm).	590 140 ± 2 500

It is immediately apparent that less radioactivity has bound to the column than in the previous experiment (table 8). In fact only 32.3% of the total applied to the column remained bound after the 4ml 5mM NH_4HCO_3 wash. Figure 3.19 shows the radioactive profile when elution was performed as before, with a linear gradient of NH_4HCO_3 from 5 to 400 mM. Here, it is evident that the biggest peak of radioactivity is in the first fraction - and figure 3.20, which is 1.6M LiCl TLC profile of 15µl from this fraction, shows that it consists mainly of [^{3}H]NAD$^+$, with possibly [^{3}H]adenosine present as well. This explains why binding to the column initially was so low, because the majority of radioactivity in this extract is present as [^{3}H]NAD$^+$, which is expected to elute at a relatively low

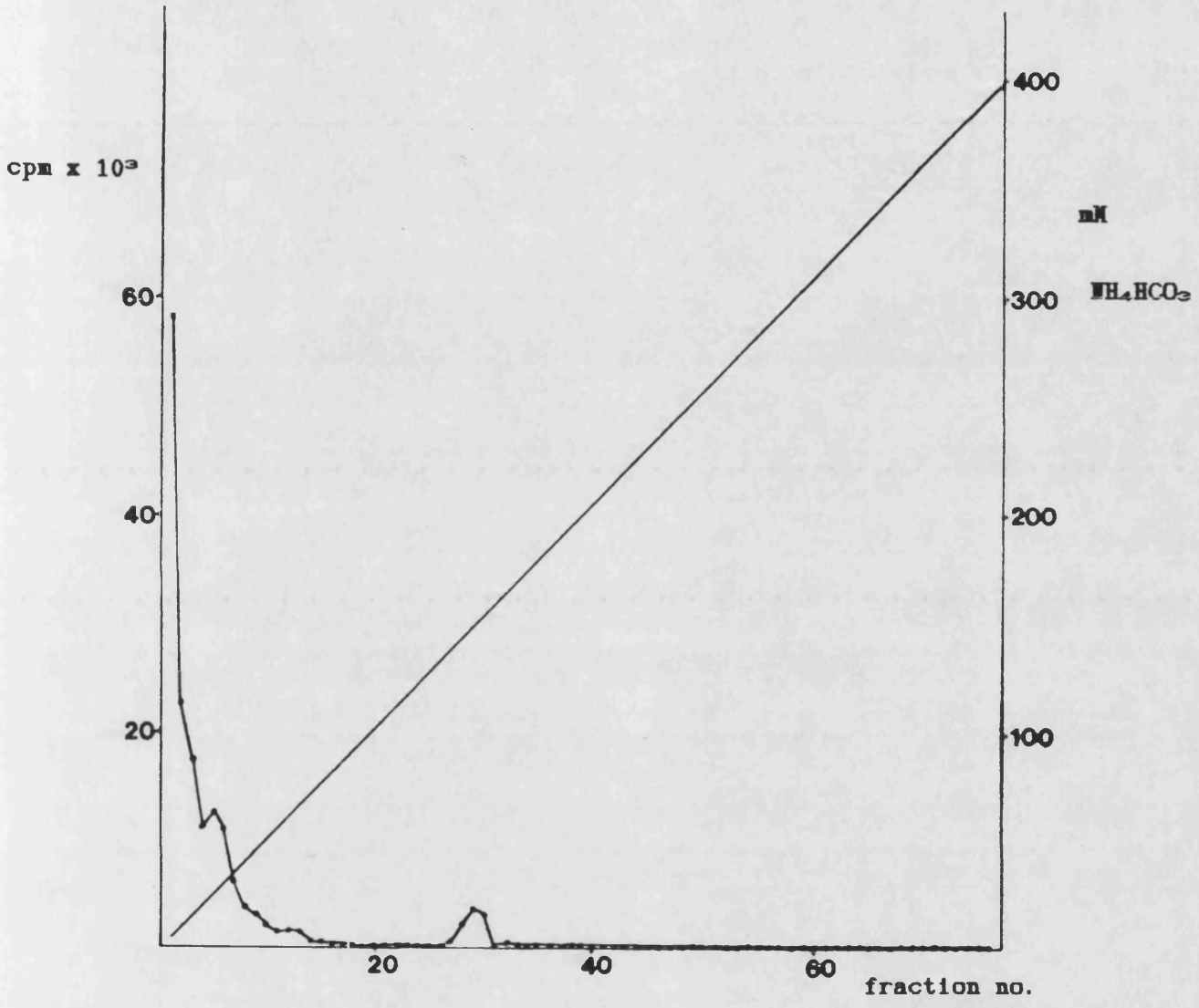

Figure 3.19.

Analysis of the nucleotide extract from permeabilised cells incubated with [³H]NAD⁺ (See text for further details) by anion-exchange chromatography on DEAE cellulose, using a linear gradient of NH_4HCO_3 (pH 8.3) from 5 mM to 400 mM. 2ml fractions were collected at 40 ml/hr and a 200µl aliquot from each was counted for radioactivity (cpm).

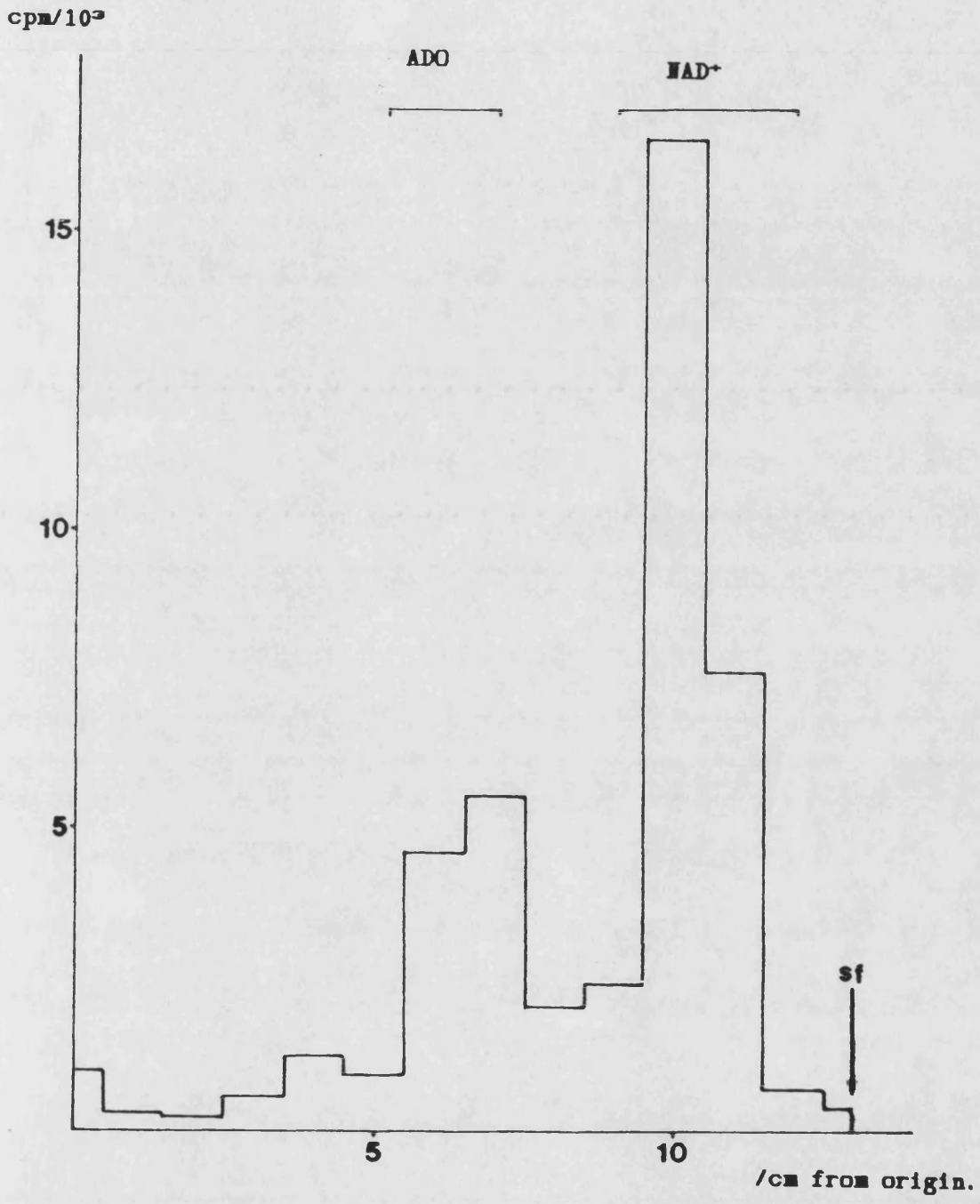

Figure 3.20.

Analysis of a 15µl aliquot from fraction 1 from the DEAE cellulose column in figure 3.19 by TLC (1.6M LiCl system).

concentration of NH_4HCO_3 owing to its positive charge (it also migrates further than Ap4A or ATP on TLC). It appears that NAD^+ is eluting at *less* than 5 mM NH_4HCO_3 - the starting point of the concentration gradient!

The second peak of radioactivity in figure 3.19 (which has not been entirely separated from the first peak) appeared in fraction 4. 20µl (10% of the total) from this fraction was subjected to 1.6M LiCl TLC analysis as before and figure 3.21 shows that the radioactivity it contains comigrates with the NAD^+ and ADP-ribose standards, as well as a small proportion which remains on the origin. The peaks migrating with ADP-ribose and NAD^+ amount to 33.3 and 30.5% of the total radioactivity, respectively, 6.4% remaining on the origin. An indication of the nature of this origin material was provided by a TLC (under identical conditions) of an equivalent amount of the fraction which had been base-treated (0.2M NaOH, overnight at room temperature). In the radioactive profile resulting (figure 3.22), the [^{3}H]NAD^+ and origin peaks have been hydrolysed to produce a single large peak of [^{3}H]ADP-ribose - although some remaining NAD^+ is evident. The disappearance of the radioactivity on the origin suggests that it may have been poly(ADP-ribose)$_n$ (where n could be 2,3..etc.), which was hydrolysed to ADP-ribose monomer. The small peak at 3.5-4.0 cm has remained unchanged by the base-treatment.

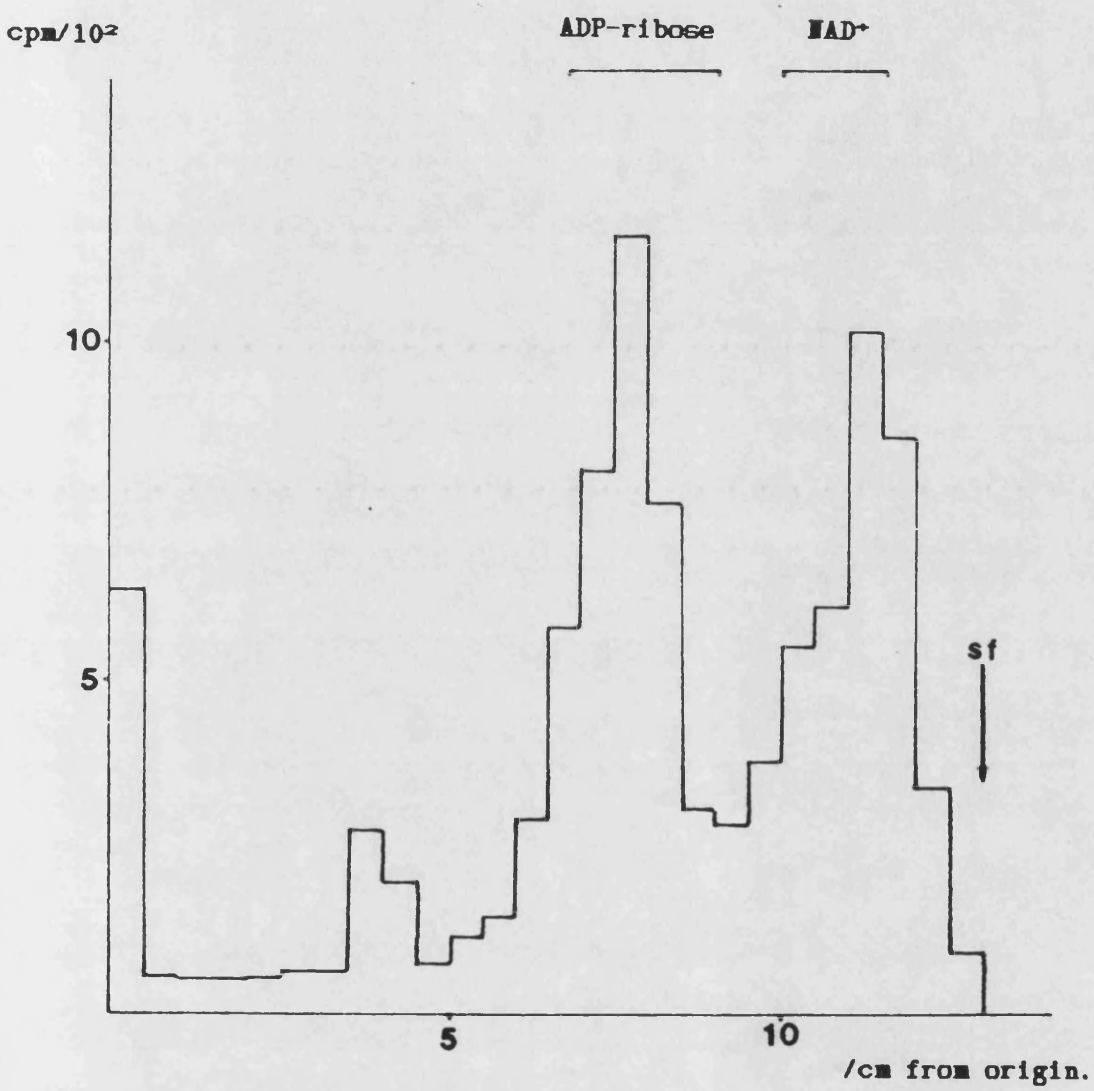

Figure 3.21.

A 15µl aliquot of fraction 4 from the DEAE cellulose column in figure 3.19 (the second major peak) was analysed by TLC (1.6M LiCl system). Note radioactivity on the origin.

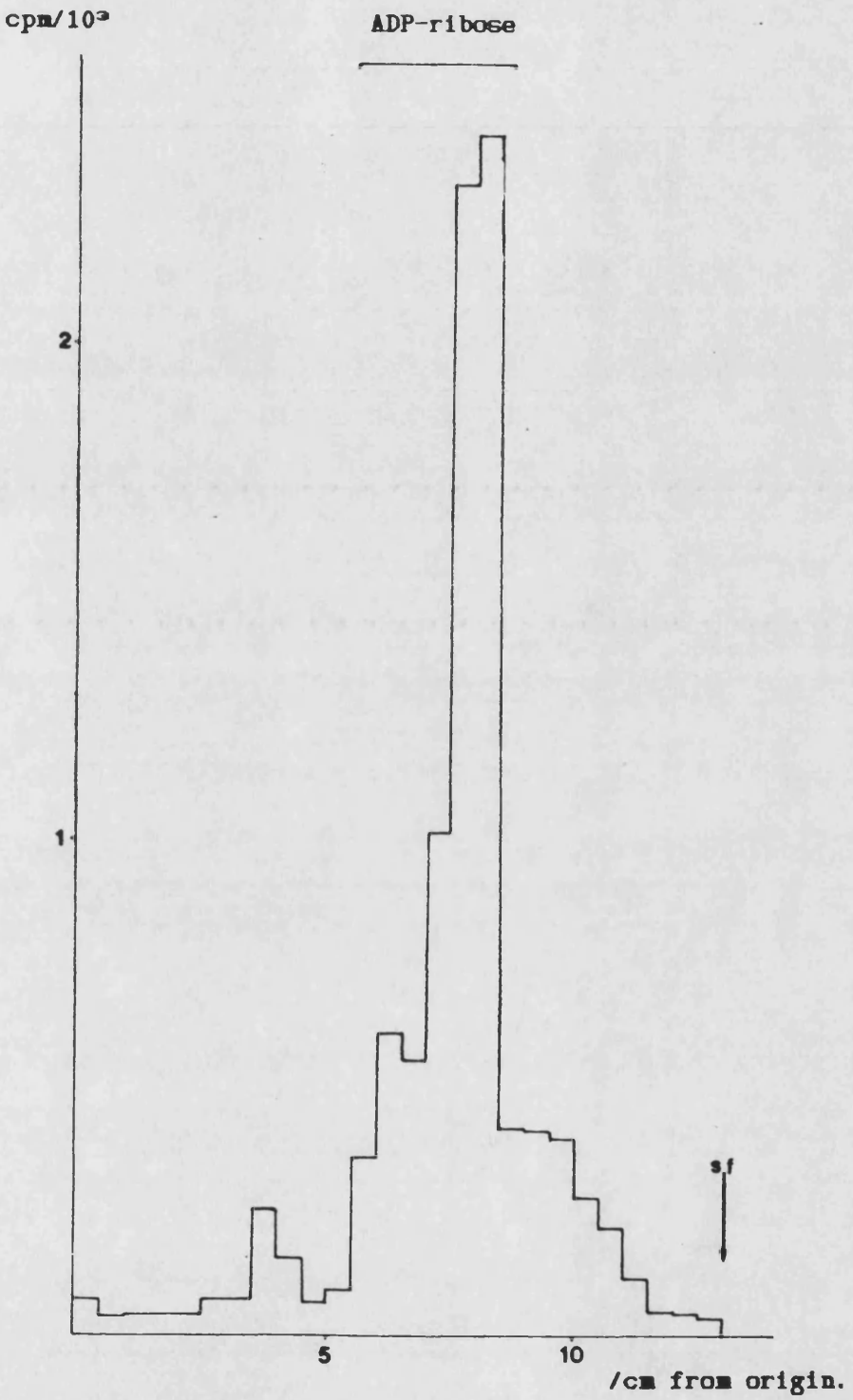

Figure 3.22.

A portion of fraction analysed in figure 3.21 was base-treated (see text) and an equivalent amount was analysed by TLC (1.6M LiCl system). Note the disappearance of the radioactivity on the origin.

The radioactivity in the third peak in figure 3.19 (fraction 28) stayed on the origin when a small portion was analysed in the acetic acid/LiCl TLC system (figure 3.23) and migrated to a position close to that of Ap4A in the 1.6M LiCl TLC system (figure 3.24) - although it is not sufficiently resolved to determine its identity further. The counterpart incubation to the one just analysed on DEAE cellulose chromatography included 100μM Ap4A, and the nucleotide extract also smeared in the 1.6M TLC system (figure 3.12(a)). When the same quantity (amounting to ≃ 3.5×10^6 cpm) of this nucleotide extract was run exactly as before on a DEAE cellulose column, a very similar radioactive profile was obtained, (figure 3.25) and the analysis of the third peak (fraction 28) in the LiCl and acetic acid/LiCl TLC systems (figures 3.26 and 3.27, respectively) show that it is similar to the analogous peak at fraction 28 in figure 3.19. The appearence and size of this peak is therefore unrelated to the presence of 100μM Ap4A in the original incubation of permeabilised cells with [^{3}H]NAD$^+$. The nucleotide extracts used in figures 3.19 and 3.25 had been stored at -20°C for two weeks prior to chromatography, and the presence of radioactivity in fraction 28 from these columns may be due to the instability of [^{3}H]NAD$^+$ (and sme of its metabolites) in aqueous solution. This seems a likely explanation, since further repeats of these experiments using fresh nucleotide extracts did not reproduce these peaks.

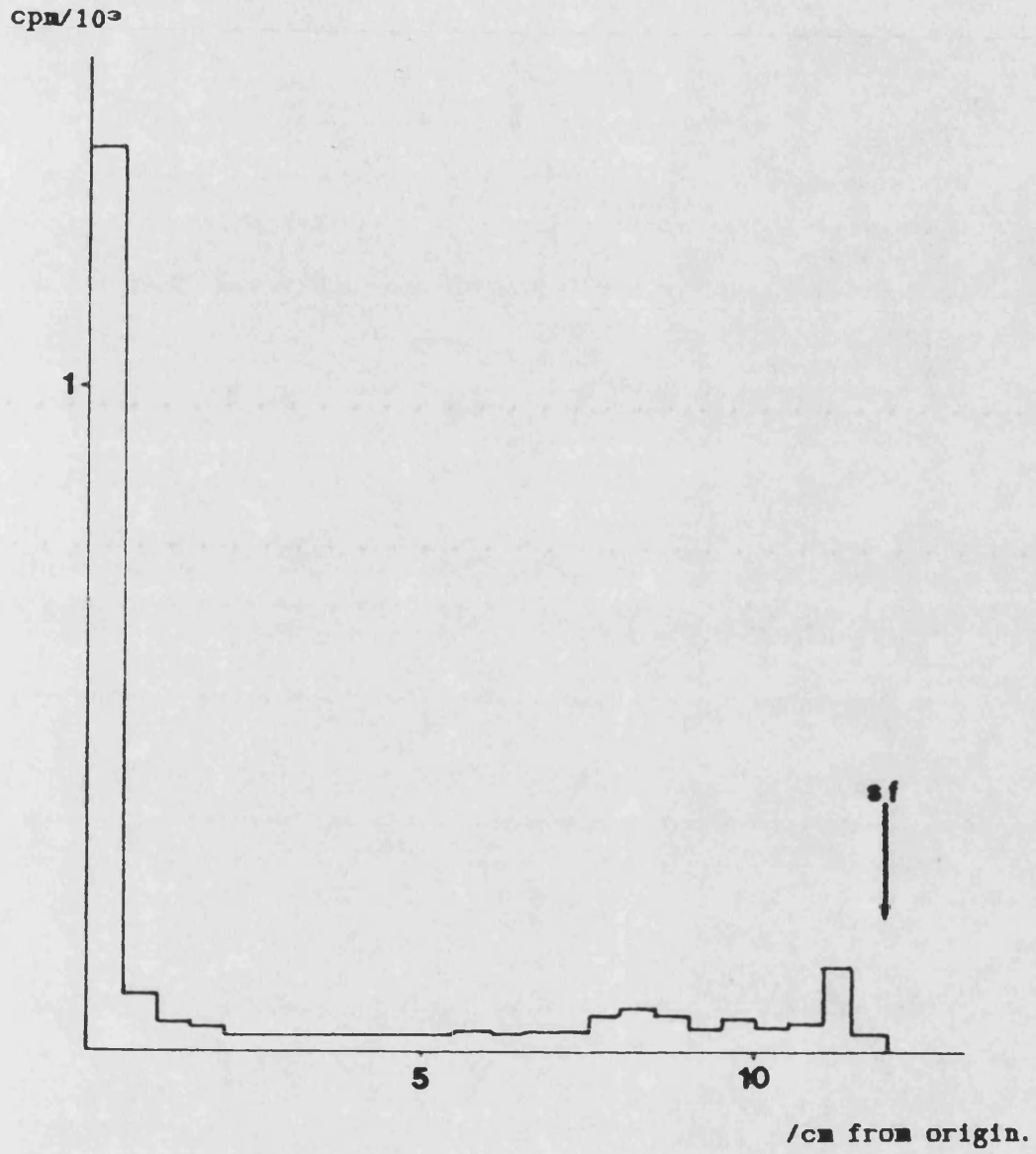

Figure 3.23.

A 15µl aliquot of fraction 28 from the DEAE cellulose column in figure 3.19 (the third major peak) was analysed by TLC in the acidic (LiCl/acetic acid) system.

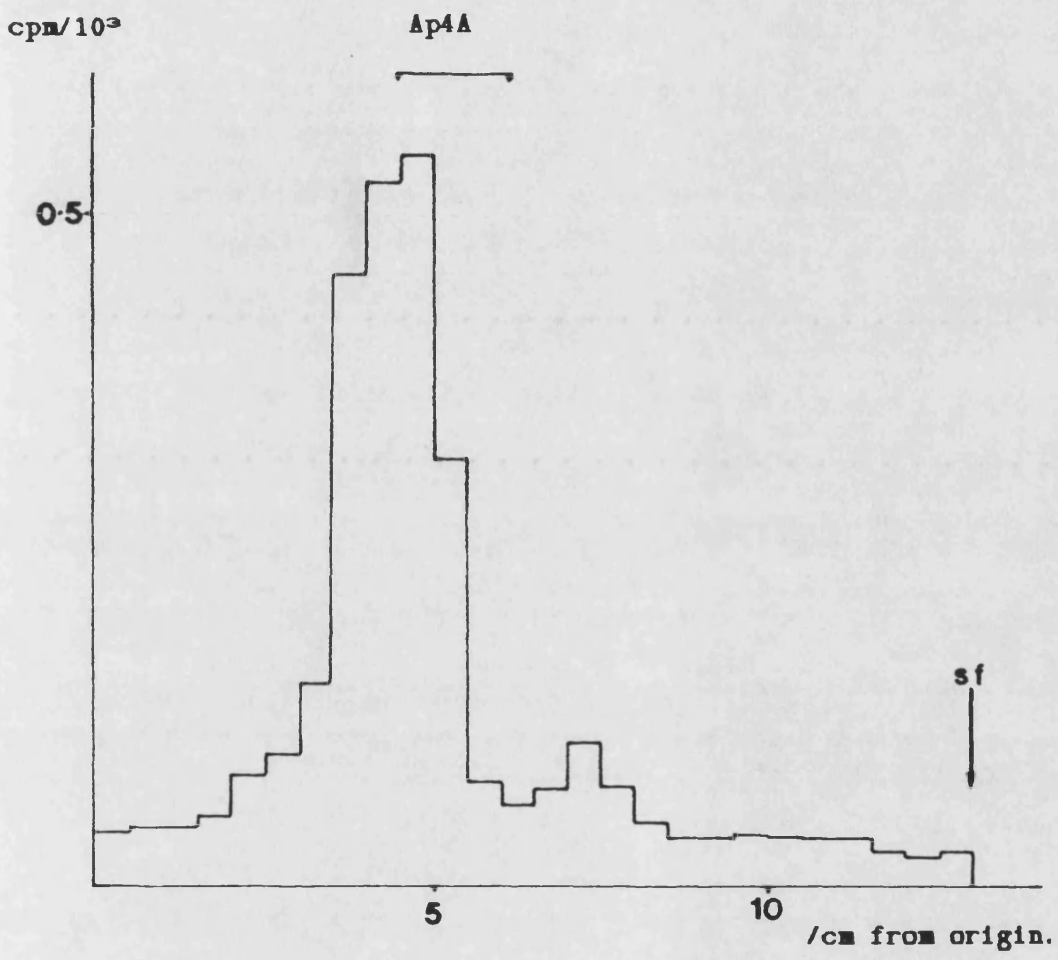

Figure 3.24.

A 15µl aliquot of fraction 28 from the DEAE cellulose column in figure 3.19 (the third major peak) was analysed by TLC in the non-acidic (1.6M LiCl) system.

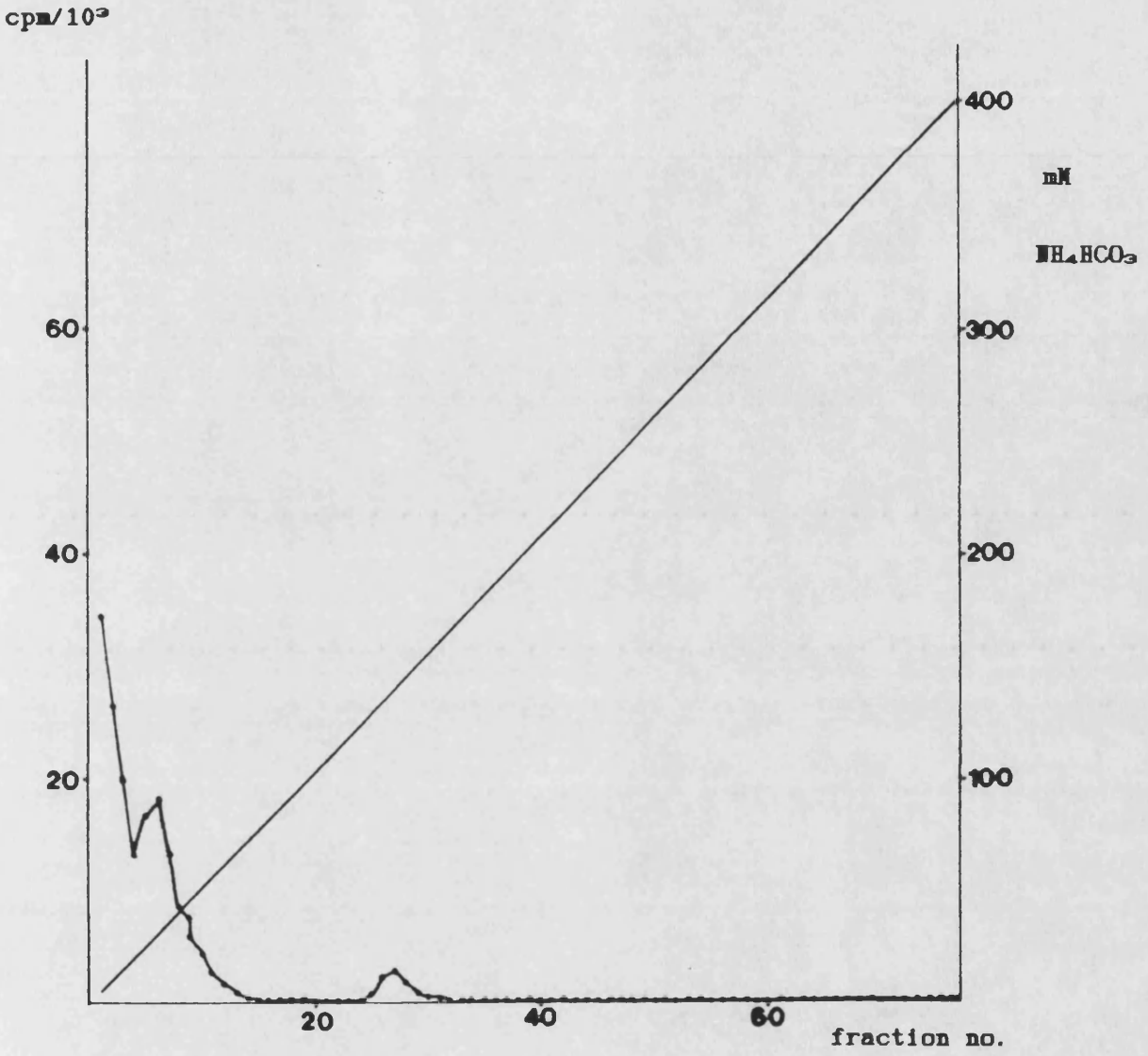

Figure 3.25.

Analysis of the nucleotide extract from permeabilised cells incubated with [^{3}H]NAD$^+$ *and 100 μM Ap4A* (cf: figure 3.19) by anion-exchange chromatography on DEAE cellulose, using a linear gradient of NH_4HCO_3 (pH 8.3) from 5 mM to 400 mM. 2ml fractions were collected at 40 ml/hr and a 200μl aliquot from each was counted for radioactivity (cpm).

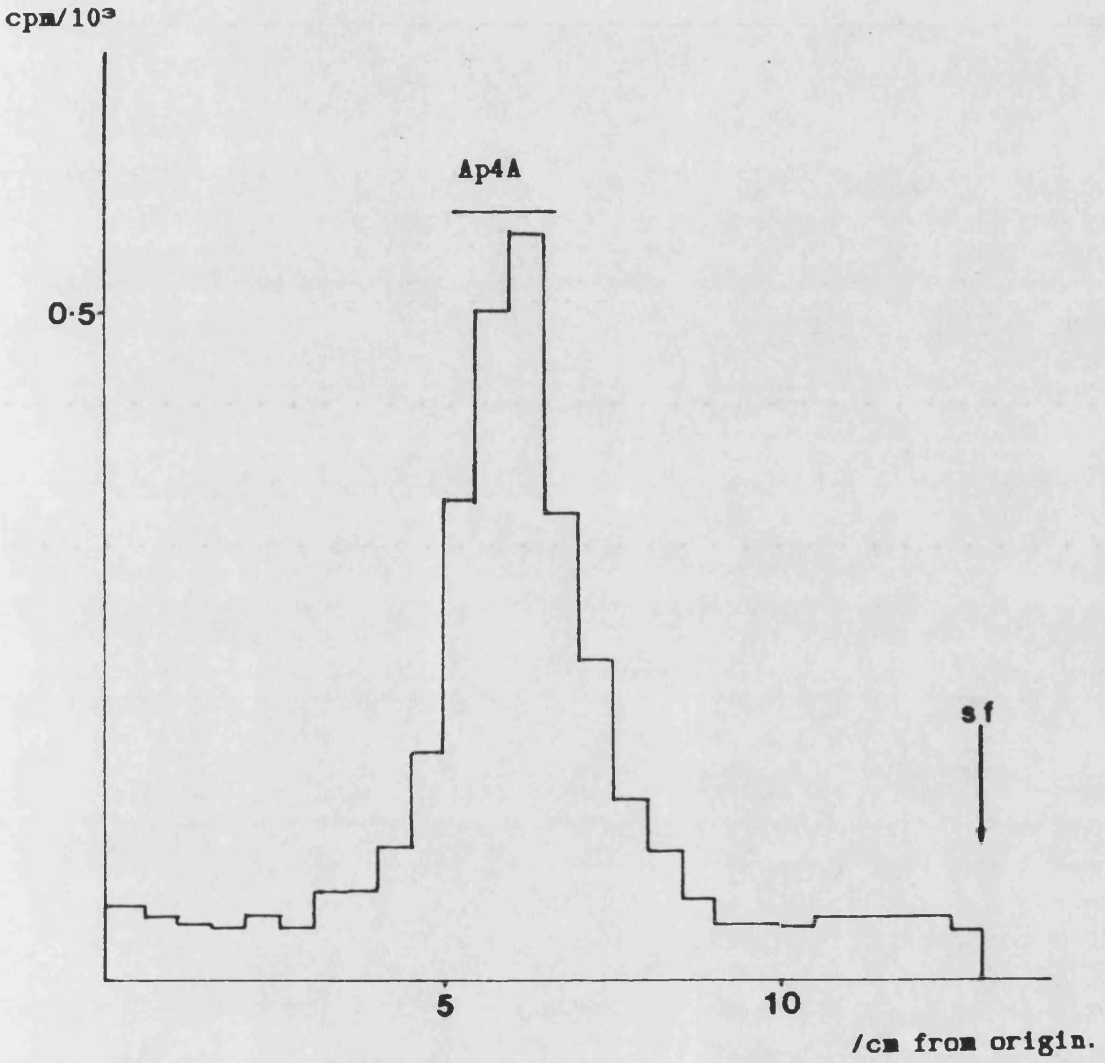

Figure 3.26.

Analysis of a 15µl aliquot of fraction 28 from the DEAE cellulose column in figure 3.25 by TLC in the non-acidic 1.6M LiCl system.

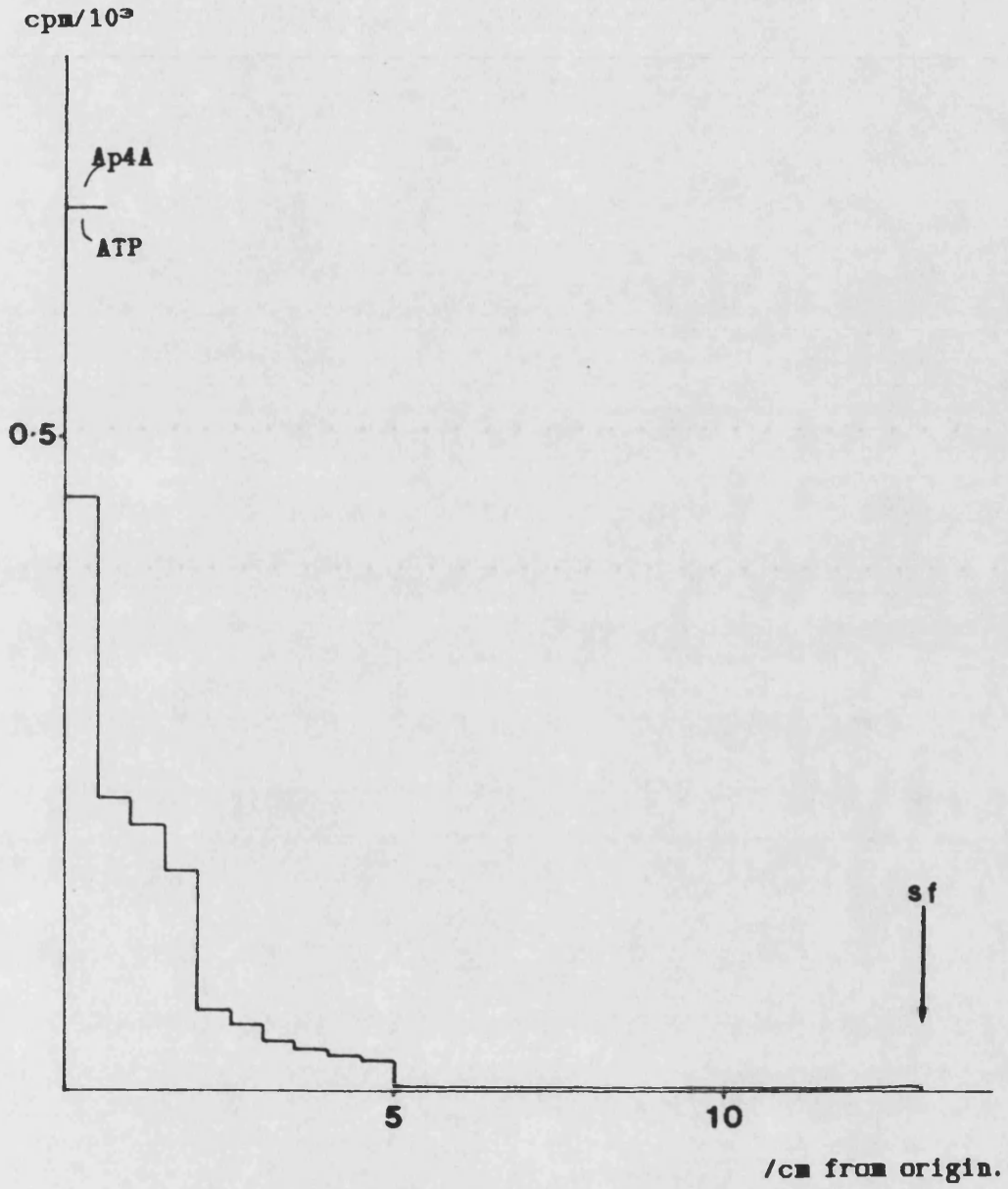

Figure 3.27.

Analysis of a 15µl aliquot from fraction 28 from the DEAE cellulose column in figure 3.25 by TLC in the acidic (LiCl/acetic acid) system.

At this stage in the project [^{32}P]NAD^{+} became available for use (see III.7(c)). It was hoped that if the (ADP-ribosyl)ating system (either extracted nuclei or permeabilised cells) were incubated with this in conjunction with some of the small quantities of [^{3}H]Ap4A which had been synthesized and purified, then the presence of (ADP-ribosyl)ated Ap4A could be detected by looking for coincidental peaks of [^{32}P] and [^{3}H] radioactivity in the elution profile of the nucleotide extract on DEAE cellulose chromatography. The effects of DNA-damage-stimulation of ADPRT (by DMS) and its inhibition by 3AB could also be examined using this method of dual labelling.

Pig thymus nuclei were extracted with salt/PEI as described in III.4 and incubated with histone H1 and DNA with 1 056 000 dpm of [^{32}P]NAD^{+} (15 pmoles) and 180 000 dpm (3 pmoles) of the "[^{3}H]Ap4A" preparation discussed in section 3, in a final volume of 520µl. The aim of this pilot experiment was to determine whether the DEAE cellulose column chromatography used in section 3 would reveal the presence of [^{3}H]Ap4A-([^{32}P]ADP-ribose)$_n$ in the nucleotide extract. After 5 minutes at 26°C, samples were taken for assaying TCA-insoluble radioactivity, and the entire incubation was diluted to 4mls with ice-cold NH_4HCO_3 (5mM, pH 8.3) and applied to a DEAE cellulose column as before. The column was then washed with a further 4ml of the same buffer. Binding figures for both [^{3}H] and [^{32}P] are shown in table 10 below.

Table 10.

	[^{3}H] dpm	[^{32}P] dpm
	σ_{n-1}	σ_{n-1}
Radioactivity initially applied to column	159000 ± 6600	1066800 ± 39600
Radioactivity left unbound to column	110 ± 110	1430 ± 110
Radioactivity in 5mM wash	2900 ± 220	57820 ± 500

The figures in table 10 imply that 98.1 ± 4.4% of the [^{3}H]dpm and 94.6 ± 3.7% of the [^{32}P]dpm have bound to the column in 5mM NH_4HCO_3. From the behaviour of [^{3}H]NAD^+ on the DEAE cellulose columns in section 3, it was expected that more [^{3}H] would bind to the column than [^{32}P], due to the greater negative charge on the [^{3}H]Ap4A increasing its affinity for the positively charged DEAE groups.

No detectable [^{3}H]dpm was incorporated into TCA-insoluble material, but a total of 42306 ± 156 dpm was recorded using the '[^{32}P] window' described in III.7(b), indicating that [^{32}P]NAD^+ had been used to (ADP-ribosyl)ate protein. Elution was performed as described with a linear gradient of NH_4HCO_3 from 5mM to 400mM, and each 2ml fraction was assayed for both kinds of radioactivity. The efficiency of counting was 78.9% for [^{32}P] and 28.3% for [^{3}H], and the Basic programme in Appendix 1 was used to process the cpm figures into dpm, correcting for efficiency and spill-over from [^{32}P] to [^{3}H]. No corrections were made for [^{32}P]-decay ($t_{½}$ 14.2 days) since the experiment was performed in a single day, and is not compared with other experiments using [^{32}P]. Figure 4.1 shows the radioactive profile of the column, with [^{32}P]dpm represented as closed circles (●) and [^{3}H]dpm as open circles (○).

It can be seen that the peak at fraction 25 (at ≈ 115mM NH_4HCO_3) contains both [^{3}H] and [^{32}P] dpm, and the remainder of this fraction

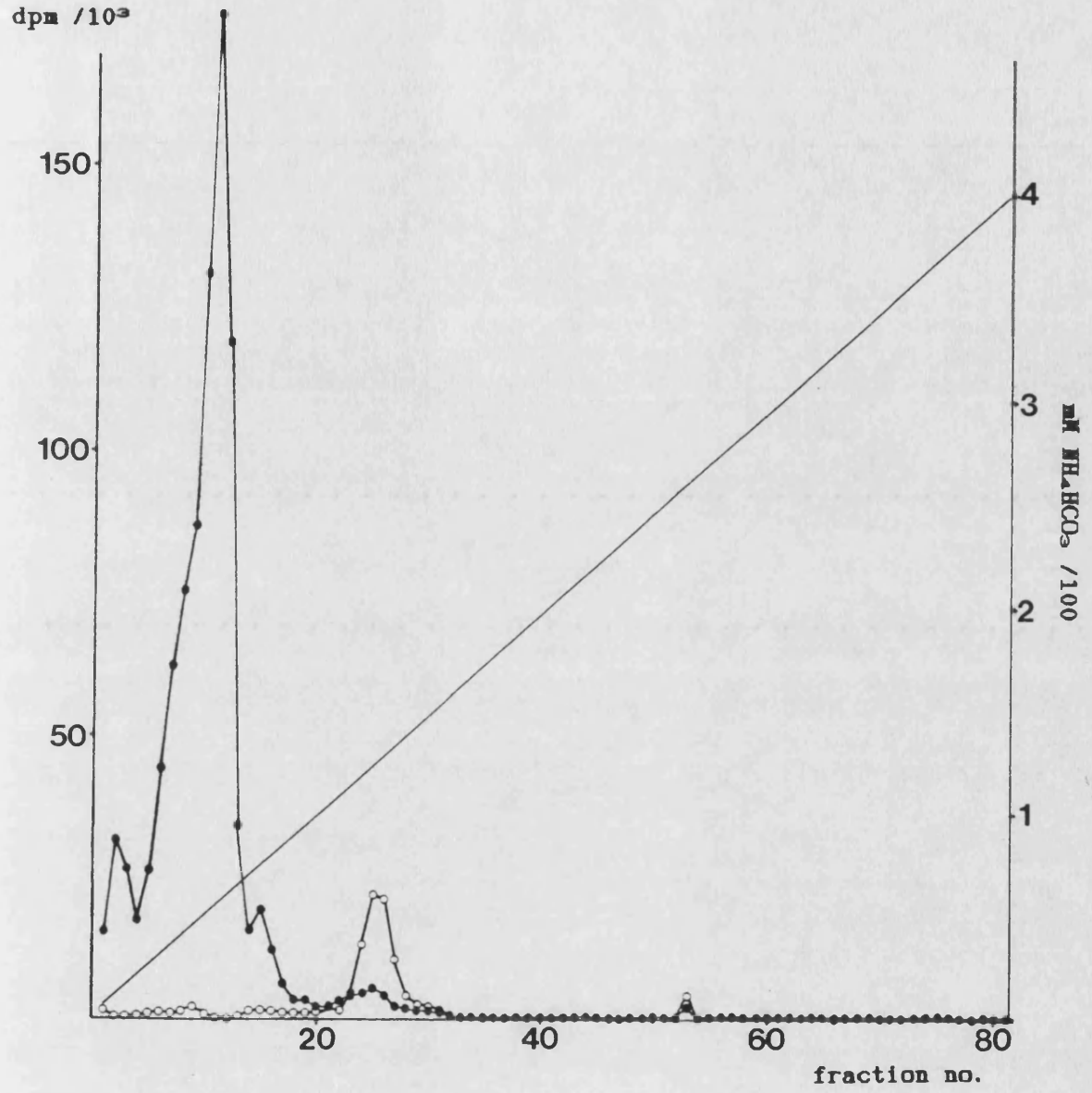

Figure 4.1.

Salt/PEI - extracted pig thymus nuclei, incubated with [^{32}P]NAD^+ and [^{3}H]Ap4A were analysed by DEAE cellulose chromatography as described in the text, the linear gradient of NH_4HCO_3 being denoted by the solid diagonal line. Each point represents the total radioactivity (in dpm) present in the 2ml fraction.

○ represents [^{3}H]dpm;

● represents [^{32}P]dpm.

was lyophilised, redissolved in a small amount of water and analysed in the 1.6M LiCl and acetic acid/LiCl TLC systems. [^{32}P] and [^{3}H] dpm for the TLC profiles were calculated as above. In the non-acidic system (figure 4.2) the [^{3}H]dpm are divided into two major peaks - one comprising 64% of the radioactivity on the plate and comigrating with the leading edge of the Ap4A standard and the trailing edge of the ADP-ribose standard. These standards were not clearly resolved, probably because lyophilisation did not remove all of the NH_4HCO_3, and the redissolving of the fraction in a final volume of 50µl resulted in a relatively high concentration of this buffer. The second [^{3}H] peak moved with the solvent front, which suggests that it is [^{3}H]adenine. This would imply that the Ap4A was being hydrolysed by enzymes in the nucleotide extract, but since the authenticity of the [^{3}H]Ap4A preparation was in some doubt (see section 3), this was not confirmed. The radioactive profile for [^{32}P] in the non-acidic system revealed one major peak, which comigrated with the ADP-ribose standard. In the *acidic* system (figure 4.3) the nucleotides (and standards) were resolved more clearly, however, it is difficult to explain the presence of at least 5 different peaks of radioactivity from a single column fraction! It is probable that [^{3}H]adenosine, as well as [^{3}H]adenine is present, since the peak at or near to the solvent front has increased from 11.6% of the total radioactivity on the plate in figure 4.2 to over 30% in figure 4.3 (adenosine has an

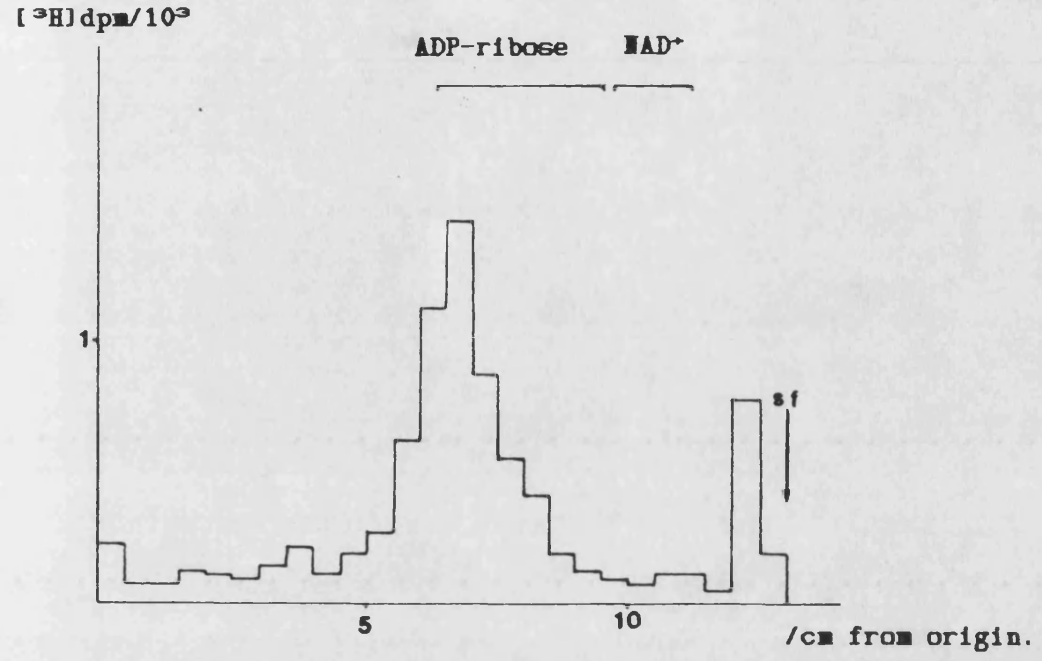

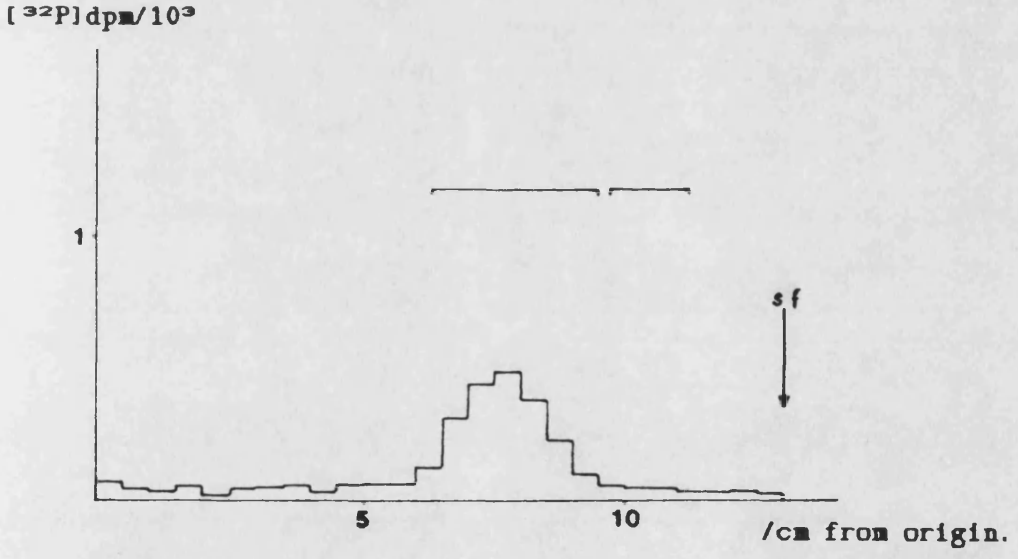

Figure 4.2.

A volume (20µl) representing 1/100th of fraction 25 from the DEAE cellulose chromatogram preceding (figure 4.1) was analysed in the 1.6M LiCl TLC system.

Top - [³H]dpm; bottom - [³²P]dpm.

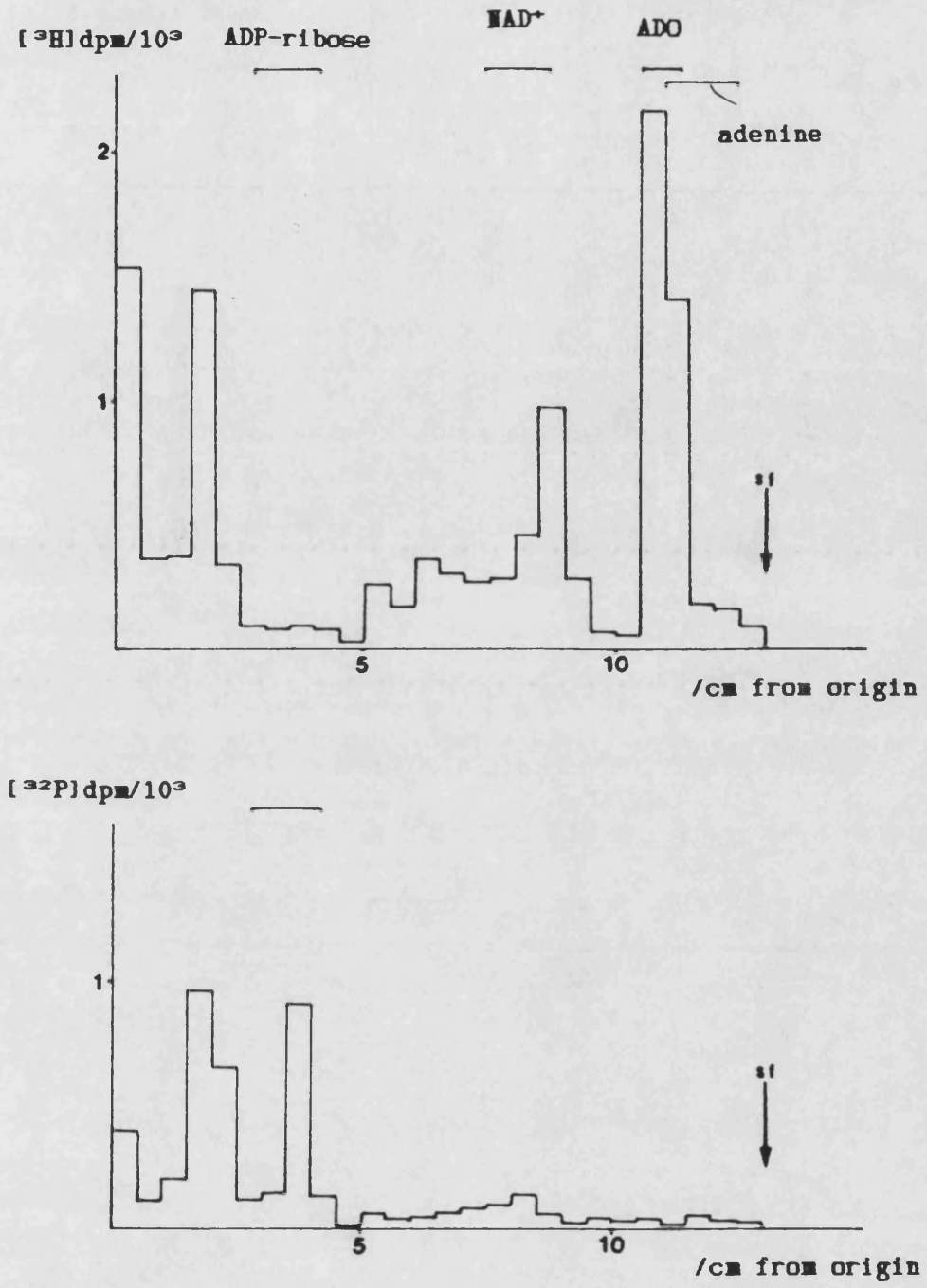

Figure 4.3.

1/100th of fraction 25 from the DEAE cellulose chromatogram in figure 4.1 was analysed in the *acidic* (LiCl/acetic acid) TLC system.

Top - [³H]dpm; bottom - [³²P]dpm

Rf value of 0.5 in neutral LiCl and runs close to the solvent front in the acidic system). Due to the complexity of this TLC profile, it was concluded that degradation of the nucleotides in the fraction had occurred, possibly as a result of the lyophilisation procedure. There was little or no radioactivity around the origin of the non-acidic TLC profile, which implies that the lyophilised fraction does not contain [^{3}H]Ap4A-([^{32}P]ADP-ribose)$_{n}$. It was decided that, ideally, enough radioactivity should be applied to the column to obviate the need for lyophilisation of the fractions of interest in order to carry out their analysis by TLC.

Pilot experiments were also carried out with permeabilised cells. Control, or DMS-treated L1210 cells were permeabilised and incubated with similar amounts of [^{32}P]NAD^{+} and the [^{3}H]"Ap4A" preparation. However, when the nucleotide extracts from these incubations were chromatographed on DEAE cellulose columns, the initial binding of radioactivity was found to be unacceptably low, with typically as much as 65-70% of the [^{32}P]dpm and ≈50% of the [^{3}H]dpm not binding at all to the column in the equilibriation buffer. Figure 4.4 shows an example, in which DMS-treated, permeabilised cells were incubated with 7.5pmoles of [^{32}P]NAD^{+} and 8.3pmoles of the [^{3}H]"Ap4A" preparation. It is obvious that a relatively large amount of [^{3}H] radioactivity is already present in fraction one, with the majority of [^{32}P] eluting at less than 75mM

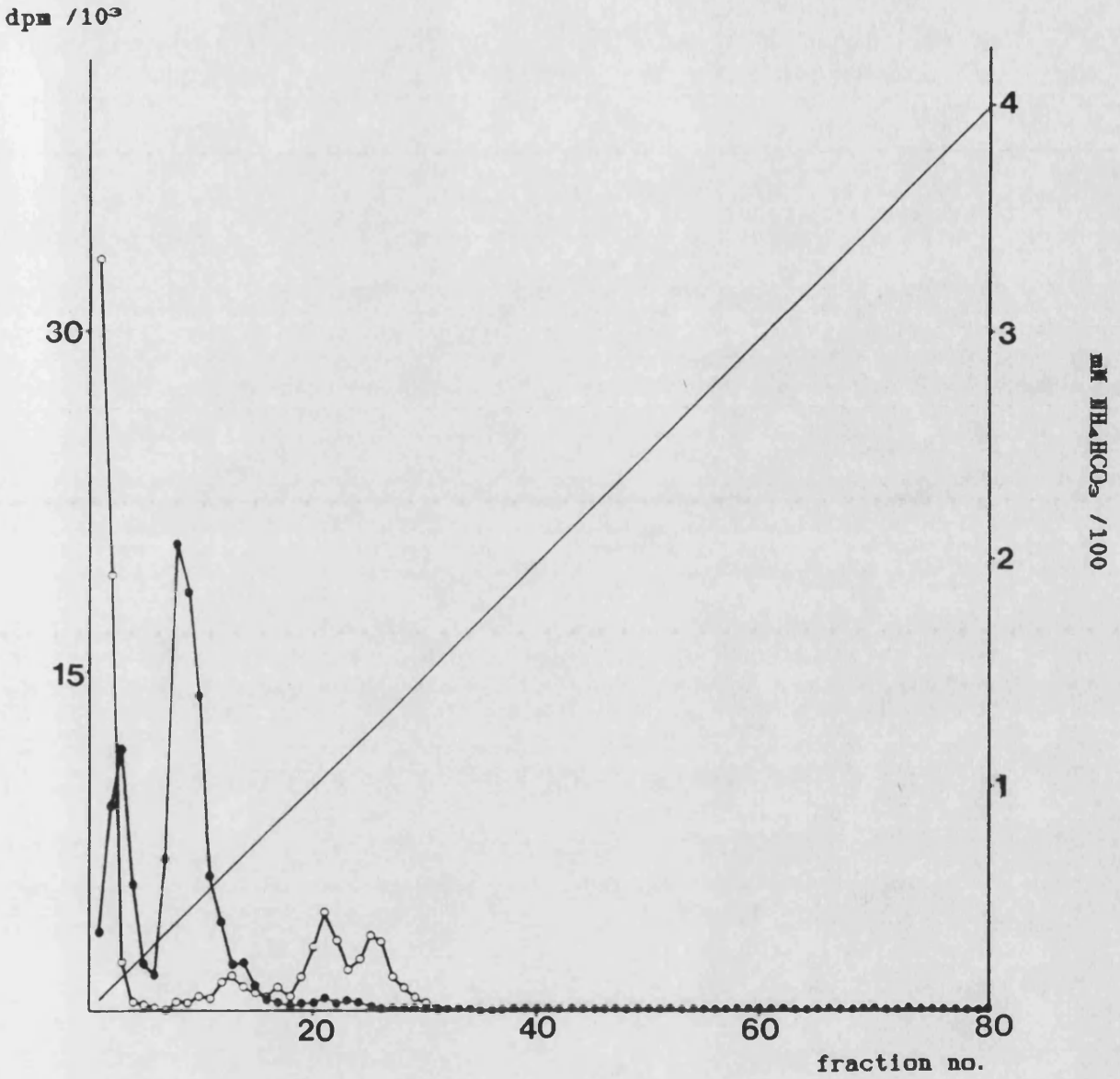

Figure 4.4.

DEAE cellulose chromatography of the nucleotide extract from permeabilised cells, incubated with 180 000 dpm (3pmol) [^{3}H]Ap4A and (1 000 000 dpm (15pmol) [^{32}P]NAD^{+}. The linear gradient was fron 5mM to 400mM NH_4HCO_3. Each point represents the total radioactivity (in dpm) present in the 2ml fraction.

○- [^{3}H]dpm

●- [^{32}P]dpm

NH_4HCO_3. Fraction one from the column profile in figure 4.4 was aspirated to 1ml under a stream of air and 20µl of this concentrate was subjected to TLC analysis in the 1.6M LiCl system. Figure 4.5 shows that the fraction appears to consist of [^{3}H]adenosine and [^{3}H]AMP, which again are probably the result of hydrolysis by the cells of the [^{3}H]"Ap4A" preparation. Fraction three from the same column was mildly concentrated in the same way, and figure 4.6 shows its profile in this TLC system, which reveals the presence of [^{32}P]NAD^+ as well as [^{3}H]adenosine and [^{3}H]AMP. The radioactive peak on the origin was not expected, since molecules eluting from the DEAE cellulose column at such a low concentration of NH_4HCO_3 (12mM) would presumably possess a less negative charge than, say, ADP-ribose. This is confirmed by the TLC profile of fraction eight, which was aspirated and analysed in the acetic acid/LiCl system (figure 4.7). The fraction appears to consist almost entirely of [^{32}P]ADP-ribose. Thus, the origin material of fraction three (in figure 4.6) was considered worthy of further investigation, particularly since it comprised of both [^{3}H] and [^{32}P] radioactive molecules.

The fact that the binding of radioactivity to the columns in these pilot experiments was so low suggests that the 'starting concentration' of the linear gradient used to elute (and thus the concentration of the equilibriation buffer - 5mM) was too high. By this reasoning it was hoped that if the gradient of NH_4HCO_3 was made

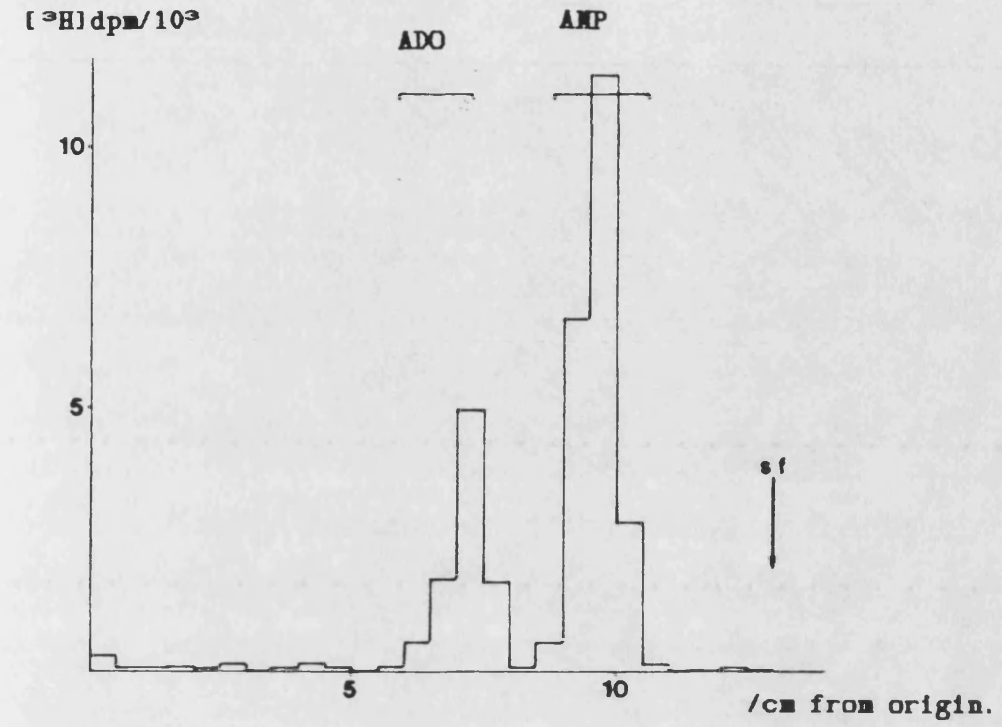

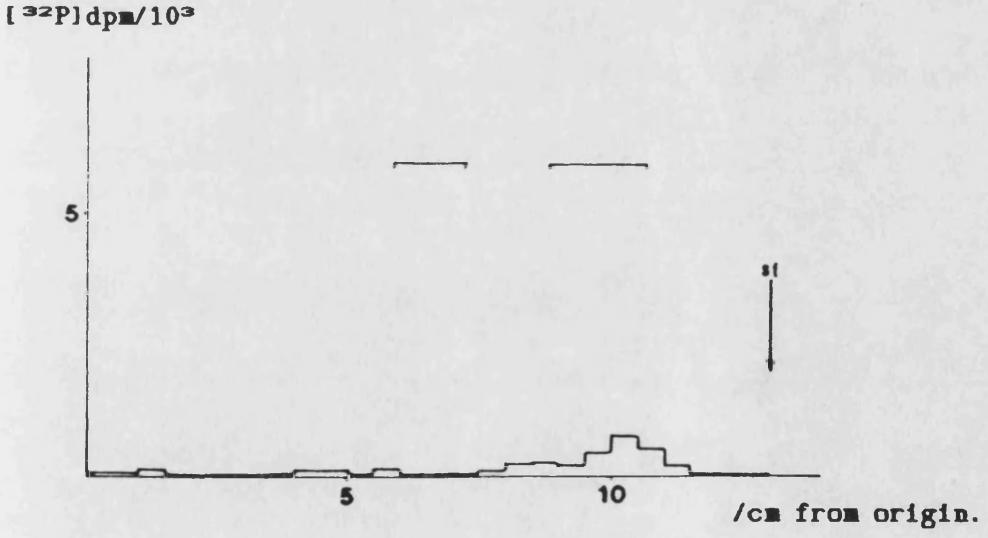

Figure 4.5

TLC analysis (in the 1.6M LiCl system) of a volume (20µl) representing 1/4 of fraction 1 from the DEAE cellulose chromatogram preceding (figure 4.4). Top - [³H]dpm; bottom - [³²P]dpm.

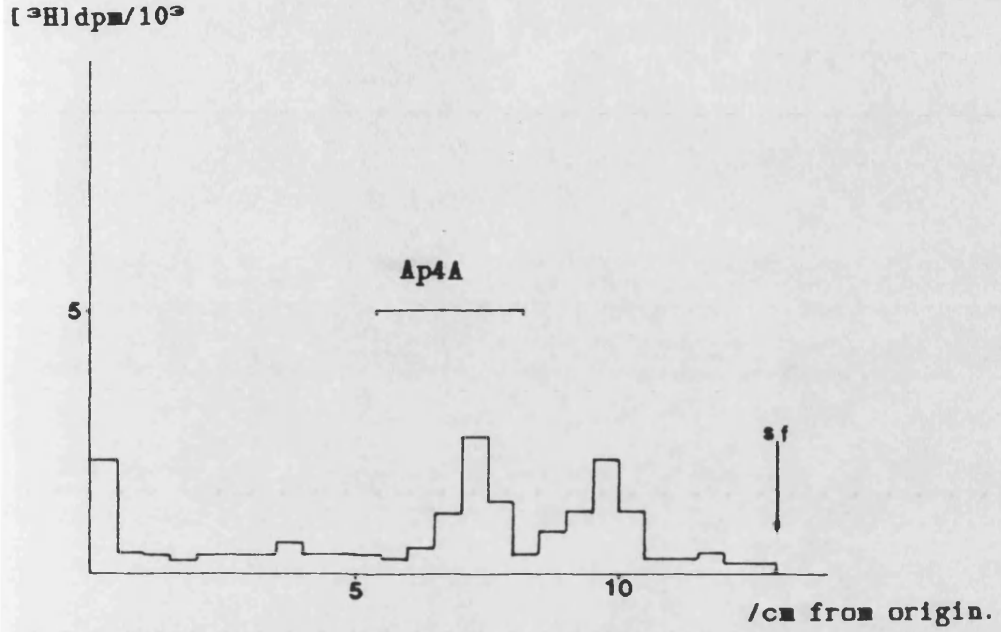

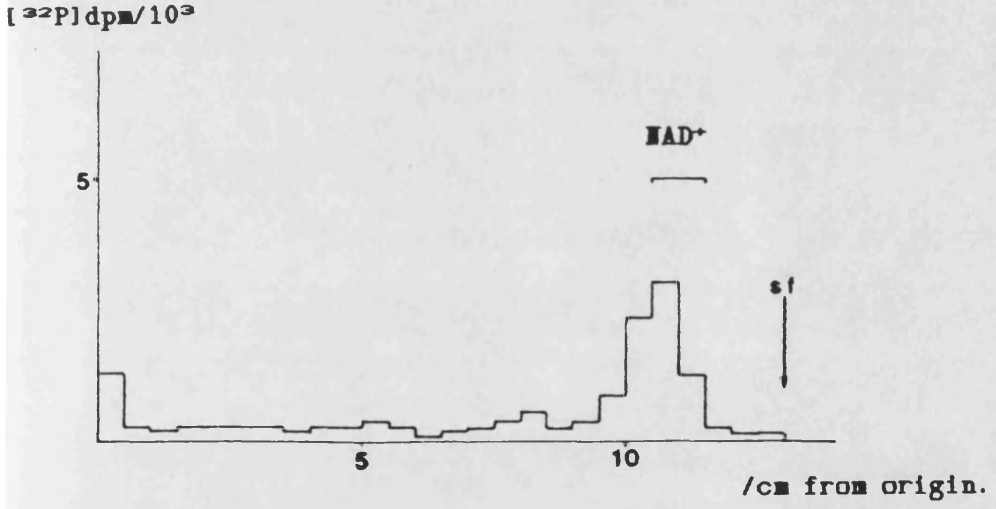

Figure 4.6.

TLC analysis (in the 1.6M LiCl system) of a volume (20µl) representing 1/2 of fraction 3 from the DEAE cellulose chromatogram in figure 4.4. Top - [³H]dpm; bottom - [³²P]dpm.

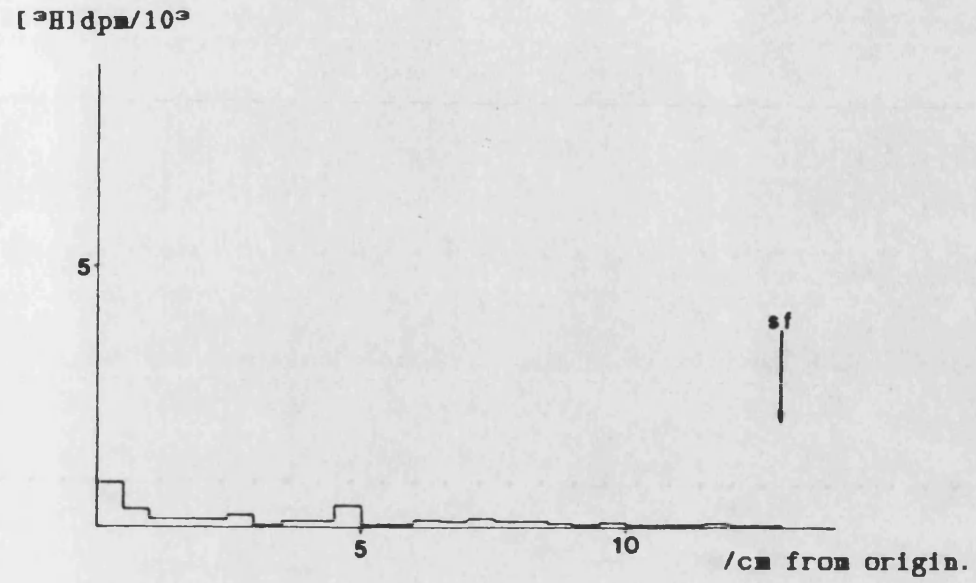

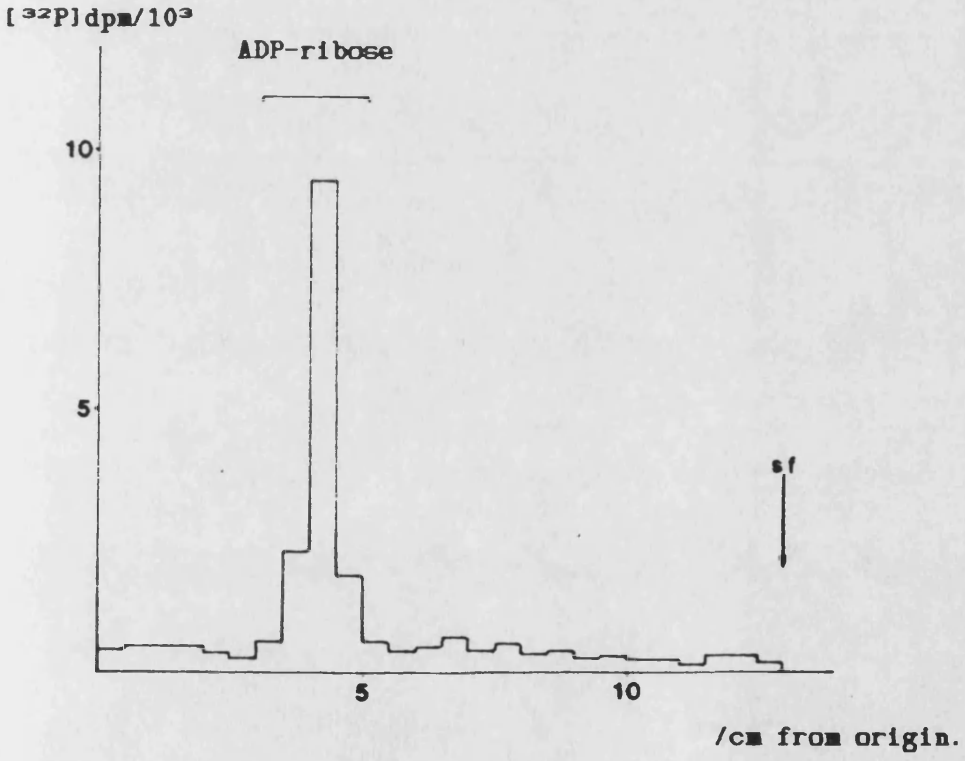

Figure 4.7.

TLC analysis (in the LiCl/acetic acid system) of a volume (20µl) of fraction 8 from the DEAE cellulose chromatogram in figure 4.4, adjusted to represent the entire fraction. Top - [³H]dpm; bottom - [³²P]dpm.

less steep by making the concentrations of the lower and higher buffers 2mM and 300mM respectively, the initial binding of the nucleotide extracts would be improved. Also, it was hoped that this would increase the resolution of adenosine, AMP, NAD^+ and ADP-ribose. These all appeared to elute at ‹75mM, producing a profile which was 'squashed up' at the lower end of the 5-400mM gradient. Successful resolution with a lower gradient would also perhaps lead to the identification of the co-[^{3}H]/[^{32}P] material in fraction three, which elutes at ≃12mM NH_4HCO_3 and yet remains upon the origin in the 1.6M LiCl system.

Again, extract of pig thymus nuclei was used to test this initially. Since the [^{3}H]"Ap4A" preparation used for the previous experiments (figures 4.1, 4.4) had been exhausted, a fresh synthesis was carried out (as described in III.12) and purification was carried out by chromatography on DEAE cellulose as described in section 3, except that a linear gradient of 2mM to 300mM NH_4HCO_3 was employed. Table 11 below shows that over 99% of the radioactivity applied to the column remained bound after washing with the new (2mM) equilibriation buffer. Figure 4.8 shows the resulting radioactive profile of the synthesis products, and three major peaks were identified. The first peak (16.5% of the total [^{3}H]dpm) was analysed by applying 30µl from fraction 6 (2ml) to a PEI TLC plate and

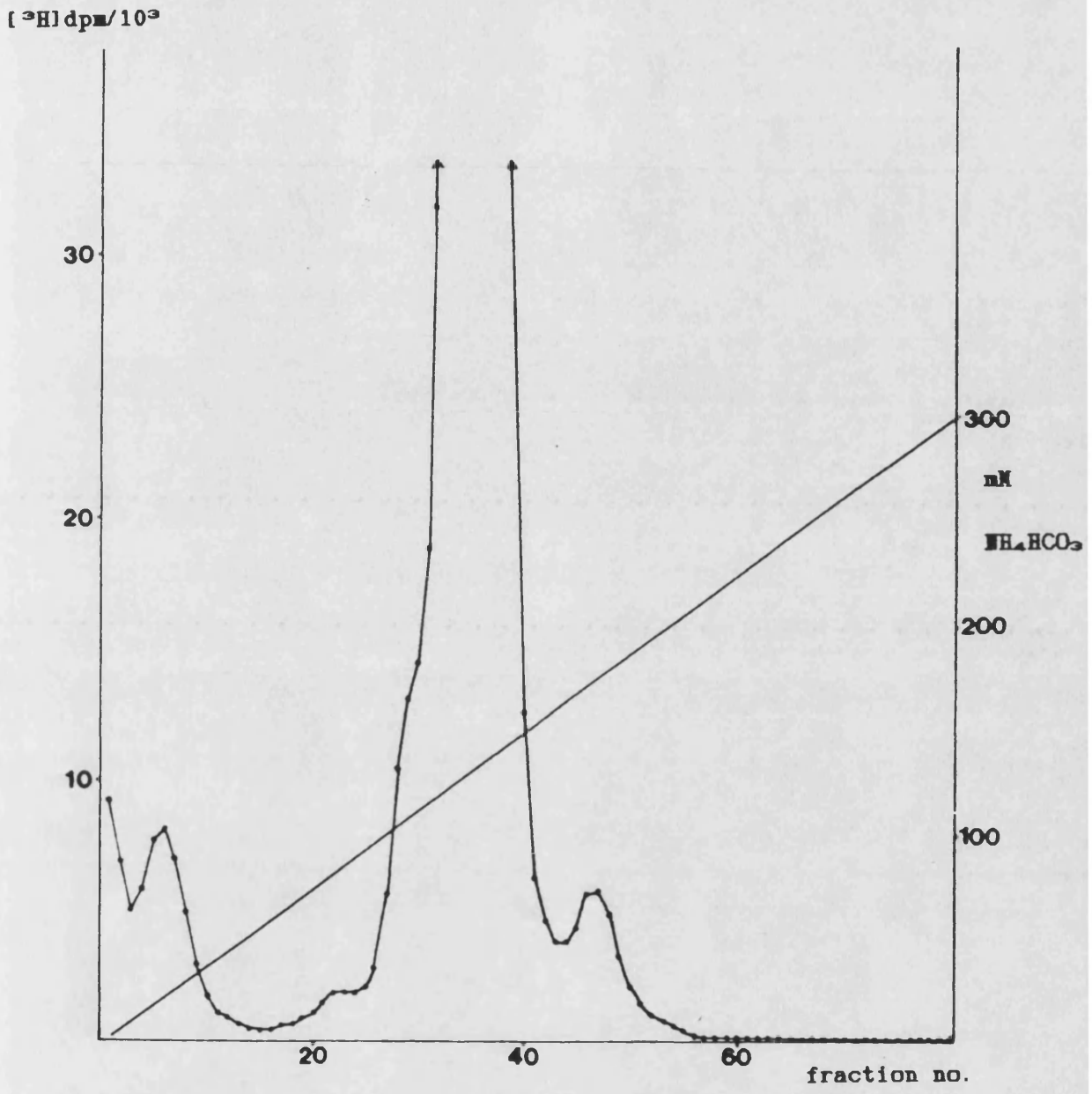

Figure 4.8.

DEAE cellulose chromatogram of the synthesis products when [³H]ATP was reacted with AMP morpholidate as described in III.12. A less 'steep' linear gradient of 2mM to 300mM NH_4HCO_3 was used. Each point represents 1/10th of the radioactivity ([³H]dpm) present in the fraction.

developing in the acetic acid/LiCl solvent system. The profile (figure 4.9) strongly suggests that the material is [^{3}H]adenosine.

Table 11.

	[^{3}H]dpm	
Radioactivity initially applied to column	44 707 750 ±	σ_{n-1} 859 750
Radioactivity remaining unbound to column	129 825 ±	1 875
Radioactivity in 2 mM wash	82 080 ±	2 080

The second (63.6% of the total [^{3}H]dpm) and third (1.7%) peaks were analysed by the application of 20µl and 50µl from fractions 38 and 48 respectively to TLC plates and developing in the same system (figures 4.10 and 4.11). Since the material in both these fractions remains on the origin, further analysis was neccessary. TLC of fraction 38 in the 1.6M LiCl system produces a single peak which co-migrates with the ATP standard (result not shown), but because minimal separation is achieved between ATP and Ap4A in this system, identification was based upon the susceptibility of the material to alkaline phosphatase. Briefly, Ap4A is known to be resistant, whereas ATP will lose successive phosphate groups to yield (in an exhaustive

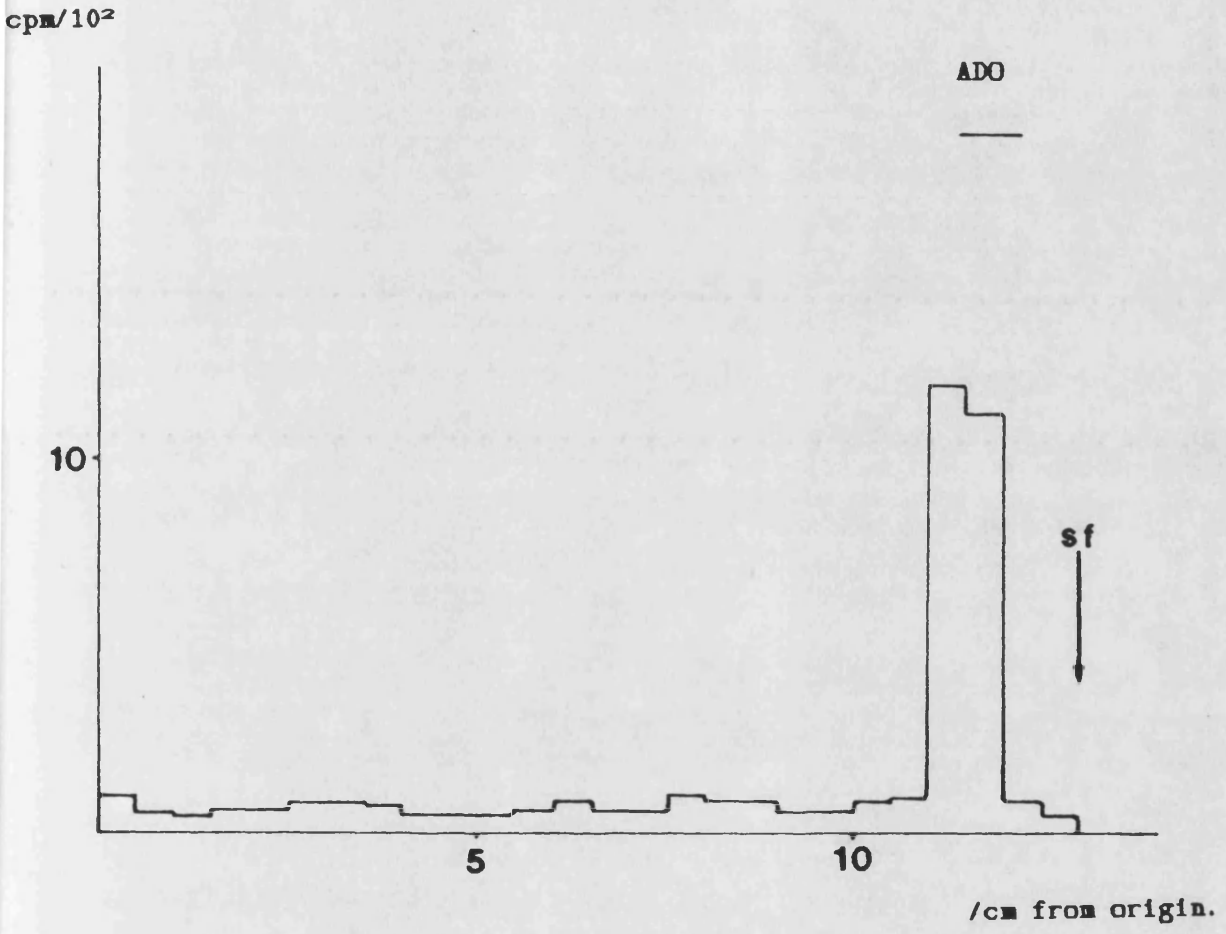

Figure 4.9.

30µl from fraction 6 of the preceding DEAE cellulose chromatogram were analysed in the LiCl/acetic acid TLC system. Top - [³H]dpm;

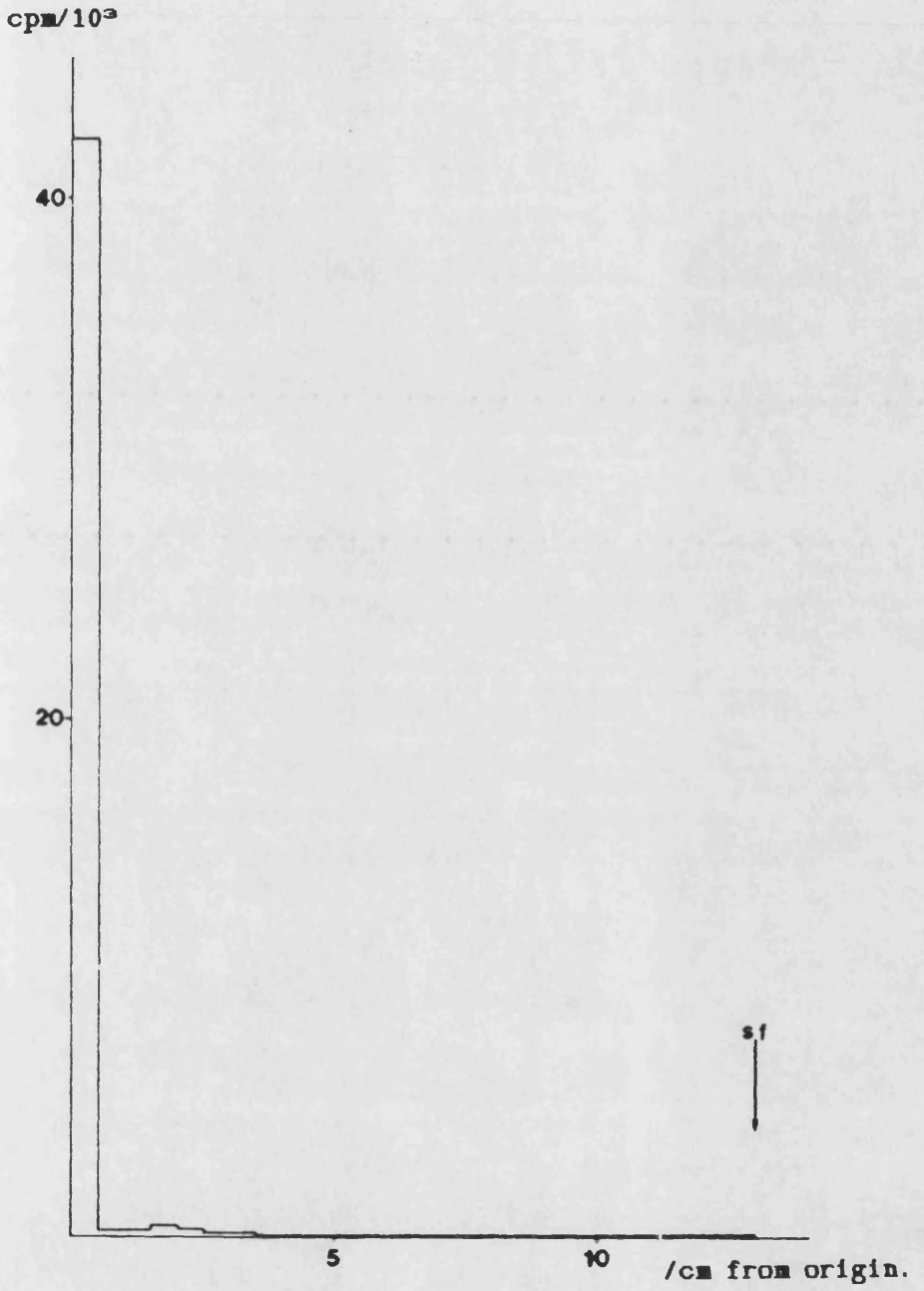

Figure 4.10.

20µl from fraction 38 of the DEAE cellulose chromatogram in figure 4.8 were analysed in the LiCl/acetic acid TLC system.

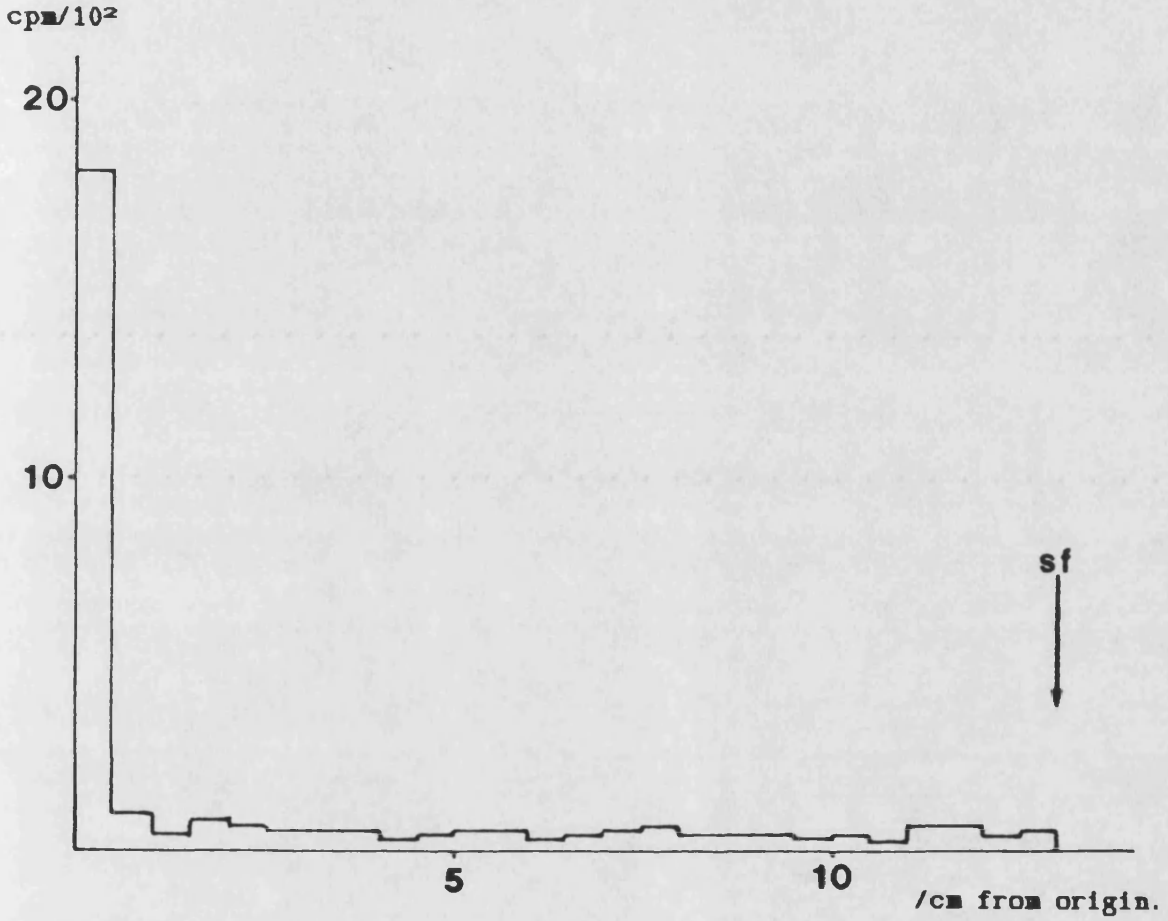

Figure 4.11.

50µl from fraction 48 of the DEAE cellulose chromatogram in figure 4.8 were analysed in the LiCl/acetic acid TLC system.

digestion) [^{3}H]adenosine (Grummt 1978). 20µl of fraction 38 and 50µl of fraction 48 were incubated for 30 minutes at 37°C with 0.2 units of alkaline phosphatase in a final volume of 52µl (at pH 8.3) and 20 µl portions were analysed in the acidic TLC system. The profiles of the digestion products (figures 4.12 and 4.13) show that the material in fraction 38 is reduced to [^{3}H]adenosine, whereas that in fraction 48 was resistant to the digestion. The latter was therefore chosen for use, and fractions 48-58 were pooled and repeatedly lyophilised to remove as much of the NH_4HCO_3 as possible. It noteworthy that this third peak (figure 4.8) eluted from the column at >175mM NH_4HCO_3 and is thus far more likely to be [^{3}H]Ap4A than the material used in the previous experiments, which eluted at 75mM !

Because of the relatively small yield of [^{3}H]Ap4A, lower overall levels of radioactivity were employed in incubations with extracted nuclei and permeabilised cells. It was thought that the amount of [^{32}P]-label in previous experiments (of which figure 4.1 is an example) was excessive in relation to the amount of [^{3}H]-label, and that even with adjustment for the spillover from the [^{32}P] to the [^{3}H] window (0.1%) of the scintillation counter, artefactual dpm may be generated in the area of the energy spectrum corresponding to [^{3}H] (*ie*: a false [^{3}H] peak may result in areas coincidental with a large [^{32}P] peak). Thus, in this experiment, salt/PEI-extracted nuclei were incubated exactly as before, but with 94 000 dpm (1.6 pmoles) of new

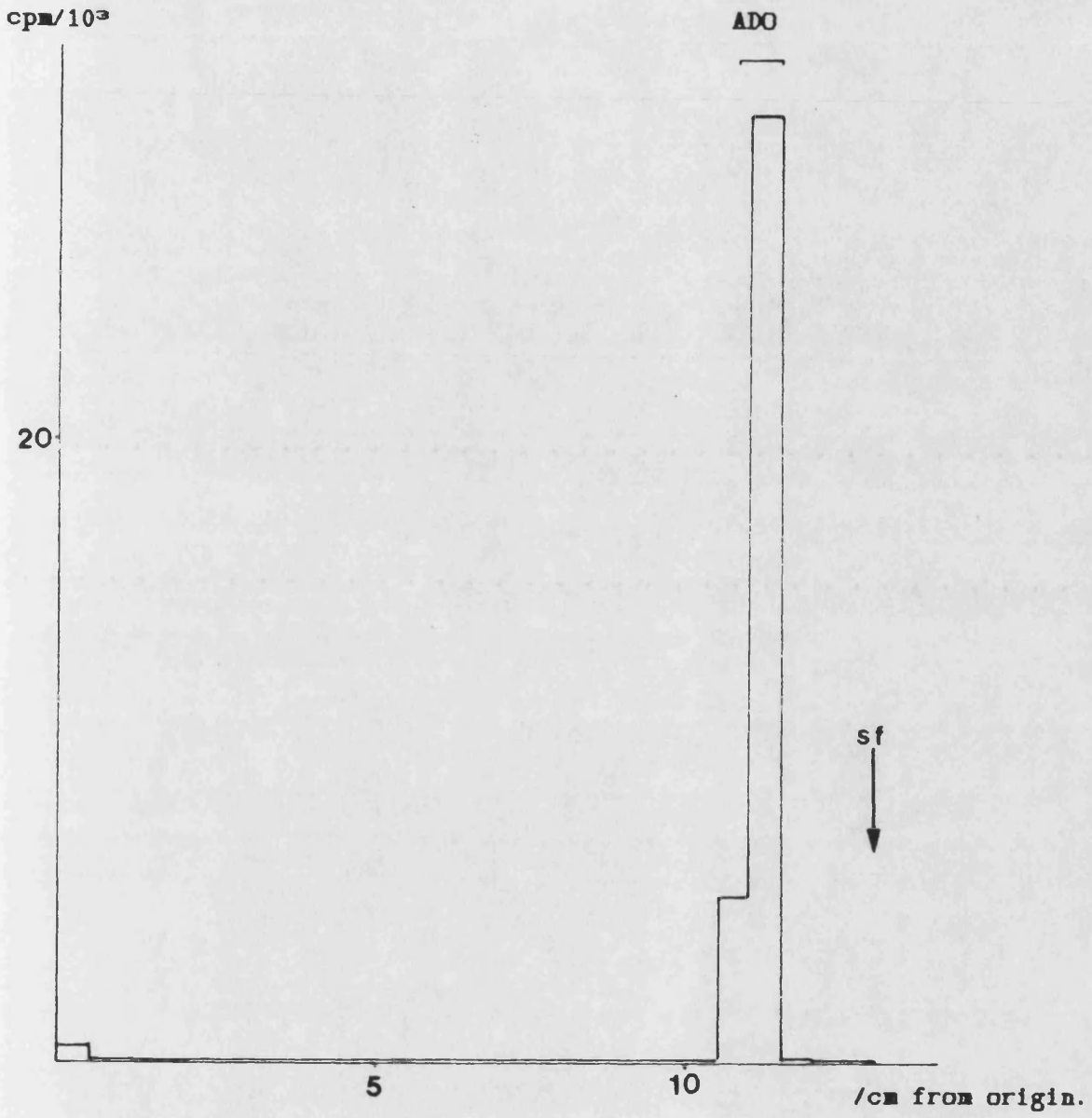

Figure 4.12.

20µl of fraction 38 from the DEAE cellulose chromatogram in figure 4.8 were digested with 0.3 units of alkaline phosphatase (see text for details) and a portion of this was analysed in the LiCl/acetic acid TLC system. Note the susceptibility to digestion.

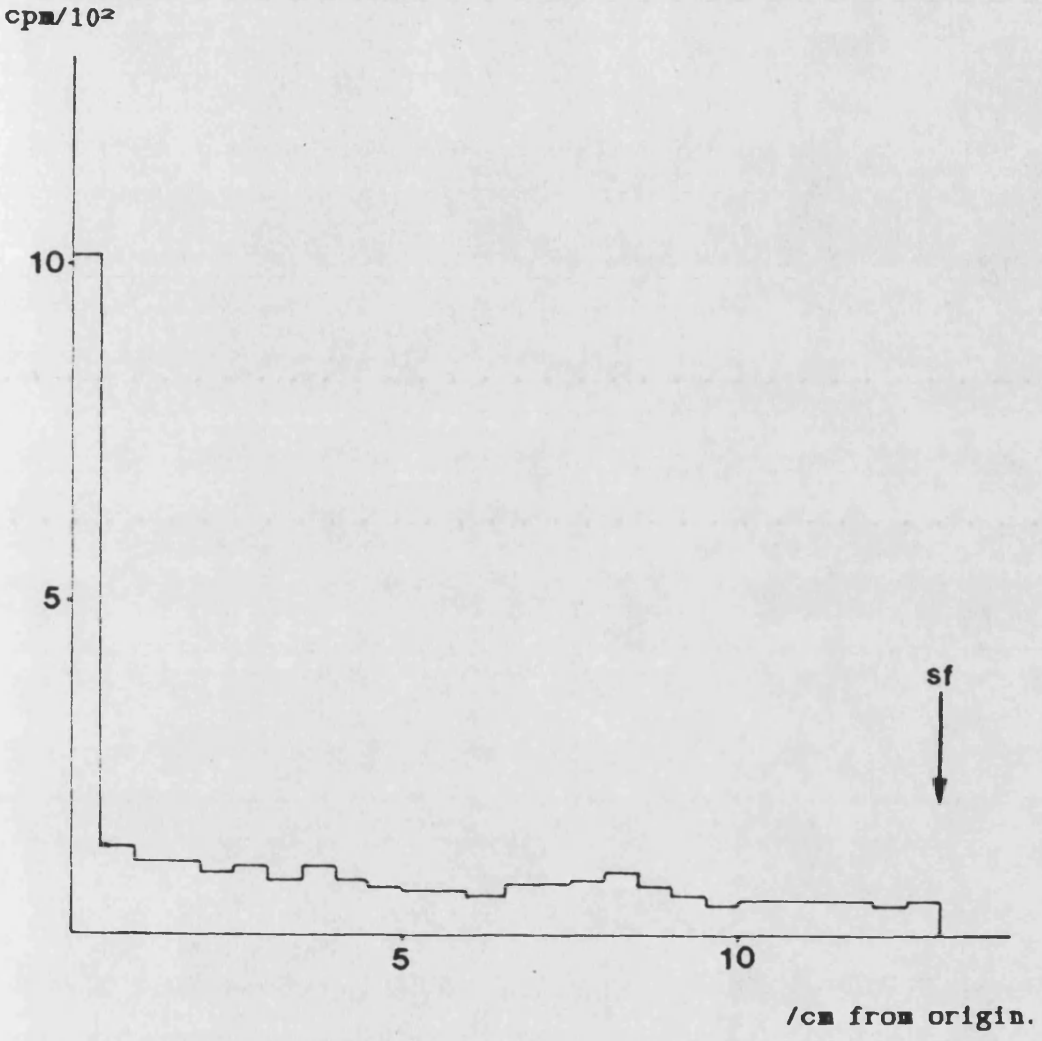

Figure 4.13.

50µl of fraction 48 from the DEAE cellulose chromatogram in figure 4.8 were digested with 0.3 units of alkaline phosphatase (see text for details) and a portion of this was analysed in the LiCl/acetic acid TLC system. Note the resistance to digestion.

[^{3}H]Ap4A preparation and 71 000 dpm (15 pmoles) of [^{32}P]NAD^{+}. After 5 minutes, aliquots were withdrawn in order to assay for TCA-insoluble radioactivity, and the entire incubation mixture was brought to 4ml with the new 'starting' buffer of 2 mM NH_4HCO_3. There was no incorporation of [^{3}H] radioactivity into TCA-insoluble material, and only 832 dpm of [^{32}P] radioactivity (cf. previously, page 168), reflecting both the lower specific activity of [^{32}P]NAD^{+} due to decay, and the lesser amounts of radioactivity initially present in the incubation.

A 3ml column of DEAE cellulose was equilibriated with excess of 2mM NH_4HCO_3 and the above sample was applied, followed, as before, with a 4ml wash with the same buffer. Elution was then carried out with a linear gradient of NH_4HCO_3 from 2 mM to 300 mM (2 x 80 ml), followed by a further 8 ml of 500 mM NH_4HCO_3. Effervescence again occurred upon attempts to pass 0.1M HCl over the column, even after excessive washing with distilled water. Table 12 shows the binding of [^{32}P] and [^{3}H] to the column before application of the gradient. Initial binding was greatly improved at this lower starting concentration of NH_4HCO_3, with 99.3% of [^{32}P] and 99.8% of [^{3}H] label remaining bound to the column after the wash. Figure 4.14 shows the elution profile of [^{3}H] and [^{32}P] radioactivity when the linear gradient was applied. Because only single aliquots were withdrawn

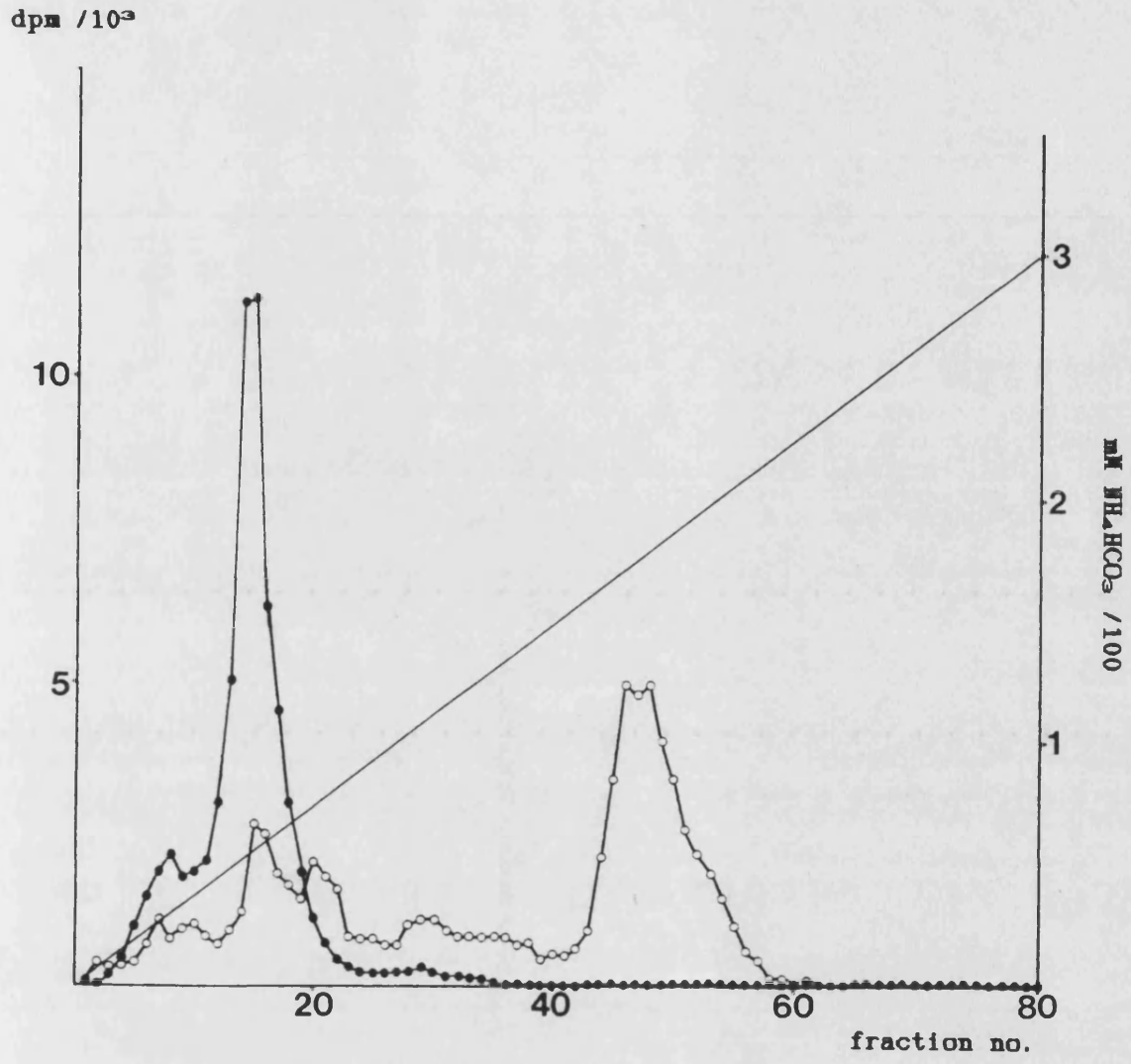

Figure 4.14.

DEAE cellulose chromatography of salt/PEI - extracted pig thymus nuclei, incubated with [^{32}P]NAD^{+} and the 'new' [^{3}H]Ap4A preparation (see text for details). Each point represents the radioactivity present in the entire fraction.

○ - [^{3}H]dpm

● - [^{32}P]dpm

from each column fraction, error estimations were not possible, but when the total amount of radioactivity eluted from the column was calculated, it was found that approximately 10% of the [^{3}H]dpm and 3% of the [^{32}P]dpm remained uneluted.

Table 12.

	[^{3}H]dpm	[^{32}P]dpm
Radioactivity initially applied to column	93 640 ± 3 534 (σ_{n-1})	71 069 ± 2 535 (σ_{n-1})
Radioactivity left unbound to column	177 ± 100	697 ± 0
Radioactivity in 2 mM wash (See text for details)	141 ± 110	457 ± 102

As before, a further 8ml of 500mM NH_4HCO_3 failed to remove any significant amount of this. The reason that more [^{3}H]dpm remain bound to the column than [^{32}P]dpm (whereas they were initially present in the incubation in the ratio of 1 : 0.76, respectively) may have been that [^{3}H] is susceptible to quenching, whereas [^{32}P] is not. When small amounts of [^{3}H]ATP were mixed with water or 100mM NH_4HCO_3 and counted, however, the NH_4HCO_3 was found to have no effect on the cpm recorded. Quenching of [^{3}H] is therefore unlikely to be responsible.

The most likely reason for this difference in retention of [^{32}P]/[^{3}H] is that the molecules bearing [^{3}H] (*ie*: Ap4A and its hydrolysis products) were more negatively charged than those bearing the [^{32}P] label (*ie*: NAD^+ and ADP-ribose *etc.*) and these therefore bound more tightly to the DEAE cellulose matrix. This retention of radioactivity by the DEAE cellulose was not considered to be unsatisfactory for the purposes of detecting (ADP-ribosyl)ated Ap4A, however, particularly since a similar analysis on DEAE cellulose by Yoshihara and Tanaka (1981) using a 5 to 400 mM NH_4HCO_3 gradient enabled them to elute mono- and poly(ADP-ribosyl)ated Ap4A whilst leaving 35% of the radioactivity bound to the column! Attempts to elute with HCl were abandoned too, since these workers found that only 5% of the total radioactivity applied were recovered in this way (*ibid.*).

The material eluting in fraction 14 (figure 4.14) was of interest, even though the NH_4HCO_3 concentration was only 50 mM at this point, because it consists of both [^{3}H] and [^{32}P]dpm. The fraction (of which ¼ had been taken to produce the profile in fig.4.14) was aspirated to dryness under a stream of air and reconstituted in 60 µl of distilled water. 20µl of this was then subjected to TLC analysis in the acidic system. Figure 4.15 shows the resulting [^{3}H] and [^{32}P] profiles. It is evident that [^{32}P]NAD^+ and ADP-ribose dpm are present, together with small quantities of [^{3}H]dpm comigrating with AMP (or possibly NAD^+) and adenosine. There is also a co-[^{3}H]/[^{32}P] peak on the

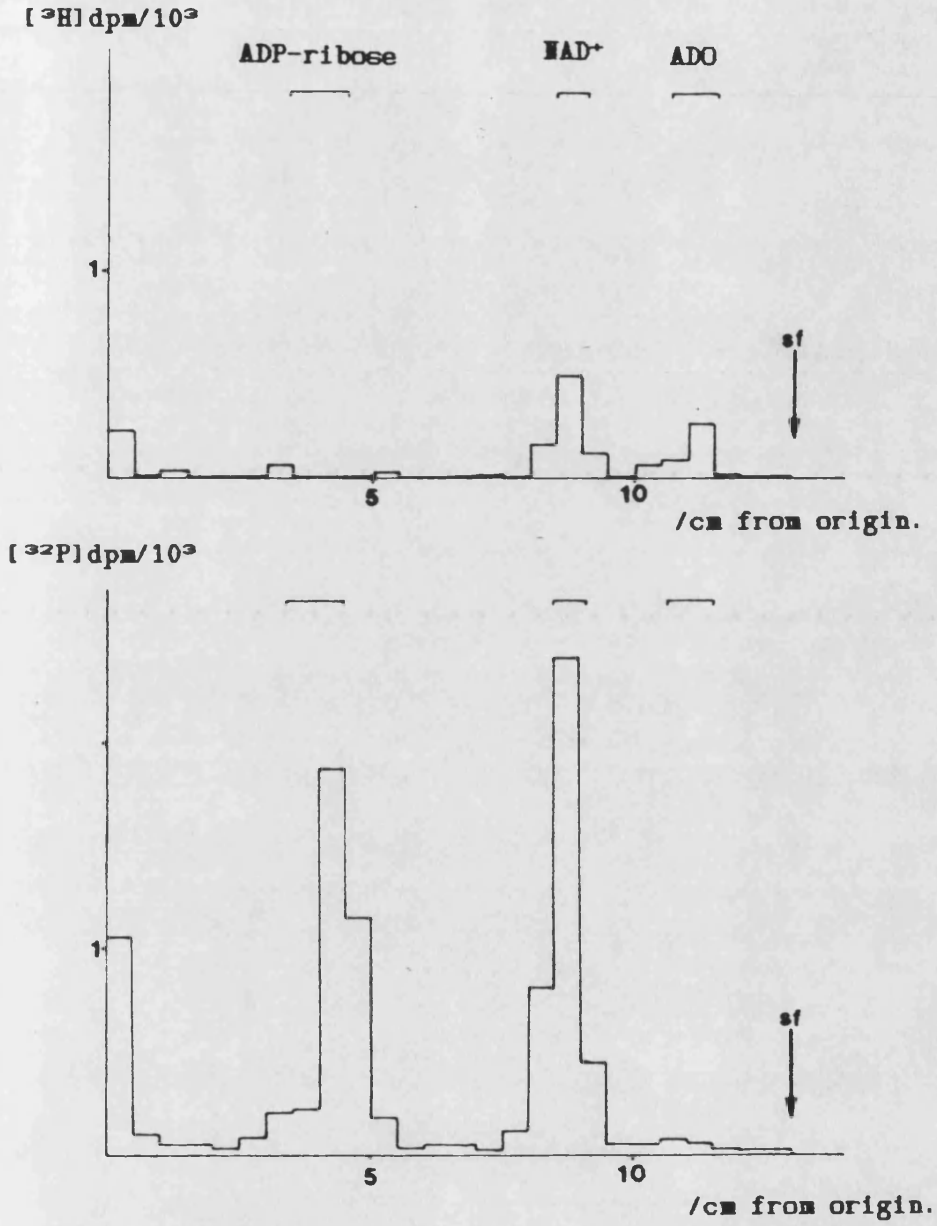

Figure 4.15.

TLC analysis (in the LiCl/acetic acid system) of 20µl (from 60µl reconstituted final volume) of fraction 14 from the preceding DEAE cellulose chromatogram (figure 4.14). Top - [³H]dpm; bottom - [³²P]dpm.

origin. It was reasoned that in the unlikely possibility that this was Ap4A-(ADP-ribose)$_n$, the concentration of NH_4HCO_3 at which it had eluted from the column was so low that n could not be greater than one. Thus, base treatment should hydrolyse the glycosidic bond between the Ap4A and ADP-ribose (Yoshihara and Tanaka (1981)), and this would be seen as the loss of [^{32}P] origin material to the [^{32}P] ADP-ribose peak. A futher 20µl of the reconstituted fraction was incubated at 0.1M NaOH, 37°C for 30 minutes in a final volume of 25µl and subjected to the same TLC analysis above (figure 4.16). This resulted in the loss of [^{32}P]NAD^+ from the profile and an increase in the size of the ADP-ribose peak (from ≈36 to ≈39% of the [^{32}P]dpm). In figure 4.15 [^{32}P]NAD^+ accounted for ≈39% of the total [^{32}P]dpm, so the small increase in the size of the ADP-ribose peak upon base-treatment does not account entirely for the disappearance of [^{32}P]NAD^+. On the contrary, the amount of [^{32}P]dpm on the origin increased from ≈10% to 20%. This suggests that the base treatment of NAD^+ is producing ADP-ribose and ATP (which stays on the origin in this TLC system). Apart from this, figure 4.16 shows that the co-[^{3}H]/[^{32}P] origin material present in fraction 14 is not [^{3}H]Ap4A linked to [^{32}P]ADP-ribose monomer.

The [^{3}H]Ap4A peak eluting at 175 mM NH_4HCO_3 (figure 4.14) was not coincident with any [^{32}P]dpm, and so analysis was not considered necessary, particularly since the large amounts of NH_4HCO_3, coupled

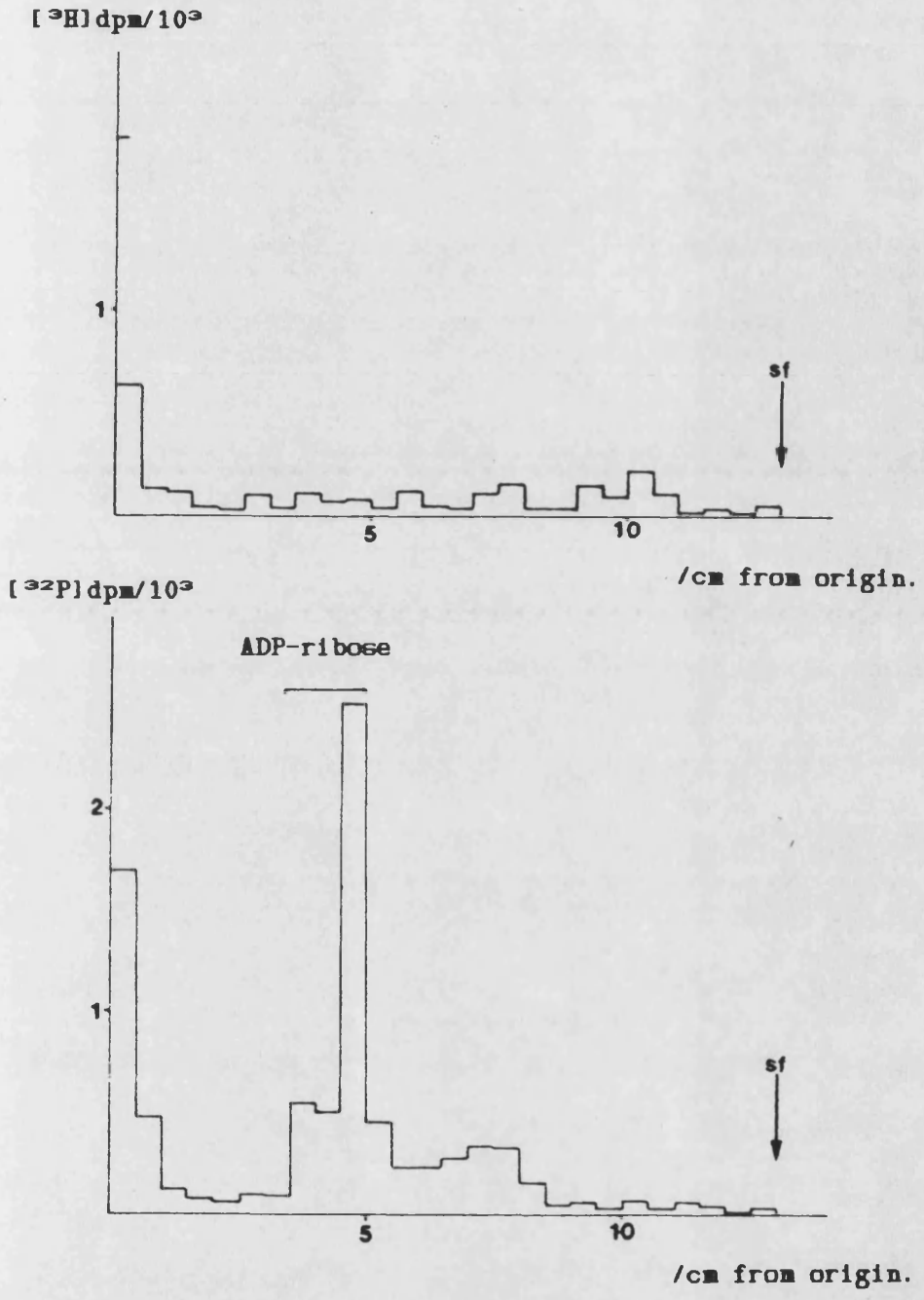

Figure 4.16.

A further 20µl of the concentrated fraction 14 from the DEAE cellulose chromatogram in figure 4.14 was base-treated (see text for details) and analysed in the LiCl/acetic acid TLC system.

with a relatively low level of radioactivity made TLC analysis difficult. The improved binding of nucleotides to the column and their increased resolution in the 2-300 mM gradient justified its use in analysing the nucleotide extract from permeabilised cells, incubated with [^{32}P]NAD$^+$ and [^{3}H]Ap4A.

The method used to synthesize [^{3}H]Ap4A was time consuming and gave low yields of the product, of which there was still uncertaintanty as to its authenticity. In order to make the maximum use of the [^{32}P]-labelled NAD$^+$ available at the time, greater amounts of *authentic* [^{3}H]Ap4A were needed before radioactive decay had depleted the specific activity of the [^{32}P]NAD$^+$ to an impractically low level. As mentioned in chapter III.12, a custom synthesis of [^{3}H]Ap4A from a commercial source is normally prohibitively expensive, however, it became possible at this time to purchase some at 4.3μCi/mmol (Amersham) and 500μCi were ordered. In the meantime, a small quantity of the [^{3}H]Ap4A preparation used above remained, and this was used together with the appropriate amount of [^{32}P]NAD$^+$ in an attempt to characterise the elution profile of the nucleotide extracts from permeabilised cells when chromatographed on DEAE cellulose in the new 2mM to 300mM NH_4HCO_3 gradient. The aim of this experiment was simply to identify some of the components present in the peaks of the profile so that their elution positions could be

recorded in readiness for the experiments to follow, which would utilise larger amounts of the commercial preparation of [^{3}H]Ap4A.

A nucleotide extract from permeabilised cells incubated with [^{32}P]NAD^{+} and [^{3}H]Ap4A preparation (see page 170) was applied to a DEAE cellulose column in 2 mM NH_4HCO_3 as before, which was then washed before appling a linear 2-300 mM gradient. Figure 4.17 shows the elution profiles of [^{3}H] and [^{32}P]dpm. [^{3}H]dpm eluted in four major peaks - at (1) 5-65 mM NH_4HCO_3, (2) 70-80 mM NH_4HCO_3, (3) 100-150 mM NH_4HCO_3 and (4) 165-200 mM NH_4HCO_3. The latter peaks (3) & (4) were assumed to be ATP and Ap4A, respectively, by implication from figure 4.8. The fact that the experiments to follow would be utilising *authentic* [^{3}H]Ap4A meant that this could be confirmed later. The [^{32}P]dpm eluted in three major peaks - A: 5-40 mM NH_4HCO_3, B: 50-70 mM NH_4HCO_3 and C: 70-80 mM NH_4HCO_3. Fractions 7 (containing [^{3}H]&[^{32}P]), 16 (containing mostly [^{32}P]) and 20 (containing [^{3}H]&[^{32}P]) were aspirated to dryness, reconstituted in distilled water and portions were analysed by TLC as before. Figure 4.18 shows the profile of fraction 7 in the acetic acid/LiCl system, in which the only significant [^{3}H]dpm comigrates with the adenosine standard, and >95% of the [^{32}P]dpm with the NAD^{+} standard. The same solvent system was used to analyse fraction 16 (figure 4.19) which appeared to consist entirely of [^{32}P]ADP-ribose. When fraction 20 was analysed in this TLC system (figure 4.20), it appeared to consist of [^{32}P]ADP-

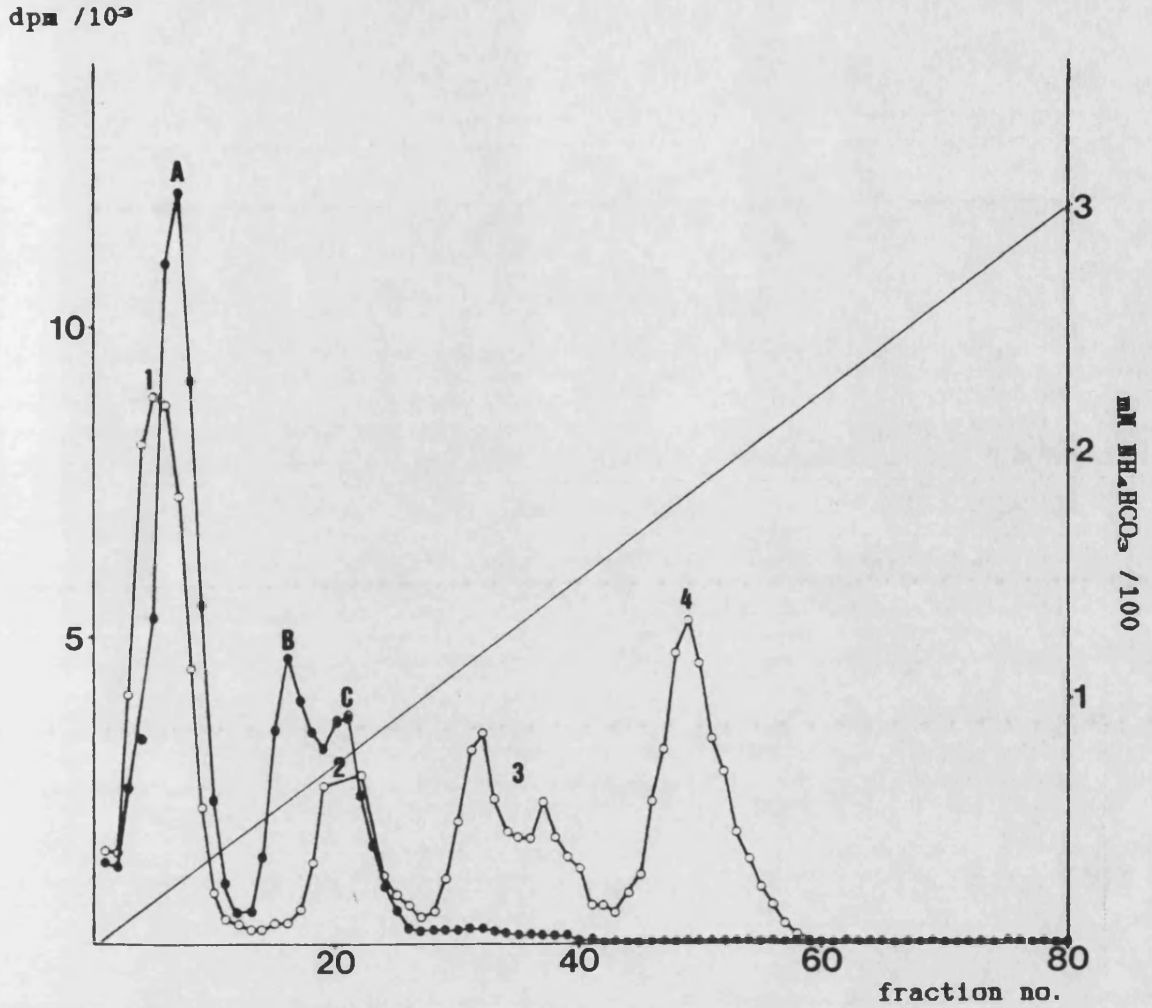

Figure 4.17.

Permeabilised cells were incubated with 7.5 pmol [^{32}P]NAD$^+$ and 8.3 pmol [^{3}H]Ap4A preparation and the nucleotide extracts were analysed by DEAE cellulose chromatography using a linear gradient of 2 to 300mM NH_4HCO_3 as in figure 4.14. The [^{3}H]-peaks eluting are assigned the numbers 1-4 and the [^{32}P]-peaks the letters A-C. See text for further details.

○- [^{3}H]dpm;

●- [^{32}P]dpm.

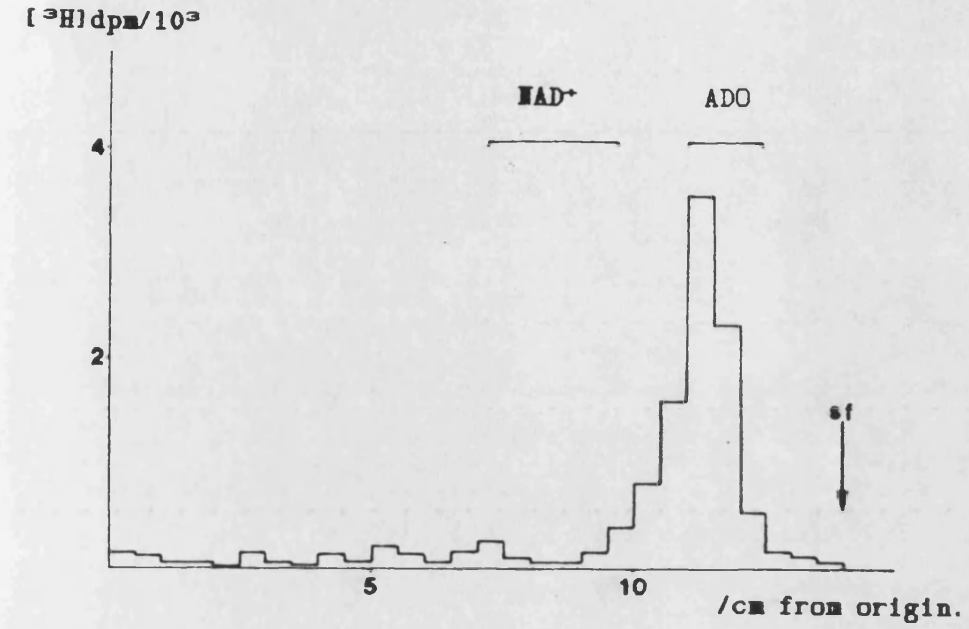

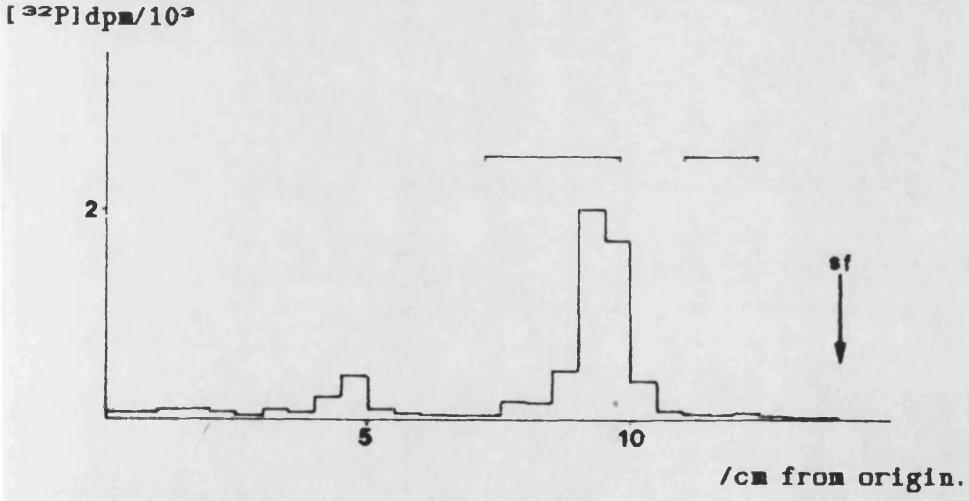

Figure 4.18.

Fraction 7 from the preceding DEAE cellulose chromatogram (figure 4.17) was analysed by TLC in the LiCl/acetic acid TLC system. The profile represents the total radioactivity present in the fraction. Top - [³H]dpm; bottom - [³²P]dpm.

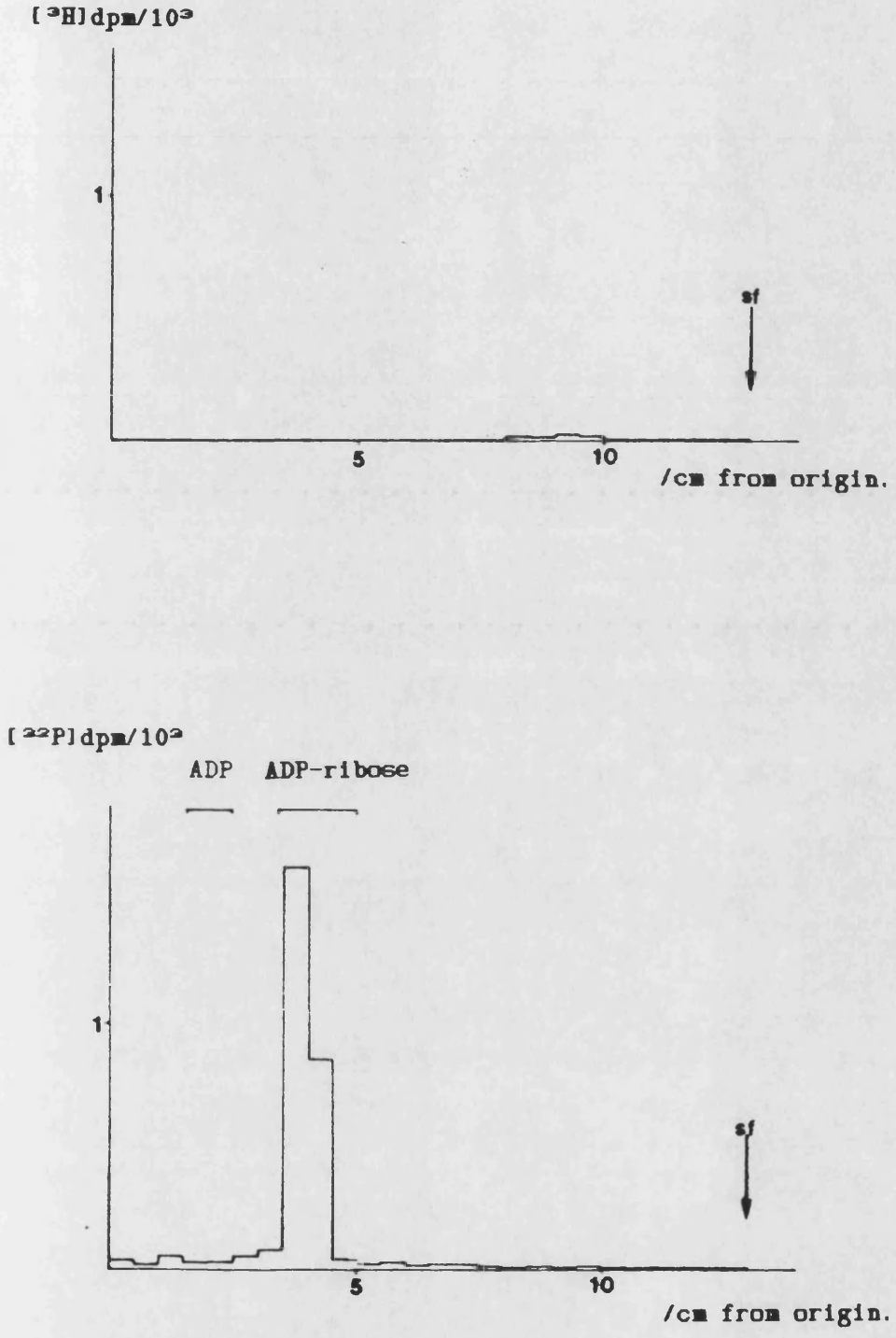

Figure 4.19.

Fraction 16 from the preceding DEAE cellulose chromatogram (figure 4.17) was analysed by TLC in the LiCl/acetic acid TLC system. The profile represents the total radioactivity present in the fraction. Top - [³H]dpm; bottom - [³²P]dpm.

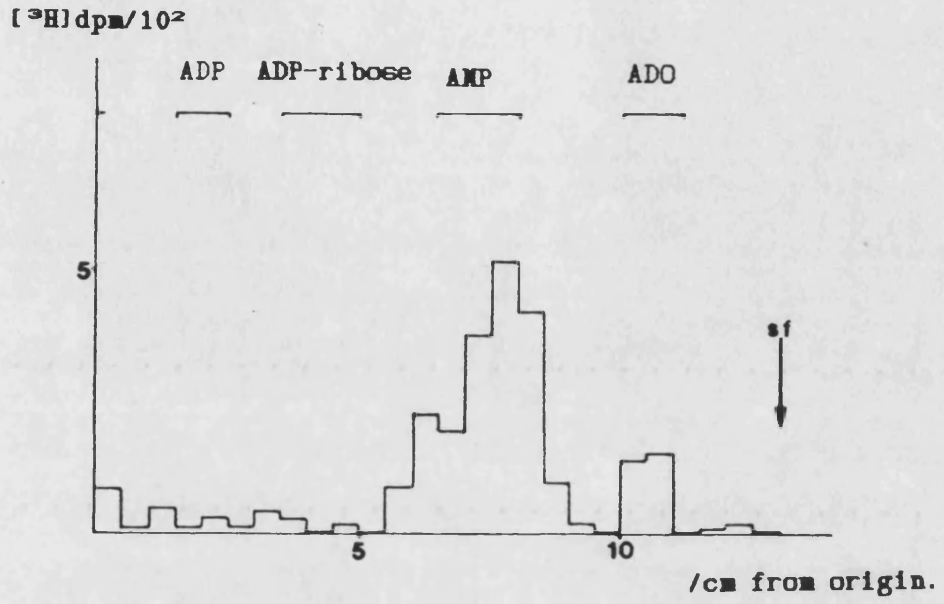

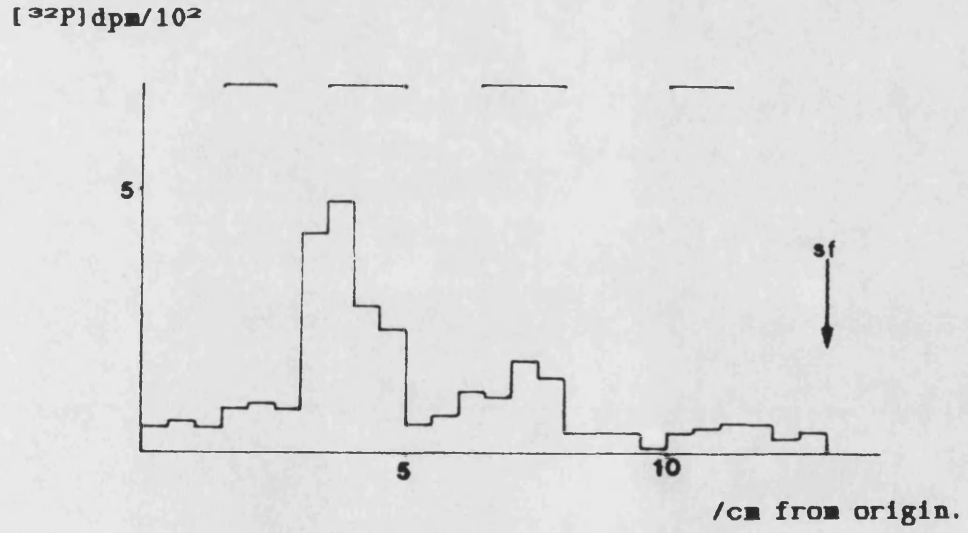

Figure 4.20.

Fraction 20 from the preceding DEAE cellulose chromatogram (figure 4.17) was analysed by TLC in the LiCl/acetic acid TLC system. The profile represents the total radioactivity present in the fraction. Top - [³H]dpm; bottom - [³²P]dpm.

ribose and [^{32}P]/[^{3}H]AMP, with negligable origin material. This implies that the fact that it appears as a co-[^{32}P]/[^{3}H] peak is an artefact of the separation of AMP and ADP-ribose in this system. Each of these TLCs (figs. 4.18,19&20) are presented as representative of the [^{3}H]/[^{32}P]dpm for the entire fraction. Further TLC analysis on portions of these fractions was performed in the 1.6M LiCl system and the results (not shown) confirm these conclusions, although not as clearly (particularly with fraction 20 where the standards smeared on the plate). Thus, we can tentatively say that adenosine is eluted slightly in front of NAD^+ below 60 mM NH_4HCO_3; then comes ADP-ribose at 50-80 mM NH_4HCO_3, followed closely by AMP. Lastly, ATP and Ap4A elute at 100 and 165 mM NH_4HCO_3 respectively. When running their DEAE cellulose chromatography, Yoshihara and Tanaka (1981) found that Ap4A linked to one (ADP-ribose) and two (ADP-ribose) molecules eluted at between 200 and 300 mM NH_4HCO_3 under identical conditions, so it was reasoned that if the cells were to generate this product, it would be revealed by chromatography of a nucleotide extract in this system.

Upon the arrival of the commercially produced [^{3}H]Ap4A (in 50% ethanol/water v/v), degradation was quickly checked for by applying 2µl to a PEI TLC plate and chromatographing in the acetic acid/LiCl system (in which authentic Ap4A remains on or around the origin).

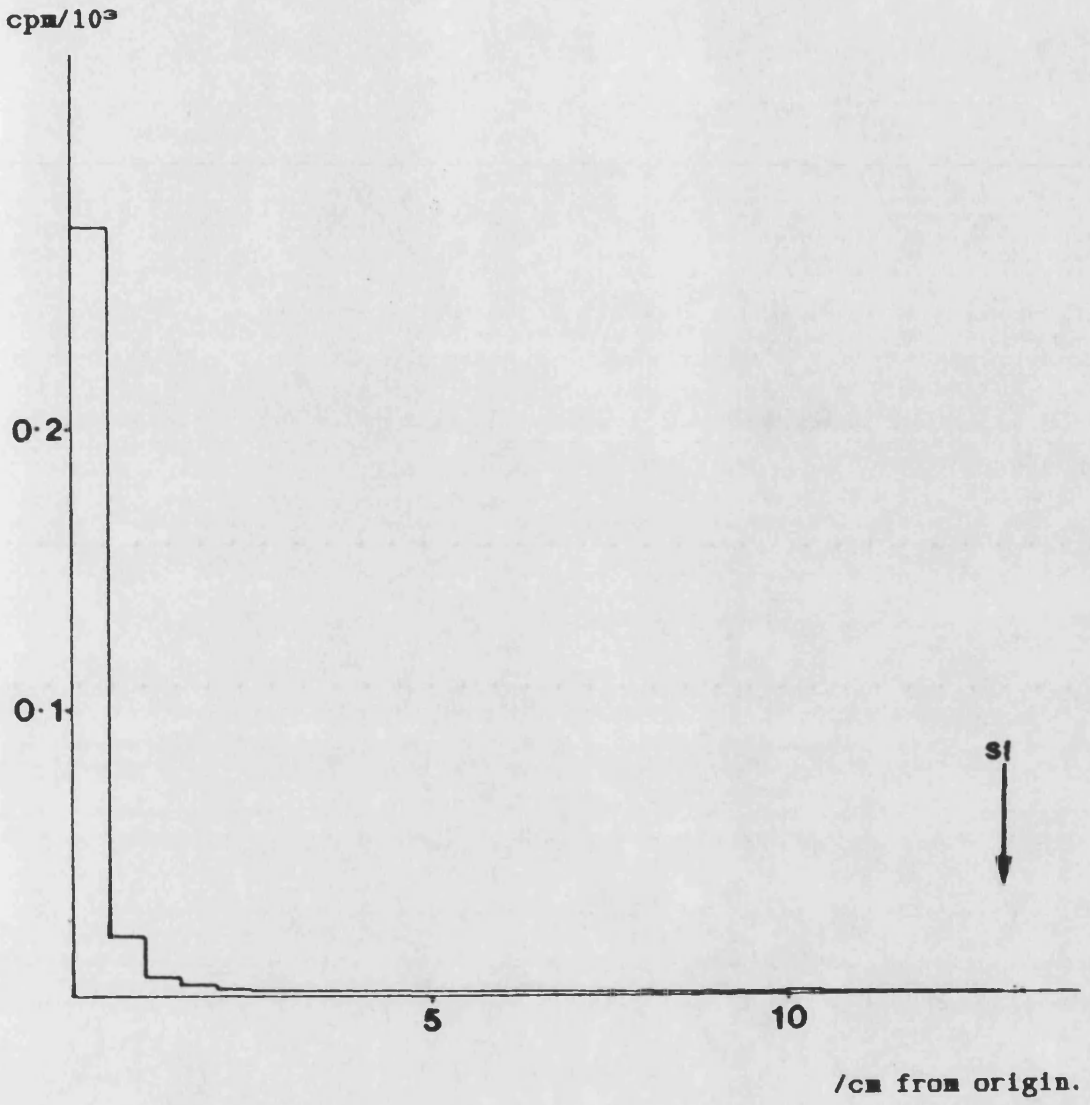

Figure 4.21.

2µl of commercially produced [³H]Ap4A (0.66 µCi - Amersham International) were analysed in the LiCl/acetic acid TLC system.

Figure 4.21 shows that 94.4% of the radioactivity remains on or around the origin of the plate, 0.5% comigrating with the adenosine standard. This agrees well with the manufacturer's (Amersham) assay 5 months earlier, of 95% purity, and indicates that negligable degradation had taken place.

The aim of the following experiments was to determine the behaviour of [^{32}P]-labelled NAD$^+$ and [^{3}H]-labelled Ap4A added in small (pM) quantities to permeabilised cells which have been treated with 200 μM DMS (or not), and the effects of including 5 mM 3AB and/or 200 μM Ap4A in the incubation. It was hoped that the observed inhibition of the (ADP-ribosyl)ation of proteins by 200 μM Ap4A (this thesis, Yoshihara and Tanaka (1981), Tanaka *et.al.*(1981a,b)) could be compared with the known inhibition of ADPRT activity by 5 mM 3AB (Durckacz *et.al.*(1980)) by the inclusion of one or both of these in the incubations, the cells in which had been subjected to DNA-damage (which is known to *stimulate* ADPRT activity (Thi Mann & Shall (1982)) or left as controls ('basal' ADPRT activity).

L1210 cells at mid-log phase were treated with 200 μM DMS (or not) for one hour and harvested as before. After permeabilisation and dilution to 10^6 viable cells / 500 μl, batches of 10^6 were incubated with [^{32}P]NAD$^+$ and [^{3}H]Ap4A in the presence or absence of Ap4A and/or 3AB as described in III.4 in a total volume of 530 μl. In each of the incubations the amount of [^{3}H]Ap4A used was 0.77 pmoles (7 326 000

dpm). The amount of [^{32}P]NAD$^+$ used was either 0.28 pmoles (429 600 dpm) or 0.27 pmoles (277 968 dpm). The incubation conditions are shown below.

Table 13. Initial incubation conditions.

batch	conditions			[^{32}P]dpm added	[^{3}H]dpm added
1	DMS-treated,	5mM 3AB,	200μM Ap4A		7326000
2	DMS-treated,	5mM 3AB,	-		
3	DMS-treated,	-	-	277968	
4	-	5mM 3AB,	200μM Ap4A		
5	-	5mM 3AB,	-		
6	-	-	-		
7	DMS-treated,	-	200μM Ap4A	429626	
8	-	-	200μM Ap4A		

At the end of the ten minute incubation, aliquots were withdrawn and assayed for TCA-insoluble radoactivity, and BSA was added, followed by freshly prepared phenol/chloroform/IAA mixture. Phenol extraction was performed as described in III.8(a). After withdrawing

the supernatant, the protein-containing disc (phenolic interface) was back-washed with 0.1M acetic acid, recentrifuged and the pooled supernatants were extracted with ether (III.8(b)). The aqueous solution was then mixed with ethanol and acetic acid to final concentrations of 50% (v/v) and 0.1M, respectively, and left to precipitate overnight at -20°C (III.8(c)). After centrifugation, the supernatant was withdrawn and the nucleic acid-containing pellet (ethanolic pellet) was back-washed with more 50% ethanol, 0.1M acetic acid at room temperature. The pooled supernatants were then frozen in glass bulbs (by immmersion in liquid nitrogen) and lyophilised.

In order to monitor the distribution of labelled material throughout this process, the phenolic interfaces and ethanolic pellets were retained and solubilised by sonication (in 8M urea, Tris-acetate pH 8.0, 0.5 and 1 ml respectively) to facilitate the accurate estimation of the radioactivity they contained. In the event, this was only partly possible, since it was found to be extremely difficult to ensure complete solubilisation, and thus homogeneity of the sample.

Table 14 shows the total amounts of [^{32}P] and [^{3}H] radioactivity (counted as described in III.7(b)) incorporated into TCA-insoluble material for each batch of 10^6 cells. Because the relative amount of [^{32}P]NAD^+ used in batches 1-6 is different from that in 7 & 8, this information is presented more usefully in table 15, which expresses

(continued on page 187)

Table 14. Total dpm incorporated into TCA-insoluble material per 10^6 cells

	TCA-insoluble [^{32}P] dpm			TCA-insoluble [^{3}H] dpm		
			σ_{n-1}			σ_{n-1}
1	135	±	81	2538	±	108
2	486	±	54	3888	±	1242
3	6021	±	81	4671	±	2187
4	189	±	27	2160	±	108
5	0	±	0	5022	±	2970
6	6480		*	3402		*
7	2943	±	837	2484	±	1674
8	1026	±	1026	2484	±	2484

277 968 dpm [^{32}P] were present initially for incubations 1-6, and 429 626 dpm [^{32}P] for 7 & 8. 7 326 000 dpm [^{3}H] were present for all incubations (1-8)
Incubation conditions initially were:-

1 DMS-treated, 5mM 3AB, 200μM Ap4A
2 DMS-treated, 5mM 3AB, -
3 DMS-treated, - -
4 - 5mM 3AB, 200μM Ap4A
5 - 5mM 3AB, -
6 - - -
7 DMS-treated, - 200μM Ap4A
8 - - 200μM Ap4A

Table 15.

	TCA-insoluble [^{32}P] dpm as % of total dpm			TCA-insoluble [^{3}H] dpm as % of total dpm		
			σ_{n-1}%			σ_{n-1}%
1	0.05	±	0.03	0.03	±	0.00
2	0.17	±	0.02	0.05	±	0.02
3	2.17	±	0.03	0.06	±	0.03
4	0.07	±	0.01	0.03	±	0.00
5	0.00	±	0.00	0.07	±	0.04
6	2.33		*	0.05		*
dms	0.69	±	0.19	0.03	±	0.02
c	0.24	±	0.24	0.03	±	0.03

* = error not available due to loss of duplicate.

Incubation conditions initially were:-

1 DMS-treated, 5mM 3AB, 200μM Ap4A
2 DMS-treated, 5mM 3AB, -
3 DMS-treated, - -
4 - 5mM 3AB, 200μM Ap4A
5 - 5mM 3AB, -
6 - - -
7 DMS-treated, - 200μM Ap4A
8 - - 200μM Ap4A

the incorporation as a percent of the total radioactivity present in the incubation initially.

Although the errors were high due to the comparatively low cpm retained on the GFC discs, it can be seen that in the presence of Ap4A (unlabelled) and/or 3AB, the amount of [^{32}P]dpm in the TCA-insoluble fraction is decreased by several times. There is no apparent stimulation of incorporation by DMS, but the absence of an error for the control measurement (due to the loss of samples) means that this might not be the case.

The amount of [^{3}H] TCA-precipitated, however, is only slightly increased upon the absence of unlabelled 200μM Ap4A, and when the errors are taken into account, there appears to be no significant difference between the [^{3}H] figure when 5mM 3AB is either present or absent. This was as expected, the (ADP-ribosyl)ation of proteins being detectable by the incorporation of ([^{32}P]ADP-ribose)$_n$ into TCA-insoluble material. The inhibition of ADPRT by 3AB and/or Ap4A would be indicated by a drop in the amount of ([^{32}P]ADP-ribosyl)ated-protein precipitated onto the GFC disc. If the observed decrease in [^{32}P]dpm detected in the TCA-insoluble fraction were due to sampling errors, one would expect the amount of [^{3}H] present to be lower as well. There is only a slight decrease in [^{3}H]dpm in the presence of 200μM Ap4A (which may be due to the 'dilution effect' discussed in the following pages) and, as demonstrated by table 14, the errors are

in excess of the difference. Thus, it was concluded that the decrease in the incorporation of [^{32}P]dpm into TCA-insoluble material in the presence of Ap4A and/or 3AB faithfully reflected the inhibition of (ADP-ribosyl)ation of proteins by these compounds in permeabilised cells.

Tables 16 and 17 represent the results from the monitoring of radioactivity ([^{32}P] and [^{3}H], respectively) 'lost' to the protein-containing phenolic interface and the nucleic-acid containing pellet produced by phenol and ethanol extraction of the cells after incubation. The information in the tables relates the amounts of radioactivity in these fractions to the total amounts of radioactivity present in the incubation initially. Figures 4.22 and 4.23 represent these data in bar chart-form.

It is interesting to note that in the case of [^{32}P] (table 16 and figure 4.22) the effect of Ap4A and 3AB is similar with regard to the losses to the phenolic interface - ie: a decrease. In the absence of either from the incubation, the losses are larger. Furthermore, if the cells are pretreated with DMS, there is a further, small increase in losses. This agrees more or less with the results obtained from the TCA-precipitation of aliquots from the incubations (table 15). A "loss" of radioactivity to the phenolic interface implies that it is

(continued on page 191)

Table 16.

Total losses of radioactivity to the phenol and ethanol extraction procedures expressed as a percent of total radioactivity present in the incubation initially (per 10^6 cells).

Percent [^{32}P]dpm.

	PHENOLIC INTERFACE (1)	ETHANOLIC PELLET (2)	SUM (1 + 2)	NUCLEOTIDE EXTRACT
	$\bar{x}_{n-1}$	$\bar{x}_{n-1}$	$\bar{x}_{n-1}$	$\bar{x}_{n-1}$
1	6.93 ± 0.1	11.14 ± 1.1	18.07 ± 1.6	78.37 ± 0.6
2	7.43 *	20.06 ± 5.2	27.48 ± 5.2	71.68 ± 1.4
3	12.50 ± 3.0	12.38 ± 3.2	24.88 ± 6.9	73.17 ± 1.9
4	6.19 *	10.65 ± 1.2	16.84 ± 1.2	69.70 ± 1.4
5	6.31 ± 0.4	12.01 ± 1.4	18.32 ± 1.7	76.38 ± 0.5
6	10.52 ± 0.3	14.48 ± 0.7	25.01 ± 1.0	45.43 ± 0.9
7	7.20 ± 0.0	11.45 ± 0.2	18.64 ± 0.2	95.70 ± 0.1
8	6.84 ± 0.0	10.27 ± 0.2	17.11 ± 0.2	86.85 ± 3.9

the total radioactivity initially (100%) was 277968dpm for 1 to 6 and 429626dpm for 7 & 8.

Incubation conditions initially were:-

1 DMS-treated, 5mM 3AB, 200μM Ap4A
2 DMS-treated, 5mM 3AB, -
3 DMS-treated, - -
4 - 5mM 3AB, 200μM Ap4A
5 - 5mM 3AB, -
6 - - -
7 DMS-treated, - 200μM Ap4A
8 - - 200μM Ap4A

Figure 4.22 shows the information above in the form of a bar chart.

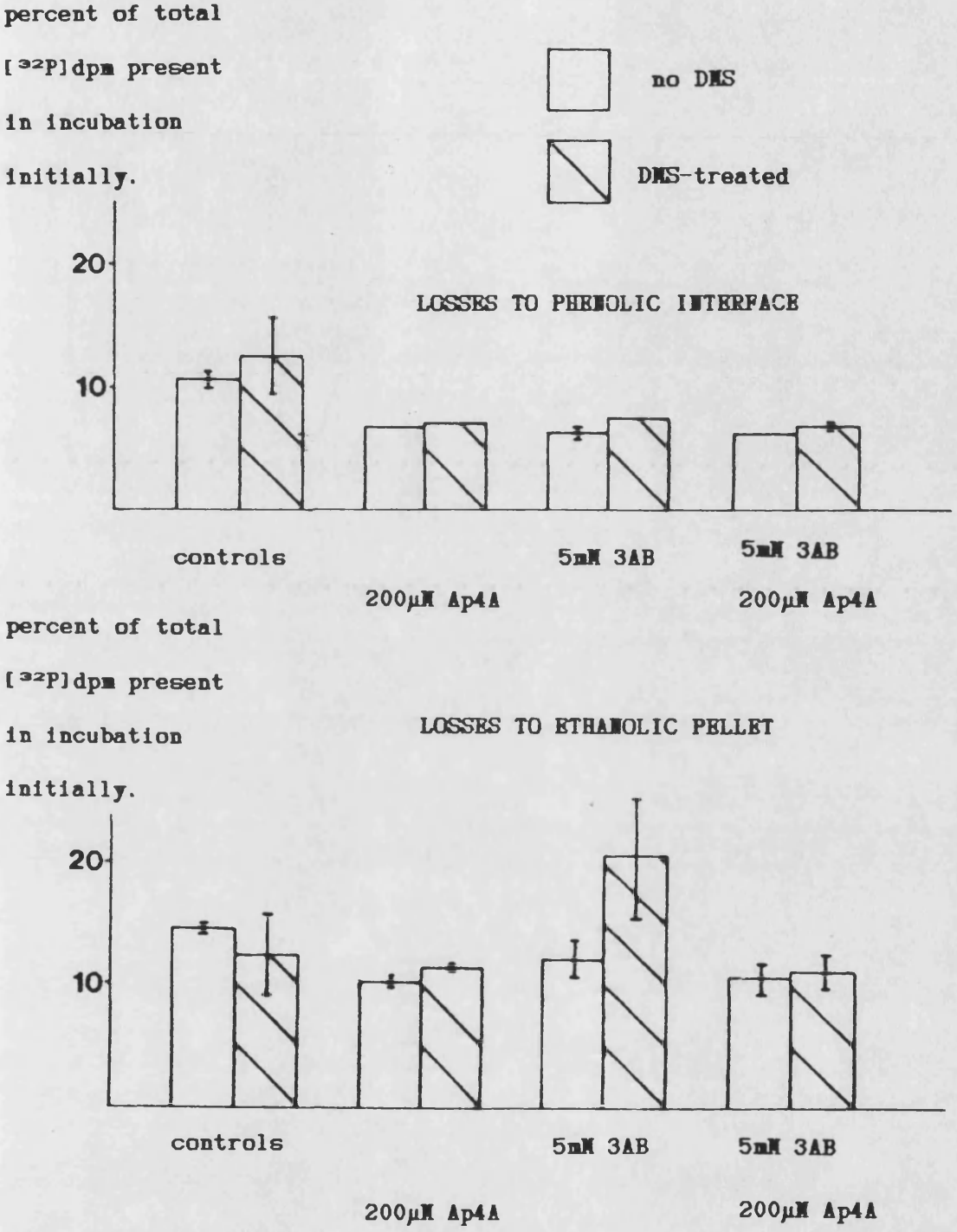

Figure 4.22.

The information in Table 16, presented in the form of a bar chart. Cells were DMS-treated (or not see key), permeabilised and incubated with [^{32}P]NAD$^+$ and [^{3}H]Ap4A in the presence or absence of 5mM 3AB and/or 200μM Ap4A. A nucleotide extraction was then performed (see III.6) and the protein-containing 'discs' resulting from phenol/chloroform/IAA extraction and nucleic acid - containing ethanolic pellets resulting from acidic ethanol extraction were solubilised by sonication in 8M urea, 0.1M Tric-acetate, pH 8. Aliquots were then counted for [^{32}P] radioactivity.

Table 17.

Total losses of radioactivity to the phenol and ethanol extraction procedures expressed as a percent of total radioactivity present in the incubation initially (per 10^6 cells).

Percent [^{3}H]dpm.

	PHENOLIC INTERFACE (1)	ETHANOLIC PELLET (2)	SUM (1 + 2)	NUCLEOTIDE EXTRACT
	σ_{n-1}	σ_{n-1}	σ_{n-1}	σ_{n-1}
1	6.3 ± 0.1	17.4 ± 1.9	23.7 ± 2.0	34.6 ± 1.1
2	17.6 ± *	5.9 ± 0.4	23.5 ± 0.4*	34.8 ± 0.9
3	18.9 ± 0.6	9.3 ± 3.9	28.2 ± 4.5	38.8 ± 1.9
4	5.4 ± *	17.1 ± 1.6	22.5 ± 1.6*	36.1 ± 1.0
5	15.5 ± 0.3	5.9 ± 0.5	21.4 ± 0.8	29.2 ± 0.2
6	15.6 ± 0.1	5.2 ± 0.1	20.8 ± 0.2	24.7 ± 0.1
7	5.9 ± 0.1	25.2 ± 0.6	31.1 ± 0.7	28.9 ± 0.3
8	6.2 ± 0.1	23.6 ± 0.2	29.8 ± 0.3	27.8 ± 0.3

The total 3H dpm present initially was 7326000 dpm for 1 to 8.

Incubation conditions initially were:-

1 DMS-treated, 5mM 3AB, 200μM Ap4A
2 DMS-treated, 5mM 3AB, -
3 DMS-treated, - -
4 - 5mM 3AB, 200μM Ap4A
5 - 5mM 3AB, -
6 - - -
7 DMS-treated, - 200μM Ap4A
8 - - 200μM Ap4A

Figure 4.23 shows the information above in the form of a bar chart.

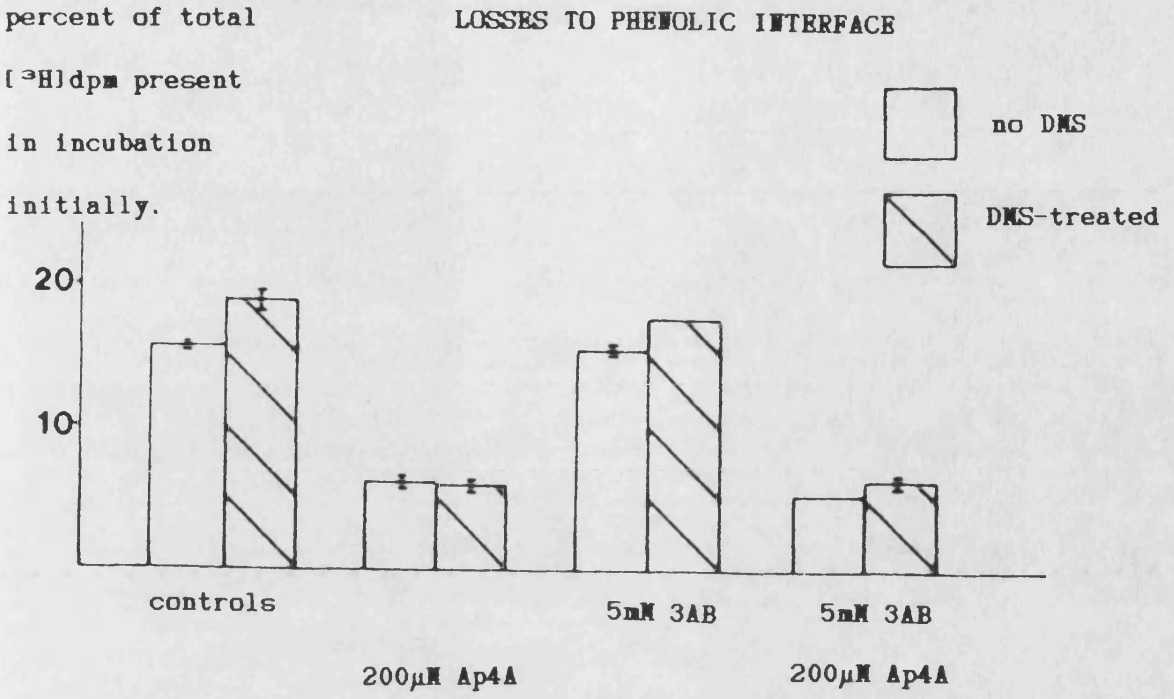

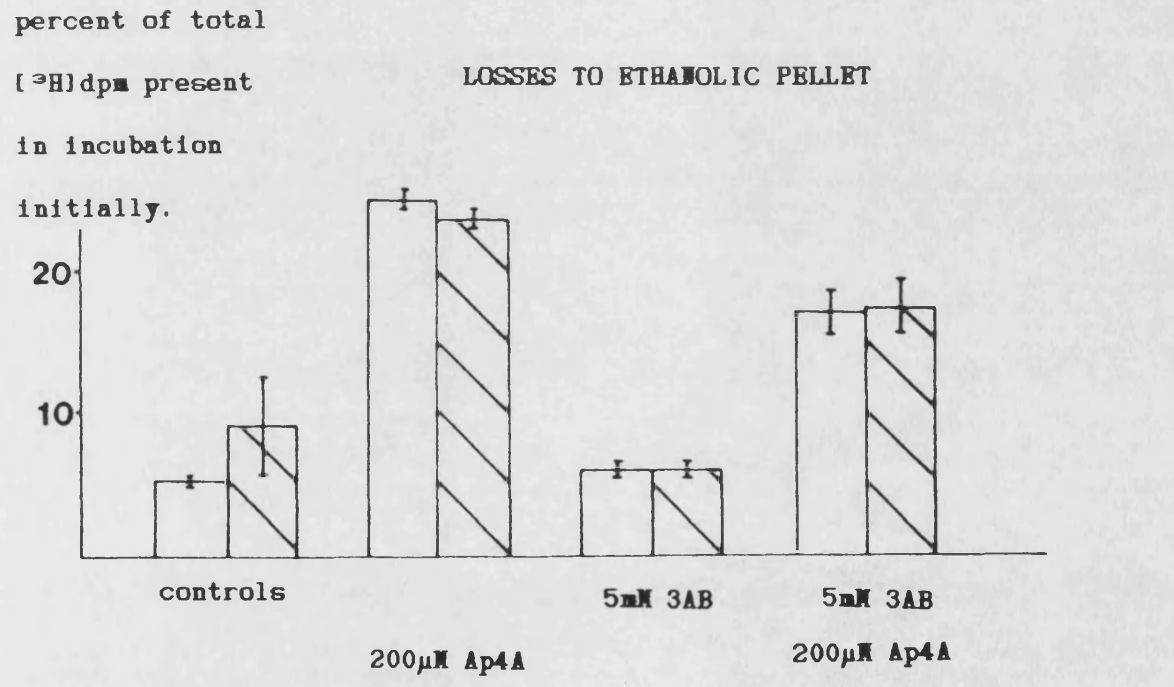

Figure 4.23.

The information in table 17, presented in the form of a bar chart. This chart concerns the losses of [³H]dpm to the nucleotide extraction procedure - see figure 4.22 for details.

incorporated into the protein-containing (phenol extracted) fraction. Thus it seems likely that the greatest loss of [^{32}P] to this fraction, observed upon treatment of the cells with DMS, is due to the stimulation of ADPRT activity. Similarly, the lowest losses of [^{32}P] are observed in the presence of 3AB and/or Ap4A, which cause the inhibition of ADPRT activity. This incorporation of [^{32}P] into the phenolic interface is the (ADP-ribosyl)ation of proteins, which are denatured by the phenol/chloroform mixture and deposited at the aqueous/non-aqueous interface by centrifugation. There is no apparent trend in losses of [^{32}P] to the ethanolic pellets, which implies that the radioactive material in them is not related to the process of (ADP-ribosyl)ation.

In the case of [^{3}H] radioactivity (table 17, figure 4.23), the presence of (unlabelled) 200μM Ap4A appears to cause an approximate three-fold increase in losses to the ethanolic pellet, whilst the losses to the phenolic interface are lower in roughly the same proportion. This results in a similar figure for the sum of these losses as for those incubations in which unlabelled Ap4A was not added. Why should the presence of 200μM Ap4A in the incubation mixture make a difference to the amounts of [^{3}H] radioactivity "lost" to the ethanol pellets ?

The presence of unlabelled Ap4A is expected to have two major effects: (a) an effective lowering of the specific activity of

[^{3}H]Ap4A by dilution. Any non-specific binding of Ap4A during the extraction procedure would therefore appear as less radioactivity in the pellet. Thus, when looking at the effects of Ap4A, a lowering of the 'losses' of [^{3}H]dpm to either the ethanol pellet or the phenolic interface would imply that this non-specific, dilution effect was the cause; (b) the inhibition of (ADP-ribosyl)ation and/or other metabolic/catabolic effects, due to the putative physiological activity of Ap4A (see chapter II).

The losses of [^{3}H] to the ethanol pellet, although small in proportion to the total radioactivity present, cannot be ruled out as non-specific phenomena of no significance, particularly with regard to the effects of 200μM Ap4A. As mentioned before, if the losses of [^{3}H] to the pellet were due to some non-specific effect, one would expect that the 'dilution' of [^{3}H]Ap4A in the reaction mixture (and throughout the extraction procedure) with 200μM unlabelled Ap4A would result in a measurable lowering of these losses.

The suprising effect is the three-fold *increase* in losses of [^{3}H]dpm to the pellet in it's presence. This is not accompanied by similar changes in [^{32}P] dpm losses, which implies that if the presence of 200μM Ap4A was causing the inhibition of (ADP-ribosyl)ation of proteins via (ADP-ribosyl)ation of itself (as observed by Yoshihara et.al. (1981)), the product does not appear in

either the phenolic or ethanolic pellets as [^{3}H] covalently linked to [^{32}P].

The opposite effect is observed in the losses of [^{3}H]dpm to the phenolic interface - the presence of unlabelled Ap4A at 200μM *reduces* these by approximately three-fold, thus suggesting that here, dilution of the [^{3}H]Ap4A (or lowering of it's specific activity) is is playing a part in this expected effect. Whether it is due to the specific or non-specific binding of Ap4A to a protein is not revealed by this information.

These changes in the distribution of [^{3}H] point to the possibility that the presence of 200μM Ap4A is causing some metabolic effect, and that the product of this becomes precipitated by the acidic ethanol and is detected in the pellet after centrifugation. As stated above, however, the fact that changes in the distribution of [^{3}H] are not accompanied by similar changes in that of [^{32}P], implies that the material precipitated by acidic ethanol is not [^{3}H]Ap4A-[^{32}P](ADP-ribose)$_{n}$.

It is also perhaps noteworthy that DNA damage, caused by DMS, does not appear to affect the amount of [^{3}H]Ap4A in the ethanol pellet. That Ap4A binds non-covalently to a protein associated with DNA polymerase α (Rapaport & Zamecnick(1981a,b) suggested it's involvement in scheduled DNA synthesis. If Ap4A were implicated in DNA repair (involving unscheduled synthesis of DNA), one might expect

changes in it's distribution also upon DNA damage, perhaps due to binding to repair polymerase(s), which were not observed.

The frozen lyophilised nucleotide extracts were carefully dissolved in 4 ml 2 mM NH_4HCO_3 (pH 8.2) one by one and applied to a 3 ml DEAE cellulose column, previously equilibriated with the same buffer. The column was then washed with a further 4 ml of the same buffer. The figures in tables 18. and 19. were produced by conversion from cpm to dpm and in the case of [^{32}P], corrected for decay so that comparisons can be made between the amount of radioactivity applied to the column, that remaining unbound after the application and that removed by the column washings. Tables 20 and 21 express these latter two as a percentage of the radioactivity initially applied to the column.

In the case of [^{32}P] (table 20) the percentage binding to the column is between 92.10 (+/-6.25) and 99.47 (+/-0.15) %. The presence of 200μM Ap4A in the original incubation is accompanied by a slight increase in binding after the wash in both DMS and untreated cells. This small difference amounts to about 3 percent and could possibly be the completely non-specific effect of an increase in ionic concentration of the nucleotide solution.

The percentage binding for [^{3}H] (table 21.) shows much larger variation - between 86.42 (+/-3.27) and 99.67 (+/-1.10) %. It can be seen that binding is always in excess of 99% in the presence of

(continued on page 197)

Table 18.:[^{32}P] binding.

	Total dpm applied	Total dpm unbound	Total dpm in wash
	σ_{n-1}	σ_{n-1}	σ_{n-1}
1	185551 ± 1521	60 ± 60	2700 ± 300
2	187580 ± 10646	940 ± 140	13900 ± 900
3	164512 ± 4816	760 ± 80	6530 ± 320
4	203206 ± 7605	720 ± 120	1500 ± 100
5	114322 ± 760	2180 ± 100	800 ± 120
6	158936 ± 3803	900 ± 100	6280 ± 640
7	279088 ± 254	680 ± 80	820 ± 60
8	253486 ± 10647	680 ± 0	1180 ± *

The figures are corrected for [^{32}P] decay so that all measurements are for the the same day

Table 19. : [^{3}H] Binding.

	Total dpm applied	Total dpm unbound	Total dpm in wash
	σ_{n-1}	σ_{n-1}	σ_{n-1}
1	2538785 ± 83350	280 ± 280	7400 ± 720
2	3157810 ± 124088	31140 ± 780	314060 ± 9260
3	2840432 ± 138382	25760 ± 640	337220 ± 11220
4	3018855 ± 86007	540 ± 140	8080 ± 640
5	2412149 ± 64997	312400 ± 13080	15160 ± 640
6	3163555 ± 127809	41240 ± 6480	22060 ± 9020
7	2119923 ± 23315	1520 *	5560 ± 80
8	2037951 ± 20905	3360 ± 280	7800 *

Column binding expressed as percent of totals applied

Table 20: percent [^{32}P] binding.

	PERCENT REMAINING UNBOUND	PERCENT IN WASH	PERCENT BOUND TO COLUMN
	σ_{n-1}	σ_{n-1}	σ_{n-1}
1	0.03 ± 0.03	1.46 ± 0.16	98.51 ± 2.70
2	0.50 ± 0.07	7.40 ± 0.48	92.10 ± 6.25
3	0.46 ± 0.05	3.96 ± 0.19	95.58 ± 3.14
4	0.35 ± 0.06	0.74 ± 0.05	98.91 ± 3.81
5	1.91 ± 0.09	0.70 ± 0.10	97.39 ± 0.89
6	0.57 ± 0.06	3.95 ± 0.40	95.48 ± 2.85
7	0.24 ± 0.03	0.29 ± 0.02	99.47 ± 0.15
8	0.00 ± 0.00	0.47 ± *	99.26 ± 4.20*

Table 21: percent [^{3}H] binding

	PERCENT REMAINING UNBOUND	PERCENT IN WASH	PERCENT BOUND TO COLUMN
	σ_{n-1}	σ_{n-1}	σ_{n-1}
1	0.01 ± 0.01	0.29 ± 0.03	99.70 ± 3.34
2	0.99 ± 0.02	10.80 ± 0.29	88.21 ± 4.21
3	0.91 ± 0.02	11.87 ± 0.40	87.22 ± 5.32
4	0.02 ± 0.00	0.27 ± 0.02	99.71 ± 2.82
5	12.95 ± 0.54	0.63 ± 0.03	86.42 ± 3.27
6	1.30 ± 0.20	7.15 ± 0.29	91.55 ± 4.49
7	0.07 *	0.26 ± 0.00	99.67 ± 1.10*
8	0.16 ± 0.01	0.38 *	99.46 ± 1.01*

These errors are the sum of the errors for 'amount initially applied','amount remaining unbound' and 'amount in wash'.

unlabelled 200μM Ap4A. One explanation may be that the [^{3}H]Ap4A (at 0.414 pmolar) is diluted some 480 x 10^6 times in the presence of 200 μM unlabelled Ap4A and non-specific effects (such as not binding to the column) would be less exaggerated. At 2 mM NH_4HCO_3, a small proportion of bound Ap4A molecules are exchanged for HCO_3^- molecules in binding to the $DEAE^+$ groups of the exchange resin. The lower the effective specific activity of the [^{3}H]Ap4A, the less visible this exchange becomes in terms of [^{3}H]Ap4A passing unbound through the column.

A linear gradient of 2 mM to 300 mM NH_4HCO_3 was then applied to elute the bound nucleotides from the column. 80 (± 2) x 2 ml fractions were collected for each chromatogram, and after mixing, 200 μl aliquots were sampled from each for [^{32}P] and [^{3}H] radioactivity. 10 ml of 500 mM NH_4HCO_3 pH 8.2 were then passed over the column and the fractions emerging were similarly analysed. It was impractical at the time to withdraw more than one aliquot per fraction, and thus errors for the total amounts of radioactivity eluted from the column were not available. For 1 to 8, an average of 96% (σ_{n-1}=4) [^{32}P]dpm and 91% (σ_{n-1}=3) [^{3}H]dpm emerged in total from the columns, which was considered to be sufficient to eliminate the possibility that significant quantities of (ADP-ribosyl)ated Ap4A remained uneluted.

As before, 500 mM NH_4HCO_3 failed to elute any significant amounts of either [^{3}H] or [^{32}P] radioactivity.

Figures 4.24 to 4.31 show the radioactive profiles of each of the incubations (1-8) described above (table 13). Figure 4.32 condenses (to scale) all of these to allow their comparison on one page. For each of these graphs, the [^{32}P]cpm present in 200µl of every fraction (measured at 78.9% efficiency) and [^{3}H]cpm (measured at 23.8% efficiency) were converted to dpm-per-fraction (2 ml). In the case of [^{32}P], these dpm were then adjusted for decay (as described in chapter III.7(b)) so that the resulting figures represented the values they would have assumed if all the chromatograms were performed on the same day (13/5/1988). The nucleotide extracts from incubations 1 to 6 were all subjected to chromatography within plus 8 days of this date (figures 4.24-29), the analysis of incubations 7 & 8 taking place 8 days earlier. Any co-[^{3}H]/[^{32}P] peaks appearing in the profiles could also be related to the equivalent *amounts* of the molecules carrying the radioactivity by calculating the decay of [^{32}P] from a known specific activity at a certain date. A "molar ratio" might then be estimated for the [^{3}H]-carrying and [^{32}P]-carrying molecules if they were to occur.

Figure 4.26 shows the radioactive profile of the nucleotide extract from incubation 3, to which there was no 3AB or unlabelled Ap4A added, and the cells were pre-treated with DMS. It is

Figures 4.24 to 31.

These are all DEAE cellulose chromatograms (using a linear gradient of NH_4HCO_3 from 2 to 300mM) of the nucleotide extracts from permeabilised cells, which had (or had not) been pre-treated with 200μM DMS, and incubated with [^{32}P]NAD^+ and commerciallly produced [^{3}H]Ap4A (see text for details) in the presence or absence of 5mM 3AB and/or 200μM Ap4A. Each point represents the total dpm for the whole fraction. In all the diagrams, [^{3}H]dpm are represented as open circles (○) and [^{32}P]dpm as closed circles (●). The numbers 1 to 8 refer to table 13 in the text.

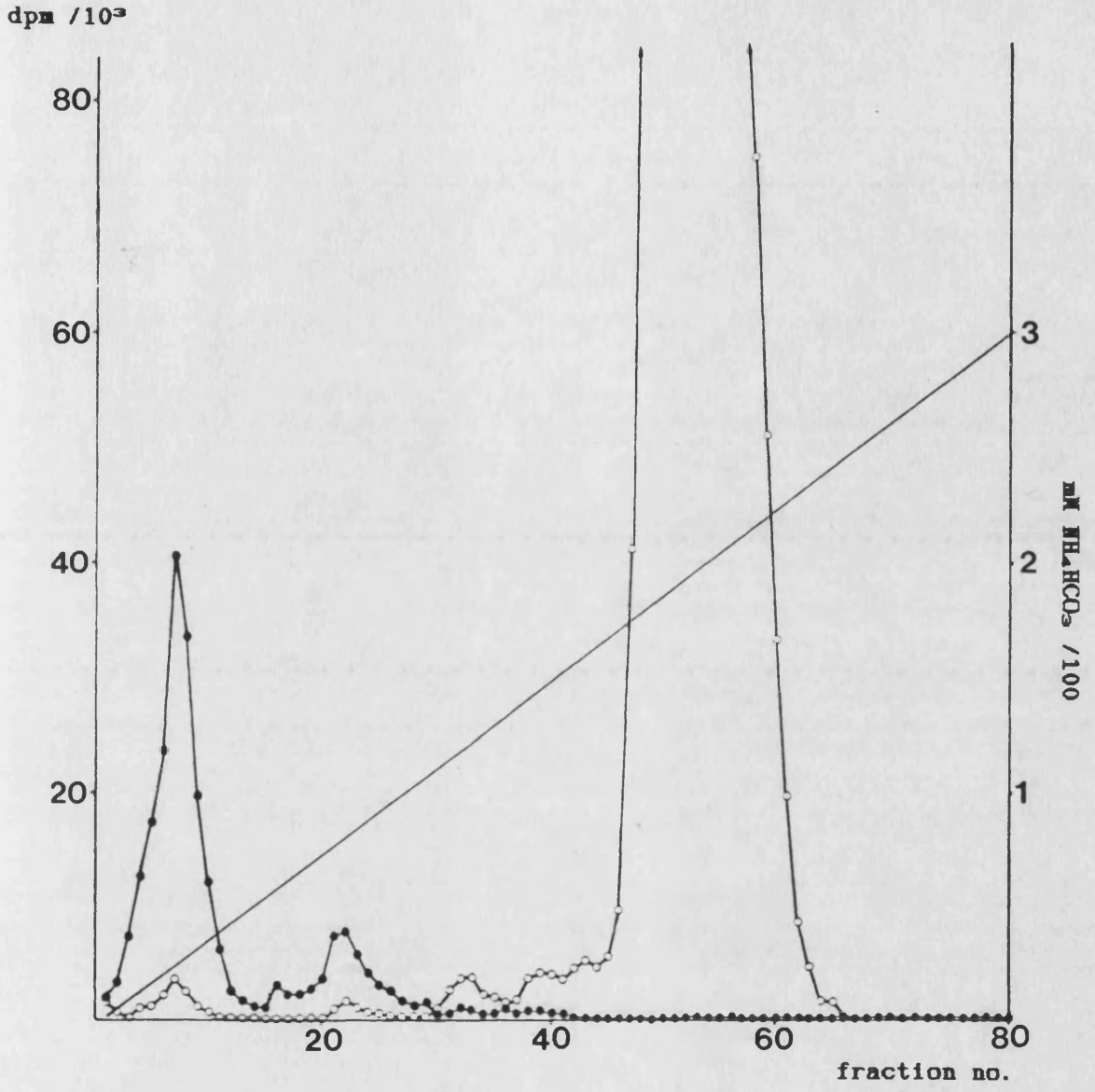

Figure 4.24.

DEAE cellulose chromatogram of the nucleotide extract from incubation "1" - DMS-treated cells; 5mM 3AB, 200μM Ap4A present.

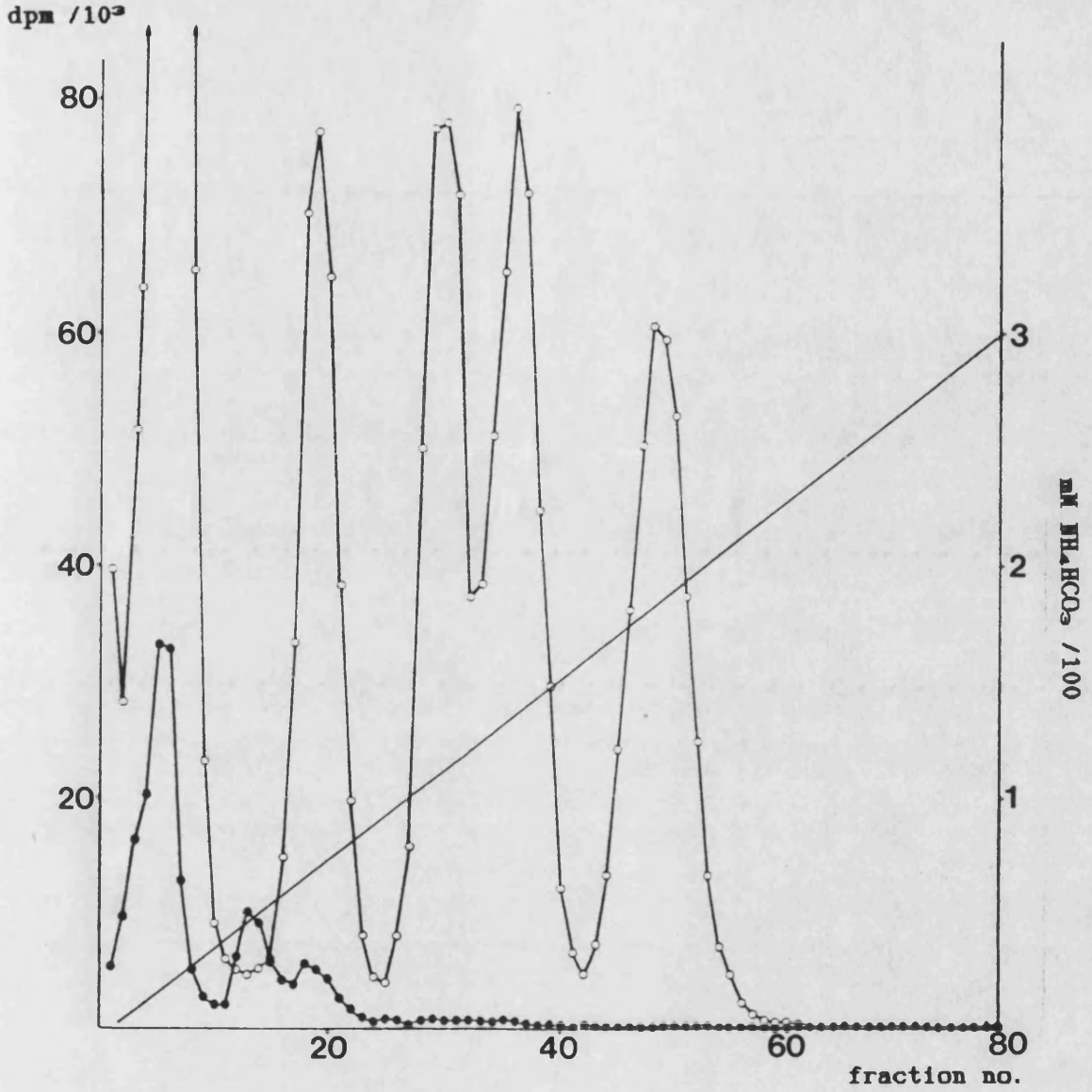

Figure 4.25.

DEAE cellulose chromatogram of the nucleotide extract from incubation "2" - DMS-treated cells; 5mM 3AB present.

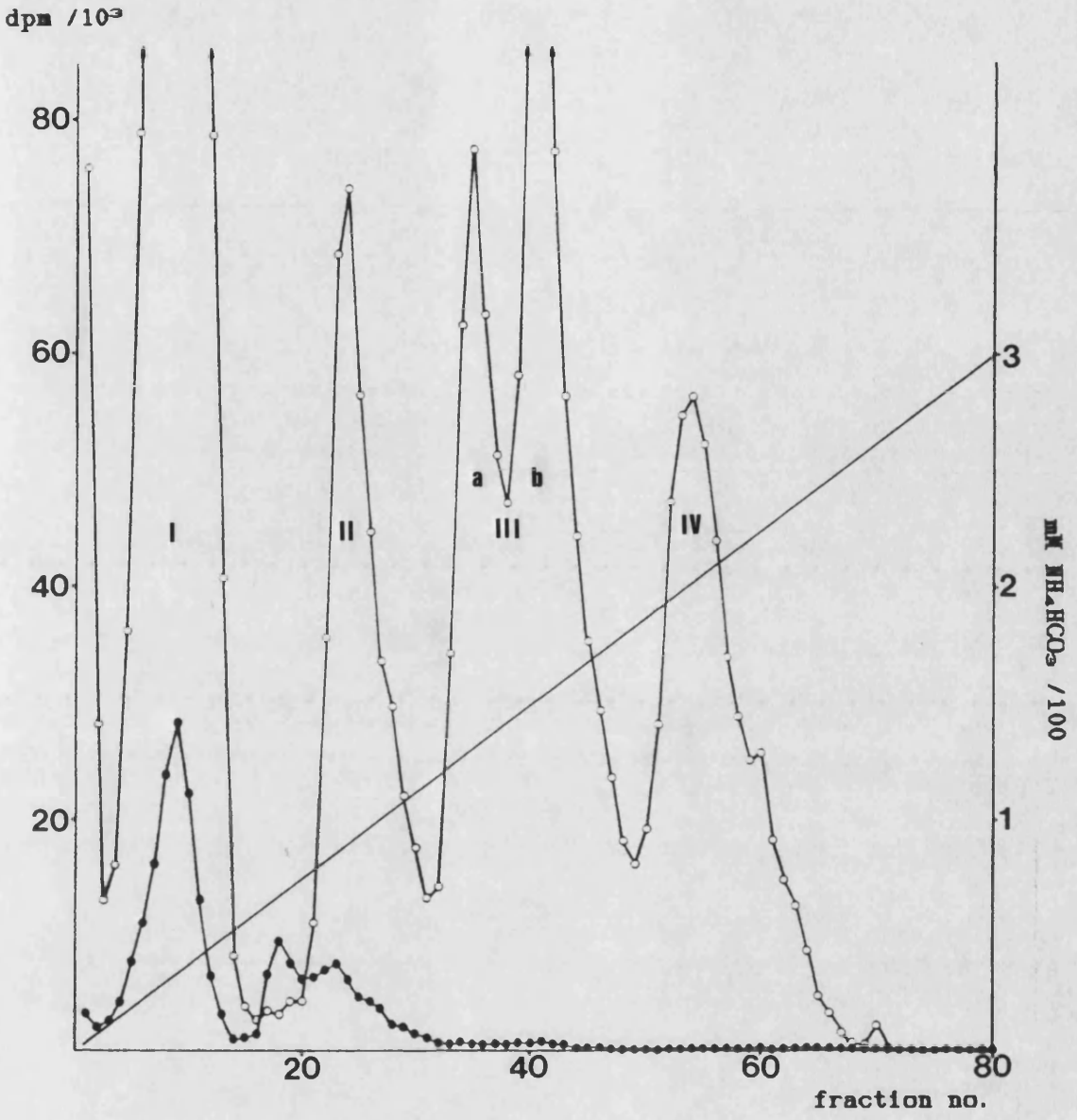

Figure 4.26

DEAE cellulose chromatogram of the nucleotide extract from incubation "3" - DMS-treated cells.

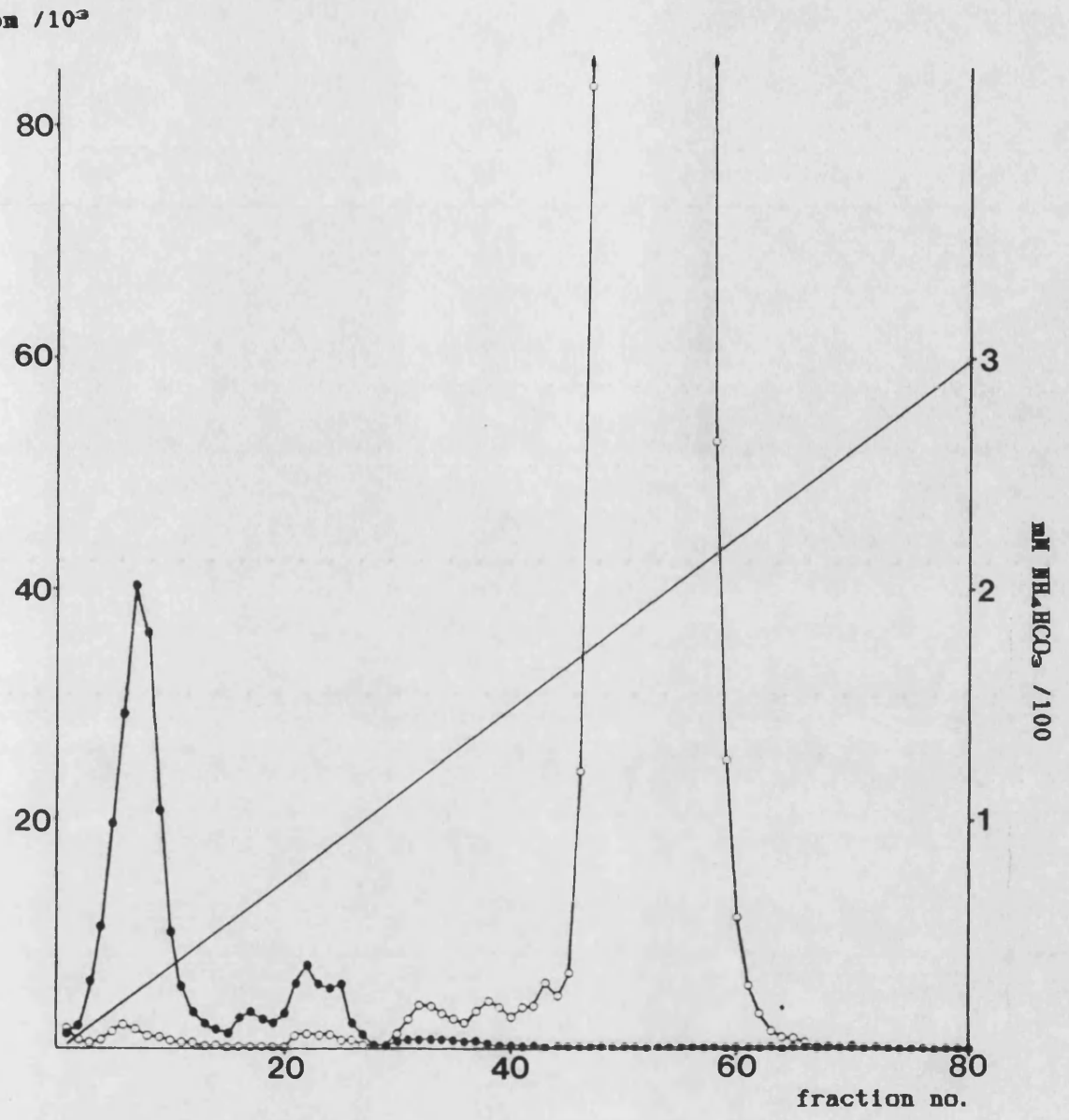

Figure 4.27.

DEAE cellulose chromatogram of the nucleotide extract from incubation "4" - control cells; 5mM 3AB, 200μM Ap4A present.

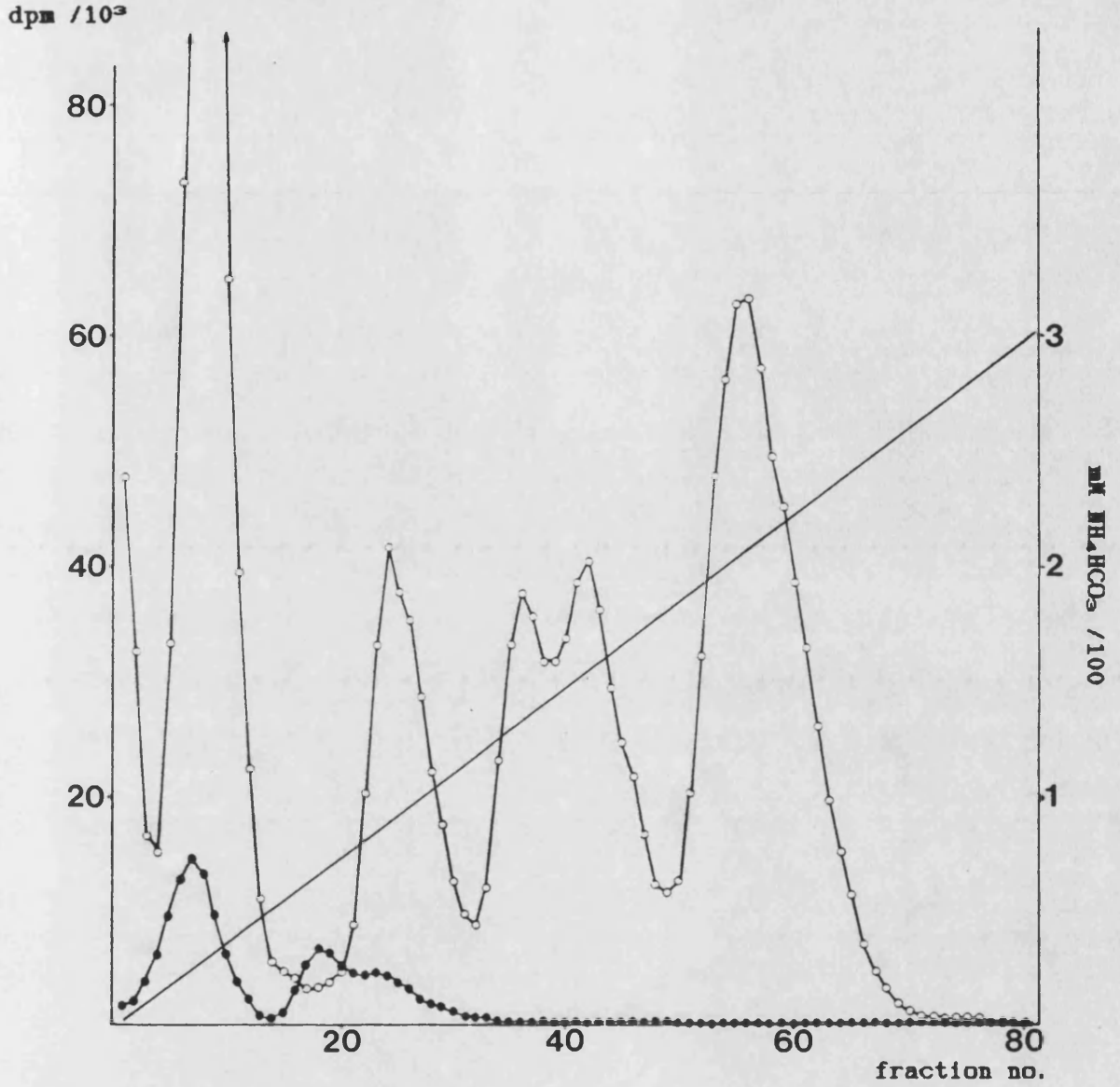

Figure 4.28.

DEAE cellulose chromatogram of the nucleotide extract from incubation "5" - control cells; 5mM 3AB present.

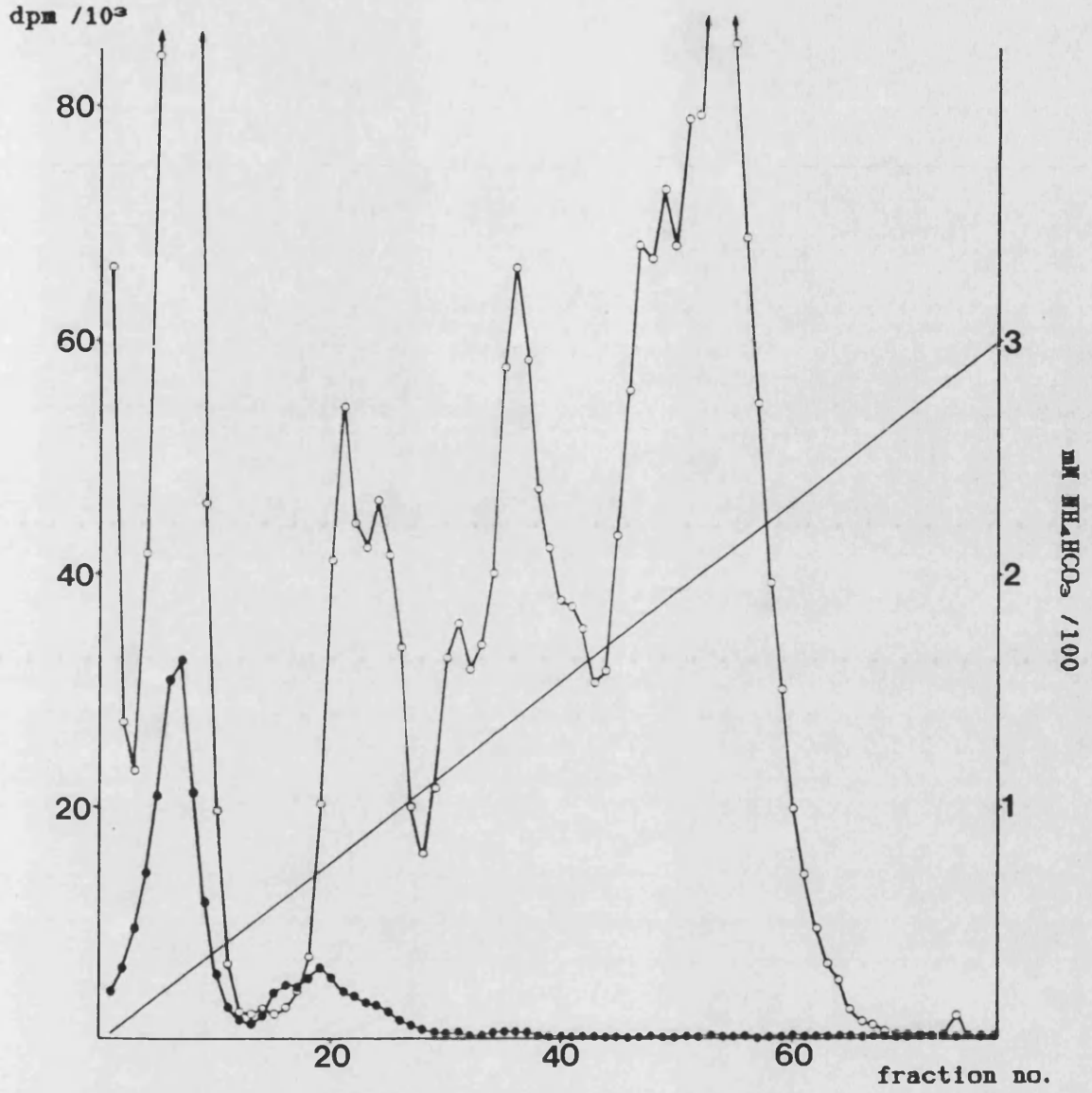

Figure 4.29.

DEAE cellulose chromatogram of the nucleotide extract from incubation "6" - control cells.

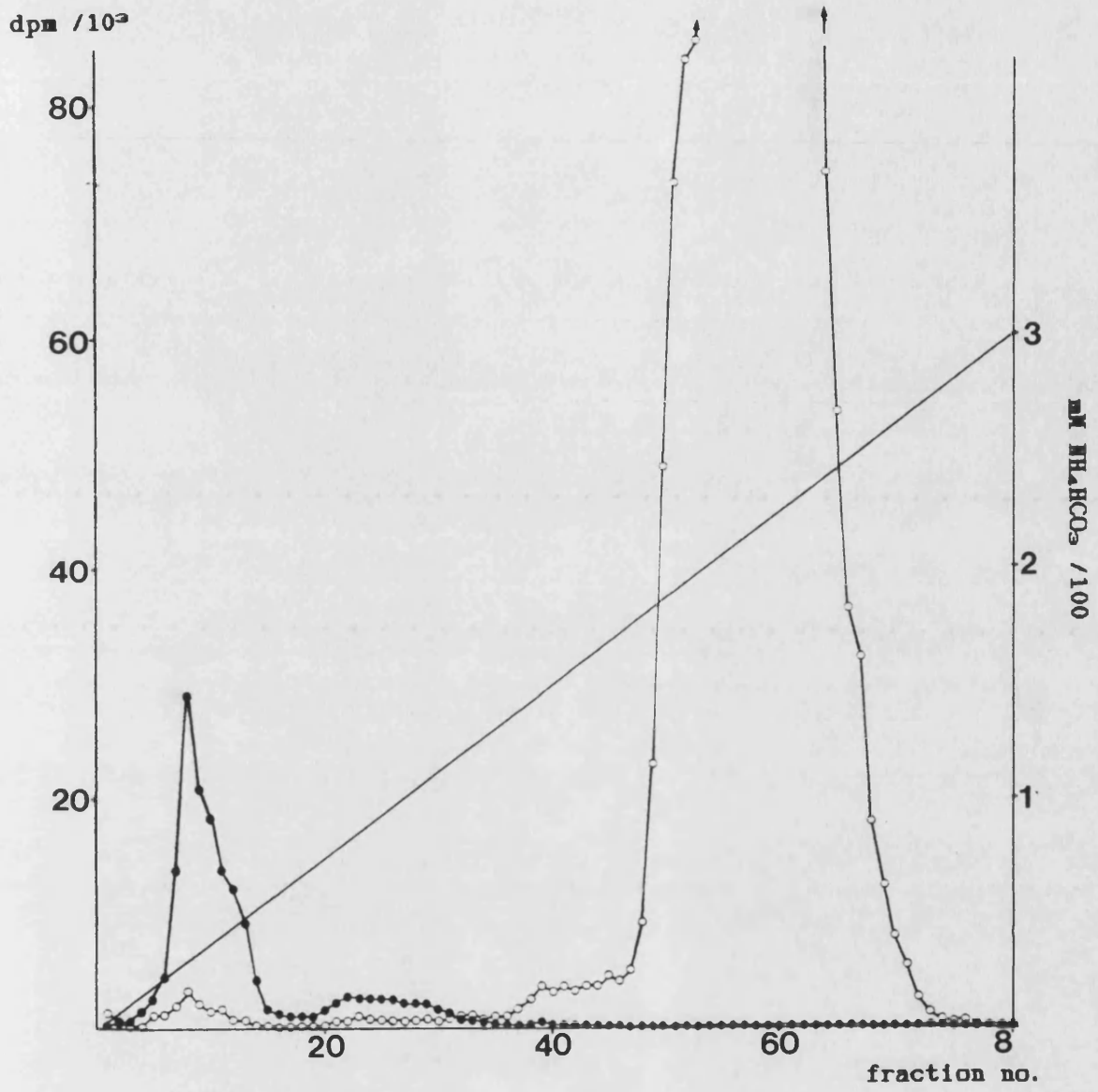

Figure 4.30.

DEAE cellulose chromatogram of the nucleotide extract from incubation "7" - DMS-treated cells; 200μM Ap4A present.

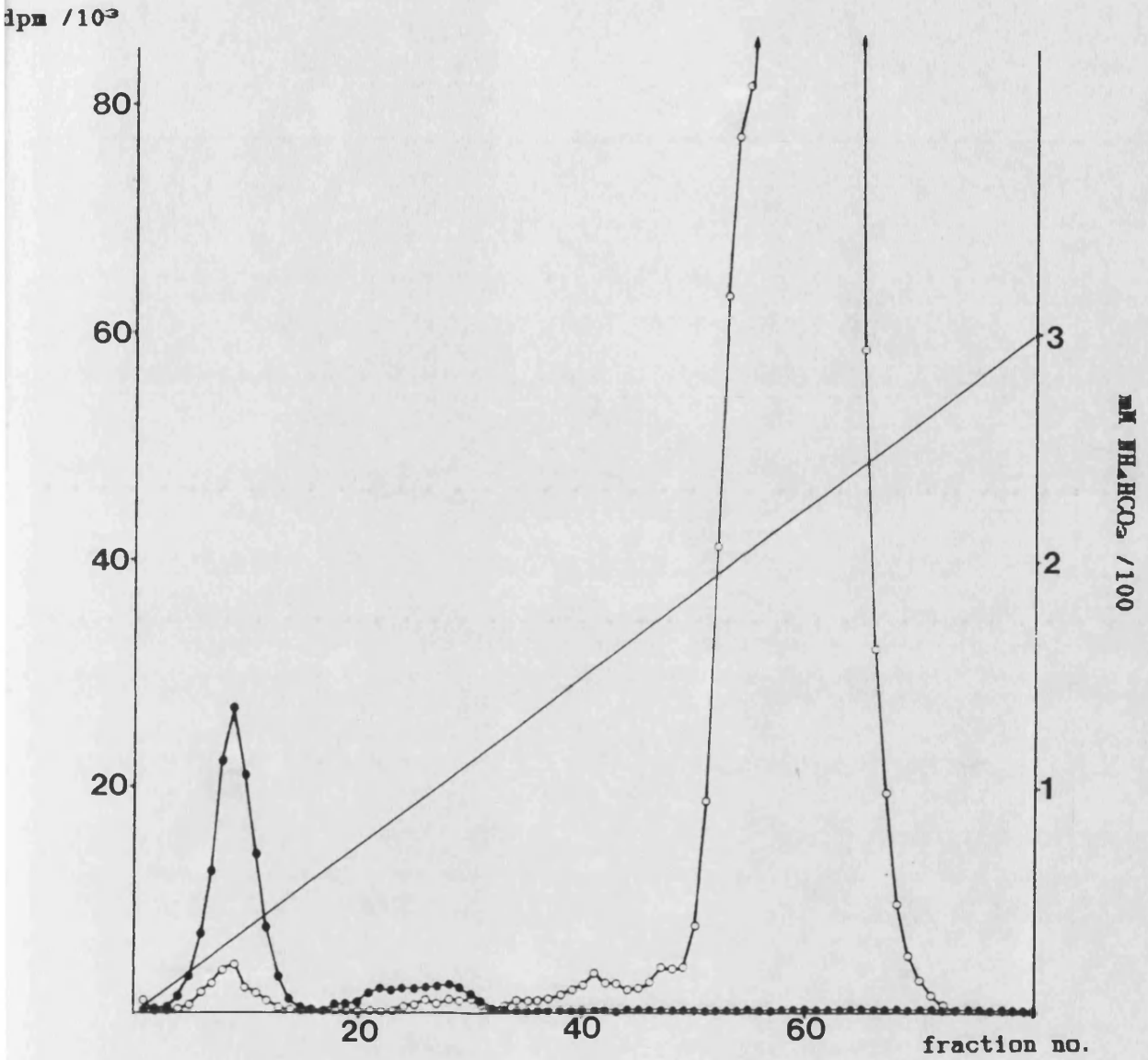

Figure 4.31.

DEAE cellulose chromatogram of the nucleotide extract from incubation "8" - control cells; 200μM Ap4A present.

(OVER) Figure 4.32.

Figures 4.24 to 4.31 were reduced and are presented together on one page for comparison. The chromatograms of the nucleotide extracts from cells which had been pre-treated with DMS are in the left-hand column. The numbers refer to the incubation conditions (± 3AB, Ap4A) of which Table 13 was a summary.

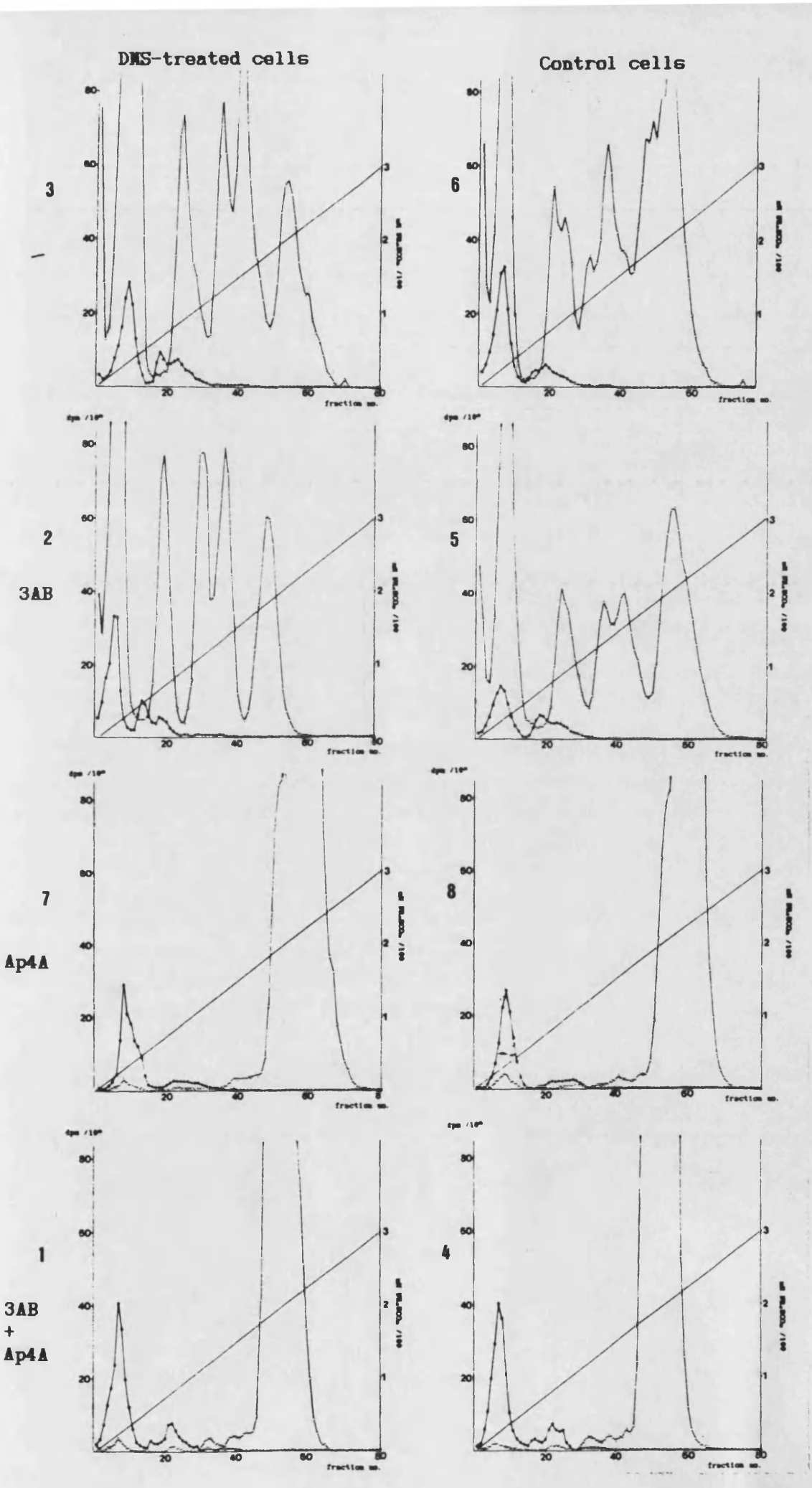
DMS-treated cells
Control cells
3
—
6
2
3AB
5
7
Ap4A
8
1
3AB
+
Ap4A
4

evident that [^{3}H]dpm is eluting already at the beginning of the gradient, and table 21 shows that relatively large amounts are present in the 2 mM NH_4HCO_3 wash, applied before the gradient. In addition to that present in the first fraction, there were four major peaks of [^{3}H]dpm, and these shall be referred to as I, II, IIIa&b and IV (peak III appearing to consist of two slightly merged peaks). The [^{32}P]dpm eluted in two major peaks, the first coinciding with I, the next appearing as two un-separated peaks between I and II (*ie*:55-100 mM NH_4HCO_3). The equivalent I peak in figure 4.17 was identified as consisting of [^{32}P]NAD^+ and [^{3}H]adenosine.

The first part of the second [^{32}P] peak was similarly identified as consisting solely of [^{32}P]ADP-ribose, whereas the second part contained [^{32}P]ADP-ribose and [^{3}H]AMP, which separated on TLC (figure 4.20). This second part also coincides with peak II in figure 4.26 and it is reasonable to assume that it, too consists of [^{3}H]AMP and [^{32}P]ADP-ribose. The double peak (III) may then be [^{3}H]ADP and [^{3}H]ATP. Peak IV is [^{3}H]Ap4A, as suggested by an (acidic) TLC of fraction 50 from figure 4.26 (see figure 4.33).

The most useful conclusions are arrived at when figure 4.26 is compared with the others, as it is in figure 4.32. Here, it can be seen that the [^{3}H] peak IV appears in all of them, in varying amounts, as do the first and second [^{32}P] peaks. The most startling changes in the profiles occur, however, when 200 μM Ap4A was present

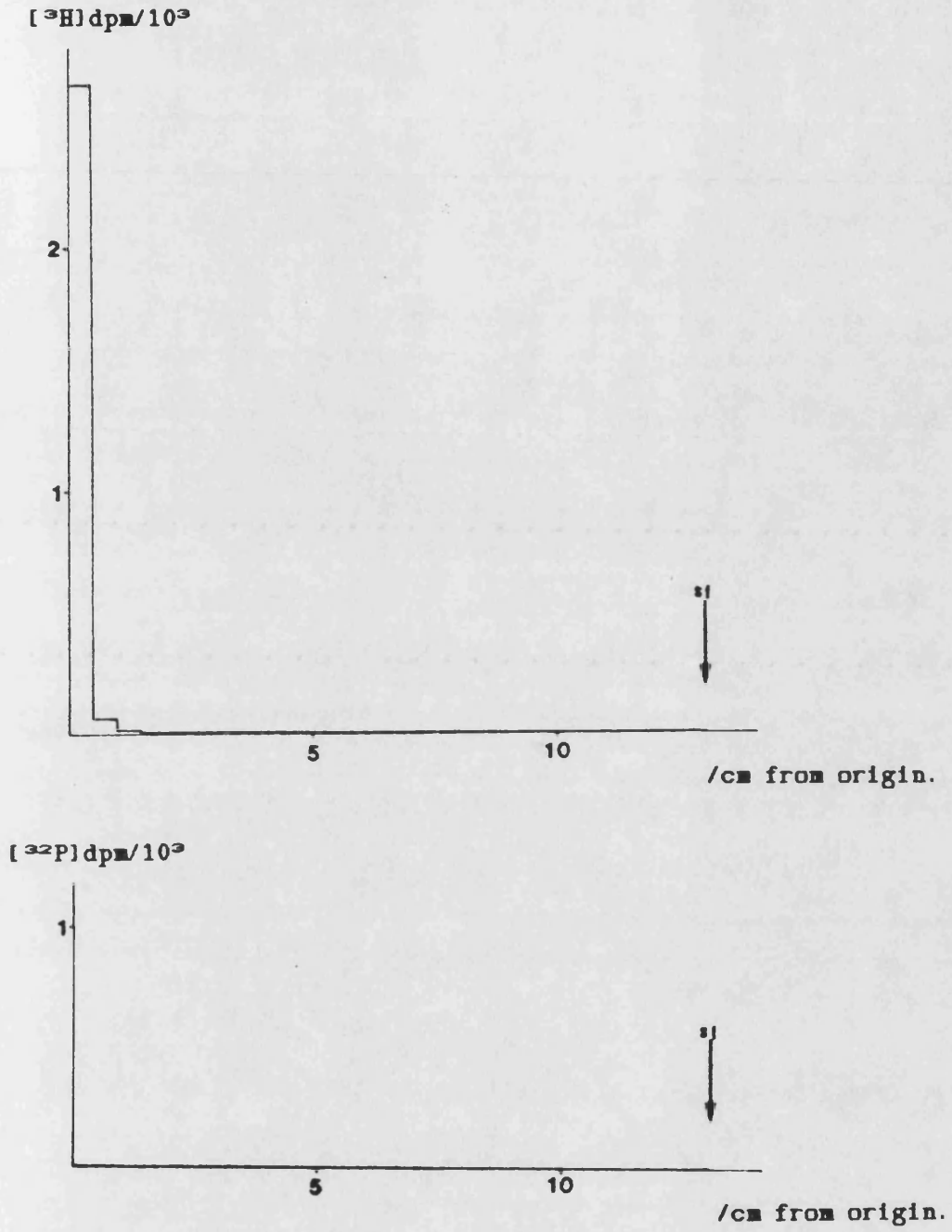

Figure 4.33.

1/200th (10µl) of fraction 58 from the DEAE cellulose chromatogram in figure 4.26 was analysed in the LiCl/acetic acid TLC system.

Top - [³H]dpm; bottom - [³²P]dpm.

in the initial incubation. The radioactivity in fraction I, peaks I, II and III all but disappear, and peak IV becomes the only major [^{3}H] peak in the profile. This change is not observed in the presence of 3AB alone, and the relative size of peak IV is not altered by its presence, or by DMS-treatment of the cells. Table 22 below shows the relative sizes of peaks I and IV (as a percentage of the total [^{3}H]dpm eluted from the column) and the variation in these between incubations 3,7,2 and 1 (DMS-treated cells). The same effect was observed in the profiles of the extracts from the control cells.

Table 22.

	(as % total [^{3}H]dpm eluted)	
Incubation	peak I	peak IV
3 (no additions)	33.8	16.6
7 (unlabelled Ap4A)	0.7	91.4
2 (3AB)	37.5	13.2
1 (Ap4A & 3AB)	0.5	95.8

This increase in peak IV and disappearance of the others may be explained by the 'dilution effect' discussed earlier. In the absence of added unlabelled Ap4A (3 & 2), a proportion of the [^{3}H]Ap4A is hydrolysed by the cells, apparently yielding adenine, adenosine, AMP, ADP and ATP. The effects of this hydrolysis are made almost invisible by the presence of 150 000 fold excess unlabelled Ap4A in the incubation, because less of the labelled Ap4A is hydrolysed. The

specific hydrolysis of Ap4A is known to occur *in vivo* (Zamecnik *et.al.*(1976); A.G.McLennan - personal communication (1988)) and in many *in vitro* systems (see chapter II for a discussion). It is likely that the products of this hydrolysis (AMP, ADP, ATP) may then be further hydrolysed by cellular phosphatases (endo and exonucleases), although it is not known whether 'adenyl-ribose glycohydrolase' activity would be responsible for the production of adenine.

Of major relevence to this thesis, however, was not the hydrolysis of Ap4A but whether DMS and/or unlabelled Ap4A caused the appearance of a co-[^{3}H]/[^{32}P] peak slightly beyond the [^{3}H]Ap4A peak at ≃ 200 mM NH_4HCO_3. The fact that this did not occur, and that the inclusion of the ADPRT-inhibitor 3AB did not make a difference (in the presence or absence of unlabelled Ap4A) suggests that the product Ap4A-(ADP-ribose)$_n$ was not being synthesised by the cells under these conditions, even though it was shown that the (ADP-ribosyl)ation of proteins was inhibited by both the 3AB and Ap4A (table 15 and 16). The possibility that (ADP-ribosyl)ated Ap4A was produced in significant amounts but remained un-eluted is unlikely, since elution with 500 mM NH_4HCO_3 in all cases yielded no significant dpm, and there was no pattern of variation in the dpm remaining bound to the column. Since the large increase in the amount of [^{3}H]dpm deposited in the ethanolic pellet from incubations containing 200 μM Ap4A was *not* accompanied by an increase in [^{32}P]dpm, it is very unlikely that

the product was lost from the nucleotide extract in this way. The analysis of the redissolved ethanolic pellets by electrophoresis in 1% agarose was only partially successful, and is dealt with in appendix 3.

Conclusion.

(V)

When permeabilised L1210 cells were incubated with [^{3}H]NAD$^+$ and the smaller molecules isolated from the rest of the cellular material by various means, no significant quantities of (ADP-ribosyl)ated nucleotide were found. Treatment of the cells with DMS did not have any effects in this respect either.

Ap4A was found to inhibit the (ADP-ribosyl)ation of proteins in both salt/PEI-extracted pig thymus nuclei and permeabilised cells in a dose-dependant manner. Could this have been due to the preferrential (ADP-ribosyl)ation of Ap4A itself ?

Although distortion made interpretation difficult, the TLC analysis of disrupted permeabilised cells which had been incubated with [^{3}H]NAD$^+$ in the presence of 200µM Ap4A revealed the increasing production with time of a labelled peak, migrating to a point just before the Ap4A standard. This did not occur in the absence of 200µM Ap4A. A suitable procedure was developed for the isolation of nucleotides from the bulk of the other cellular components, utilising phenol/chloroform/IAA extraction of proteins, followed by acidic ethanol precipitation of DNA and RNA. The analysis of this nucleotide extract on TLC was also unsatisfactory in terms of the distortion and lack of resolution of nucleotides. However, the "Ap4A - dependant" peak appeared here, too, though in much smaller relative amounts. The material in this peak was shown to be resistant to base-treatment,

and thus it was considered unlikely that it consisted of (ADP-ribosyl)ated Ap4A, since the Ap4A - ADP-ribose bond has been shown to be base - sensitive (Yoshihara and Tanaka (1981)).

The more satisfactory analysis of nucleotide extracts from permeabilised cells incubated with [^{3}H]NAD^{+} by DEAE cellulose column chromatography showed that the inclusion of unlabelled Ap4A in the incubation made no significant difference in terms of their radioactive profiles.

In order to distinguish between the adenosine moieties of Ap4A and NAD^{+}, they were labelled with [^{3}H] and [^{32}P] respectively. If a particular set of incubations were to cause the production of (ADP-ribosyl)ated Ap4A by permeabilised cells then it would be detected as a co-[^{3}H]/[^{32}P] peak of radioactivity (of greater negative charge than Ap4A) when the nucleotide extracts were subjected to DEAE cellulose chromatography. The inclusion of 5mM 3AB in incubations with permeabilised cells, on its own or together with 200μM unlabelled Ap4A, allowed comparisons to be made between the effects of the two with respect to (ADP-ribosyl)ation. Similarly, the pre-treatment of some of the cells with DMS allowed the effects of DNA damage to be examined. Both DMS - treatment and 5mM 3AB alone had no significant effect on the radioactive profiles of the nucleotide extracts with respect to the control. The presence of 200μM Ap4A (with or without 3AB) masked the extensive hydrolysis of [^{3}H]Ap4A by

the cells - as shown by the radioactive profiles of their nucleotide extracts. It also caused an unexpected three-fold increase in the loss of [^{3}H]dpm to the ethanolic pellet during the extraction of RNA/DNA. The fact that this was not accompanied by an increased loss of [^{32}P] means that the precipitated material is not (ADP-ribosyl)ated Ap4A. This is supported by the fact that the phenomenon occurs both in the presence and absence of inhibiting levels of 3AB.

It is thus concluded that the inhibitory effect of Ap4A upon (ADP-ribosyl)ation of proteins in permeabilised L1210 cells is probably not due to its serving as a preferrential acceptor for poly(ADP-ribose), unless the product ([^{3}H]Ap4A-([^{32}P]ADP-ribose)$_{n}$) is so rapidly degraded in the cells that is not detectable after ten minutes. Perhaps its effects are due to the stimulated proteolytic processing of ADPRT observed by Berger and Surowy (1983a,b). If this is the case, then it is occurring at much lower levels of Ap4A (10 to 100-fold lower). The deposition of increased amounts of [^{3}H]dpm with nucleic acids in the presence of 200μM Ap4A is interesting and worthy of further investigation, although it may just be due to increased ionic concentration of the mixture being precipitated. Until specific roles for Ap4A and nuclear (ADP-ribosyl)ation in eukaryotes can be established, there is no firm evidence to date that the two are connected.

Appendices.

Appendix 1

In order to facilitate the differential counting of [^{32}P] and [^{3}H] radioactivity, the 'windows' of separate channels in scintillation countere were tuned to the optimum part of the emission spectrum, such that the [^{32}P] window excluded all [^{3}H]-derived counts, and the [^{3}H] window allowed only 0.1% of [^{32}P]-derived counts to register. This unavoidably involved a drop in efficiency, such that it was neccessary to convert the [^{32}P] cpm (counted at 78.9% efficiency) and [^{3}H] cpm (counted at 23.8% efficiency) into disintegrations per minute. The 0.1% spillover of [^{32}P] → [^{3}H] also had to be taken into account. Finally, in order to compare experiments, a decay-chart was employed to calculate the value of [^{32}P] on a particular day - eg. two experiments, separated by 14 days (≃ 1 half-life) could be related to one another by multiplying the [^{32}P] dpm by a correction factor, producing [^{32}P] figures as if the experiments were performed on the same date.

All of this was made very much easier (particularly when used with DEAE cellulose chromatograms, of 80 fractions) by using the Basic program shown over.

The cpm from an experiment were entered into a file (from the [^{32}P] and [^{3}H] windows), together with notes (which are not read by the programme). When the programme is run, it prompts for the file, which is subsequently displayed, together with the notes accompanying

```
10 REM ************use to convert cpm from files to dpm*****************
20 :
30 ZONE (13)
40 INPUT "file name   ";x$
50 DISPLAY x$
60 INPUT "enter volume of aliquotes",p
70 INPUT "enter total vol. of fractions",   q
80 r=q/p
90 INPUT "enter no. of fractions   ",w
100 INPUT "enter date you wish to correct 32P figures to",l$
110 INPUT "when was radioactivity counted?  ",v$
120 DISPLAY "correct"
130 REM: "correct" is 32P decay chart
140 INPUT "enter correction factor    ",t
150 DIM a(w),b(w)
160 OPEN "i",1,x$
170 FOR x=1 TO w
180 INPUT £1,a(x)
190 NEXT
200 FOR x=1 TO w
210 INPUT £1,b(x)
220 NEXT
230 PRINT "are you ready to print out ? Type CONT to do so."
240 STOP
250 LPRINT  x$"  performed on "v$
260 LPRINT "                                          corrected for decay
 "
270 LPRINT "           32P  ";"            tritium ";"total p32 ";"total 3H "
280 LPRINT "
          "
290 LPRINT "   fraction";" cpm";"   dpm";"     cpm";"    dpm";"   dpm";"     d
"
300 LPRINT"
       "
310 FOR x=1 TO w
320 f=1/0.789*(a(x)-15)
330 g=1/0.283*((b(x)-5)-0.01*a(x))
340 LPRINT USING" ######";x,a(x),f,b(x),g,
350 IF f<0 THEN f=0
360 IF g<0 THEN g=0
370 y=y+f
380 z=z+g
390 LPRINT USING" ######";r*f*t, r*g
400 NEXT
410 LPRINT "total 32P dpm:        ",USING"#######";r*y*t
420 LPRINT"total 3H dpm:        ",USING"#######";r*z
430 LPRINT "
  "
440 LPRINT x$ ", of "v$"."
450 LPRINT "only TOTAL 32P figures corrected to ",l$
460 LPRINT "(correction factor ",t,")"
470 LPRINT w" fractions "
480 RESET
490 END
```

Basic programme (used with Amstrad PCW8256)

it. Other details are then prompted for, such as the number and volume of the aliquots v fractions, and the date of the experiment v the 'correction date'. The [^{32}P] decay chart (shown below) (LKB) is then called and displayed and the appropriate correction factor is entered. The file then sequentially reads [^{32}P]cpm no.1 together with [^{3}H]cpm. no.1, [^{32}P] no.2, [^{3}H] no.2 etc. from the file and displays the calculated figures as shown on the following page. A graph can then be drawn for [^{3}H] and [^{32}P]dpm.

Decay chart for [^{32}P] (LKB).

days from zero	1/factor	factor
0	1.000	1.000
1	.953	1.049
2	.908	1.101
3	.865	1.156
4	.824	1.214
5	.785	1.274
6	.748	1.337
7	.712	1.404
8	.679	1.473
9	.647	1.546
10	.616	1.623
11	.587	1.704
12	.559	1.789
13	.533	1.808
14	.507	1.972
20	.379	2.639
30	.234	4.274
40	.144	6.944
50	.089	11.236
60	.055	18.181

Example print-out.

tlc1.5 performed on 19/5/87

	32P		tritium		corrected for decay total p32	total 3H
fraction	cpm	dpm	cpm	dpm	dpm	dpm
1	23	10	24	66	14	66
2	33	23	74	243	31	243
3	25	13	50	158	17	158
4	30	19	17	41	25	41
5	31	20	19	48	27	48
6	29	18	58	186	24	186
7	25	13	8	10	17	10
8	34	24	136	462	32	462
9	24	11	40	123	15	123
10	37	28	8	9	37	9
11	34	24	18	45	32	45
12	34	24	15	34	32	34
13	27	15	17	41	20	41
14	35	25	280	970	34	970
15	29	18	73	239	24	239
16	32	22	79	260	29	260
17	31	20	73	239	27	239
18	22	9	9	13	12	13
19	25	13	6	3	17	3
20	35	25	4	-5	34	0
21	37	28	5	-1	37	0
22	25	13	5	-1	17	0
23	42	34	12	23	46	23
24	39	30	18	45	41	45
25	34	24	24	66	32	66
26	25	13	20	52	17	52

total 32P dpm: 690
total 3H dpm: 3378

tlc1.5, of 19/5/87.
only TOTAL 32P figures corrected to 13/5/87
(correction factor 1.337)
26 fractions

(*N.B.* the "cpm" columns are raw data. The "dpm" columns have been adjusted to take account of the background radiation, and in the case of [^{32}P], radioactive decay over the period shown (6 days) was also compensated for.

Snake venom phosphodiesterase (from both C.durissus and C.adamanteus) was purified as described fully in chapter III.11 - after Oka *et.al.*(1978). Figure A2.1 shows the results when a batch of phosphodiesterase from C.adamanteus (type II, Sigma.) subjected to affinity chromatography on blue sepharose (synthesized as described in III.11), using stepwise increases in potassium phosphate concentration as indicated. Assays were made for non-specific phosphatase and phosphodiesterase activities, and also for protein concentration using Coomassie Blue as described in III.11 and 13, respectively. Using the fact that the extinction coefficient of p-nitrophenol (at 400nm) is quoted by Sigma as 17000 $cm^2.mol^{-1}$, it was found that 54% of the original phosphodiesterase activity eluted in the 30mM potassium phosphate (representing 40% of the total protein applied) and the pooled fractions were concentrated and washed as described in III.11. To test for phosphatase and/or nucleotidase activity, two aliquots of [^{3}H]ATP in water (2.5 x 10^6 cpm) were incubated for 1hr with either 50µl 10mM magnesium chloride, 50mM Tris-acetate, pH8.8 or 50µl of the same solution containing 0.1 unit of the purified enzyme. (one unit was defined as that liberating 1 µmole of p-nitrophenol per minute under these conditions). Figure A2.2 shows the result when 15µl from the above two incubations, and it can be seen that the enzyme nearly entirely digests the [^{3}H]ATP to

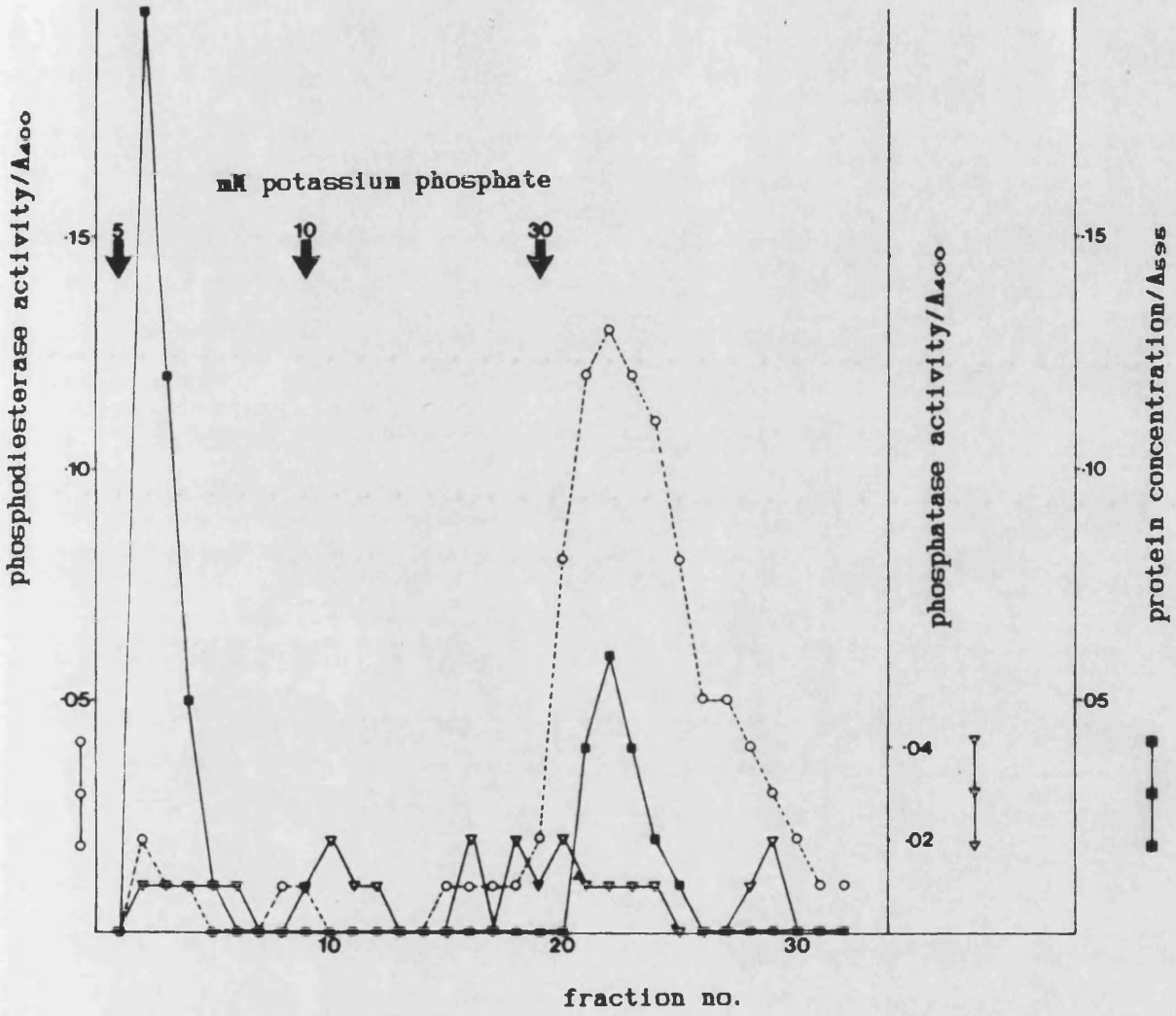

Figure A2.1.

Affinity chromatography of snake venom phosphodiesterase on Blue Sepharose, performed as described in chapter III.11. Each fraction was assayed for phosphodiesterase activity (O), phosphatase acivity (▽) and protein concentration (■). The points at which the potassium phosphate concentration was raised are indicated (arrows).

(OVER)Figure A2.2.

The 30mM -phosphate fractions from figure A2.1 were pooled and washed in an Amicon filtration unit as described in chapter III.11.

[^{3}H]ATP was incubated for 1hr at 37°C with either an amount equivalent to one unit of the enzyme or an equal amount of the buffer in which it was contained (see text for details). The products were analysed by TLC in the LiCl/acetic acid TLC system. Top - radioactive profile of the control incubation (undigested); bottom - profile of the incubation containing the enzyme (digested).

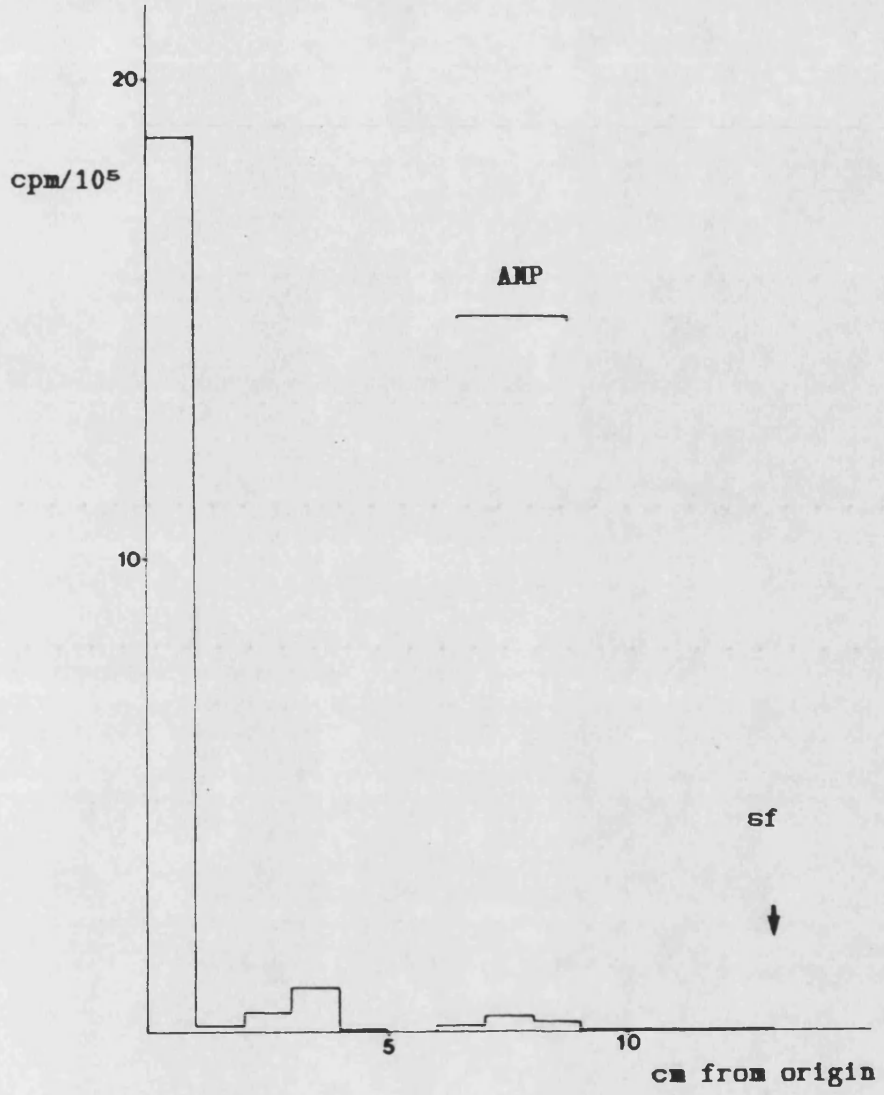
20
cpm/10⁵
AMP
10
sf
5
10
cm from origin

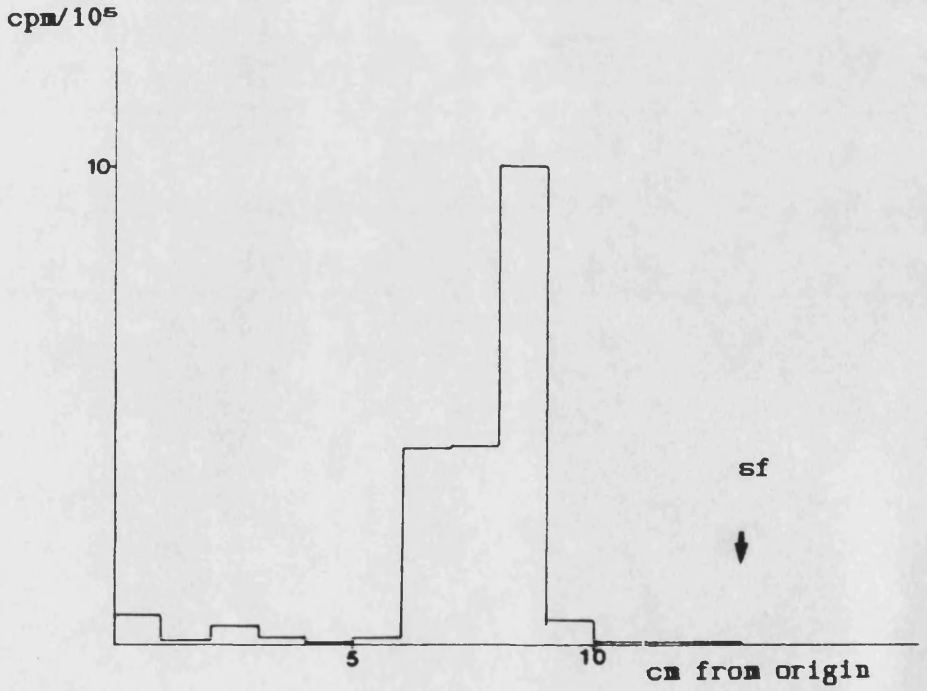
cpm/10⁵
10
sf
5
10
cm from origin

[^{3}H]AMP. That there is no phosphatase activity present is indicated by the absence of [^{3}H]adenosine - which would have been produced by such exonucleolytic digestion. It appears, then, that the ATP is serving as a substrate for either snake venom phosphodiesterase itself, or that contaminating nucleotidase activity remains.

Even though it was not accompanied by similar changes in [^{32}P]dpm, the increase in the 'loss' of [^{3}H]dpm to the nucleic acid pellet caused by the inclusion of 200 μM Ap4A in the incubation was considered worthy of investigation by other means.

It was thought that the nature of the radioactive material in the ethanolic pellets produced by the nucleotide extraction procedure might be further characterised by its electrophoretic mobility in 1% agarose gels. If the gels were run only a short distance, the nucleotides might be retained and visualised by cutting up and counting the gel slices for radioactivity. The specific activity of the [^{32}P] and [^{3}H] radioactivity was such that if [^{32}P]ADP-ribose and [^{3}H]Ap4A were bound together in equimolar amounts, the presence of approximately 1200 dpm of [^{32}P] should be accompanied by 10 000 dpm of [^{3}H]. With 200 μM Ap4A present in the initial incubation, the lowering of its specific activity meant that the same amount of [^{32}P] dpm should be accompanied by 0.067 dpm of [^{3}H]! In the event, this technique proved to be of little value due to these and other, practical difficulties. As described in chapter III.10(b), two types of gel were run, of 6 and 13.5 cm in length. In both cases, however, the amounts of [^{32}P] and [^{3}H] dpm retained by the gels did not exceed 20% of the total amounts applied to the wells. Unfortunately, the buffer at the (-ve) starting end of the gels was not monitored, and

so it is not known whether all the material actually entered the gels. Figure A3.1 shows the radioactive profile obtained when 2 x 20µl (from 100 µl total volume) of the redissolved ethanolic pellet from incubation "3" (no additions; DMS-treated cells) were run alongside each other in the shorter gel system. The bromophenol Blue marker was allowed to run a third of the length of the gel, which was then cut into 1 mm slices (see III.10(a)), each of which were solubilised and counted for radioactivity. It can be seen that no significant [^{32}P] dpm had been retained (whereas the ratio of [^{3}H]:[^{32}P] dpm in the samples applied was 16:1). 91.9% of the [^{3}H] dpm, however, appeared in a triple peak at and beyond the leading edge of the bromophenol Blue band. The photograph in figure A3.1 shows the gel, visualised under *uv* light. The two prominent bands (double-stranded DNA or RNA with sufficient tertiary structure to allow the intercalation of ethidium bromide) were not associated with any significant amounts of radioactivity.

It was decided that a longer gel run for the same distance might retain more of the labelled material. Larger wells were also employed, to facilitate the entry of the sample into the gel. The same quantity (40%) of the redissolved ethanolic pellet from incubation "7" (200 µM Ap4A; DMS-treated cells) was run in two adjacent tracks in the longer gel system. As described in III.10(b), restriction fragments from λ plasmids were run in another track, as

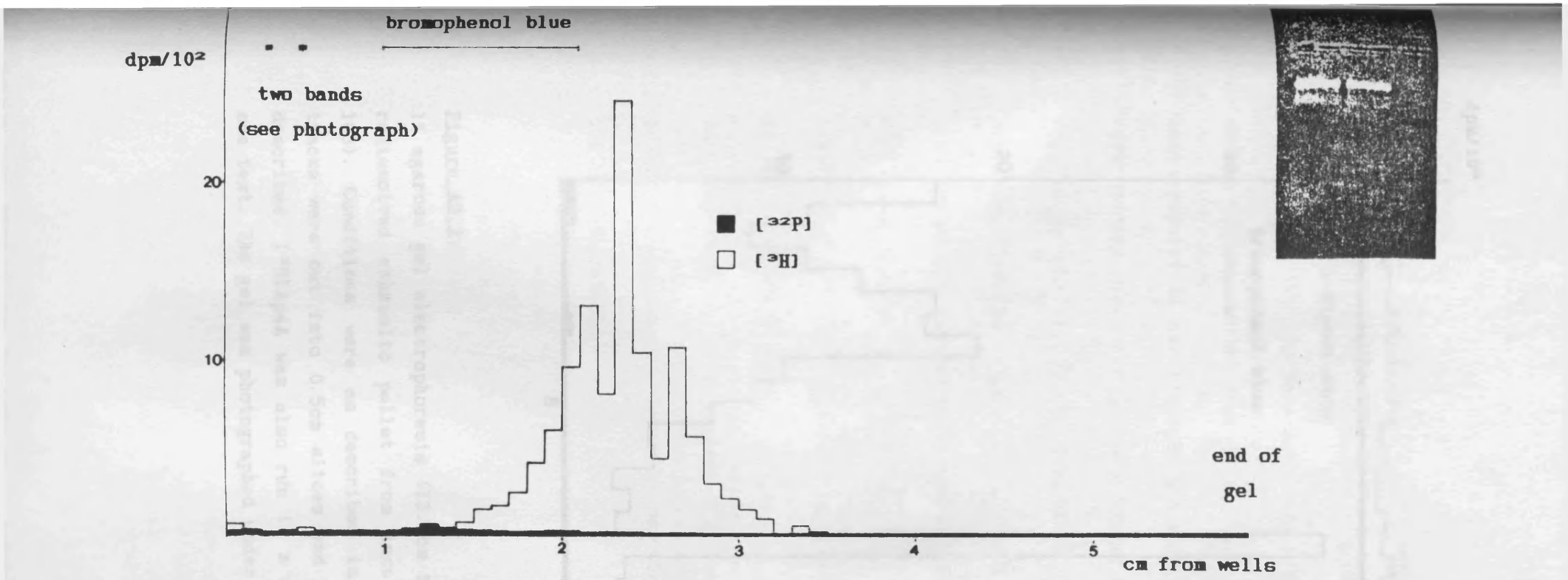

Figure A3.1.

1% agarose gel electrophoresis (6cm in length) of 2 x 20µl of the redissolved ethanolic pellet from incubation number "3" (see page 183). Conditions were as described in chapter III.10(b). The gel was photographed under *uv* light, enabling the visualisation of material intercalating with ethidium bromide. The two tracks (adjacent) were cut into 1mm slices and counted for [^{3}H] and [^{32}P] radioactivity as described. The photograph is shown in the top right hand corner.

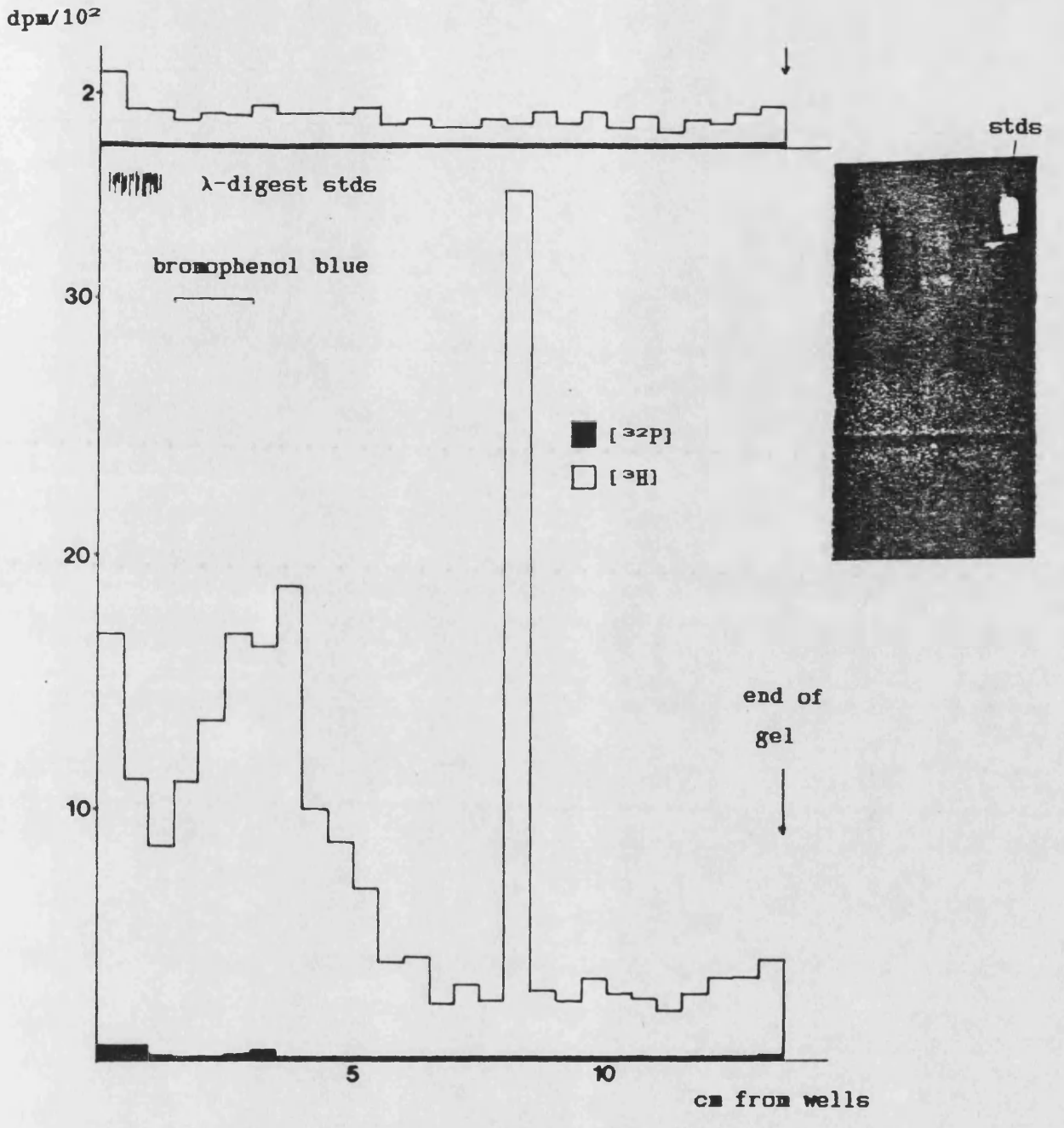

Figure A3.2.

1% agarose gel electrophoresis (13.5cm in length) of 2 x 20µl of the redissolved ethanolic pellet from incubation number "7" (see page 183). Conditions were as described in chapter III.10(b). The two tracks were cut into 0.5cm slices and counted for radioactivity as described. [³H]Ap4A was also run in a separate track (top graph) - see text. The gel was photographed under *uv* as in figure A3.1.

well as 2 µl of [^{3}H]Ap4A (4.3µCi/nmole) in a fourth. Figure A3.2 shows the resulting radioactive profile, and again, negligable amounts of [^{32}P] dpm were retained, although the ratio of [^{3}H]:[^{32}P] dpm in these samples was 10:1. There was no discernable peak of radioactivity in the [^{3}H]Ap4A standard track, and monitoring of the 'end' buffer accounted for only 10% of the total [^{3}H] dpm originally applied to the gel. Apart from this, there was a peak of [^{3}H]dpm migrating (as in figure A3.1) with the leading edge of the bromophenol Blue marker in figure A3.2 . In addition, a further large [^{3}H] peak occured at ≈8 cm. Bearing in mind that in the case of figure A3.2 the [^{32}P]dpm should be present in excess over the [^{3}H]dpm if the material in a peak consists of [^{3}H]Ap4A-(ADP-ribose)$_n$ it was concluded that no such product had been deposited in the ethanolic pellet, either in the presence or absence of 200 µM Ap4A in the initial incubation.

References.

Adamietz, P., Wielckens, K., Bredehorst, R., Lengyel, H. & Hilz, H.
Biochem. Biophys. Res. Commun. 101 (1981) p96-103

Adamietz, P. & Rudolph, A.
J. Biol. Chem. 259 no. 11 (1984) p6841-46

Adolph, K. W.
Arch. Biochem. Biophys. 253 no. 1 (1987) p176-188

Adolph, K. W. & Song, M. H.
Biochem. Biophys. Res. Commun. 126 no. 2 (1985a) p840-47

Adolph. K. W. & Song, M. H.
FEBS 2355 182 no. 1 (1985b) p158-162

Alkhatib, H. M., Chen, D., Cherney, B., Bhatia, K., Notario, V., Giri, C., Stein, G., Slattery, E., Roeder, R. G. & Smulson, M.
Proc. Natl. Acad. Sci. USA 84 (1987) p1224-1228

Allan, J., Hartman, P. G., Crane-Robinson, C. & Aviles, F. X.
Nature 288 (1980) p675-679

Aloya, U. J.
Anal. Biochem. 99 (1979) 161-64

Alvarez-Gonzalez, R., Moss, J., Niedergang, C. & Althaus, F.
in Abstr. 8th. Int. Symp. ADP-ribosylation. (1987) no. 9

Aubin, R. J., Dam, V. T., Miclette, J., Brousseau, Y., Huletsky, A. & Poirier, G. G.
Can. J. Biochem. 60 (1982) p1085-94

Baril, E., Bonin, P., Burstein, D., Mara, K. & Zamecnik, P. C.
Proc. Natl. Acad. Sci. USA 80 (1983) p4931-4935

Ben-Ishai, R., Hacham, H. & Hilz, H.
in *Abstr. 8th. Int. Symp. ADP-ribosylation.* (1987) no. 99

Benjamin,R.C., & Gill,D.M.
J.Biol.Chem. 255 (1980) p10502-10508

Berger,N.A.,Weber,G.,& Kaichi,A.
Biochem.Biophys.Acta. 519 (1978) p87-104

Berger,N.A. & Sikorski,G.W.
Biochemistry 20 (1981) p3610-3614

Berger,N.A.& Cohen,J.J.
in *"ADP-ribosylation reactions* ."(eds. Hayaishi,O.& Ueda,K.) (1982)
Academic Press. p547-560

Berger,N.A.,Berger,S.J.& Catino,D.M.
Nature 299 (1982) p271

Berger,N.,Surowy,C.& Petzold,S.J. *in "ADP-ribosylation of proteins"*
(Eds. Althaus,F.,Hilz,H.& Shall,S.) (1985) p129-38

Böhme,H.J., Kopperschläger,G., Schulz,J. & Hofman,E.
J.Chromatogr. 69 (1972) 209-14

Bohr,V. & Klenow,H.
Biochem.Biophys.Res.Commun. 102 (1981) p1254-1261

Borek,C.,Morgan,W.F.,Ong,A.& Cleaver,J.E.
Proc.Natl.Acad.Sci.USA 81 (1984) p243-7

Bradford, A.
Anal.Biochem. 72 (1976) 248-54

Bredehorst,R.,Goebel,M.,Renzi,F.,Kittler,M.,Klapproth,K.& Hilz,H.
Hoppe-Seyler's Z.Physiol.Chem. 360 (1979) p1737-43

Bredehorst,R.,Wielckens,K.,Adamietz,P.,Steinhagen-Theissen,E. &
Hilz,H.
Eur.J.Biochem. 120 (1981) p267-274

Brevet,A.,Coste,H.,Fromant,M.,Plateau,P.& Blanquet,S.
Biochemistry 26 (1987) p4763-4768

Burzio,L.O. & Koide,S.S.
Biochem.Biophys.Res.Commun. 40 (1970) p1013-1020

Burzio,L.O., Riquelme,P.T.,& Koide,S.S.
J.Biol.Chem. 254 no.8 (1979) p3029-37

Burzio,L.O., Koide,S.S.,Puigdomenech,P., Ruiz-Carrillo,A.
in *"Novel ADPRibosylation of Regulatory enzymes and proteins"*
(eds.Smulson,M.E. & Sugimura,T.) (1980) Elsevier, Amsterdam.p345-53

Burzio,L.O.
in *"ADP-ribosylation reactions".* (eds. Hayaishi,O.& Ueda,K.)
Academic Press (1982) p103-115

Butt,T.& Smulson,M. in *"ADP-ribosylation reactions"* (Eds.
Hayaishi,O.& Ueda,K.) Academic Press (1982) p173-191

Chan,J.Y.H.,Becker,F.F.,German,J. and Ray,J.H.
Nature 325 (1987) p357-358

Chang,L.,Plevani,P.& Bollum,F.
Proc.Natl.Acad.Sci.USA 79 (1982) p758-61

Chambon,P.,Weill,J.D.& Mandel,P.
Biochem.Biophys.Res.Commun. 11,(1963) p39-43

Cherney,B.A.,Midura,R.J.,& Kaplan,A.
in *"ADPRibosylation of Proteins"* (Eds.Althaus,F.R.,Hilz,H. &
Shall,S.) (1985) . Springer-Verlag, Berlin. p389-404

Cleaver,J. in *"The Metabolic Basis of Inherited Disease"* (eds,
Stanbury,J., Wyngararden,J.& Frederickson,D.) (1978) 4th ed.
Elsevier. p1072-1075

Cleaver, J.E., Bodell, W.J., Morgan, W.F. & Zelle, B.
J. Biol. Chem. 258 (1983) p9059-9068

Cleaver, J.E. & Morgan W.F.
Mut. Res. 150 (1985) p69-76

Cleaver, J.E.
Mut. Res. 131 (1984) p123-7

Coleman, J.E. in *"Zinc Enzymes"*. (Ed. Spiro, T.G.) (1983)
Wiley & Sons NY.

Cornelissen, A.W.C.A., Michels, P.A.M., Borst, P., Spanjer, J.A.M., Versluis-Broers, C., Van der Meer, C., Farzaneh, F. & Shall, S.
in *Abstr. 8th. Int. Symp. ADP-ribosylation.* (1987) no.105

Creissen, D. & Shall, S.
Nature 296 (1982) p271-272

Dam, T.V., Brousseau, Y., Miclette, J., Faribault, G., Aubin, R. & Poirier, G.G.
in *"ADP-ribosylation reactions ."* (eds. Hayaishi, O. & Ueda, K.)
Academic Press (1982) p324-337

Durkacz, B.W., Omidiji, O., Gray, D.A., & Shall, S.
Nature 283 (1980) p593-596

Edwards, M.J. & Taylor, A.M.R.
Nature 287 (1980) p745-747

Farzaneh, F. & Pearson C.K.
Biochem. Biophys. Res. Commun. 84 (1978) p537-543

Farzaneh, F., Shall, S. & Zalin, R.
in *"Novel ADPRibosylation of Regulatory Enzymes and Proteins"*
(eds. Smulson, M.E. & Sugimura, T.) (1980) Elsevier, Amsterdam. p217-224

Farzaneh,F.,Shall,S. & Johnston,A.P.
FEBS 189 (1985) p62

Farzaneh,F.,Panayotou,G.N.,Bowler,L.D.,Broom,T. & Shall,S.
in *8th Int.Symp.ADPRibosylation.*(1987) no.86

Friedberg,E.C.
"DNA repair". (1985) Freeman

Furneaux,H.M. & Pearson,C.K.
Biochem.J. 187 (1980) p91-103

Gaal,J.C.& Pearson,C.K.
Biochem.J. 230 (1985) p1-18

Ghani,Q.P. & Hollenberg,M.
Biochem.J. 170 (1978) p387-394

Greer,W.L. & Kaplan, J.G.
in *"Growth, Cancer and the cell cycle"* (Eds.Skehan,P. &
Freedman,S.) (1984) . Humana Press, New Jersey. p125

Greer,W.L. & Kaplan,J.G.
in *"ADPRibosylation of Proteins"* (Eds.Althaus,F.R.,Hilz,H. &
Shall,S.) (1985) . Springer-Verlag, Berlin. p417

Grummt,F.
Proc.Natl.Acad.Sci.USA 751 (1978) p371-375

Grummt,F.
Plant.Mol.Biol. 2 (1983) p41-44

Grummt,F.Waltl,G.,Jantzen,H.M.,Hamprecht,K.,Hübscher,U.& Kuenzle,C.C.
Proc.Natl.Acad.Sci.USA 76 (1979) p6081-6085

Grummt,F.,Albert,W.,Zastrow,G.& Schnabel,A.
in *"Proteins involved in DNA replication"* (Eds.Hübscher,U.&
Spadari,S.) (1984) p373

Grummt,F.,Weinmann-Dorsch,C.,Schneider-Schaulies & Lux,A.
Exp.Cell.Res. 163 (1986) p191-200

Guranowski,A.& Blanquet,S.
J.Biol.Chem. 260 (1985) p3542-3547

Hatekeyama,K.,Nemoto,Y.,Ueda,K.& Hayaishi,O.
J.Biol.Chem. 261 no.32 (1986) p14902-14911

Hayaishi,O & Ueda,K.
Ann.Rev.Biochem. 46 (1977) p95-116

Hayaishi,O.& Ueda,K.
"ADP-ribosylation reactions" (1982) Academic Press

Heynes,W. & De Moor, P.
Biochemica et Biophysica Acta 358 (1974) p1-13

Hilz,H.
Hoppe-Seyler's Physiol.Chem. 362 (1981) p1415-25

Hilz,H.,Koch,R.,Fanick,W.,Klapproth,K.& Adamietz,P.
Proc.Natl.Acad.Sci.USA 81 (1984) p3929-33

Honjo,T.,Nishizuka,Y.,Hayaishi,O.& Kato,I.
J.Biol.Chem. 243 (1968) p3553-55

Holtlund,J.,Kristensen,T.,Østvold,A.C.& Laland,S.G.
Eur.J.Biochem. 130 (1981) p309-314

Huletsky,A.,Niedergang,C.,Fréchette,A.,Aubin,R.,Gaudreau,A.&
Poirier,G.G.
Eur.J.Biochem. 146 (1985) p277-285

Ikai,K.,Ueda,K.,Fukushima,M.,Nakamura,T.& Hayaishi,O.
Proc.Natl.Acad.Sci.USA 77 (1980) p3682-85

Ikai, K. Ikejima, M., Bohannon, D., Gill, D. M. & Thompson, L. H.
Mut. Res. 128 (1984) p213-220

Ikejima, M., Bohannon, D., Gill, M. & Thomson, L. H.
Mutation Research 128 (1984) p213-220

Ikejima, M., Marsischky, G. & Gill, D.
in *Abstr. 8th. Int. Symp. ADP-ribosylation.* (1987) no. 13

Ittel, M. E., Jongstra-Bilen, J., Niedergang, C., Mandel, P& Delain, E.
in *Abstr. 7th. Int. Symp. ADP-ribosylation reactions.* (1984) p55

Jacob, S. T., Kurl, R. N. & Mealey, J. F.
in *8th Int. Symp. ADPRibosylation.* (1987) no 87.

Jackowski, G., Danilczyk, U., Buki, K. G. & Kun, E.
in *Abstr. 8th. Int. Symp. ADP-ribosylation.* (1987) no. 109

Jacobson, M. K., Levi, V., Juarez-salinas, H., Barton, R. A., & Jacobson, E. L
Cancer. Res. 40 (1980) p1797-1802

Jacobson, E. L., Antol, K. M., Juarez-salinas, H., & Jacobson, M. K.
J. Biol. Chem. 258 (1983) p103-107.

Janßen, O. & Hilz, H.
in *Abstr. 8th. Int. Symp. ADP-ribosylation.* (1987) no. 108

Jongstra-Bilen, J., Ittle, M. E., Jongstra, J. & Mandel, P.
Biochem. Biophys. Res. Commun. 103 (1981) p383-390

Jump, D. B. & Smulson, M. E.
Biochemistry 19 (1980) p1024-1030

Kanai, Y., Tanuma, S. & Sugimura, T.
Proc. Natl. Acad. Sci. USA 78 (1981) p2801-2804

Kahn, Z. & Francis, G. E.
in *Abstr. 8th. Int. Symp. ADP-ribosylation.* (1987) no. 111

Kameshita, I., Matsuda, Z., Taniguchi, T. & Shizuta, Y.
J. Biol. Chem. 259 no. 8 (1984) p4770

Kameshita, I. *et. al.*
in *Abstr. 8th. Int. Symp. ADP-ribosylation.* (1987)

Kawaichi, M., Ueda, K. & Hayaishi, O.
J. Biol. Chem. 225 (1980) p816-819

Khorana, H. G.
J. Org. Chem. 76 (1954) p3517-3522

Kidwell, W. P.
J. Biochem. 77 (1975) p6.

Kitabetake, S., Dombou, M., Tomioka, I. & Nakejima, H.
Biochem. Biophys. Res. Commun. 140 no. 1 (1987) p173-178

Koide, S. S.
in *"ADP-ribosylation reactions"* eds. Hayaishi, O & Ueda, K. (1982)
Academic Press. p363

Koide, S. S., Ellison, R. P., Burzio, L. O., & Koide, S. L.
Biol. Bull . (Woods Hole, Mass.) 151 (1976) p4165-417

Konishi, Y., Denda, A. & Tsutsumi, M.
in *Abstr. 8th. Int. Symp. ADP-ribosylation.* (1987) no. 45

Kornberg, A.
"DNA Replication" (1980) San Fransisco. Freeman.

Kreimeyer, A., Wielckens, K., Adamietz, P. & Hilz, H.
J. Biol. Chem. 259 no. 2 (1984) p890-96

Kun, E., Chang, A. C. Y., Sharma, M. L., Ferro, A. M. & Nitecki, D.
Proc. Natl. Acad. Sci. USA 80 (1976) p3131-35

Leduc, Y., de Murcia, G., Lamarre, D. & Poirer, G. G.
Biochem. Biophys. Acta. 885 (1986) p248-55

Lee, P.C., Bochner, B.R. & Ames, B.N.
J. Biol. Chem. 258 (1983) p6827

Lehmann, A.R., Kirk-Bell, S., Shall, S. & Whish, W.J.D.
Exp. Cell. Res. 83 (1974) p63-72

Lindahl, T.
Nature 298 (1982) p424-425

Lötscher, P., Alvarez-Gonzalez, R. & Althaus, F.R.
in *Abstr. 3rd. Eur. Workshop. ADP-ribosylation of Proteins.* (1985)
Poster no. 12

Lubet, R.A., McCarvill, J.T., Putman, D.L., Schwarz, J.L. & Schechtman, L.M.
Carcinogenesis 5 (1984) no.4 p449-462

Lunec, J., George, A.M., Hedges, M., Cramp, W.A., Whish, W.J.D. & Hunt, B.
Br. J. Cancer 49 (1984) Suppl. VI p19-25

Mathis, G. & Althaus, F.
in *Abstr. 8th. Int. Symp. ADP-ribosylation.* (1987) no.93

Mazen, A., Gradwhol, G., Lamarre, D. & de Murcia, G.
in *Abstr. 8th. Int. Symp. ADP-ribosylation.* (1987) no. 19

Mennella, M., Quesada, P., Farina, B., Leone, E. & Jones, R.
Biochem. J. 221 (1984) p223-33

Milam, K.M. & Cleaver, J.E.
Science 223 (1984) (4636) p589-591

Minaga, T. & Kun, E.
J. Biol. Chem. 258 no.9 (1983) p725

Miwa, M., Saikawa, N., Yamaizumi, Z., Nishimura, S. & Sugimura, T.
Proc. Natl. Acad. Sci. USA 76
(1979) p595-599

Miwa, M., Kanai, M., Kondo, T., Hoshino, H. Ishihara, K& Sugimura, T.
Biochem. Biophys. Res. Commun. 100 (1981) p463-470

Miwa, M., Ishihara, M., Takishima, S., Takasuka, N., Maeda, M., Yamaizumi, Z. & Sugimura, T.
J. Biol. Chem. 256 (1981) p2916-21

Moss, J., Tsai, S., Adamik, R., Chen, H. & Stanley, S.
in *Abstr. 8th. Int. Symp. ADP-ribosylation.* (1987) no. 1

deMurcia, G., Huletsky, A., Lammarre, D., Gaudreau, A., Pouyet, J., Daune, M. & Poirier, G. G.
J. Biol. Chem. 261 no. 15 (1986) p7011-17

Mullen, W. H.
PhD. Thesis. (University of Bath) (1983)

Nagao, M., Yameda, M., Miwa, M. & Sugimura, T.
Biochem. Biophys. Res. Commun. 48 (1972) p219-225

Niedergang, C., deMurcia, G., Ittel, M., Pouyet, J. & Mandel, P.
Eur. J. Biochem. 146 (1985) p185-191

Nishizuka, Y., Ueda, K., Nakazawa, K. & Hayaishi, O.
J. Biol. Chem. 238 (1967) p3164-71

Nishizuka, Y., Ueda, K., Honjo, T. & Hayaishi, O.
J. Biol. Chem. 243 (1968) p3765-67

Nolde, S. & Hilz, H.
Br. J. Cancer. 26 (1972) p299-303

Nomura, H., Kitamura, A., Yoshinori, T., Tsuchiya, M., Ueki, M., Sugimoto, O. & Shimoyama, M.
Biochem. Biophys. Acta. 781 (1984) p112

Ohashi, Y., Ueda, K., Kawaichi, M., & Hayaishi, O.
Proc. Natl. Acad. Sci. USA 80 (1983) p3604-3607

Oka,J.,Ueda,K.& Hayaishi,O.
*Biochem.Biophys.Res.Commun.*80 no.4 (1978) p841-848

Oka,,J.,Ueda,K.,Hayaishi,O.,Komura,H.& Nakanishi,K.
J.Biol.Chem 259no.2 (1983) p986-995

Okayama,H.,Honda,M.& Hayaishi,O.
*Proc.Natl.Acad.Sci.USA*75 no.5 (1978) p2254-57

Okayama,H.,Edson,C.M.,Fukushima,Ueda,K.& Hayaishi,O.
J.Biol.Chem. 252 (1977) p7000-7005

Panyim,S.& Chalkley,R.
J.Biol.Chem. 246 (1971) p7557-60

Patel,B.N.,Dover,M.B.J.& Skidmore,C.J.
in *Abstr. 8th.Int.Symp.ADP-ribosylation.* (1987) no.113

Pearson,C.K.
in *"ADPRibosylation reactions"* eds. Hayaishi,O & Ueda,K. (1982)
Academic Press p407-421

Pearson,C.K.& Gaal,J.C.
in *Abstr. 8th.Int.Symp.ADP-ribosylation.* (1987) no.96

Plateau,P.,Mayaux,J.& Blanquet,S.
Biochemistry 20 (1981) p4654-4662

Plateau,P.,Fromant,M.,Kepes,F.& Blanquet,S.
*J.Bacteriol.*169 no.1 (1987) p419-422

Poirier,G.G.,deMurcia,G.,Jongstra-Bilen,J.,Niedergang,C.& Mandel,P.
*Proc.Natl.Acad.Sci.USA*79 (1982) p3423-27

Politi,L. & Moriggi,M.
J.Chromatogr. 267 (1983) 403-408

Porteus,J.W. & Pearson,C.K.
in *"ADPRibosylation reactions"* eds. Hayaishi,O & Ueda,K. (1982)
Academic Press. p423-437

Purnell,M.R.& Whish,W.J.D.
Biochem.J. 185 (1980a) p775-777

Purnell,M.R.& Whish,W.J.D.
Biochem.Soc.Trans. 8 (1980b) p175-6

Randerath,K., Janeway, C.M., Stephenson,M. & Zamecnik, P.C.
Biochem,Biophys.Res.Commun. 24 (1966) p98-105

Rapaport,E.& Zamecnik,P.C.
*Proc.Natl.Acad.Sci.USA*73 no.11 (1976) p3984-3988

Rapaport,E., Zamecnik,P.C. & Baril, E.G.
*Proc.Natl.Acad.Sci.USA*78 (1981a) p838-842

Rapaport,E.,Zamecnik,P.C.& Baril,E.F.
J.Biol.Chem. 256 no.23 (1981b) p12148-12151

Rapaport,E.& Feldman,L.
Eur.J.Biochem. 138 (1984) p111-115

Rechsteiner,M.,Hillyard,D.& Olivera,B.M.
Nature 259 (1976) p695-696

Reddy,G.P.V.& Pardee,A.B.
*Proc.Natl.Acad.Sci.USA*77 (1980) p3312-3316

Rees,A.R.& Sternberg,M.J.E. *"From cells to atoms"* (1984)
Blackwell Scientific Pubs.

Reiss, J.R. & Moffat , J.G.
J.Org.Chem. 30 (1965) p3381-3387

Renz, M. & Day, L. A.
Biochemistry. 15 (1976) p3320-8

Riquelme, P. T., Burzio, L. O. & Koide, S. S.
J. Biol. Chem. 254 no. 8 (1979) p3018-28

Roitt, I. M.
Biochem. J. 63 (1956) p300-307

Sastry, S. S. & Kun, E.
in *Abstr. 8th. Int. Symp. ADP-ribosylation.* (1987) no. 85

Sauermann, G. & Wesierska-Gadek, J.
Biochem. Biophys. Res. Commun. 139 no. 2 (1986) p523-9

Scovassi, A. I., Stefanini, M., Izzo, R., Lagomarsini, P. & Bertazzoni, U.
in *Abstr. 8th. Int. Symp. ADP-ribosylation.* (1987) no. 114

Segal, E. & Le Pecq, J.
Exp. Cell. Res. 167 (1986) p119-126

Shall, S., Brightwell, M., O'Farrell, M. K., Stone, P. & Whish, W. J. D.
Hoppe Zeyler's Physiol. Chem. 353 (1972) p846-7

Shall, S. in *"ADPRibosylation reactions"* (Eds. Hayaishi, O. and Ueda, K.)
(1982) Academic Press. p477-520

Shaikh, B., Huang, S. K. S. & Pontzer, N. J.
Chem. Biol. Interact. 30 (1980) p253-256

Shinohara, Y., Miyata, Y., Muraski, G., Nakanishi, K., Yoshimura, T. & Ito, N.
Gann. 68 (1977) p397-404

Skidmore, C. J., Jones, J. & Patel, B. N.
in *Abstr. 8th. Int. Symp. ADP-ribosylation.* (1987) no. 23

Smulson, M.E., Henrickson, O. & Rideau, C.
Biochem. Biophys. Res. Commun. 43 (1971) p1266-1273

Smulson, M.E., Stark, P., Gazzoli, M. &Roberts, J.H.
Exp. Cell. Res. 90 (1975) p175-182

Smulson, M.E., Schein, P., Mullins, D.W. and Sudhakar, S.
Cancer. Res. 37 (1977) p3006-3012

States, J.C. & Janakivedi, K.
Bioscience Reports. 3 (1983) p847-56

Stone, P.R., Lorimer, W.S. & Kidwell, W.R.
Eur. J. Biochem. 81 (1977) p9-18

Surowy, C. & Berger, N.
J. Biol. Chem. 258 no.1 (1983a) p579-83

Surowy, C. & Berger, N.A.
Biochem. Biophys. Acta. 740 (1983b) p8-18

Suzuki, H., Uchida, K., Shima, H., Sato, T., Okamoto, T., Kimura, T. & Miwa, M.
Biochem. Biophys. Res. Commun. 146 no.2 (1987) p403-409

Tanaka, Y., Hayaishi, K., Sakura, H., Miwa, M., Matsushima, T. & Sugimura, T.
Nucleic Acids Res. 5 (1978) p3183-94

Tanaka, Y., Matsunami, Y. & Yoshihara, K.
Biochem. Biophys. Res. Commun. 99 no.3 (1981a) p837-43

Tanaka, Y., Matsunami, N., Itaya, A. & Yoshihara, K.
J. Biochem. 90. (1981b) p1131-39

Tanaka, Y., Yoshihara, K., Itaya, A., Kamiya, T. & Koide, S.S.
J. Biol. Chem. 259 (1984) p6579-6585.

Tanaka, Y., Ito, K., Yoshihara, K. & Kamiya, T.
J. Biochem. 155 (1986) p19-25

Tanigawa,Y. & Shimoyama,M.
J.Biol.Chem. 258 no.15 (1983) p9184.

Tanuma,S.,Yagi,T.& Johnson,G.S.
Arch.Biochem.Biophys. 237 no.1 (1985) p38-42

Tanuma,S.,Kawashima,K. & Enda,M.
BBRC 135 no.3 (1986) p979-86

Tanuma,S.& Kanai,M.
J.Biol.Chem. 257 (1982) p6565-70

Thi Man,N.& Shall,S.
Eur.J.Biochem 126 (1982) p83-88

Thoma,F.& Koller,T.
J.Mol.Biol. 149 (1981) p709-735

Travers,A.& Krug,A.
Nature 327 (1987) p280-281

Ueda,,K.& Hayaishi,O. in *"ADP-ribosylation reactions"*
(eds.Hayaishi,O.& Ueda,K.) (1982a) . Academic Press. p561-572

Ueda,K.,Kawaichi,M.& Hayaishi,O.in *"ADP-ribosylation reactions"*
(eds.Hayaishi,O.& Ueda,K.) (1982b) Academic Press. p118-150

Ueda,K. & Hayaishi,O.
Ann.Rev.Biochem. 54 (1985) p73

Ueda,K. & Yamamura,H.
in "Methods in enzymology" (Eds. McCormick,D.B. & Wright,L.D.).
Vol 18B .(1970) Academic Press, New York. p60-67

Vallejo,C.G.,Lobaton,C.D.,Quintanilla,M.,Sillero,A.& Sillero,M.A.G.
*Biochem.Biophys.Acta.*438 (1976) p304-309

Varshavsky, A.
J. Theor. Biol. 105 (1983) p707-714

Walker, I.G., Th'ng, J.P.H., Schrader, T.J. & Norry, T.W.
Can. J. Biochem. Cell. Biol. 62 (1984) p329-334

Walker, J. & Pearson, C.K.
Biochem. J. 199 (1981) p813-17

Weinmann-Dorsch, C., Pierron, G., Wick, R., Sauer, H. & Grummt, F.
Exp. Cell. Res. 155 (1984a) p171-177

Weinmann-Dorsch, C. Hedl, A., Grummt, I., Albert, W., Ferdinand, F., Fris, R.,
Pierron, G., Moll, W. & Grummt, F.
Eur. J. Biochem. 138 (1984b) p179-183

Weinmann-Dorsch, C. & Grummt, F.
Exp. Cell. Res. 160 (1985) p47-53

Weisbrod, S. & Weintraub, H.
Proc. Natl. Acad. Sci. USA76 (1979) p630-34

West, R.E. & Moss, J.
Biochemistry 25 (1986) p8057-62

Whish, W.J.D., Davies, M.I. & Shall, S.
Biochem. Biophys. Res. Commun. 65 (1975) p722-730

White, I.
PhD. thesis. University of Bath. (1988).

Wielckens, K., Schmidt, A., George, E., Bredehorst, R. & Hilz, H.
J. Biol. Chem. 257 no.21 (1982) p12872-77

Williams, G.T., Taylor, R., Jenkinson, E.J., Hill, M., Griffin, E., Kingston, R.
and Owen, J.T.
in *Abstr. 8th. Int. Symp. ADP-ribosylation.* (1987) no.100

Willis, A.E. & Lindahl, T.
Nature 325 (1987) p355-357

Wu, M., Zaun, R., Aboul-Ela, N. & Jacobson, M.
in *Abstr. 8th. Int. Symp. ADP-ribosylation.* (1987) no.101

Yoshihara, K., Hashida, T. & Koide, S.S.
Biochem. Biophys. Res. Commun. 59 (1974) p658-665

Yoshihara, K., Tanigawa, Y., Burzio, L.O., & Koide, S.S.
Proc. Natl. Acad. Sci. USA 72 (1975) p289-293

Yoshihara, K., Hashida, T., Tanaka, T., Yoshihara, H. & Kamiya, T.
J. Biol. Chem. 253 (1978) p6459-66

Yoshihara, K. & Tanaka, Y.
J. Biol. Chem. 256 (1981) p6756-6761

Yoshihara, K., Itaya, A., Tanaka, Y., Ohashi, Y., Kamiya, T., Teraoka, H.,
Tsukada, K. & Matsukage, A.
in *Abstr. 7th. Int. Symp. ADP-ribosylation Reactions.* (1984) p.108

Yoshihara, K., Itaya, A., Tanaka, Y., Ohashi, Y., Kamiya, T., Teraoka, H.,
Tsukada, K. & Matsukage, A. *& Kamiya, T.*
Biochem. Biophys. Res. Commun. 128 (1985) p61-67

Yoshihara, K., Hironaka, T., Itaya, A. & Kamiya, T.
in *Abstr. 8th. Int. Symp. ADP-ribosylation.* (1987) no.7

Yost, D.A. & Moss, J.
J. Biol. Chem. 258 (1983) p4296

Zahradka, P. & Ebisuzaki, K.
Eur. J. Biochem. 142 (1984) p503-9

Zamecnik, P.C., Stephenson, M.L. & Janeway, C.M.
Biochem. Biophys. Res. Commun. 24 no.1 (1966) p91-97

Zatman, L., Kaplan, N. & Colowick, S.
J. Biol. Chem. 200 (1953) p197-212

Zimmerman, S., Little, J., Oshinsky, C. & Gellert, M.
Proc. Natl. Acad. Sci. USA 57 (1967) p1841-48

Zhang, J., Kalemegham, R. & Ebisuzaki, K.
in *Abstr. 8th. Int. Symp. ADP-ribosylation.* (1987) no.30

Zourgi, L., Tharaud, D., Solari, A., Litvak, S. & Tarrago-Litvak, L.
Biochem. Biophys. Acta. 846 (1986) p222-232

Bibligraphy of Reviews.

"DNA Repair"
Friedberg,E.C.
W.H.Freeman. (1985)

"Eukaryotic nuclear ADP-ribosylation reactions".
Gaal,J.C. and Pearson,C.K.
Biochem.J. 230 (1985) p1-18

"Ap4A: a putative chemical messenger of cell proliferation control and inducer of replication".
Grummt,F.
Plant Mol.Biol. 2 (1983) 41-44

"ADP-ribosylation reactions"
Hayaishi,O. and Ueda,K.(Eds.)
Academic Press.1982

"ADP-Ribosylation"
Hayaishi,O. and Ueda,K.
Ann.Rev.Biochem. 46 (1977) p95-116

"ADP-Ribosylation of Proteins"
Hilz,H.
Hoppe-Seyler's Z.Physiol.Chem. 362 no.11 (1981) p1415-1425

"Research overview: ADPR'n of nuclear proteins".
Purnell,M., Stone,P.R. and Whish,W.J.D.
Biochem.Soc.Trans. 8 (1980) p215-27

Review.
Ueda,K.,Ogata,N.Kawaichi,M.,Ineda,S.,and Hayaishi,O.
Curr.Topics.Cell.Regulat. 21 (1982) p175-87